

# **Teashirts in the mammalian urinary tract**

**by Claire Michelle Lye**

A thesis submitted to the University of London in  
fulfilment of the requirement for the degree of Doctor of  
Philosophy

July 2008

Nephro-Urology Unit  
UCL Institute of Child Health  
University College London



UMI Number: U591619

All rights reserved

INFORMATION TO ALL USERS

The quality of this reproduction is dependent upon the quality of the copy submitted.

In the unlikely event that the author did not send a complete manuscript and there are missing pages, these will be noted. Also, if material had to be removed, a note will indicate the deletion.



UMI U591619

Published by ProQuest LLC 2013. Copyright in the Dissertation held by the Author.  
Microform Edition © ProQuest LLC.

All rights reserved. This work is protected against  
unauthorized copying under Title 17, United States Code.



ProQuest LLC  
789 East Eisenhower Parkway  
P.O. Box 1346  
Ann Arbor, MI 48106-1346

## **Declaration**

I, Claire Michelle Lye (née Gannon), confirm that the original studies presented in the results chapters of this thesis are my own work. I have acknowledged various important reagents used, as appropriate, especially generation of Tshz3 transgenic mice and polyclonal antibodies. Where work was done in collaboration with others, for example, optical projection tomography and certain histology stains, this has also been indicated in my thesis. Where information has been derived from other sources, this has been indicated in my thesis.

*To Ed*

## Abstract

*Teashirt* genes encode putative transcription factors, and were first identified in *Drosophila melanogaster*. *Teashirt* genes regulate various aspects of *Drosophila* and vertebrate embryonic development, and there is evidence of functional conservation of *Teashirts* between species. Since *Teashirt* genes are expressed during (and may play a role in) the development of the *Drosophila* renal system, I hypothesised that *Teashirt* genes play a role in the development of the mammalian renal system/urinary tract.

To investigate this possibility I sought the expression of the mouse *Teashirt* genes (*mTshz1*, *mTshz2* and *mTshz3*) in the kidneys of mice at various stages of development using polymerase chain reaction based methods. I found that all mouse *Teashirt* genes were expressed in metanephric kidneys from inception and through their maturation, findings consistent with my hypothesis. In order to develop reagents to further define the expression patterns of *Teashirt* genes in urinary tracts (including kidneys) of embryonic and adult mice I had polyclonal antibodies designed and generated to specifically recognise proteins encoded by *mTshz1*, *mTshz2* and *mTshz3*, and tested their reactivity and specificity.

Secondly, I used a mutant mouse (in which *mTshz3* had been inactivated by replacing the majority of its coding sequence with a *lacZ* reporter construct) to investigate the expression and function of *mTshz3* in the urinary tract. By following *lacZ* expression in heterozygous transgenic mice, I found that *mTshz3* was expressed in kidney medullary stroma, and in mesenchymal cells of the ureters and urinary bladder. Homozygous (*mTshz3* null) transgenic mice displayed a striking, bilateral hydronephrosis and hydroureter phenotype. I showed that this phenotype develops due to a failure of ureteric smooth muscle differentiation, leading to defective peristalsis, and therefore urine accumulates in the proximal ureter and renal pelvis. Thus *mTshz3* is required during mouse urinary tract development for the differentiation of ureteric smooth muscle.

## Table of Contents

Declaration .....	2
<b>Abstract</b> .....	4
List of figures and movies .....	14
Acknowledgements .....	19
List of Abbreviations .....	22
<b>Chapter One – Introduction</b> .....	27
Overview of Thesis .....	27
The <i>Teashirt</i> gene family .....	29
Teashirt structure, evolution and functional conservation .....	29
Teashirt gene functions in <i>Drosophila</i> .....	33
Teashirt genes and the Malpighian tubule .....	35
Teashirt gene functions in vertebrates .....	39
Expression studies .....	39
Functional studies .....	41
Why study Teashirt genes in developing mouse urinary tracts? .....	42
The development of the ureter .....	55
Cell lineages in ureter development .....	58
Molecular control of ureter development .....	58
Initiation of ureteric bud formation, and restriction of budding site .....	58
Development of the epithelium and mesenchyme of the ureter .....	60
Ureteropelvic junction formation .....	65

Vesicoureteric junction formation.....	68
<b>Chapter Two – Materials and Methods .....</b>	<b>70</b>
Mice.....	70
Cell culture.....	71
Culturing embryonic mouse ureters .....	73
Analysis of ureter growth.....	73
Quantitative analysis of peristalsis.....	76
Qualitative analysis of peristalsis.....	76
Reverse transcriptase-PCR and real time-PCR experiments .....	77
Design of primers.....	77
Isolation of kidneys/metanephri from mice .....	77
Isolation of RNA from dissected tissue .....	79
Isolation of RNA from confluent cells.....	79
Removal of residual genomic DNA.....	79
Reverse transcription of DNase treated RNA into single stranded cDNA .....	80
PCR .....	80
Real-time PCR .....	81
Design and production of polyclonal antibodies.....	87
Overexpression of cMyc-tagged proteins in HEK293 cells.....	93
Preparation of plasmids to be transfected into HEK293 cells.....	94
Transfection of Myc-tagged Teashirts in HEK293 cells.....	97
Western Blotting .....	98
Preparation of protein.....	98
SDS-PAGE.....	99

Electroblotting.....	100
Blocking and addition of antibodies .....	101
Chemiluminescence .....	101
Control experiments to ensure specificity of antibody binding .....	105
Stripping blots.....	105
Immunocytochemistry of transfected HEK293 cells.....	105
Growing and fixing of cells onto slides .....	105
Staining procedure .....	106
Immunohistochemistry.....	106
Preparation of paraffin embedded sections of urinary tracts and treatments prior to blocking and the addition of antibodies.....	110
Preparation of frozen sections of urinary tracts and treatments prior to blocking and the addition of antibodies.....	111
Quenching of endogeneous peroxidase activity and prevention of non-specific antibody binding.....	111
Application of antibodies.....	112
Histochemical detection of HRP.....	113
Photomicroscopy.....	113
Control experiments to ensure specificity of antibody binding .....	113
Verification of observed staining patterns .....	114
Immunofluorescence.....	114
X-gal detection of $\beta$ -galactosidase activity.....	117
Masson's trichrome histology.....	118
Phenotypic analysis of renal tracts from <i>Tshz3</i> null embryos.....	118
Optical projection tomography .....	118



Injection of India ink into lumens of urinary tracts.....	119
Detection and quantification of proliferating cells.....	119
Detection and quantification of apoptotic cells.....	120
<b>Results Part I – Chapter Three</b> .....	122
Expression of <i>Tshz1</i> , 2 and 3, and <i>Larp</i> in kidneys and renal cell-lines.....	122
Introduction.....	122
Results.....	122
Reverse transcriptase PCR on embryonic and mature kidneys.....	122
Reverse transcriptase PCR on renal cell lines.....	125
Real time-PCR on embryonic and mature kidneys.....	130
Interpretation and Discussion.....	136
Reverse transcriptase PCR on embryonic and mature kidneys.....	136
Reverse transcriptase PCR on renal cell lines.....	136
Real time-PCR on embryonic and mature kidneys.....	137
<b>Results part I - Chapter Four</b> .....	139
Raising and characterising antibodies against <i>Tshz1</i> , 2 and 3.....	139
Introduction.....	139
Results.....	140
Design and generation of antibodies.....	140
Characterising antibody reactivity and specificity.....	140
Transfected HEK293 express Myc-tagged proteins, as determined by	
Western blotting.....	141

Testing reactivity of anti-Tshz antibodies, using protein from transfected HEK293 cells .....	144
Anti-Tshz1 and Anti-Tshz3 antibodies are specifically reactive against the Tshz of interest, they do not react with other Tshz protein family members .....	154
Testing reactivity of anti-Tshz3 antibody in immunocytochemistry experiments .....	159
Tshz3 protein is approximately 250 kDa in size, as observed by western blotting using three different antibodies.....	162
Using anti-Tshz1 and anti-Tshz3 antibodies to investigate the expression of Tshz proteins in urinary tract tissue .....	165
Western blots on mouse urinary tract tissue .....	165
Immunohistochemistry on mouse urinary tract tissue .....	171
Discussion .....	171
Reactivity of antibodies raised against Tshz1, 2 and 3 .....	171
Tshz3 is a nuclear protein .....	173
Western blot banding patterns and size of Tshz proteins.....	173
Using the antibodies to detect endogeneous Tshz proteins.....	176
<b>Results Part II - Chapter Five.....</b>	<b>179</b>
The expression of <i>Tshz3</i> in the developing mouse urinary tract.....	179
Introduction.....	179
Results.....	180
Tshz3 is expressed in the embryonic kidney.....	180
Tshz3 is expressed in the embryonic ureter.....	185

Tshz3 is expressed in the embryonic bladder .....	185
Tshz3 is expressed in the adult kidney and ureter.....	194
Discussion .....	199
The Tshz3- $\beta$ -galactosidase fusion protein is a nuclear protein.....	199
The embryonic expression of Tshz3 suggests a role for Tshz3 in the development of the kidneys, ureter and bladder .....	199
Tshz3 is expressed in the adult kidney and ureter, suggesting additional roles for Tshz3 in the mature urinary tract .....	201
<b>Results Part II - Chapter Six</b> .....	204
The function of <i>Tshz3</i> in the developing urinary tract; <i>in vivo</i> studies .....	204
Introduction.....	204
Results.....	205
Gross anatomy by external examination.....	205
Gross anatomy of the kidney by optical projection tomography .....	208
Prevalance of the phenotype .....	208
Ontogeny of the phenotype .....	209
Histology .....	210
Hydronephrosis and hydroureter is not caused by overt anatomical obstruction .....	226
Defects in ureteric smooth muscle in Tshz3 <sup>-/-</sup> mice.....	230
Lack of ureteric smooth muscle in Tshz3 <sup>-/-</sup> mutants is probably caused by a failure of smooth muscle cell precursor differentiation .....	239
The expression of Bmp4 in the ureter, which is important for the development of ureteric smooth muscle, is unaffected in Tshz3 <sup>-/-</sup> mice .....	259

Other populations of $\alpha$ SMA expressing cells in the urinary tracts of Tshz3 <sup>-/-</sup> mice appear to be unaffected.....	262
Urothelial differentiation is unaffected in Tshz3 <sup>-/-</sup> mutant mice.....	267
The expression of Pax2, a gene that is important for controlling early events in nephrogenesis, is normal in Tshz3 <sup>-/-</sup> null mice .....	270
The kidneys of Tshz3 <sup>-/-</sup> mutant mice appear normal, other than they are hydronephrotic .....	270
Discussion .....	284
Tshz3 <sup>-/-</sup> develop bilateral hydronephrosis and hydroureter .....	284
Hydronephrosis and hydroureter in Tshz3 <sup>-/-</sup> mice do not result from physical obstruction.....	284
Ureters from Tshz3 <sup>-/-</sup> mice lack smooth muscle in their proximal portions, and have attenuated smooth muscle distally .....	285
The attenuation of smooth muscle in Tshz3 <sup>-/-</sup> ureters is probably due to a failure of smooth muscle differentiation .....	286
Bmp4 expression, which is required for ureteric smooth muscle development, is not affected in Tshz3 <sup>-/-</sup> ureters .....	287
Abnormalities in cell shape may be the cause of the failure of smooth muscle differentiation.....	287
Other than in the ureter, expression of $\alpha$ SMA is not affected in urinary tracts of Tshz3 <sup>-/-</sup> mice. ....	289
Other than the defect in ureteric smooth muscle development, leading to hydronephrosis and hydroureter, no abnormalities could be found in the development of urinary tracts.....	290

<b>Results Part II - Chapter Seven</b> .....	293
The function of <i>Tshz3</i> in the developing urinary tract; <i>in vitro</i> studies .....	293
Introduction .....	293
Results .....	294
Quality of peristalsis .....	294
Frequency of peristalsis .....	295
Differentiation of ureters <i>in vitro</i> .....	299
Elongation of ureters <i>in vitro</i> .....	300
Discussion .....	309
Peristalsis is defective in <i>Tshz3</i> <sup>-/-</sup> ureters .....	309
$\alpha$ SMA expression is not affected in <i>Tshz3</i> <sup>-/-</sup> ureters <i>in vitro</i> .....	311
Ureter Elongation is impaired in <i>Tshz3</i> <sup>-/-</sup> ureters .....	313
 <b>Chapter Eight - Final Discussion</b> .....	 316
Summary of main findings .....	316
<i>Teashirt3</i> and mesenchymal cell lineages in urinary tract development .....	318
<i>Teashirt 3</i> is required for ureter development, a site of mesenchymal-epithelial interactions .....	322
Teashirt 3 as a player in the genetic network regulating ureter development..	325
Transcriptional pathways that may link <i>Teashirt3</i> to smooth muscle differentiation .....	333
Teashirt3 may promote smooth muscle differentiation by regulating cell shape .....	334
Teashirt3 is required for normal ureteric peristalsis, <i>in vitro</i> .....	335
Teashirt3 is required for the elongation of the ureter, <i>in vitro</i> .....	335

Teashirt3 <sup>-/-</sup> mice as a model of human pelviureteric junction obstruction .....	336
Regionalisation of the ureter .....	337
Possible role for <i>Teashirt 3</i> in the development of the renal stroma .....	339
Possible role for <i>Teashirt 3</i> in the development of the bladder .....	341
Possible role for <i>Teashirt3</i> in the adult kidney .....	342
A role for <i>Teashirt1</i> , <i>Teashirt 2</i> and <i>Larp</i> (a putative transcriptional target of <i>Teashirts</i> ) in urinary tract development? .....	343
<b>Chapter Nine – References</b> .....	349
<b>Appendix</b> .....	365

## List of figures and movies

<i>Figure 1.1 A comparison of Teashirt protein structure</i>	31
<i>Figure 1.2 teashirt genes and Malpighian tubule development</i>	37
<i>Figure 1.3 Teashirt interactors</i>	43
<i>Figure 1.4 Reciprocal signalling between epithelial and mesenchymal cell populations is required for kidney and ureter development</i>	56
<i>Figure 2.1 Analysis of growth of cultured ureters</i>	74
<i>Figure 2.2 Real Time Polymerase Chain Reaction; Generating and Using a Standard Curve</i>	83
<i>Figure 2.3 Real Time Polymerase Chain Reaction; Typical Melting Curve</i>	85
<i>Figure 2.4 The position of epitopes to which antibodies were raised within the Tshz proteins</i>	90
<i>Figure 2.5 Maps of plasmids used to overexpress cMyc tagged proteins in HEK293 cells</i>	95
<i>Figure 3.1 Early development of the mouse kidney (metanephros)</i>	123
<i>Figure 3.2 Reverse transcriptase PCR for Tshz1, 2 and 3 and Larp on metanephric kidneys from E11 and E12 mice</i>	126
<i>Figure 3.3 Reverse transcriptase PCR for Tshz1, 2 and 3 and Larp on kidneys from E14, E18, neonatal and adult mice</i>	128
<i>Figure 3.4 Reverse transcriptase PCR for Tshz1, 2 and 3 and Larp on renal cell lines</i>	131
<i>Figure 3.5 Real Time PCR for Tshz1, 2 and 3 and Larp on kidneys from E14, E18, neonatal and adult mice</i>	134
<i>Figure 4.1 Transfected cells express Myc-tagged proteins</i>	142
<i>Figure 4.2 Anti-Tshz1 antibody is reactive against Myc-tagged Tshz1 protein</i>	146
<i>Figure 4.3 Anti-Tshz2 antibody is not reactive against Myc-tagged Tshz2 protein</i>	149
<i>Figure 4.4 Anti-Tshz3 antibody is reactive against Myc-tagged Tshz3 protein</i>	152
<i>Figure 4.5 Anti-Tshz1 antibody does not react against Tshz2 and Tshz3 proteins</i>	155
<i>Figure 4.6 Anti-Tshz3 antibody does not react against Tshz1 and Tshz2 proteins</i>	157
<i>Figure 4.7 Immunocytochemistry on cells transfected with pcDNA3-MycTshz3</i>	160
<i>Figure 4.8 Western blotting for Tshz3 using three different anti-Tshz3 antibodies</i>	163
<i>Figure 4.9 Western blot for Tshz1 on kidney tissue</i>	166

<i>Figure 4.10 Western blot for Tshz3 on kidney and ureter tissue</i>	169
<i>Figure 5.1.1 Immunohistochemistry for <math>\beta</math>-galactosidase in kidneys from E15 – E18 Tshz3<sup>+/-</sup> mice</i>	181
<i>Figure 5.1.2 Negative control immunohistochemistry for <math>\beta</math>-galactosidase in kidneys from E15 – E18 Tshz3<sup>+/-</sup> and Tshz3<sup>+/+</sup> mice</i>	183
<i>Figure 5.2.1 Immunohistochemistry for <math>\beta</math>-galactosidase in ureters from E15 and E18 Tshz3<sup>+/-</sup> mice</i>	186
<i>Figure 5.2.2 Negative control immunohistochemistry for <math>\beta</math>-galactosidase in ureters from E15 and E18 Tshz3<sup>+/-</sup> and Tshz3<sup>+/+</sup> mice</i>	188
<i>Figure 5.3.1 Immunohistochemistry for <math>\beta</math>-galactosidase in bladders from E15 – E18 Tshz3<sup>+/-</sup> mice</i>	190
<i>Figure 5.3.2 Negative control immunohistochemistry for <math>\beta</math>-galactosidase in bladders from E15 – E18 Tshz3<sup>+/-</sup> and Tshz3<sup>+/+</sup> mice</i>	192
<i>Figure 5.4.1 X-gal staining of Tshz3<sup>+/-</sup> kidneys and Tshz3<sup>+/+</sup> controls</i>	195
<i>Figure 5.4.2 Double <math>\alpha</math>SMA and X-gal staining of Tshz3<sup>+/-</sup> kidneys and Tshz3<sup>+/+</sup> controls</i>	197
<i>Figure and Movies 6.1 Tshz3<sup>-/-</sup> develop hydroureter and hydronephrosis</i>	206
<i>Figure 6.2.1 Histology of the urinary tracts from E15 Tshz3<sup>-/-</sup> mice and their littermates</i>	212
<i>Figure 6.2.2 Histology of the urinary tracts from E16 Tshz3<sup>-/-</sup> mice and their littermates</i>	214
<i>Figure 6.2.3 Histology of the urinary tracts from E17 Tshz3<sup>-/-</sup> mice and their littermates</i>	216
<i>Figure 6.2.4 Histology of the urinary tracts from E18 Tshz3<sup>-/-</sup> mice and their littermates</i>	218
<i>Figure 6.3 Histology of the metanephric region of E12 Tshz3<sup>-/-</sup> mice and their littermates</i>	220
<i>Figure 6.4 Histology of the nephrogenic zones of kidneys from E18 Tshz3<sup>-/-</sup> mice and their littermates</i>	222
<i>Figure 6.5 High magnification view of histology staining of E15 proximal ureters from Tshz3<sup>-/-</sup> mice and their littermates</i>	224
<i>Figure 6.6 Injection of ink into renal pelves of Tshz3<sup>-/-</sup> mice</i>	228
<i>Figure 6.7.1 Immunohistochemistry for <math>\alpha</math>SMA in kidneys and ureters from E15 Tshz3<sup>-/-</sup> mice and their littermates</i>	231
<i>Figure 6.7.2 Immunohistochemistry for <math>\alpha</math>SMA in kidneys and ureters from E16 Tshz3<sup>-/-</sup> mice and their littermates</i>	233



<i>Figure 6.7.3 Immunohistochemistry for <math>\alpha</math>SMA in kidneys and ureters from E17 Tshz3<sup>-/-</sup> mice and their littermates</i>	235
<i>Figure 6.7.4 Immunohistochemistry for <math>\alpha</math>SMA in kidneys and ureters from E18 Tshz3<sup>-/-</sup> mice and their littermates</i>	237
<i>Figure 6.8.1 Scatter plots showing the percentage of proliferative cells in E15 Tshz3<sup>-/-</sup> and Tshz3<sup>+/+</sup> proximal ureters</i>	242
<i>Figure 6.8.2 Scatter plots showing the percentage of proliferative cells in E16 Tshz3<sup>-/-</sup> and Tshz3<sup>+/+</sup> proximal ureters</i>	244
<i>Figure 6.8.3 Representative PCNA staining of proximal ureters Tshz3<sup>-/-</sup> and Tshz3<sup>+/+</sup> mice</i>	246
<i>Figure 6.9.1 Scatter plots showing the percentage of apoptotic cells in E15</i>	250
<i>Figure 6.9.2 Scatter plots showing the percentage of apoptotic cells in E16</i>	252
<i>Figure 6.9.3 TUNEL staining of proximal ureters</i>	254
<i>Figure 6.10 Immunohistochemistry for <math>\beta</math>-galactosidase in proximal ureters from E18 Tshz3<sup>-/-</sup> and Tshz<sup>+/-</sup> mice</i>	257
<i>Figure 6.11 Immunohistochemistry for Bmp4 in kidneys and proximal ureters from E15 Tshz3<sup>-/-</sup> and Tshz<sup>+/-</sup> mice</i>	260
<i>Figure 6.12 Immunohistochemistry for <math>\alpha</math>SMA in bladders from E15-E18</i>	263
<i>Figure 6.13 Immunohistochemistry for <math>\alpha</math>SMA in kidneys from E18 Tshz3<sup>-/-</sup> mice and their littermates</i>	265
<i>Figure 6.14 Immunohistochemistry for Up1b in the proximal ureters of Tshz3<sup>+/+</sup> and Tshz3<sup>-/-</sup> mice</i>	268
<i>Figure 6.15 Immunohistochemistry for Pax2 in the metanephric region of E12 Tshz3<sup>-/-</sup> mice and their littermates</i>	271
<i>Figure 6.16 Immunohistochemistry for Pax2 in the kidneys of E18 Tshz3<sup>-/-</sup> and Tshz3<sup>+/+</sup> kidneys</i>	274
<i>Figure 6.17 Immunohistochemistry for podoplanin in the kidneys of Tshz3<sup>+/+</sup> and Tshz3<sup>-/-</sup> mice</i>	277
<i>Figure 6.18 Immunohistochemistry for uromodulin in the kidneys of E18 Tshz3<sup>-/-</sup> and Tshz3<sup>+/+</sup> kidneys</i>	280
<i>Figure 6.19 Immunohistochemistry for aquaporin 2 in the kidneys of E18 Tshz3<sup>-/-</sup> and Tshz3<sup>+/+</sup> kidneys</i>	282
<i>Movies 7.1 Timelapse movies of ureters cultured for five days in serum free conditions</i>	296

<i>Figure 7.1 Analysis of movies of ureters cultured in serum free conditions for five days</i>	297
<i>Figure 7.2.1 Expression of <math>\alpha</math>SMA and Up1b in cultured ureters</i>	301
<i>Figure 7.2.2 Expression of <math>\alpha</math>SMA and Up1b in the proximal section of cultured ureters</i>	303
<i>Figure 7.2.3 Expression of <math>\alpha</math>SMA and Up1b in the middle section of cultured ureters</i>	305
<i>Figure 7.2.4 Expression of <math>\alpha</math>SMA and Up1b in the distal section of cultured ureters</i>	307
<i>Figure 8.1 The expression of Tshz3 during the development of the kidney and ureter</i>	319
<i>Figure 8.2 Failed ureteric development in Tshz3<sup>-/-</sup> mouse</i>	323
<i>Figure 8.3 Tshz3 may act downstream of BMP4, and upstream of myocardin, to control smooth muscle differentiation in the ureter</i>	327

## List of tables

<i>Table 1.1.1 Molecules that physically interact with Teashirt</i>	45
<i>Table 1.1.2 Genes that are genetically downstream of Teashirt</i>	48
<i>Table 1.1.3 Genes that are genetically upstream of Teashirt</i>	51
<i>Table 1.2.1 Genes required for the development of the ureter</i>	64
<i>Table 1.2.2 Genes required for ureteropelvic junction (or pelvic) development</i>	67
<i>Table 2.1 Cell lines and culture conditions</i>	72
<i>Table 2.2 Primers used for reverse transcriptase PCR and real time PCR</i>	78
<i>Table 2.3 Peptides to which Tshz antibodies were raised</i>	89
<i>Table 2.4 Antibody Production Schedule</i>	92
<i>Table 2.5 Titre 's of bleeds of animals used for antibody production</i>	93
<i>Table 2.6 Antibodies used for Western blotting</i>	102
<i>Table 2.7 Primary antibodies</i>	107
<i>Table 2.8 Confocal Imaging Parameters</i>	116
<i>Table 6.1 Proliferation of Cells in the Proximal Ureter</i>	241
<i>Table 6.2 Apoptosis of Cells in the Proximal Ureter</i>	249

## Acknowledgements

I thoroughly enjoyed undertaking the research contained in this thesis, and would like to take this opportunity to thank those who helped, supported and encouraged me throughout my PhD.

Firstly I would like to thank Professor Adrian Woolf, Dr Helen Skaer and Professor Peter Scambler for allowing me the opportunity to work on this project, for their intellectual and technical guidance, and for their interest in and encouragement of my research. Special thanks goes to Adrian Woolf for helping me to develop this project, and for always being available when I needed his advice or dissection skills, and to Helen Skaer (and members of her laboratory, in particular Kyra Campbell) for introducing me to the wonders of working on the developing renal system whilst I was an undergraduate at Cambridge. I would also like to thank the Biotechnology and Biological Sciences Research Council for funding my PhD.

Much of the work in this thesis was only possible due to the generosity of collaborators, with their time, reagents and ideas. Thanks go to Dr Laurent Fasano, Dr Xavier Caubit and Elise Martin (Institute of Developmental Biology Marseilles-Luminy, Marseilles, France), and other members of their laboratory, for allowing me to work with them on the renal system of the *Tshz3* transgenic mouse, as well as providing me with valuable reagents, and for very enjoyable and productive research visit to their laboratory. Thanks also go to Dr Jamie Davies, Julie Moss and Jane Armstrong (Centre of Integrative Physiology, University of Edinburgh) for OPT imaging the renal systems of *Tshz3* transgenic mice. Finally thanks to all of Helen Skaer's laboratory for keeping me up to date with their research, and for always making me welcome when I turned up out of the blue to see them.

I would also like to thank Tung-Tien Sun (Sackler Institute, New York University Medical Center, USA) for providing me with the anti-Up1b antibody and Leila Romio (Nephro-Urology Unit, UCL Institute of Child Health) for donating plasmids containing Myc-tagged GFP. Thanks goes to staff at the UCL Confocal Unit (UCL

Department of Anatomy and Developmental Biology, UCL), in particular Daniel Ciantar, for technical assistance with confocal imaging. Special thanks goes to Dyanne Rampling (Chief Biomedical Scientist, Department of Histopathology, Great Ormond Street Hospital) for performing Masson's Trichrome staining on my behalf.

My colleagues within the Nephro-Urology Unit deserve many thanks, both for technical and academic advice, and for providing a friendly working environment. In particular I would like to thank David Long for his patience and generosity in sharing his technical knowledge and skills with me, for his advice about how to keep my project going in the right direction and for his advice on this manuscript. David, you have been like supervisor to me, and for this I can't thank you enough. Thanks also to Dagan Jenkins for his help with RT-PCR experiments, and to Karen Price for her advice on transfecting cells. Thanks to other Nephro-Urology Unit members past and present including: Shun-Kai Chan, Miliyun Chui, Paul Winyard (where would have been without you to rescue me from broken computers and mis-behaving microscopes?), Ambrose Gullet, Maggie Godley, Jazz Dinza, Jolanta Pitera, Leila Romio, Larissa Kerecuk and Michiel Schreuder; I have learnt from all of you, and had fun working with you all.

On a personal note I would like to thank my Mum and Dad, sister Elizabeth, and the rest of my family and friends for all their support and understanding throughout the preparation of this thesis. I especially would like to thank my husband. Ed, I couldn't have done it without your support, encouragement and love.

#### ***Acknowledgements of others work that contributed to this thesis***

Laurent Fasano, and members of his laboratory, carried out many of the dissections of whole renal tracts (but dissection of ureters used in organ culture experiments were performed by myself), and were responsible for collecting and genotyping the *Tshz3/lacZ* embryos.

Laurent Fasano performed computer-aided analysis of ureter culture movies (Chapter Seven).

The injection of Indian ink into the renal pelves of embryonic mice at autopsy (detailed in Chapter Six) was carried out by Laurent Fasano and myself.

Professor Adrian Woolf performed some dissections of E11 and E12 mouse metanephroi (Chapter Three), made the initial identification of the renal tract phenotype of *Tshz3/lacZ* transgenic mice (Chapter Six) and helped set up the ureter dissections and cultures (Chapter Seven).

Dyanne Rampling carried out all Masson's trichrome staining on paraffin embedded sections (Chapter Six), and performed some of the embedding and sectioning of renal tracts (Chapters Five and Six).

Julie Moss and Jane Armstrong, members of Jamie Davies' laboratory (Centre of Integrative Physiology, University of Edinburgh) carried out the Optical projection tomography imaging of embryonic kidneys (Chapter Six).

## List of Abbreviations

aa	amino acid
adb-A	abdominal A
AD	acidic domain
Agtr1a	angiotensin receptor one a
Agtr1b	angiotensin receptor one b
ANOVA	analysis of variance
antp	antennapedia
arm	armadillo
BCA	bicinchoninic acid
Bmp	bone morphogenetic protein
BrdU	bromodeoxyuridine
brk	brinker
BSA	bovine serum albumin
C2	second cervical vertebra
CaCl <sub>2</sub>	calcium chloride
CD	compact disc
cDNA	copy deoxyribonucleic acid
ci	cubitus interruptus
Cnb1	calcineurin subunit b, isoform one
CO <sub>2</sub>	carbon dioxide
CtBP	C-terminal binding protein
cTshz	chick teashirt
Da	Daltons
DAB	3,3'-diaminobenzidine
dac	dacshund
DEPC	diethylpyrocarbonate
disco	disconnected
Dlgh1	discs large homologue one
dNTPs	deoxynucleotide (triphosphate)
dteashirt	Drosophila teashirt

dtiptop	Drosophila tiptop
DNA	deoxyribonucleic acid
dpp	decapentaplegic
dUTP	deoxyuridine triphosphate
E	embryonic day
EGFr	epidermal growth factor receptor
ELISA	enzyme linked immunosorbent assay
ETDA	ethylenediaminetetraacetic acid
exd	extradenticle
eya	eyes absent
eye	eyeless
Fgf	fibroblast growth factor
ftz	fushi tarazu
GC	guanine cytosine
Gdnf	glial cell line-derived neurotrophic factor
GdnfR $\alpha$	glial cell line-derived neurotrophic factor receptor alpha
GFP	green fluorescent protein
gug	grunge
HB-EGF	heparin binding EGF-like growth factor
HCl	hydrochloric acid
HD	homeodomain (homeobox)
HEK293	human embryonic kidney cell line 293
Hprt	hypoxanthine-guanine phosphoribosyltransferase
HRP	horseradish peroxidase
hth	homothorax
IgG	immunoglobulin G
IgY	immunoglobulin Y
IMCD3	inner medullary collecting duct cell line three
ITS	insulin transferrin selium
KDa	kilo Daltons
KLH	keyhole limpet hemocyanin
lab	labial
larp	la-related protein



LEF	lymphoid enhancer-binding factor
M	molar
M5	mesenchymal cell line five
MDCK	Madin-Darby canine kidney
MET	mesenchymal to epithelial transition
mg	milligrams
MgCl <sub>2</sub>	magnesium chloride
ml	millilitres
mm	millimetres
mM	milli-molar
MM	metanephric mesenchyme
MpT	Malpighian tubule
mRNA	messenger ribonucleic acid
mTshz	mouse teashirt
n	number
NCBI	National Center for Biotechnology Information (US)
ng	nanograms
nm	nanometres
NP40	nonidet P40
OPT	optical projection tomography
P	postnatal day
PAS	periodic acid Schiff
Pax	paired box
pb	proboscipedia
PBS	phosphate buffered saline
PCNA	proliferating cell nuclear antigen
PCR	polymerase chain reaction
PI3K	phosphoinositide 3-kinase
pmol	pico-moles
Ptc1	patched one
PUJO	pelviureteric junction obstruction
R <sup>2</sup>	correlation co-efficient
RA	retinoic acid

Raldh2	retinaldehyde dehydrogenase two
RAR	retinoic acid receptor
RNA	ribonucleic acid
RT+	reverse transcriptase positive sample
RT-	reverse transcriptase negative sample
RT-PCR	reverse transcriptase polymerase chain reaction
Real Time-PCR	real time polymerase chain reaction
RIPA	radioimmunoprecipitation assay
rpm	revolutions per minute
scr	sex combs reduced
SDS	sodium dodecyl sulphate
SDS-PAGE	sodium dodecyl sulphate polyacrylamide gel electrophoresis
SEM	standard error of the mean
sFRP	secreted frizzled related protein
sgg	shaggy
Shh	sonic hedgehog
SMC	smooth muscle cell
SM-MHC	smooth muscle myosin heavy chain
so	sine oculis
SRF	serum response factor
Tbx18	T-box eighteen
Tcf	transcription factor (specifically of the Tcf/LEF family)
TEMED	N,N,N-N-tetramethylethylenediamine
tio	tiptop
TGF $\alpha$	transforming growth factor alpha
TGF $\beta$	transforming growth factor beta
tsh	<i>Drosophila</i> teashirt
Tshz	teashirt (mouse unless otherwise specified)
TUNEL	terminal deoxynucleotidyl transferase-mediated dUTP nick end labelling
U	units
UB	ureteric bud
ubx	ultrabithorax

Up1b	urolakin one b
UPJ	ureteropelvic junction
UV	ultraviolet
V	volts
VEGF	vascular endothelial growth factor
vg	vestigial
vTshz	vertebrate Teashirt
wg	wingless
Wnt	wingless-type MMTV integration site family member
Wt1	Wilms' tumour gene one
X-Gal	5-bromo-4-chloro-3-indolyl- beta-D-galactopyranoside
XTeashirt	<i>Xenopus</i> teashirt
ZnF	zinc finger
$\alpha$ SMA	alpha smooth muscle actin
$\mu$ g	micrograms
$\mu$ l	microlitres
$^{\circ}$ C	degrees Celsius

## Chapter One – Introduction

### Overview of Thesis

This thesis, which is entitled “Teashirt genes in the mammalian urinary tract”, describes research undertaken to address the expression and function of *Teashirt* genes in the mammalian (specifically mouse) urinary tract, with a strong emphasis on the expression and function of *Teashirt* genes in the developing (embryonic) urinary tract.

The rationale underlying these studies comes from the observations that, mouse *Teashirt* (*mTshz*) genes have been shown to be functionally conserved with *Drosophila teashirt* (*dtsh*) (Manfroid et al., 2004), and both *dTsh* and *Drosophila Tiptop* (*dtio*, the second *Drosophila teashirt* family gene) are expressed in the renal (Malpighian) tubules of *Drosophila melanogaster* during embryonic development (Denholm et al., 2003; Laugier et al., 2005). Given that the development of both the vertebrate urinary tract and the Malpighian tubules of *Drosophila* require complex interactions between epithelial and mesenchymal cells (Denholm et al., 2003), it is an attractive possibility that *Teashirt* genes may be involved in regulating the development of both of these renal systems.

In this thesis, I took two approaches to explore whether *Teashirt* genes are involved in the regulation of mouse urinary tract development. Firstly, I used polymerase chain reaction (PCR) based methods, and developed antibodies to undertake an expression analysis of *Teashirt* genes in the mouse urinary tract. These experiments concentrated on defining the expression of mouse *Teashirt 1* (*mTshz1*), mouse

*Teashirt 2 (mTshz2)*, and mouse *Teashirt 3 (mTshz3)* in kidneys from their inception, throughout development, and in mature adult mice. Secondly, I used a mutant mouse (in which *mTshz3* had been inactivated by replacing the majority of its coding sequence with a *lacZ* reporter construct) to investigate the expression and function of *mTshz3* in the urinary tract. I investigated *lacZ* expression in urinary tracts from heterozygotes to explore the expression of *mTshz3*, and undertook phenotypic analysis of urinary tracts from homozygotes to explore the function of *mTshz3* in mouse urinary tract development.

I found that *mTshz1*, *mTshz2* and *mTshz3* were expressed in metanephric kidneys from inception and through their maturation (Chapter Three). *mTshz3* was expressed in kidney medullary stroma, and in mesenchymal cells of the ureters and urinary bladder (Chapter Five). Homozygous (*mTshz3* null) transgenic mice displayed a striking, bilateral hydronephrosis and hydroureter phenotype, resulting from maldevelopment of their ureters (Chapters Six and Seven). Interestingly, no defects in the development of the kidneys or bladders of *mTshz3* null mice were apparent, despite expression of *mTshz3* in these organs during their development (Chapter Six).

In this introduction I summarise the published literature on *Teashirt* genes, in order that the reader can appreciate the implications of my findings in relation to what is already known about *Teashirt* gene function. As I found a role for *mTshz3* in the development of the mouse ureter, I also discuss what is already known about the control of mouse ureter development.

## The *Teashirt* gene family

### *Teashirt* structure, evolution and functional conservation

The *teashirt* gene, which encodes a transcription factor with three atypical widely spaced zinc-finger motifs (Cx2Cx12HMx4H) (Caubit et al., 2000; Manfroid et al., 2004), was first identified in *Drosophila melanogaster* and was named *teashirt* due to its characteristic expression pattern in the trunk region of the *Drosophila* embryo (Fasano et al., 1991). Alexandre et al. (1996) demonstrated, using band shift and DNase 1 protection assays, that the zinc-finger motifs of *Drosophila* Teashirt can bind to DNA *in vitro*. Also, (*Drosophila* and mouse) Teashirt has been shown to act as a transcriptional repressor when transfected into mammalian cells (Waltzer et al., 2001; Manfroid et al., 2004). Recently, a second *teashirt*-like gene, *tiptop*, has been described in *Drosophila melanogaster*. The global identity of the proteins encoded by *dteashirt* and *dtiptop* is about 28%. The region of highest identity, which is about 51%, coincides with the three atypical widely spaced zinc-fingered motifs. *dteashirt* has two exons, whilst *dtiptop* is a three exon gene (Laugier et al., 2005). *Teashirt* gene family members were subsequently identified in many species. Whilst members of the *Drosophilidae* family each have two *teashirt* genes, other insects have only one (Laurent Fasano, Institute of Developmental Biology Marseilles-Luminy, personal communication). Three *Teashirt* genes have been identified in mice (Caubit et al, 2000; Manfroid et al., 2004), and each has an orthologue in humans (Caubit et al., 2000; Laurent Fasano, personal communication; Ensembl genome browser) and chickens (Manfroid et al., 2006). It has also been reported that there are three *Teashirt* genes in *Xenopus* (Onai et al., 2007), whereas there are thought to be five in zebrafish (Laurent Fasano, personal communication). All

vertebrate Teashirt proteins appear to be encoded by two exons (Fasano, personal communication; Ensembl database).

The defining feature of Teashirt family proteins is the possession of the three atypical widely spaced zinc-finger motifs (Cx2Cx12HMx4H), which are located towards the amino-terminal of the protein (Caubit et al., 2000). Additionally, Teashirt proteins possess an acidic domain near their amino-terminal (Caubit et al., 2000), and a five amino-acid PLDLS (in *Drosophila*) or a PIDLT (in vertebrate) domain, which have been shown to be required for physical interaction with the transcriptional corepressor C-terminal binding protein (CtBP) (Manfroid et al., 2004). In addition to these domains possessed by all Teashirt proteins, dTiptop possesses a fourth zinc finger motif towards its carboxy-terminal and vertebrate Teashirt proteins possess two zinc-finger motifs and a homeodomain towards their carboxy-terminal (Caubit et al., 2000; Onai et al., 2007). A comparison of Teashirt protein structures is depicted in Figure 1.1. There is a high degree of divergence between vertebrate and *Drosophila teashirt* gene family members. Conservation is essentially restricted to the region containing the three (Cx2Cx12HMx4H) zinc-finger motifs and the acidic domain, with approximately 30% amino acid identity between murine and *Drosophila* sequences in this region.

## **Figure 1.1 A comparison of Teashirt protein structure**

A diagram to compare the functional domains possessed by different Teashirt proteins. *Drosophila* Teashirt, *Drosophila* Tiptop, and vertebrate Teashirt (vertebrate Teashirt proteins are similar to each other, all possessing the same main functional domains). Based on Caubit et al. (2000) and personal communication with Laurent Fasano.

PLDLS – PLDLS motif

PIDLT – PIDLT motif

AD – acidic domain

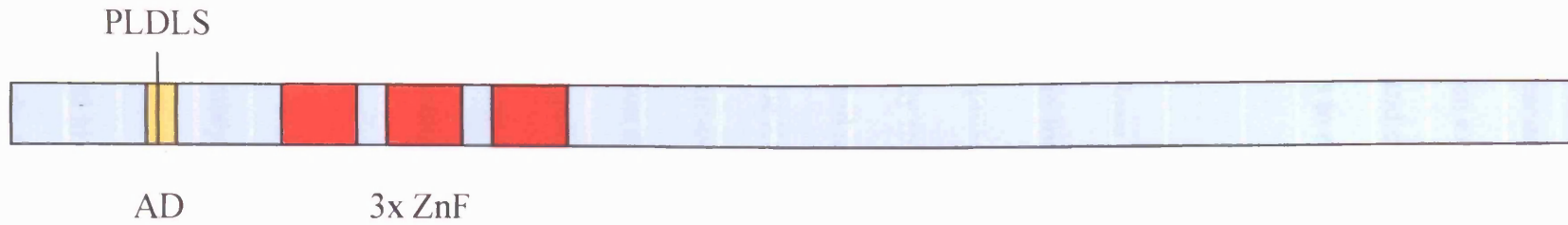
ZnF – zinc finger domain

HD – homeodomain

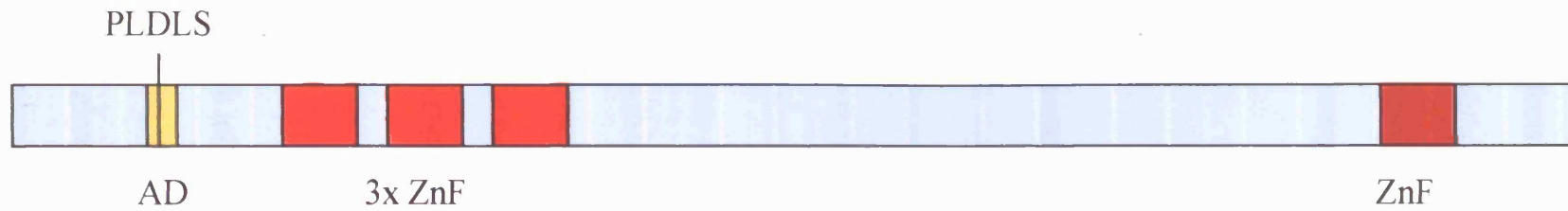


**Figure 1.1 - A comparison of Teashirt protein structure**

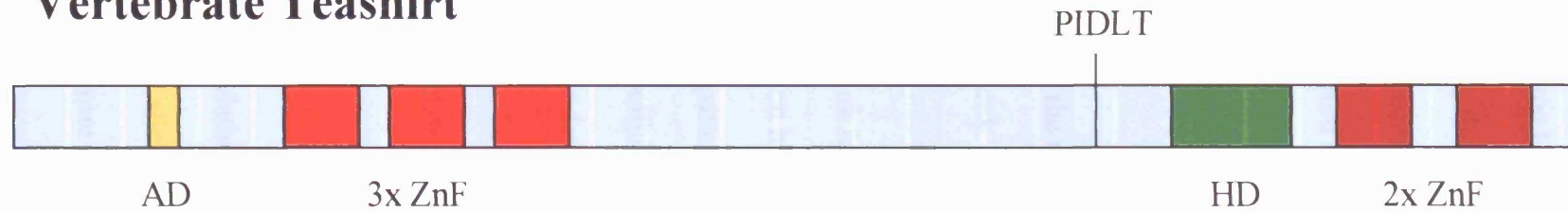
***Drosophila* Teashirt**



***Drosophila* Tiptop**



**Vertebrate Teashirt**



Despite a high degree of divergence between *Drosophila* and vertebrate genes “conservation of function” has been demonstrated, because each of the three mouse *Teashirt* genes can rescue the developmental defects of a *Drosophila teashirt* loss-of-function mutant (when expressed during *Drosophila* embryogenesis using the *UAS Gal4* system), and ectopic expression of murine *Teashirt* genes produces similar abnormalities to ectopic expression of *Drosophila teashirt* (Manfroid et al., 2004).

### ***Teashirt gene functions in Drosophila***

The first reported role for *teashirt* in *Drosophila* was the development of the ventral trunk, as Teashirt expression was observed in the trunk and the ventral trunk developed abnormally in *teashirt* mutants (Fasano et al., 1991). *tsh* was subsequently identified as a homeotic gene responsible for specifying trunk identity (Roder et al., 1992; de Zulueta et al., 1994) and has been shown to function in parallel with homeotic-complex (HOM-C) proteins in anterior-posterior patterning of the embryo (Robertson et al., 2004). In addition to its general role in specifying ‘trunk fate’, *tsh* is required specifically for prothorac segment identity (Roder et al., 1992; Taghli-Lamalle et al., 2007). *tsh* has also been implicated in naked cell fate choice (absence of denticles) in the larval trunk (Gallet et al., 1998; Angelats et al., 2002).

In the *Drosophila* embryo *tsh* also plays a role in midgut development (Mathies et al., 1994; Staehling-Hampton and Hoffman, 1994; Waltzer et al., 2001; Saller et al., 2002) and is involved in the regulating salivary gland development (Andrew et al., 1994; Henderson et al., 1999; Myat et al., 2000).

*tsh* is required to specify the proximo-distal domain of the adult leg of *Drosophila melanogaster* (Erkner et al., 1999; Wu and Cohen, 2000) and analysis of behaviour of cell clones ectopically expressing *tsh* suggests that *tsh* expression contributes to differences in cell-cell adhesive properties between proximal and distal leg cells (Erkner et al., 1999). *tsh* has also been implicated in wing development; *tsh* has been proposed to play a role in specifying wing hinge structures (Azpiazu and Morata, 2000) and indeed, *aeroplane* mutants (a regulatory allele of *Teashirt*) display a defect in the hinge region of the wing, resulting in the proximal wing and haltere being fused to the body cuticle (Soanes and Bell, 2001; Soanes et al., 2001).

*tsh* has complex roles in eye development. *tsh* is expressed in the region of the early eye disc where the eye primordium will form (Bessa and Casares, 2005) and has been reported to be capable of inducing ectopic eyes (Pan and Rubin, 1998; Bessa and Casares, 2005). However, *tsh* can also suppress eye development, and has been proposed to have different functions in different parts of the eye, e.g. promoting eye development dorsally and suppressing it ventrally (Bessa et al., 2002; Singh et al., 2002). Bessa et al. (2002) report that *tsh* is expressed anterior to the morphogenetic furrow in the developing eye, and here it is required with other transcription factors to promote proliferation of presumptive eye cells and to block expression of late-acting transcription factors (Bessa et al., 2002).

Much less is known about the function of *tiptop* than that of *teashirt*. *tiptop* is expressed in many of the same places as *teashirt* including the trunk epidermis and the midgut visceral mesoderm. However *tiptop* mutants are viable and fertile,

showing that *tiptop* does not have functions that are essential for survival. However, *tiptop* mutants that have the *teashirt* function reduced by RNAi, have a stronger phenotype in the trunk than do *teashirt* mutant embryos, revealing a function for *tiptop* in patterning of the trunk (Laugier et al., 2005). It therefore appears that *teashirt* and *tiptop* have some redundant functions in the development of *Drosophila melanogaster*, but that *teashirt* also has non-redundant functions.

#### *Teashirt genes and the Malpighian tubule*

In addition to the diverse roles of *teashirt* and *tiptop* discussed above, these genes are also important for the development of the renal (Malpighian) tubules of *Drosophila melanogaster*. The Malpighian tubules (MpT; of which there are four) are made up of two epithelial cell types; the principal cells and the stellate cells. The principal cells are derived from an ectodermal primordium at the junction between the hindgut and the midgut, whereas the stellate cells are derived from a subpopulation of the visceral mesoderm (Denholm et al., 2003; Barry Denholm, Nan Hu and Helen Skaer, University of Cambridge, personal communication). Denholm et al. (2003) showed that during development this subset of visceral mesodermal cells remained associated with the MpTs as the caudal visceral mesodermal cells migrated forward. The tubule-associated cells subsequently undergo mesenchymal to epithelial transition (MET) and integrate into the MpTs between the principal cells. The observation that MET occurs in *Drosophila* nephrogenesis provides a striking parallel between the development of the apparently dissimilar renal systems of *Drosophila* and vertebrates, as the nephrons of the mammalian kidney are derived from metanephric mesenchyme that has undergone MET. Furthermore, Denholm et al. (2003) showed that the stellate cells express *Teashirt*, and thus *Teashirt* may be required for the

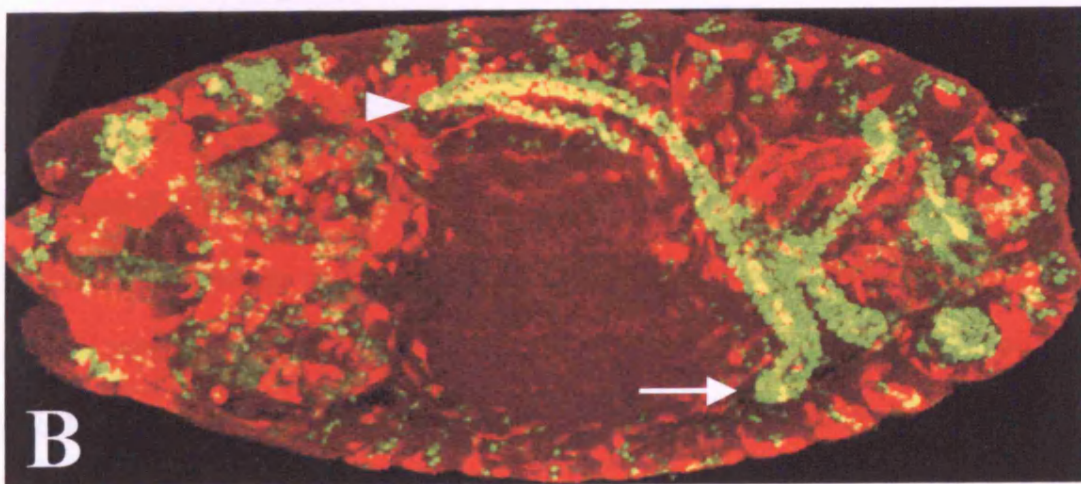
MET of stellate cells and their integration into the MpTs. Subsequently Laugier et al. (2005) showed that Tiptop is also expressed in the developing MpTs, and this has been verified by Nan Hu, Barry Denholm and Helen Skaer (personal communication) who observed that Tiptop is initially expressed by the principal cells, and later is co-expressed with Teashirt by the stellate cells (Figure 1.2 A). Recent evidence (Nan Hu, Barry Denholm and Helen Skaer, personal communication) suggests that Teashirt and Tiptop act redundantly to promote MpT elongation and stellate cell integration. Although tubule elongation and stellate cell integration occur normally in both *teashirt* and *tiptop* null mutants, when *teashirt* function is reduced by RNAi in *tiptop* null mutant embryos a reduction in the number of stellate cells in the MpTs is observed, and this is associated with abnormal MpT elongation (Figure 1.2 B). Therefore, in *Drosophila*, the *teashirt* family genes are required for renal system (MpT) development: specifically for the proper elongation of MpTs and to promote stellate cell integration (perhaps through the regulation of the occurrence of MET).

## Figure 1.2 *teashirt* genes and Malpighian tubule development

**A** A stage 16 wildtype embryo stained with anti-Tio (green) and anti-Tsh (red) antibodies. Note the stellate cells (arrowheads) of the Malpighian tubule co-express Tsh and Tio (appearing yellow), whereas the tip cell of the Malpighian tubule (arrow) expresses Tio but not Tsh. **B** A stage 16 *tiptop* null mutant embryo that has been injected (from the side) with *teashirt* RNAi (dorsal view). The development of the anterior Malpighian tubule on the injected side (arrow) is affected; it is shorter and contains fewer (yellow) stellate cells than the other unaffected anterior Malpighian tubule (arrowhead). Malpighian tubules are stained green (using an anti-Cut antibody), whilst stellate cells appear yellow as they express Cut and also are stained red with an anti- $\beta$ -galactosidase antibody (G447.2-GAL4 driving UAS-lacZ).

*Figure kindly supplied by Nan Hu, Barry Denholm and Helen Skaer, prior to publication.*

**Figure 1.2 - *Teashirt* genes and Malpighian tubule development**



## ***Teashirt gene functions in vertebrates***

### *Expression studies*

The first published data on vertebrate *Teashirt* expression patterns described the global expression of two *Teashirt* genes during mouse development (Caubit et al., 2000). *mTshz1* transcripts were first detected at E9-9.5 and are present in the neural tube, in some somites, a region of the foregut, the first and second branchial arches and the mesenchyme of the forelimb bud. *mTshz2* transcripts were first detected at E9-9.5 in the mesenchyme of the forelimb bud, and later expression was also seen in some somites and in the hindgut, neural tube and whisker pads. These expression patterns are consistent with a possible role for these transcription factors in the specification of anterior-posterior identity along the primary axis, and in the control of limb development (Caubit et al., 2000). The expression of *mTshz3* has not been reported in detail, but has been noted to be similar, though not identical, to *mTshz1* (Manfroid et al., 2004).

*mTshzs* have since also been reported as being expressed in the developing and adult forebrain (Caubit et al., 2005). *mTshz1-3* have overlapping but distinct spatiotemporal expression patterns in the diencephalon, telencephalon and olfactory bulb. The major changes in expression levels were observed to coincide with compartmental boundaries leading to the speculation that *mTshzs* are required for the establishment of regional identity and specification of cell types in the developing forebrain (Caubit et al., 2005).

Long et al. (2001a) have investigated the reported expression of *mTshz1* in limb-buds and branchial arches in some detail using *in-situ* hybridisation. They report that



*mTshz1* is predominately expressed in the mesenchyme of these structures, and that this expression is (at least to some extent) dependent on the presence of the overlying epithelium.

An expression study in chick has also lead to the speculation that *cTshz3* (orthologue of *mTshz3*) is involved in the development of tendons. *cTshz3* is expressed in the syndetome of somites, which is a compartment composed of tendon progenitors (Manfroid et al., 2006). *cTshz3* is also expressed at other sites during chick development including the neural tube, lateral mesoderm, a region of the foregut, the limb-bud mesenchyme and branchial arches, the smooth muscle of the gizzard and intestine, the condensing mesenchyme of the forming cartilage, the feather anlagen and the lung. Considering its wide expression pattern *cTshz3* is likely to have diverse roles during chicken development, and many of these roles are likely to be conserved in mouse development (as *mTshz3* has a similar expression pattern).

The reported expression of *zTshz1* in zebrafish in the spinal cord, pectoral fins and dorsal forebrain (Wang et al., 2007), is also reminiscent of the *mTshz* expression patterns and provides evidence that *Tshz* genes might have conserved functions in vertebrate development.

It is important to note that despite the accumulating data on the expression of *Teashirt* genes in vertebrates, no information on *Teashirt* expression in the urinary tract of any vertebrate was available in the literature at the time of writing this thesis.

### *Functional studies*

The analysis of the *mTshz1* null mouse (Core et al., 2007) provided functional evidence for a homeotic role of mouse *Teashirt* genes, which had previously been speculated based on expression patterns, the known homeotic role of *Teashirt* in *Drosophila*, and apparent functional conservation (Caubit et al., 2000; Manfroid et al., 2004). Homozygous null *mTshz1*<sup>-/-</sup> mice have abnormalities in the development of the axial skeleton, particularly in the cervical vertebrae (Core et al., 2007).

*mTshz1* is expressed in the sclerotome of the somites (which gives rise to future vertebrae), suggesting that *mTshz1* is required in the sclerotome to allow for the correct specification of future vertebrae, in particular the identity of the second cervical vertebra (C2) (Core et al., 2007). *mTshz1*<sup>-/-</sup> mice also have abnormalities in the soft palate and middle ear, suggesting that *mTshz1* is required during the development of structures in which epithelial-mesenchymal interactions play an important role (Core et al., 2007).

*Xenopus* studies have also been important in beginning to define the roles of the *Teashirt* family of genes in the regulation of vertebrate development. *Xenopus* morpholino and overexpression studies have revealed that *XTshz1* is involved in the specification of the hindbrain and the midbrain/hindbrain boundary, as well as in determination of cranial neural crest cell identity. Therefore, in *Xenopus*, *XTshz1* appears to have at least two functions during development, i.e. determining positional identity along the anterior-posterior axis and control of segmental migration of cranial neural crest cells (Koebernick et al., 2006). Meanwhile, *XTshz3* has been shown to play an essential role in dorsal determination and possibly also in anterior-posterior patterning (Onai et al., 2007).

### *Teashirt Genes – Genetic and biochemical interactors*

A number of genes have been shown to interact with *Teashirt* genes. Further, *Teashirt* proteins have been shown to bind to a number of different proteins, prompting the idea that *Teashirt* might act in a protein complex(es). Details of these interactions can be seen in Figure 1.3 and Tables 1.1.1, 1.1.2 and 1.1.3), and are important when considering how *Teashirt* genes may be involved in regulatory genetic pathways that control urinary tract development (see Discussion).

### ***Why study Teashirt genes in developing mouse urinary tracts?***

From the discussion of *Teashirt* gene functions above, it is clear that this gene family has multiple functions in the development of many different species of animal.

Whilst some of these functions are likely only to be relevant to particular species (for example wing development), other functions (such as the role of *Teashirt* genes in the patterning of the anterior posterior axis of the embryo) appear to be conserved.

Indeed, *mTshz* genes have been shown to be functionally conserved with *dTsh* (at least in the context of the development of the *Drosophila* trunk) (Manfroid et al., 2004).

### **Figure 1.3 *Teashirt* interactors**

A diagram to illustrate proteins that physically interact with *Teashirt* (double arrowhead) and signalling factors/genes that are upstream and downstream of *Teashirt* genes. Arrowheads depict positive interactions, whilst flat arrowheads depict inhibition. This diagram summarises information presented in Tables 1.2.1, 1.2.2 and 1.2.3. Species in which interaction has been shown for each gene/protein is shown in brackets: C – chicken; M – mouse; Z – zebrafish; D – *Drosophila*; X; *Xenopus*. Where genes/proteins are referred to in abbreviated form, please refer to the list of abbreviations at the beginning of this thesis.

## Figure 1.3 - *Teashirt* interactors

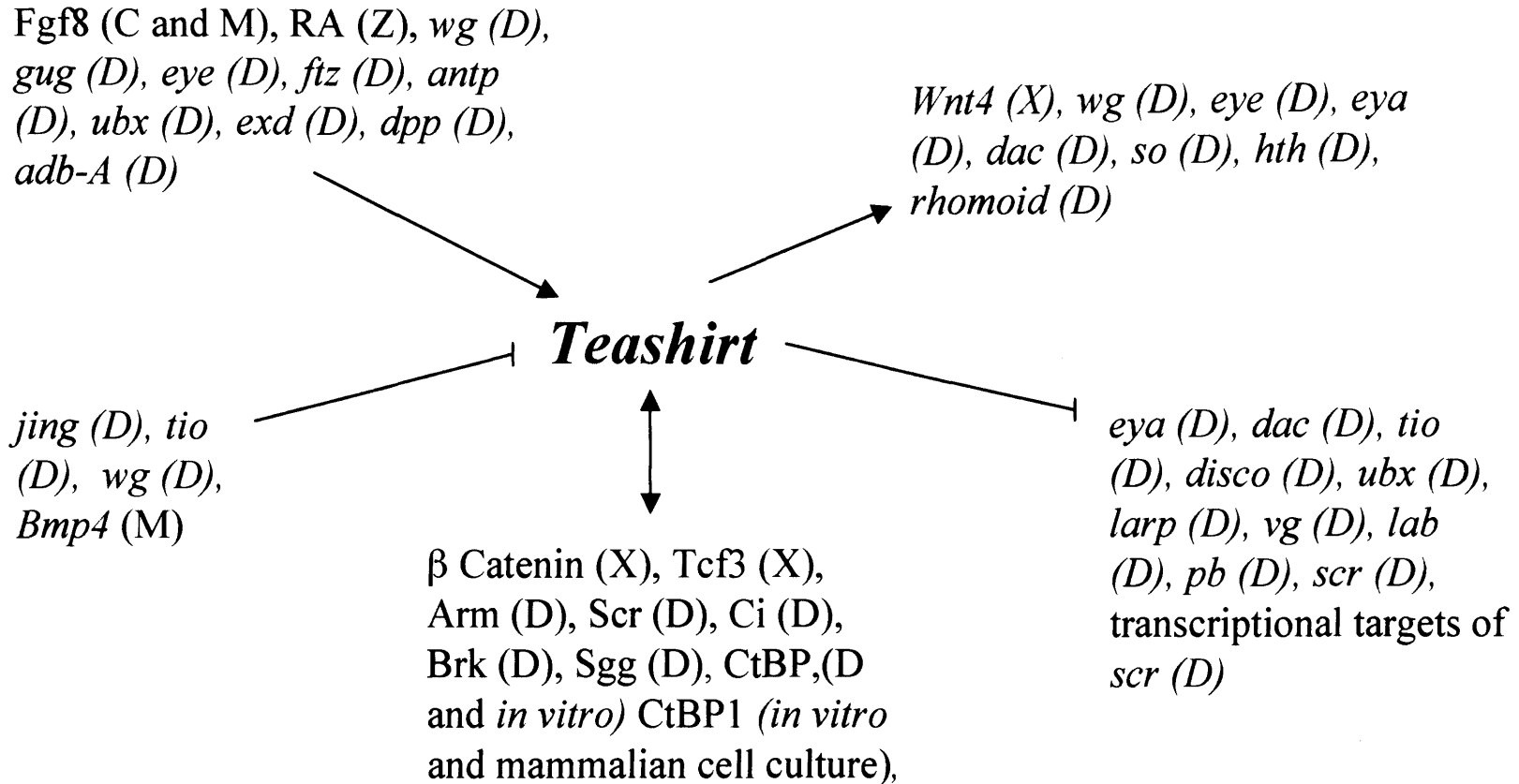


**Table 1.1.1 Molecules that physically interact with Teashirt**

<b>Tsh</b>	<b>Domain of Tsh involved in interaction (and consequences of interaction)</b>	<b>Interacts with</b>	<b>Species/context</b>	<b>Experimental evidence</b>	<b>Reference</b>
XTshz3	amino-terminal (increased nuclear localisation of $\beta$ catenin)	$\beta$ catenin (downstream effector of Wnt signalling pathway)	<i>Xenopus</i> / dorsal axis determination	Co-immunoprecipitation. Additionally, injection of XTshz3 transcripts increases nuclear $\beta$ -catenin whilst injection of XTshz3 morpholino reverses nuclear localisation of $\beta$ -catenin in response to Wnt1.	(Onai et al., 2007)
XTshz3	carboxy terminal	Transcription factor 3 (Tcf3, a DNA binding protein downstream effector of Wnt signalling pathway)	<i>Xenopus</i> / dorsal axis determination	Co-immunoprecipitation.	(Onai et al., 2007)
dTsh	acidic domain	Sex Combs Reduced (Scr, a HOM-C/Hox protein)	<i>Drosophila melanogaster</i> / prothorax	Yeast two hybrid.	(Taghli-Lamalle et al., 2007)
dTsh	PLDLS motif	C-terminal binding protein (CtBP, a transcriptional corepressor)	<i>in vitro</i>	GST pulldown assay. Deletion of PLDLS motif prevents this binding.	(Manfroid et al., 2004)

mTsh1, 2 and 3	PIDLT motif	C-terminal binding protein1 (CtBP1)	<i>in vitro</i> and in mammalian cell culture	GST pulldown assays. Deletion of PIDLT motif affects levels of repressive activity demonstrated by mTsh1 in MDCK cells.	(Manfroid et al., 2004)
dTsh	Not reported	Cubitus interruptus (Ci, transcription factor downstream of Hedgehog signalling)	<i>Drosophila melanogaster</i> /trunk	GST pulldown assay and Co-immunoprecipitation (hyperphosphorylated dTsh and Ci).	(Angelats et al., 2002)
dTsh	Not reported	Brinker (Brk, a DNA binding transcriptional repressor)	<i>Drosophila melanogaster</i> /midgut	GST pulldown assay.	(Saller et al., 2002)
dTsh	Not reported	C-terminal binding protein (CtBP)	<i>Drosophila melanogaster</i> /midgut	GST pulldown assay.	(Saller et al., 2002)
dTsh	(promotion of phosphorylation and nuclear accumulation of dTsh)	Armadillo (Arm, <i>Drosophila</i> $\beta$ catenin), C-terminal end	<i>Drosophila melanogaster</i> /trunk (naked cell fate choice)	Co-immunoprecipitation (hypophosphorylated dTsh with Arm) and GST pulldown assays.	(Gallet et al., 1999)
dTsh	Not reported	Shaggy (Sgg, a serine/threonine kinase, which promotes degradation of Arm in the absence of Wg signalling)	<i>Drosophila melanogaster</i> /trunk (naked cell fate choice)	Co-immunoprecipitation.	(Gallet et al., 1999)

dTsh	Not reported	Armadillo (Arm)	<i>Drosophila melangaster</i> / trunk (naked cell fate choice)	Co-immunoprecipitation and GST pulldown assays.	(Gallet et al., 1998)
------	--------------	-----------------	--	--	--------------------------



**Table 1.1.2 Genes that are genetically downstream of *Teashirt***

<b><i>Tsh</i></b>	<b>Type of interaction</b>	<b>Interacts with</b>	<b>Species/ context</b>	<b>Experimental evidence</b>	<b>Reference</b>
<i>XTshz1</i>	induces	<i>Wnt4</i>	<i>Xenopus</i> / brain and spinal cord	<i>Wnt4</i> expression is reduced in <i>XTshz1</i> morphants.	(Koebernick et al., 2006)
<i>dtsh</i>	induces	<i>eyeless (eye)</i> (and <i>eyes-absent</i> , <i>eya</i> and <i>dacshund</i> , <i>dac</i> , when dpp [a TGF $\beta$ ] signalling is also present)	<i>Drosophila melanogaster</i> / larval eye disc	Ectopic expression of <i>dtsh</i> in disc regions that are usually destined to form head capsule causes ectopic expression of <i>eye</i> (and also <i>eya</i> and <i>dac</i> in regions where dpp signalling is present).	(Bessa and Casares, 2005)
<i>dtsh</i>	represses	<i>tiptop (tio</i> , a teashirt family gene)	<i>Drosophila melanogaster</i> / anterior-posterior patterning of early embryo	Ectopic expression of <i>tio</i> in the trunk of <i>dtsh</i> null embryos. Ectopic expression of <i>dtsh</i> represses <i>tio</i> expression.	(Laugier et al., 2005)
<i>dtsh</i>	represses	<i>disconnected (disco</i> , which encodes a zinc-finger transcription factor)	<i>Drosophila melanogaster</i> / trunk	<i>disco</i> is misexpressed in the trunk in <i>dtsh</i> null embryos.	(Robertson et al., 2004)
<i>dtsh</i>	represses	<i>ultrabithorax (ubx</i> , a <i>Hox</i> gene)	<i>Drosophila melanogaster</i> / midgut	Overexpression of <i>dtsh</i> throughout mesoderm causes downregulation of <i>ubx</i> in mesoderm (anterior to the midgut constriction).	(Saller et al., 2002)

<i>dtsh</i>	represses (in collaboration with <i>eyeless</i> , <i>eye</i> , and <i>homothorax</i> , <i>hth</i> )	<i>eyes-absent (eya)</i> and <i>dacshund (dac)</i>	<i>Drosophila melanogaster/eye</i> (domain anterior to morphogenetic furrow)	Clone experiments show that simultaneous expression of <i>tsh</i> , <i>hth</i> and <i>eye</i> efficiently repress <i>eya</i> and <i>dac</i> .	(Bessa et al., 2002)
<i>dtsh</i>	induces	<i>homothorax (hth, a Hox gene)</i>	<i>Drosophila melanogaster/Suppression of eye development</i>	Ectopic expression of <i>dtsh</i> induces <i>hth</i> expression.	(Singh et al., 2002)
<i>dtsh</i>	represses	<i>ultrabiothorax (ubx, a Hox gene)</i> and <i>labial (lab, a Hox gene)</i>	<i>Drosophila melanogaster/embryonic midgut</i>	<i>ubx</i> and <i>lab</i> expression domains are expanded in <i>dtsh</i> null embryos.	(Waltzer et al., 2001)
<i>dtsh</i>	induces	<i>rhomoid</i> (which encodes a component of EGF receptor)	<i>Drosophila melanogaster/trunk</i>	<i>rhomoid</i> expression is missing from the epidermis of <i>dtsh</i> null embryos.	(Gallet et al., 2000)
<i>dtsh</i>	induces	<i>wingless (wg, which encodes a Wnt extracellular signalling protein)</i>	<i>Drosophila melanogaster/trunk</i>	<i>wg</i> expression is downregulated in <i>dtsh</i> null embryos.	(Gallet et al., 2000)
<i>dtsh</i>	represses	<i>proboscipedia (pb, a Hox gene)</i>	<i>Drosophila melanogaster/trunk</i>	<i>dtsh</i> null embryos display weak ectopic expression of <i>pb</i> in the first thoracic segment.	(Rusch and Kaufman, 2000)
<i>dtsh</i>	Represses	<i>la-related protein (larp, which encodes a protein of unknown function)</i>	<i>Drosophila melanogaster/trunk</i>	<i>dtsh</i> deficient embryos have ectopic expression of <i>larp</i> in the ectoderm of parasegment three.	(Chauvet et al., 2000).



<i>dtsh</i>	represses (in collaboration with <i>Homothorax</i> , <i>Hth</i> )	<i>vestigial</i> ( <i>vg</i> , which encodes a transcription factor)	<i>Drosophila melanogaster</i> / wing hinge	<i>hth</i> expression is induced, and <i>vg</i> repressed, in clones of cells ectopically expressing <i>dtsh</i> .	(Casares and Mann, 2000)
<i>dtsh</i>	induces	<i>eyeless</i> ( <i>eye</i> ), <i>sine oculis</i> ( <i>so</i> ), <i>dacshund</i> ( <i>dac</i> ), <i>eyes absent</i> ( <i>eya</i> ) (all of which encode transcription factors)	<i>Drosophila melanogaster</i> / antennal imaginal discs	Gain of function <i>dtsh</i> mutations and ectopic expression of <i>dtsh</i> (under control of a heatshock promotor) induce ectopic eyes; this is associated with induction of <i>eye</i> , <i>dac</i> and <i>so</i> expression. Eye specific mutations in <i>eya</i> , <i>so</i> and <i>dac</i> suppress <i>dtsh</i> -induced ectopic eyes.	(Pan and Rubin, 1998)
<i>dtsh</i>	represses	<i>sex combs reduced</i> ( <i>scr</i> , a <i>Hox</i> gene)	<i>Drosophila melanogaster</i> / salivary gland	In <i>dtsh</i> null embryos <i>scr</i> is ectopically expressed (in parasegment three).	(Andrew et al., 1994)
<i>dtsh</i>	represses	Transcriptional targets of <i>sex combs reduced</i> ( <i>scr</i> )	<i>Drosophila melanogaster</i> / salivary gland	In <i>dtsh</i> null embryos, ectopic expression of <i>scr</i> (under the control of a heat-shock promotor) can induce <i>dCREB-A</i> expression (in parasegments three to thirteen).	(Andrew et al., 1994)
<i>dtsh</i>	represses	<i>labial</i> ( <i>lab</i> )	<i>Drosophila melanogaster</i> / trunk	In <i>dtsh</i> homozygotic null embryos <i>lab</i> is ectopically expressed (in parasegments four to thirteen).	(Roder et al., 1992)

**Table 1.1.3 Genes that are genetically upstream of *Teashirt***

<b>Tsh</b>	<b>Type of interaction</b>	<b>Interacts with</b>	<b>Species/ context</b>	<b>Experimental evidence</b>	<b>Reference</b>
<i>zTshz1</i>	induced by	Retinoic acid (a signalling molecule produced by vitamin A metabolism)	Zebrafish/ brain and spinal cord	Exogenous retinoic acid causes ectopic <i>zTshz1</i> expression. <i>zTshz1</i> is downregulated in <i>neckless</i> mutants (missense mutation in <i>Raldh2</i> , which is required for retinoic acid synthesis).	(Wang et al., 2007)
<i>cTshz3</i>	induced by	Fibroblast Growth Factor 8 (Fgf8)	Chick/ somites of trunk	Fgf8 coated beads implanted into trunk somites cause upregulation of expression of <i>cTshz3</i> .	(Manfroid et al., 2006)
<i>dtsh</i>	repressed by	<i>jing</i> (which encodes a zinc-fingered transcription factor)	<i>Drosophila melanogaster</i> / small domain of wing-disc that will give rise to alula	Ectopic expression of <i>dtsh</i> in <i>jing</i> negative clones.	(Culi et al., 2006)
<i>dtsh</i>	repressed by	<i>tiptop (tio)</i>	<i>Drosophila melanogaster</i> / Anterior-posterior patterning of early embryo	<i>dtsh</i> is ectopically expressed in the clypeolabrum of <i>tio</i> homozygotic null embryos. Ectopic expression of <i>tio</i> represses <i>dtsh</i> expression.	(Laugier et al., 2005)
<i>dtsh</i>	repressed by	wingless (wg) signalling	<i>Drosophila melanogaster</i> / wing hinge in larvae	<i>dtsh</i> is ectopically expressed in <i>arrow</i> (wg co-receptor) negative clones and clones expressing dominant-negative dTCF.	(Zirin and Mann, 2004)

<i>mTshz1</i>	induced by	Fibroblast Growth Factor 8 (Fgf8)	Mouse/ limb buds and branchial arches	Fgf8 coated beads implanted into limb-buds and branchial arches cause upregulation of expression of <i>mTshz1</i> .	(Long et al., 2001a)
<i>mTshz1</i>	repressed by	Bone Morphogenetic Protein 4 (Bmp4, a TGFβ signalling protein)	Mouse/ limb buds and branchial arches	Bmp4 coated beads implanted into limb-buds and branchial arches cause downregulation of expression of <i>mTshz1</i> .	(Long et al., 2001a)
<i>dtsh</i>	induced by	<i>grunge</i> ( <i>gug</i> , which encodes an Atrophin-like protein which localises to the nucleus)	<i>Drosophila melanogaster</i> / leg (proximo-ventral domain)	<i>dtsh</i> expression is downregulated in <i>gug</i> negative clones.	(Erkner et al., 2002)
<i>dtsh</i>	downstream of	wingless ( <i>wg</i> ) signalling	<i>Drosophila melanogaster</i> / embryonic midgut	When <i>wg</i> or constitutively active <i>arm</i> are overexpressed in a <i>dtsh</i> homozygotic null embryo, <i>ubx</i> is not repressed (usually <i>ubx</i> is repressed by ectopic <i>wg</i> signalling).	(Waltzer et al., 2001)
<i>dtsh</i>	induced by	<i>eyeless</i> ( <i>eye</i> )	<i>Drosophila melanogaster</i> / antennal imaginal discs	<i>dtsh</i> expression is induced by ectopic <i>eye</i> expression (which also leads to ectopic eye formation).	(Pan and Rubin, 1998)
<i>dtsh</i>	induced by	<i>fushi-tarazu</i> ( <i>ftz</i> , a “pair rule” gene that encodes a transcription factor)	<i>Drosophila melanogaster</i> / Even numbered segments	<i>dtsh</i> is downregulated in <i>Ftz</i> homozygotic null embryos. <i>dtsh</i> is expressed ectopically when <i>ftz</i> is expressed ubiquitously. <i>Ftz</i> protein can bind to a Tsh enhancer sequence <i>in vitro</i> .	(Core et al., 1997)
<i>dtsh</i>	induced by	<i>antennapedia</i> ( <i>antp</i> , a Hox gene)	<i>Drosophila melanogaster</i> / trunk	In <i>antp</i> null embryos <i>dtsh</i> expression is downregulated in the thoracic epidermis.	(McCormick et al., 1995)
<i>dtsh</i>	induced by	<i>ultrabithorax</i> ( <i>ubx</i> )	<i>Drosophila melanogaster</i> / trunk	In <i>ubx</i> null embryos <i>dtsh</i> expression is downregulated in the abdominal mesoderm.	(McCormick et al., 1995)

<i>dtsh</i>	induced by	<i>extradenticle (exd, a Hox gene)</i>	<i>Drosophila melanogaster</i> / midgut visceral mesoderm	<i>dtsh</i> expression is absent in midgut of embryos lacking <i>exd</i> .	(Rauskolb and Wieschaus, 1994)
<i>dtsh</i>	induced by	<i>decapentaplegic (dpp, which encodes a TGFβ signalling protein)</i>	<i>Drosophila melanogaster</i> / midgut visceral mesoderm	Ectopic expression of <i>dpp</i> in the visceral mesoderm induces ectopic expression of <i>dtsh</i> .	(Stahling-Hampton and Hoffmann, 1994)
<i>dtsh</i>	induced by	<i>antennapedia (antp), ultrabithorax (ubx), abdominal A (adb-A, a Hox gene), wingless (wg) and decapentaplegic (dpp)</i>	<i>Drosophila melanogaster</i> / midgut visceral mesoderm	<i>dtsh</i> expression is downregulated in <i>antp</i> mutants. <i>dtsh</i> expression is lost in some cells of the visceral mesoderm in <i>antp/ubx</i> double mutants. <i>dtsh</i> expression is lost in cells around the middle midgut constriction in <i>adb-A</i> mutants. <i>dtsh</i> expression is reduced in embryos that lack Dpp in the central midgut. <i>dtsh</i> expression is absent in the central midgut in temperature sensitive <i>wg</i> mutants.	(Mathies et al., 1994)

Both *teashirt* and *tiptop* are expressed in the Malpighian tubules of *Drosophila melanogaster* during embryonic development (Denholm et al., 2003; Laugier et al., 2005) and appear to be involved in regulating their development (Barry Denholm, Nan Hu and Helen Skaer, personal communication). Despite the lack of structural similarity between the vertebrate urinary tract and the Malpighian tubules of *Drosophila*, epithelial-mesenchymal interactions are required for the development of both (Denholm et al., 2003). Thus, it is an attractive possibility that *Teashirt* genes are involved in the development of both of these somewhat dissimilar renal systems. Indeed *Teashirt* genes have been implicated in the development of other mouse tissues that require epithelial-mesenchymal interactions for their development, such as the middle ear, soft palate, limb-buds and branchial arches (Long et al., 2001a; Core et al., 2007) and is expressed at a number of sites where epithelial-mesenchymal interactions are known to occur in chick including the feather anlagen, limb-buds, branchial arches and the lung (Manfroid et al., 2006). Therefore *Teashirt* genes may have conserved roles in regulating epithelial-mesenchymal interactions in the development of diverse tissues in different species. Furthermore, *Larp* (whose expression is regulated by *teashirt* in *Drosophila*) is expressed in mouse in developing organs where epithelial-mesenchymal interactions occur, including the kidney (Chauvet et al., 2000). Investigation of the role of *Teashirt* genes in the development of the urinary tract of mice, and the role of *teashirt* genes in the development of Malpighian tubules of *Drosophila melanogaster*, may well cast light on the question of whether *Teashirt* genes have conserved functions in the regulation of mesenchymal-epithelial interactions during development in addition to possibly defining further specific roles of *Teashirt* genes in the development of animals. In this thesis I investigate the role of *Teashirt* genes

in the development of mouse urinary tracts through expression studies and phenotypic analysis. Meanwhile, the role of *teashirt* genes in the development of the Malpighian tubules of *Drosophila* is being further investigated in Helen Skaer's laboratory.

### **The development of the ureter**

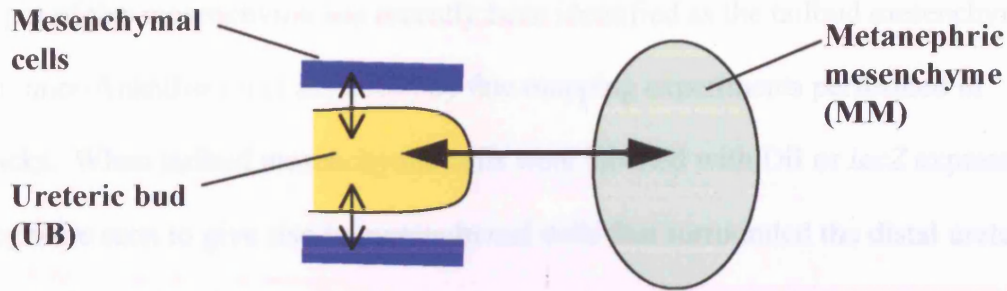
The control of ureter development has been attracting an increasing amount of attention over the past ten years, and the analysis of the renal phenotype in several mouse mutants has been particularly important in uncovering some of the genes involved regulating the development of this important tube (Airik and Kispert, 2007). It has become apparent from these studies that, as with kidney development, reciprocal signalling between the epithelial and mesenchymal components of the embryonic ureter are vital for its correct differentiation (Figure 1.4).



**Figure 1.4 Reciprocal signalling between epithelial and mesenchymal cell populations is required for kidney and ureter development**

Interactions between the metanephric mesenchyme and the ureteric bud are required for kidney development. Interactions between the stalk of the ureteric bud (i.e. the unbranched portion, that does not invade the metanephric mesenchyme) and the surrounding mesenchymal cells are required for the development of the ureter.

**Figure 1.4**

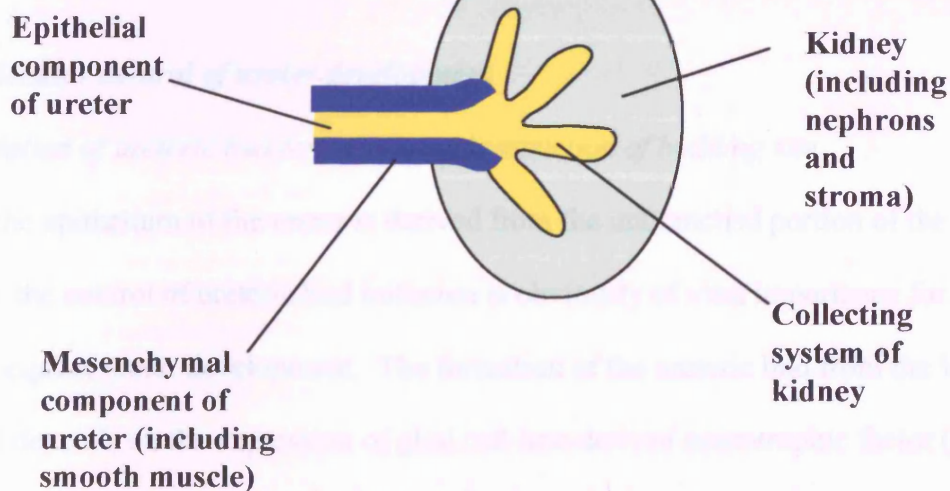


**Reciprocal signalling between UB stalk and the surrounding mesenchymal cells causes:**

1. Stalk of ureteric bud to differentiate into the specialised epithelium of the ureter.
2. The surrounding mesenchymal cells to condense and differentiate into the mesenchymal components of the ureter.

**Reciprocal signalling between UB and MM causes:**

1. UB tip to branch extensively and give rise to the collecting system.
2. Some cells of the MM to undergo mesenchymal-to-epithelial transition to give rise to nephrons



### ***Cell lineages in ureter development***

The ureter develops from the unbranched stalk of the ureteric bud (whereas the branched portion of the ureter bud gives rise to the collecting system of the kidney), which itself buds from the Wolffian duct, and the surrounding mesenchyme. The origin of this mesenchyme has recently been identified as the tailbud mesenchyme (Brenner-Anantharam et al., 2007) by fate mapping experiments performed in chicks. When tailbud mesenchymal cells were labelled with *DiI* or *lacZ* expression they were seen to give rise to mesenchymal cells that surrounded the distal ureteric bud stalk and the cloaca. These tailbud mesenchymal cells express bone morphogenetic protein 4 (*Bmp4*) and continue to express *Bmp4* after they come into contact with the distal ureteric bud stalk and cloaca. A similar *Bmp4* expression pattern is observed in mice, suggesting that the results of the cell lineage analyses performed in chick are also applicable to mammalian development. Data from Schmidt-Ott et al. (2006) suggest that the ureteral mesenchymal cells may not be derived entirely from the tailbud mesenchyme, as c-kit positive cells, which are thought to derive from a central population of mesenchyme ventral and lateral to the dorsal aorta, are also present in the mesenchymal cell layer of the developing ureter.

### ***Molecular control of ureter development***

#### ***Initiation of ureteric bud formation, and restriction of budding site***

As the epithelium of the ureter is derived from the unbranched portion of the ureteric bud, the control of ureteric bud initiation is obviously of vital importance for subsequent ureter development. The formation of the ureteric bud from the Wolffian duct depends on the expression of glial cell line-derived neurotrophic factor (*Gdnf*) in the metanephric mesenchyme, which signals to the cells of the Wolffian duct via

its receptors Ret (a tyrosine kinase receptor) and GdnfR $\alpha$  (Treanor et al., 1996), causing the ureteric bud to evert from the Wolffian duct (Moore et al., 1996; Pichel et al., 1996; Sanchez et al., 1996; Schuchardt et al., 1996; Sainio et al., 1997). The induction of the ureteric bud is tightly regulated to ensure that only one bud forms per Wolffian duct, and that the bud forms at the correct position. Failure of this regulation can lead to severe malformations of the kidney and urinary tract including ectopic and duplicated ureters (Ichikawa et al., 2002). As the formation of the ureteric bud is dependent upon Gdnf signalling, the site of its formation is dependent in part upon the expression domain of Gdnf. *Foxc1* homozygous mutants have double ureters (and duplex kidneys) due an expansion of the normal Gdnf expression domain, suggesting that *Foxc1* normally acts to limit Gdnf expression (Kume et al., 2000). *Slit2* and *Robo2* (which encode a ligand, and one of its receptors, respectively) have also been shown, by analysis of knockout mice, to be required to limit the Gdnf expression domain and restrict the site of formation of the ureteric bud so that only one ureteric bud grows from each Wolffian duct (Grieshammer et al., 2004).

Although it is clear that the expression domain of Gdnf is important for controlling the site of ureteric bud formation, Gdnf (and Ret) have fairly wide expression domains, so other molecules must also play a role in the regulation of the ureteric bud budding site (Ichikawa et al., 2002). Several genes encode molecules that have been shown to have such a role. For example, *Sprouty1*, which encodes a receptor tyrosine kinase antagonist: homozygous null *Sprouty1* mice have multiple ureters and multiplex kidneys due to multiple ureteric buds being induced as a result of a lack of antagonism of Gdnf/Ret signalling in the Wolffian duct (Basson et al., 2005).

Bmp4 has also been proposed to restrict the site of ureteric bud formation through the inhibition of Gdnf/Ret signalling (Ichikawa et al., 2002). In conclusion, Gdnf signalling from the metanephric mesenchyme to the Wolffian duct is essential for the initiation of the ureteric bud (and thus for ureter development), but regulation of this signalling is also crucial to ensure that only two ureters form.

#### *Development of the epithelium and mesenchyme of the ureter*

As previously mentioned, interaction between epithelial and mesenchymal components of the ureter are essential for its development. Yu et al. (2002) demonstrated that sonic hedgehog (Shh), which is expressed in the ureteric epithelium, is important for the control of proliferation and differentiation of the ureteric mesenchymal cells. Conditional *Shh* mutant mice, in which *Shh* was genetically deleted in the epithelium of the renal tract, have a delay in the development of the smooth muscle layer of the ureter and an absence of the ureteral stromal cell layer (Yu et al., 2002). Somewhat paradoxically the authors show that Shh acts to inhibit smooth muscle differentiation in the ureter and promotes proliferation of the ureteric mesenchymal cells. However, this is explained by their finding that Shh induces the expression of Bmp4 in the ureter (Yu et al., 2002), which has been shown (in other studies) to be important for the development of ureteric smooth muscle. Bmp4 is expressed in ureteric mesenchyme, initially uniformly and later exclusively in the smooth muscle layer (Miyazaki et al., 2000; Miyazaki et al., 2003). *Bmp4* null heterozygotes have a reduced number of alpha smooth muscle actin ( $\alpha$ SMA)-positive cells in their ureters (Miyazaki et al., 2003) and treatment of cultured kidneys and ureters with Bmp4 leads to enhanced  $\alpha$ SMA expression (Raatikainen-Ahokas et al., 2000). Furthermore, addition of Bmp4 to

kidney culture can cause ectopic expression of  $\alpha$ SMA within the kidney, and cause the branched portions of the ureteric buds to express uroplakin, which is a characteristic of urothelial development (Brenner-Anantharam et al., 2007). Therefore Bmp4 appears to promote ureteral differentiation both within the mesenchymal and epithelial cell populations. Thus, as well as its role in ureteric smooth muscle development, Bmp4 is a good candidate for a signalling factor responsible for mesenchymal-to-epithelial communication during ureter development. The exact mechanisms by which Bmp4 promotes smooth muscle and urothelial development are unknown, but Bmp4 has been shown to promote the condensation (increased cell density) of ureteral mesenchymal cells in culture (mesenchymal cells accumulate and form several layers surrounding Bmp4-coated beads), and Boyden chamber assays demonstrate that Bmp4 is a chemoattractant for ureteric mesenchymal cells (Miyazaki et al., 2003). Thus Bmp4 may function to bring smooth muscle precursor cells close together, and close to the urothelium, to allow their subsequent differentiation (Miyazaki et al., 2003). Whilst Bmp4 certainly appears to be important for the development of the ureter, particularly the smooth muscle, it is important to note that if Bmp4 function is lost in mice after E12.5 (using a tamoxifen-inducible Cre-lox system), the ureter develops normally (Brenner-Anantharam et al., 2007). As ureteric smooth muscle does not begin to differentiate until approximately E15 (Yu et al., 2002), it seems certain that other factors must be important for ureteric smooth muscle differentiation, and that Bmp4 controls earlier aspects of ureteral development (such as proliferation and condensation of mesenchymal cells).

The *T-box 18 (Tbx18)* homozygous null mouse also has abnormal ureter development, specifically a failure of the differentiation of the urothelium and the ureteric smooth muscle (Airik et al., 2006). *Tbx18* is expressed in the ureteric mesenchymal cells and is required for the condensation of these cells around the urothelium (Airik et al., 2006). Additionally the rate of proliferation is reduced in both the epithelial and mesenchymal compartments in *Tbx18* homozygous null mice. The expression of *Patched1* (the Shh receptor) and *Bmp4* is downregulated in *Tbx18* homozygous null mice, and the lack of *Bmp4* along with the lower number of mesenchymal cells present in the mutant ureter (as some cells mislocalise to the periphery of the kidney) is the likely cause of both the failure of smooth muscle and urothelial development. Additionally, secreted frizzled related protein two (sFRP2) expression (a modulator of wingless-type MMTV integration site family member (Wnt) signalling) is downregulated in *Tbx18* mutant ureteral mesenchyme, which suggests that Wnt signalling may also be involved in ureter development.

Another gene shown to be involved in ureter development is *discs large homologue one (Dlgh1)*, which encodes a PDZ domain protein and is expressed in the epithelium and smooth muscle of the ureter (Mahoney et al., 2006). *Dlgh1* homozygous null mice do not have ureteric stromal (Raldh2 positive) cells and the circular smooth muscle layers are misaligned (longitudinally) leading to defects in peristaltic function (Mahoney et al., 2006). Additionally, these mice have short ureters (Mahoney et al., 2006; Iizuka-Kogo., 2007), probably as a result of decreased proliferation of urothelial cells (Iizuka-Kogo et al., 2007). Therefore *Dlgh1* is important for aspects of epithelial and mesenchymal development in the ureter. Importantly, the expression of Shh, *Patched1* and *Bmp4* is unaffected in *Dlgh1*<sup>-/-</sup>

ureters (Mahoney et al., 2006), suggesting that other regulatory networks are also important for ureteric development. Indeed Bush et al. (2006) identified candidate signalling-factors that may act *in vivo* to control ureteric development. In particular they identified factors that may regulate the development of ureteric smooth muscle; they found that *in vitro* epidermal growth factor (EGF) and other ligands of the epidermal growth factor receptor (EGFr), heparin binding EGF-like growth factor (HB-EGF) and transforming growth factor alpha (TGF $\alpha$ ), inhibited smooth muscle development, whilst phosphoinositide 3-kinase (PI3kinase)-dependent signalling promoted smooth muscle development (Bush et al., 2006). Also mutant mice lacking both *angiotensin receptor one a* (*Agtr1a*) and *angiotensin receptor one b* (*Agtr1b*) receptors have reduced (although not absent) ureteric smooth muscle postnatally (as assessed by thickness of the smooth muscle layer), implicating angiotensin signalling in the promotion of ureteric smooth muscle development (Miyazaki et al., 1998).

In conclusion several genes have been implicated in the regulation of ureter development and Shh and Bmp4 have been identified as signalling factors involved in epithelial-mesenchymal interactions during the development of this organ. Table 1.2.1 summarises the genes involved in the regulation of ureter development. Consideration of the literature allows for the conclusion that other signalling factors are also probably involved in ureter development.



**Table 1.2.1 Genes required for the development of the ureter**

<b>Gene</b>	<b>Expression</b>	<b>Function</b>	<b>Reference(s)</b>
<i>sonic hedgehog</i> ( <i>Shh</i> )	ureteric epithelium	Proliferation and differentiation of ureteric mesenchymal cells (in part through its ability to induce Bmp4 expression in the ureteric mesenchyme).	(Yu et al., 2002)
<i>bone morphogenetic protein four</i> ( <i>Bmp4</i> )	ureteric mesenchyme (initially uniformly, later in smooth muscle only)	Promotion of smooth muscle formation (possibly by promoting condensation of ureteric mesenchymal cells). Promotion of urothelial development.	(Miyazaki et al., 2000; Rattikainen-Ahokas et al., 2000; Miyazaki et al., 2003; Brenner-Anantharam et al., 2007)
<i>T-box 18</i> ( <i>Tbx18</i> )	ureteric mesenchymal cells	Differentiation of ureteric smooth muscle (possibly through promoting condensation of ureteric mesenchymal cells) and urothelium. Promotion of proliferation of ureteric (mesenchymal and epithelial) cells. Promotes expression of Ptch1, Bmp4 and sFRP2.	(Airik et al., 2006)
<i>Discs large homologue one</i> ( <i>Dlgh1</i> )	ureteric epithelium and ureteric smooth muscle	Alignment of circular smooth muscle. Ureteric stromal cell development. Promotion of ureteric elongation and proliferation of urothelial cells.	(Mahoney et al., 2006; Iizuka-Kogo et al., 2007)
<i>angiotensin 1 receptors</i> ( <i>Agtr1a</i> and <i>Agtr1b</i> )	not reported	Promotion of ureteric smooth muscle development.	(Miyazaki et al., 1998)

### *Ureteropelvic junction formation*

Unlike the bladder, the kidney is attached to the ureter from the beginning of its development. However, the ureteropelvic junction (UPJ) is an important component of the urinary tract and “obstruction” of the UPJ is a clinically important cause of hydronephrosis in humans (Han et al., 2006).

Several genes have been implicated in the development/maturation of the UPJ in mice. ADAMTS1 is an ADAM family protease and is expressed in urothelium of the UPJ (Shindo et al., 2000). *ADAMTS1*<sup>-/-</sup> null mice develop hydronephrosis that is associated with a thickening of the collagenous layer (which lies between the urothelium and the smooth muscle) at the UPJ. Therefore, ADAMTS1 is likely to be required for the remodelling of the fibrous layer in the development of the UPJ (Shindo et al., 2000). *Id2* encodes an inhibitor of basic helix-loop-helix transcription factors and is expressed in ureteric smooth muscle; and *Id2*<sup>-/-</sup> and *Id2*<sup>+/-</sup> mice develop hydronephrosis (Aoki et al., 2004). This hydronephrosis is associated with hypertrophic and irregular muscle (and alteration of expression of *Agtr1* and *Bmp4*) at the UPJ, indicating that *Id2* acts in a genetic network to control proper development of the UPJ (Aoki et al., 2004).

The role for angiotensin signalling via *Agtr1a* and *Agtr1b* in the development of the UPJ was first demonstrated by Miyazaki et al. (1998): they report that in mice lacking both *Agtr1a* and *Agtr1b* receptors the renal pelvis fails to form (associated with a postnatal reduction of proliferation of smooth muscle cells in the region that normally forms the pelvis), which leads to hydronephrosis. A similar phenotype is seen in mice in which a *Calcineurin* subunit gene (*Cnb1*) is ablated in the

mesenchyme of the developing urinary tract. In these mice the funnel shaped extension of the renal pelvis fails to develop, associated with a defect in pyeloureteral peristalsis and hydronephrosis (Chang et al., 2004). In conclusion, the development of the specialised UPJ is not very well understood, but several different genes have been implicated (and these are summarised in Table 1.2.2).

**Table 1.2.2 Genes required for ureteropelvic junction (or pelvic) development**

<b>Gene</b>	<b>Expression</b>	<b>Function</b>	<b>Reference</b>
<i>ADAMTS1</i>	urothelium of uteropelvic junction (UPJ)	Remodelling of fibrous layer of UPJ.	(Shindo et al., 2000)
<i>Id2</i>	ureteric smooth muscle	Required for appropriate development of smooth muscle at UPJ and for appropriate expression of <i>Agtr1</i> and <i>Bmp4</i> .	(Aoki et al., 2004)
<i>angiotensin 1 receptors (Agtr1a and Agtr1b)</i>	not reported	Required for proper development of pelvis, in particular to promote proliferation of pelvic smooth muscle cells post-natally.	(Miyazaki et al., 1998)
<i>Calcineurin subunit B, isoform one (Cnb1)</i>	ureteric and kidney mesenchyme and epithelia	Required for proper development of pelvis, in particular to promote proliferation of pelvic cells post-natally.	(Chang et al., 2004)

### *Vesicoureteric junction formation*

The junction between the ureter and the bladder forms during development by a complex process of morphogenesis, involving apoptosis of the common nephric duct (the part of the Wolffian duct that lies between the ureter and the urogenital sinus; the primitive bladder) and detachment of the ureters from the mesonephric duct to come into contact with the bladder wall. The ureters then “tunnel” through the bladder wall into the bladder trigone to form the vesicoureteric junction (Batourina et al., 2005). The vesicoureteric junction forms a valve mechanism, which is important to prevent retrograde flow of the urine from the bladder to the kidneys (so called “vesicoureteric reflux”) (Murawski and Gupta, 2006). Defects with vesicoureteric junction formation can lead to vesicoureteric reflux (when the flapvalve mechanism is defective), and even to hydroureter and hydronephrosis (if the vesicoureteric junction completely fails to form, causing a physical obstruction at the ends of the ureters) (Mackie and Stephens, 1975, Murawski and Gupta, 2006). Failure of the common nephric duct to apoptose (as occurs when vitamin A signalling is impaired in *Raldh2* deficient mice (Batourina et al., 2005)) prevents the vesicoureteric junction from forming, and the ureter will remain attached to the mesonephric duct or end blindly. Problems with vesicoureteric junction formation also occur when the ureteric bud (the stalk of which will form the ureter) branches from the mesonephric duct at an abnormal position. When this occurs, nephric duct apoptosis will not bring the ureter to the required position for its normal insertion into the bladder. It has been proposed that if the ureteric bud forms too cranially along the ureteric bud, the ureter will attach to the urethra, rather than to the bladder. If the ureteric bud develops more caudally than usual then the ureteric orifice will be situated in the

bladder, but lateral to the bladder trigone (Mackie and Stephens, 1975; Schwartz et al., 1981).

*Summary of ureter development*

In summary, the initial budding of the ureteric bud, communication between the epithelial and mesenchymal components of the ureter and the development of the ureteropelvic and vesicoureteric junctions are all vital aspects of ureter development, and each of these events requires careful regulation.

## Chapter Two – Materials and Methods

Reagents were obtained from Sigma-Aldrich Company Limited (Poole, UK) unless otherwise stated.

### Mice

A wildtype, outbred mouse strain, CD1 mice (Charles River Mouse Farms, Margate, UK) was used in experiments detailed in Chapters Three and Four. Mice were maintained at the UCL Institute of Child Health Animal Facility. Mice were killed by Home Office Schedule One approved methods.

A transgenic strain of mice, in which the majority of the *Tshz3* coding sequence has been replaced by a *lacZ* reporter construct was used in experiments detailed in Chapters Five, Six and Seven. These mice were generated by Xavier Caubit and Laurent Fasano (Institute of Developmental Biology Marseilles-Luminy, Marseilles, France) and were maintained on a CD1 background. Details of how these mice were generated can be found in Caubit et al. (submitted). These mice were maintained and sacrificed at the Institute of Developmental Biology Marseilles-Luminy (Marseilles, France) according to local ethical requirements. Urinary tract tissue from these mice was generously provided by Laurent Fasano. Additionally Laurent Fasano hosted me at his laboratory where I performed *in vitro* organ culture studies using embryonic ureters from the *Tshz3/lacZ* mice.

When wildtype or *Tshz3* transgenic embryonic mice were required, adult mice were mated overnight; and when vaginal plugs were found the females were assumed to

pregnant. The morning that the plugs were found was taken to be embryonic day (E) zero, and the mothers were sacrificed an appropriate number of days later (depending upon which stage embryos were required).

### **Cell culture**

Cell lines were maintained in monolayers in ten centimetre cell culture plates (obtained from Corning Incorporated, New York, USA) in appropriate media, at an appropriate temperature in a humidified, sterile environment with 5 % CO<sub>2</sub>. Details of cell lines used, and their specific culture conditions, can be found in Table 2.1

All cells were passaged when 80-90 % confluent by addition of trypsin (1000 U/ml, 0.02 % EDTA) for five minutes at 37°C after washing in sterile phosphate buffered saline (PBS). Cells were then centrifuged at 800 revolutions per minute (rpm) for 5 minutes to remove trypsin and resuspended into fresh sterile media and placed in fresh tissue culture dishes

Cell culture media, fetal calf serum, sterile PBS (DPBS without calcium chloride or magnesium chloride), 0.05 % trypsin-EDTA and MEM 10 mM non-essential amino acids solution were obtained from Invitrogen (Paisley, UK).

Cultured cells were observed using an Olympus IX70 inverted microscope (Olympus, Middlesex, UK) with Olympus UPlanF1 objective lens. Photographs of cultured cells were taken using an Olympus Camedia C-3030 zoom 3.3 megapixel camera mounted to this microscope.



**Table 2.1 Cell lines and culture conditions**

<b>Cell line</b>	<b>Details of cell line</b>	<b>Culture media</b>	<b>Culture temperature</b>
M5 (mesenchymal clone 5)	Conditionally immortal clonal cell-line derived from the metanephric mesenchyme of an E11, transgenic ( <i>H-2K<sup>b</sup>-tsA58</i> ) mouse expressing a temperature sensitive mutant of the SV-40 T antigen inducible by $\gamma$ -interferon (Woolf et al., 1995).	Dulbecco's modified Eagle's medium/Ham's F12 medium plus Glutamax, with 10 % fetal calf serum, 1 % antibiotic/antimycotic solution and $\gamma$ -interferon (0.08U/ml)	33 °C
IMCD3 (inner medullary collecting duct 3)	Immortal, clonal cell-line derived from the inner medullary collecting ducts of a transgenic mouse expressing the SV-40 large T antigen (Rauchman et al., 1993).	Dulbecco's modified Eagle's medium plus Glutamax with 10 % fetal calf serum and 0.1 mM non essential amino acids	37°C
HEK293 (human embryonic kidney 293)	Immortal cell-line derived from human embryonic kidney cells that were transformed by exposure to sheared fragments of adenovirus type 5 DNA (Graham et al., 1977).	Dulbecco's modified Eagle's medium plus Glutamax with 10 % fetal calf serum and 1 % antibiotic/antimycotic solution	37°C

### **Culturing embryonic mouse ureters**

Ureters were dissected from E15 *Tshz3* transgenic mice in Leibovitz's L15 media (+ L-Glutamine + L-amino acids) (Invitrogen) and transferred to six well tissue culture plates (Corning Incorporated) containing Millicell-CM inserts (0.4  $\mu$ m pore, 30 mm diameter) (Millipore, Billerica, USA) and 1.1 ml culture media. Culture media consisted of Dulbecco's modified Eagle's medium/Ham's F12 medium (+ L-Glutamine + 15mM HEPES), 1% antibiotic/antimycotic suspension (containing penicillin, streptomycin and amphotericin B) and either 10 % fetal calf serum (with serum) or 1 % ITS liquid media supplement (which contains 1.0 mg/ml insulin, 0.55 mg/ml transferrin, and 0.5  $\mu$ g/ml sodium selenite) (serum-free). Ureters from three litters of embryos were used for each culture condition. Ureters were maintained for six days (37 °C, 5 % CO<sub>2</sub>, humidified and sterile environment).

### ***Analysis of ureter growth***

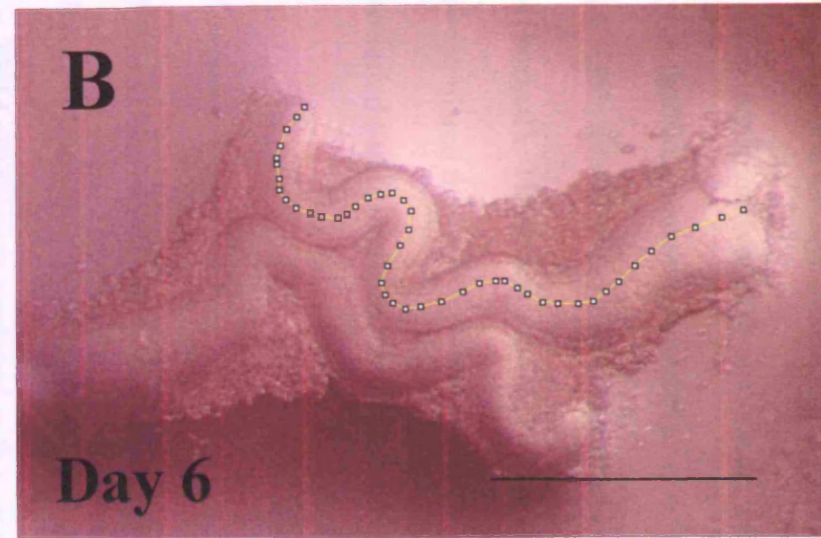
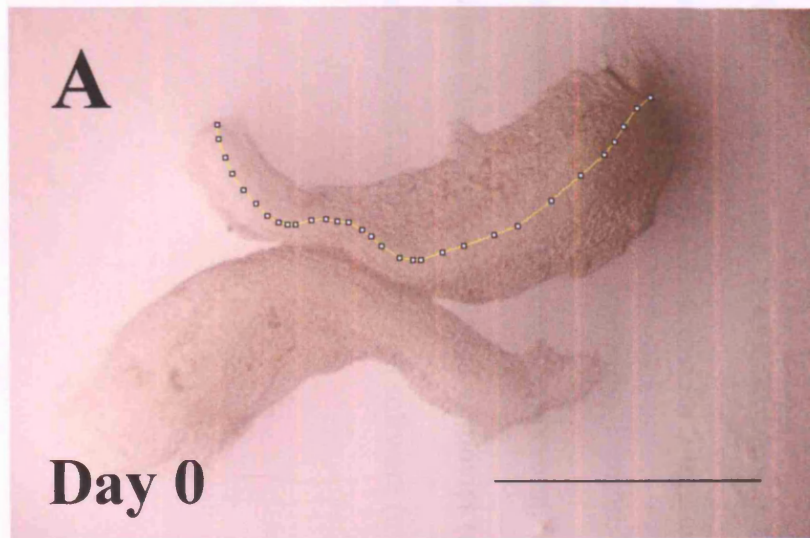
Photographs were taken of the ureters viewed under a Binocular Leica MZFL III dissecting microscope with a variable zoom lens (Leica Microsystems, Wetzlar, Germany) using a Nikon Dxm 1200 camera (Nikon, Tokyo, Japan) at the beginning and end of the experiment. (The magnification used and size and resolution of image was the same at each timepoint.) Image J was used to measure the lengths of the ureters at each time point (by drawing a line along the middle of the ureter, and measuring its length in pixels, see Figure 2.1), and the percentage change in length calculated for each ureter using Microsoft Excel (Microsoft Corporation, Seattle, USA).

## **Figure 2.1 Analysis of growth of cultured ureters**

Photographs were taken of the cultured ureters on the first and last day of culture, and ImageJ software was used to draw a line (yellow, fragmented) along the centre of the ureter at each timepoint. The software was then used to measure the length of the line in pixels. As the photographs were taken at the same magnification and the same resolution, the lengths of these lines could then be used to calculate the percentage increase in ureter length over the time of the culture period. **A** shows a pair of ureters on the first day of culture (one of which has a line drawn along it in order to measure its length), and **B** shows the same pair of ureters on the final day of culture. Scale bars - 500 $\mu$ m.

**Figure 2.1**

75



### ***Quantitative analysis of peristalsis***

Peristaltic frequency was recorded on days three and four of culture. Each ureter was observed under a dissecting microscope for one minute, twice a day for two consecutive days. Any contraction seen was recorded as one “peristalsis” (but note here the word peristalsis refers to any observable contraction and does not mean that the peristaltic wave was normal). The average number of peristalses per minute over the two-day period was calculated for each individual ureter and SPSS (Chicago, USA) used to perform two-tailed t-tests (independent samples).

### ***Qualitative analysis of peristalsis***

Timelapse microscopy was used to image peristaltic movements in wildtype (n=36) and mutant (n=35) cultured ureters, after five days in culture. Ureters were imaged on an inverted Axiovert 200M microscope equipped with a spinning disc confocal head (Perkin Elmer, Waltham, USA) and a 5x objective lens (Carl Zeiss, Oberkochen, Germany). Images were acquired every 0.5 second for 2 minutes by using a cooled, 14-bit CCD camera (CoolSnap HQ; Roper Scientific, Trenton, USA) operated by Metamorph Image Software (Universal Imaging Corporation, West Chester, USA). Images were imported into Quicktime to be played as movies (at approximately 4x actual speed) and were analyzed using Metamorph software (n=5 each for wildtype and mutant).

## **Reverse transcriptase-PCR and real time-PCR experiments**

### ***Design of primers***

Primers used in reverse transcriptase-PCR and real time-PCR reactions were designed by myself using Primer 3 software specifying GC content close to 50% and preferred melting temperature of 60°C (available online from Biology Workbench at <http://workbench.sdsc.edu/>) and sequence information from Genbank, NCBI (*Tshz1*, 2 and 3, *Larp* and *Hprt* sequences are available under the accession numbers AF191309, AF207880, AY063491, XM\_126172 and NM\_013556), and produced by Operon (Cologne, Germany). Theoretical specificity was ensured by selection of primers that would amplify sequences specific to the gene of interest (determined by NCBI nucleotide BLAST searching the amplified region against the mouse genomic and transcript database). Details of primers can be found in Table 2.2.

### ***Isolation of kidneys/metanephri from mice***

Kidneys/metanephroi were dissected in Leibovitz's L15 media (+ L-glutamine + L-amino acids) using a Stemi SV6 dissection microscope (Carl Zeiss) from wild-type outbred mice (CD1) of the following ages; E11, 12, 14, E18, neonatal and adult (6-7 weeks old, male). Care was taken to remove all extraneous tissue from the kidneys/metanephroi (ureters were removed just below their junction with the metanephros).

**Table 2.2 Primers used for reverse transcriptase PCR and real time PCR**

	Forward Primer Sequence	Reverse Primer Sequence	Product Size	Corresponding nucleotides of region amplified (Genbank accession number)
<i>Tshz1</i>	GAAGGAGGAG TCGCAGTGTC	TGCAGTCTTTG CACCTGAAC	467	246-712 (AF191309)
<i>Tshz2</i>	AGTCCGTCCT GAACAACCAC	GTGGAGACTT CGCTCGAAAC	418	2285-2702 (AF207880)
<i>Tshz3</i>	GGACAGCGAG TCTCACATCA	CGCGATAGTG ACCTGTCTCA	506	348-853 (AY063491)
<i>Larp</i>	TGAAGGACTG AGCACACAGG	GCGACAAGTG AGTCACAGGA	296	5699-5995 (XM_126172)
<i>Hprt</i>	AAGCTTGCTG GTGAAAAGGA	GCAAATCAAA AGTCTGGGGA	354	629-982 (NM_013556)

### ***Isolation of RNA from dissected tissue***

Kidney tissue (approximately twenty E11, ten E12, five E14, two E18 or one neonatal kidney(s) or an eighth of an adult kidney) was homogenised in 1ml Tri-Reagent and RNA isolated by chloroform extraction followed by isopropanol precipitation. The resulting pellet was washed in 70% ethanol, dried and resuspended in 75 µl DEPC-water.

### ***Isolation of RNA from confluent cells***

Cells were grown in a monolayer in ten centimetre culture plates until confluent as detailed previously. The cell culture media was then removed from the culture dish and the cells rinsed in ice cold sterile PBS. 1 ml of Tri-Reagent was added and the cells scraped to ensure disruption. RNA was then isolated as described for dissected tissue.

### ***Removal of residual genomic DNA***

Isolated RNA was treated with *DNase* (Invitrogen) to remove any contaminating genomic DNA. 0.01 U/µl *DNase I* was added to samples for 15 minutes at 37 °C, in the presence of 0.5 U/µl *RNase* Inhibitor (Invitrogen), 5 mM MgCl<sub>2</sub> (Biorad, Hemel Hempstead, UK), 10 mM dithiothreitol (DTT, Invitrogen) and 0.1 M sodium acetate (pH 5.3). Following treatment, *DNase* was removed from the samples by extracting twice with phenol/chloroform/isoamylalcohol and once with chloroform. RNA was precipitated in 0.06 M sodium acetate and 70 % ethanol and the resulting pellet was washed in 70 % ethanol, dried and resuspended in DEPC-water.



### ***Reverse transcription of DNase treated RNA into single stranded cDNA***

RNA was quantified using a spectrophotometer to measure the absorbance at 260 nm, and 5 µg was used to make cDNA. RNA was incubated at 70 °C and then held on ice until addition of reverse transcriptase reaction mix [1x first strand buffer (Invitrogen), 1 µM dNTPs (Promega, Southampton, UK), 5 µM DTT, 2.5 ng/µl oligo(dT) (Invitrogen), 0.25 U/ µl *RNase* inhibitor and 10 U/µl reverse transcriptase (Superscript II, Invitrogen)]. The reaction was incubated in a PCR machine at 26°C for 8 minutes then 41°C for 90 minutes.

### ***PCR***

Ten µl PCR reactions were set up consisting of 1.67 mM MgCl<sub>2</sub>, 1.6 mM NH<sub>4</sub><sup>+</sup> (Biorad), 0.2mM dNTPs, 1 pmol/µl forward and reverse primers (detailed in Table 2.2), 1 µl cDNA and 0.1 U/µl *HotStarTaq* polymerase (Qiagen, Crawley, UK). Products of reverse transcription reactions in which reverse transcriptase had been substituted with water were used as negative controls.

PCRs consisted of a hot start step of 5 minutes at 95 °C, followed by cycles of denaturing (95 °C, 45 seconds), annealing (45 seconds) and extension (72 °C, 1 minute) steps. After cycling, a final extension of 72 °C for 7 minutes was carried out. Annealing temperatures of 61°C (*Tshz2*, *Tshz3* and *Larp*, tissue and cell-lines), 63 °C (*Tshz1*, tissue) or 65 °C (*Tshz1*, cell-lines) were used. PCRs were carried out for 30 cycles (except for *Tshz3* PCRs on M5 cell-lines which were carried out for 36 cycles due to low levels of expression).

PCR products were run on a 1 % agarose gel (prepared in TAE buffer; 0.04 M Tris-acetate, 0.001 M EDTA, pH 8.0) containing 100 ng/ml ethidium bromide. 1 µl of loading dye was added to 5 µl of each sample before samples were loaded into the wells. The gel was run at 80 volts for 45 minutes in a horizontal electrophoresis tank (Biorad) containing TAE buffer, and bands visualised under UV light. Band sizes were identified by comparison to a DNA ladder marker.

To ensure primer specificity, a PCR product for each primer pair was sequenced (by Qiagen). The sequences were verified as corresponding to the correct gene sequence by BLAST searching (which showed the sequence to correspond, with at least 98 % homology, to the gene sequence being investigated).

### ***Real-time PCR***

50 µl reactions were set up using 2 µl cDNA and 25 µl iQSYBR Green Supermix (which consists of SYBR Green I dye, optimised buffer, dNTPs, Hot Start Taq polymerase and fluorescein; Biorad) per reaction and primers (detailed in Table 2.1) were used at a final concentration of 0.2 pmol/µl. Reactions were run using Opticon real-time PCR detection system (MJ Research Incorporated, Waltam, USA) with annealing temperatures of 61 °C (*Tshz2*, *Tshz3* and *Larp*) or 65 °C (*Tshz1*). The PCR reactions consisted of a hot start step of 5 minutes at 95 °C, followed by cycles of denaturing (95 °C, 30 seconds), annealing (30 seconds) and extension (72 °C, 30 seconds) steps for 60 cycles. After cycling, a final extension of 72 °C for 10 minutes was carried out. Each reaction was run twice to ensure reproducibility. Negative control reactions (in which cDNA was substituted with H<sub>2</sub>O) were run for each

primer set. Data was analysed using Opticon (MJ Research Incorporated) and Microsoft Excel software.

Measurements of the fluorescence of each reaction mixture (plate reads) were taken after each cycle, and amplification plots drawn of cycle number against fluorescence. Threshold levels were set above baseline fluorescence, in the log-linear phase range of the PCR amplification. “Neonatal” cDNA was serially diluted and used to generate standard curves, which were used to calculate the initial template concentration of the test samples from their threshold cycle number as described in Figure 2.2.

To check that the fluorescent signal observed is the result of the dye binding to a single (specific) PCR product, melting curve analyses of the products were carried out. The temperature was slowly increased from 65 °C to 95 °C (the plate was read every 0.3 °C, and the temperature was held for 1 second between reads) upon completion of the PCR reaction. Because different PCR products denature at different temperatures (depending on characteristics such as length and GC content) a graph of the first derivative of the melting curve should have a single peak if only one product is present (Figure 2.3 shows an example). Data was only accepted for analysis if melting curves showed that one (specific) PCR product had been produced in the PCR reaction.

## **Figure 2.2 Real Time Polymerase Chain Reaction; Generating and Using a Standard Curve**

**A** An amplification plot showing fluorescence signal plotted against cycle number, for standard samples (different samples are portrayed by lines of different colours) undergoing a PCR reaction to detect transcripts of *Hprt* (this is an example taken from my data). Standard samples were prepared by serially diluting neonatal kidney cDNA. Two samples of each concentration (except the lowest concentration) were analysed. The dotted line (parallel to the x-axis) is the threshold level, which has been set above baseline fluorescence (see **B**): this line was used to determine the threshold cycle number, the C(T), for each standard sample. The C(T) for a particular sample is the cycle at which its amplification plot crosses the threshold level.

**B** An amplification plot presenting the same data as **A**, but with log fluorescence signal plotted against cycle number. The threshold fluorescence level is set using this semi-log graph, in the log-linear phase range of the PCR amplification.

**C** The C(T) (x-axis) of each sample (as determined in **A**), was then plotted against the log of the initial template quantity (which had been assigned a value according to its dilution factor; y-axis) to produce a straight line of best fit. The correlation coefficient was calculated ( $R^2$  value,  $R^2$ ) to ensure that the line adequately represented the standard sample results. ( $R^2$  should be greater than 0.95, in this case  $R^2=0.997$ ). Provided that the  $R^2$  value was satisfactory the equation of the line (in this case  $y = -0.31x + 8.93$ ) could be used to calculate the initial template quantity of test samples from their C(T) values.

**Figure 2.2A**

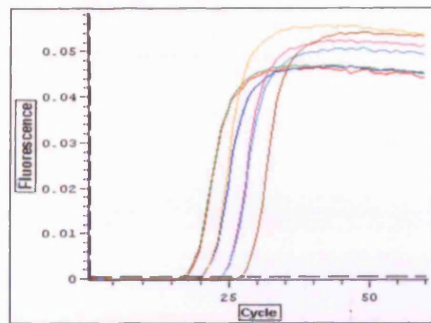


**Figure 2.2B**

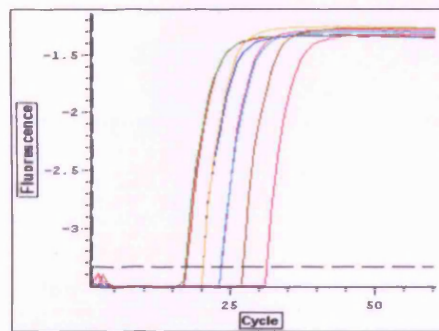


**Figure 2.2C**

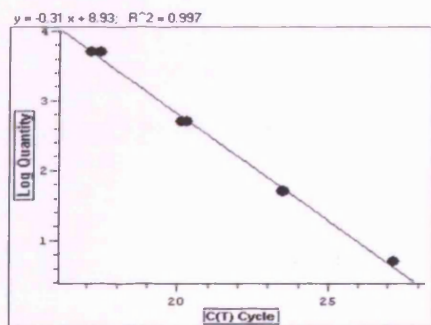


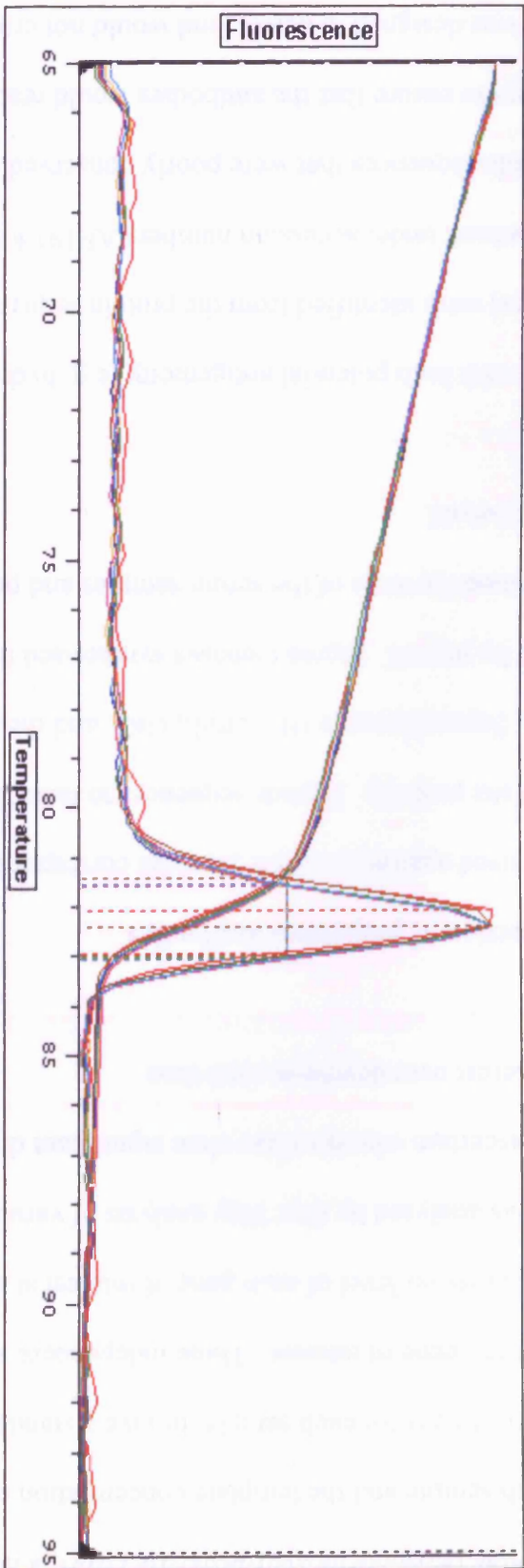
### **Figure 2.3 Real Time Polymerase Chain Reaction; Typical Melting Curve**

A graph showing the melting curves of PCR products from several samples which have undergone a PCR reaction to detect transcripts of *Hprt* (different samples are portrayed by lines of different colours) (this is an example, taken from my data).

The temperature of the reaction mixture containing the products was gradually increased, and the fluorescent signal recorded every 0.3 °C. As the temperature was increased the fluorescent signal decreased, due to the PCR being denatured to become single stranded. The temperature at which this denaturing occurs depends on the physical properties of the product, and in this case is between 80 and 85°C.

Note that the melting curves for all the samples follow the same path, with only minor variations. The first derivatives of the melting curves were also plotted on the same graph, and show a single peak around 82.5 °C, indicating that only single PCR products were present.

Figure 2.3



The template concentration (on an arbitrary scale) of both the gene of interest and *hypoxanthine-guanine phosphoribosyltransferase* (*Hprt*; a house-keeping gene) were determined for each sample and the template concentration of the gene of interest was divided by that of *Hprt* for each sample, to give a standardised measure of the expression level of the gene of interest. Three independent samples were used to find the average expression level of each gene of interest at each developmental timepoint. Data was analysed by One Way analysis of variance (ANOVA) using SPSS software to ascertain whether there were significant differences in expression of each gene of interest over developmental time.

### **Design and production of polyclonal antibodies**

Antibodies were raised against synthetic peptides corresponding to specific sequences of the Tshz proteins. Peptide sequences to raise the antibodies against were suggested by Sigma Genosys (Haverhill, UK), and the specific ones to be used were then selected by myself. Sigma Genosys synthesised the peptides, raised the antibodies, determined the titres of the serum samples and performed IgY purification on my behalf.

Peptide sequences with high potential antigenicity (e.g. hydrophilic regions, predicted beta-turns) were identified from the protein sequences of each of the Tshzs (obtained from Genbank under accession numbers AF191309, AF207880 and AY063491). Peptide sequences that were poorly conserved between the Tshzs were chosen in an attempt to ensure that the antibodies would react specifically against the Tshz the antibody was designed to detect (and would not cross react with other members of the Tshz family). The peptide sequences that fulfilled these criteria were



BLAST searched (protein, short near exact matches) to check whether homologous sequences were present in other mouse proteins. Initially, one peptide for each Tshz was chosen, synthesised and had antibodies raised against them in rabbits.

(However, for Tshz1, the rabbits elicited a poor immune response when injected with the peptide, as seen from the ELISA results of the first bleed. Therefore a second peptide was chosen for Tshz1 and another antibody raised, this time in chickens.)

Table 2.3 shows details of the peptides chosen, along with their predicted antigenic properties, and a summary of the results of the BLAST results for these peptides.

Figure 2.4 shows the positions of the epitopes chosen within the Tshz proteins.

Peptides were synthesised (with a preceding, or succeeding, cysteine residue) and conjugated to Keyhole Limpet Hemocyanin (KLH) to improve antigenicity. New Zealand white rabbits, or Rhode Island Red chickens, were immunized subcutaneously with the peptides in adjuvant, and their serum collected, according to schedule set out in Table 2.4. Antibodies were produced in two animals for each peptide, in case of non-reactivity of an animal to the immunizations of peptide.

ELISA's were performed to determine the titres of the 1<sup>st</sup> bleed and final bleed (in comparison to the pre-immune serum), in order to establish a relative measurement of the quantity of peptide specific antibody present in the serum samples. Results of ELISA's are shown in Table 2.5. The bleeds with the highest titres for each Tshz protein (i.e. demonstrating the best response) were used for subsequent experiments.

When chickens were used eggs were also collected, and IgY was purified from the yolks of some of the eggs. Remaining yolks were stored at -20°C for subsequent IgY purification if desired.

**Table 2.3 Peptides to which Tshz antibodies were raised**

<b>Protein</b>	<b>Host</b>	<b>Peptide</b>	<b>Antigenic Properties</b>	<b>BLAST results (mouse proteins)</b>
Tshz1	Rabbit	CKGSDSETG KAKKES (corresponding to residues 685-698 of Tshz1 protein)	Hydrophilic, contains one $\beta$ -turn	57% homology with G kinase anchoring protein 1 (testis specific gene), a protein of approximately 42KDa in size (NCBI Genbank accession number NP_062806)
Tshz1	Chicken	CMQERKIKE ETEDAT (corresponding to residues 503-516 of Tshz1 protein)	Hydrophilic	50% homology with unnamed protein product, a predicted protein 294 amino acids long (therefore predicted to be approximately 32KDa in size). (NCBI Genbank accession number BAC38332).
Tshz2	Rabbit	HQSSNDTGT DEELEC (corresponding to residues 111-124 of Tshz2 protein)	Hydrophilic, contains four $\beta$ -turns	none
Tshz3	Rabbit	CKMKEPEG KLSPPKR (corresponding to residues 627-640 of Tshz3 protein)	Hydrophilic, contains two $\beta$ turns	57% homology with Transmembrane protease, serine 6, a protein of approximately 90KDa in size (Uniprot accession number Q9DBI0)

**Figure 2.4 The position of epitopes to which antibodies were raised within the Tshz proteins**

Schematic representation of Tshz1, Tshz2 and Tshz3 mouse proteins (not to scale).

All proteins contain an acidic domain (yellow box, AD), three zinc-finger motifs towards their N-terminal of the *Cx2Cx12HMx4H* type (bright red boxes, ZnF), a PIDLT motif (black line, PIDLT), a homeodomain (green box, HD) and two zinc finger motifs near their C-terminal of the *Cx2Cx12Hx3-4H* type (dark red boxes, ZnF).

Epitopes which were made as synthetic peptides and used for antibody production are shown as blue boxes. R denotes that these peptides were used to immunise rabbits : C denotes that this peptide was used to immunise chickens. Additionally the 108 amino acid epitope used by A.Garrat (Max-Delbruck-Center for Molecular Medicine, Berlin) to raise antibodies against Tshz3 protein (in both guinea-pigs and rabbits, see materials) is shown as blue diagonally lined box (and is denoted Garrat Abs).

**Figure 2.4**

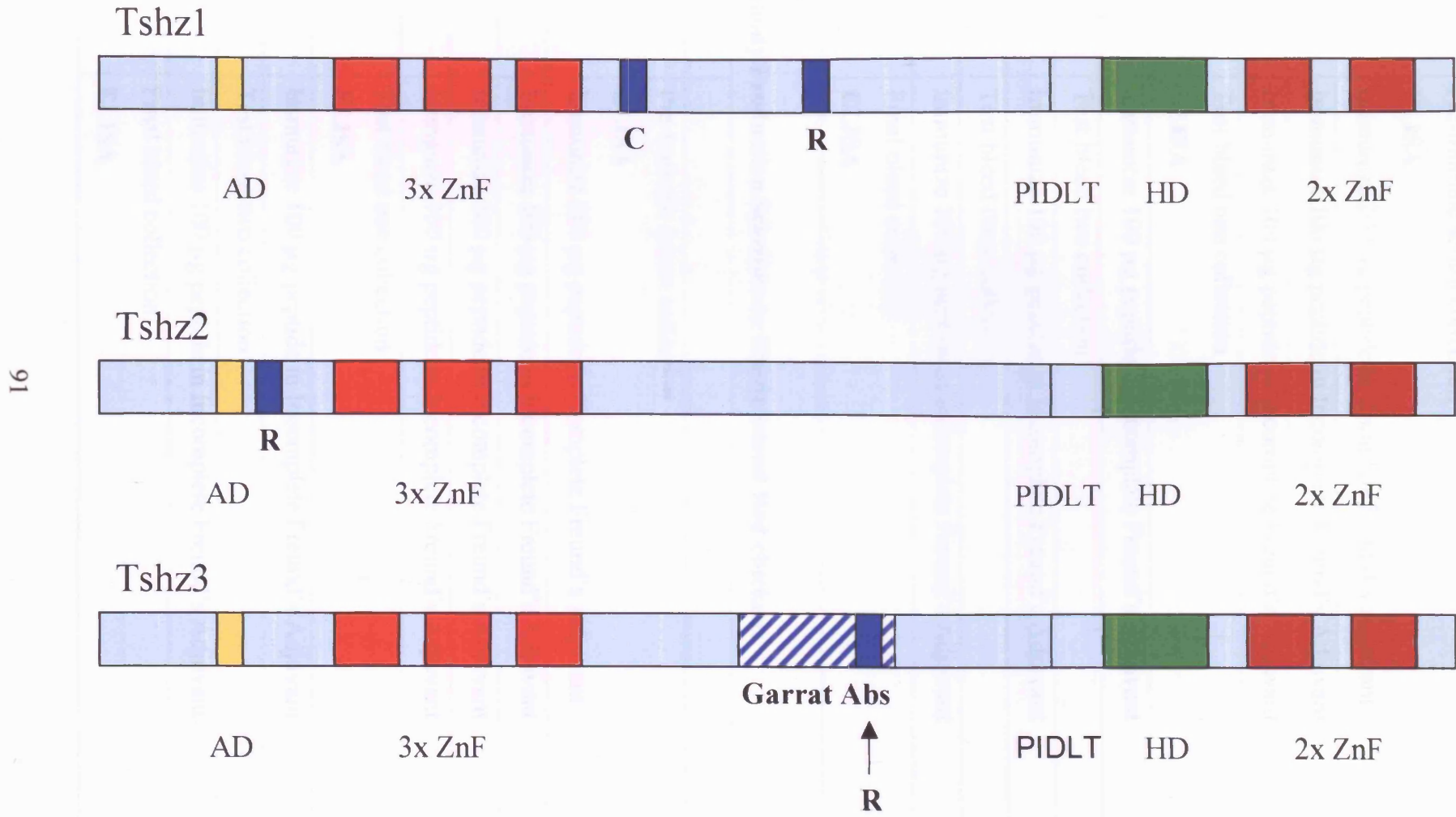


**Table 2.4 Antibody Production Schedule in New Zealand White rabbits**

Day	
0	Pre-immune serum collection <b>ELISA</b> Immunize 200 µg peptide in Complete Freund's Adjuvant
14	Immunize 100 µg peptide in Incomplete Freund's Adjuvant
28	Immunize 100 µg peptide in Incomplete Freund's Adjuvant
35	Test bleed one collection <b>ELISA</b>
42	Immunize 100 µg peptide in Incomplete Freund's Adjuvant
49	Test bleed two collection
56	Immunize 100 µg peptide in Incomplete Freund's Adjuvant
63	Test bleed three collection
70	Immunize 100 µg peptide in Incomplete Freund's Adjuvant
77	Final bleed collection <b>ELISA</b>

**Antibody Production Schedule in Rhode Island Red chickens**

Day	
0	Pre-immune serum collection <b>ELISA</b> Immunize 200 µg peptide in Complete Freund's Adjuvant
14	Immunize 100 µg peptide in Incomplete Freund's Adjuvant
28	Immunize 100 µg peptide in Incomplete Freund's Adjuvant
42	Immunize 100 µg peptide in Incomplete Freund's Adjuvant
49	Test bleed one collection <b>ELISA</b>
56	Immunize 100 µg peptide in Incomplete Freund's Adjuvant
63	Test bleed two collection
70	Immunize 100 µg peptide in Incomplete Freund's Adjuvant
77	Final bleed collection <b>ELISA</b>

**Table 2.5 Titre's of first and final bleeds of animals used for antibody production**

<b>Protein</b>	<b>Host</b>	<b>Animal number</b>	<b>Titre of 1<sup>st</sup> bleed</b>	<b>Titre of final bleed</b>
Tshz1	Rabbit	1	No response	1: 20 000
Tshz1	Rabbit	2	No response	1: 15 000
<b>Tshz1</b>	<b>Chicken</b>	<b>1</b>	<b>1: 500 000</b>	<b>1: 500 000</b>
Tshz1	Chicken	2	1: 150 000	1: 500 000
Tshz2	Rabbit	1	1: 5000	1: 15 000
<b>Tshz2</b>	<b>Rabbit</b>	<b>2</b>	<b>1: 20 000</b>	<b>1: 20 000</b>
<b>Tshz3</b>	<b>Rabbit</b>	<b>1</b>	<b>1: 50 000</b>	<b>1: 150 000</b>
Tshz3	Rabbit	2	1: 50 000	1: 20 000

Bold indicates that serum, or IgY, derived from these animals was used in subsequent experiments, as they had the highest titres, and therefore should contain the highest concentration of specific antibody.

### **Overexpression of cMyc-tagged proteins in HEK293 cells**

Myc tagged full length Tshz proteins were overexpressed in HEK293 cells by transient transfection: Myc tagged GFP was used as a control. Myc tagged DNAs were encoded in plasmids [gifts from L.Fasano (Manfroid et al., 2004) and L.Romio (Romio et al., 2003), see Figure 2.5 for maps of plasmids]. Protein was extracted from the overexpressing cells for use in Western blots, or the overexpressing cells were used for immunocytochemistry.

### ***Preparation of plasmids to be transfected into HEK293 cells***

TOP10 Chemically Competent Bacteria (Invitrogen) were transformed with 10-20  $\mu$ l of plasmid DNA by incubation on ice for 30 minutes, followed by heatshock for 90 seconds at 42 °C. 250  $\mu$ l SOC media (Invitrogen) was added to the bacteria and they were shaken at 200 rpm at 37 °C for 4 hours. Transformants were then spread on pre-warmed selective LB agar plates (containing 50  $\mu$ g/ml ampicillin: to select for plasmid containing bacteria) and incubated at 37 °C overnight. Individual colonies were picked and grown overnight at 37 °C in 4 ml of LB broth containing 50  $\mu$ g/ml ampicillin. The resulting suspension was centrifuged for 10 minutes at 13000 rpm and the supernatant discarded. Plasmid DNA was prepared from the bacterial pellet using a Miniprep kit (Qiagen), according to manufacturer's instructions.

**Figure 2.5 Maps of plasmids used to overexpress cMyc tagged proteins in HEK293 cells**

**A** Map of pcDNA3.1 plasmid containing cMyc tagged *GFP* gene

**B** Map of pcDNA3 plasmid containing cMyc tagged *Tshz1 (mTsh1)* gene

**C** Map of pcDNA3 plasmid containing cMyc tagged *Tshz2 (mTsh2)* gene

**D** Map of pcDNA3 plasmid containing cMyc tagged *Tshz3 (mTsh3)* gene

All plasmids contain a CMV promotor (pCMV), T7 promotor, Myc tagged full-length cDNA of interest, Sp6 promotor, BGH polyadenylation signal (BGH polyA), F1 origin of replication (F1 ori), SV40 promotor and origin (SV40 ori), neomycin resistance gene (Neomycin), SV40 polysdenylation signal (SV40 polyA), ColE1 origin (ColE1 ori) and Ampicillin resistance gene (Ampicillin).

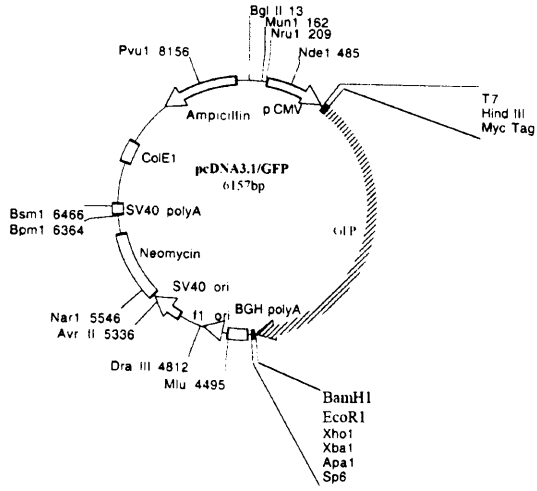
Note some of the restriction sites are also shown for each plasmids. In **D** restriction sites within the *Tshz3(mTsh3)* gene are also shown.

Plasmid maps **B-D** were provided by Laurent Fasano. Plasmid map **A** was redrawn after Romio et al. (2003; personal communication).

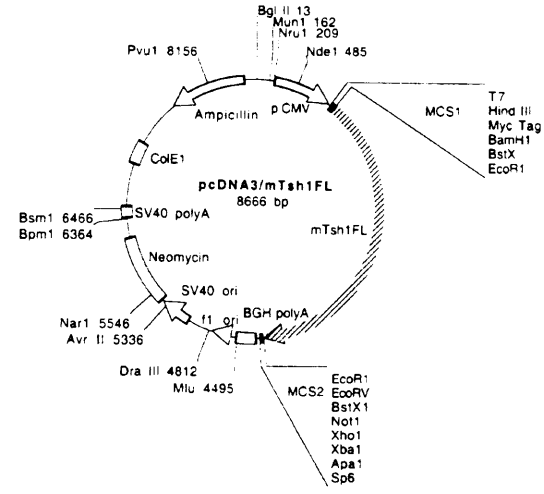


# Figure 2.5

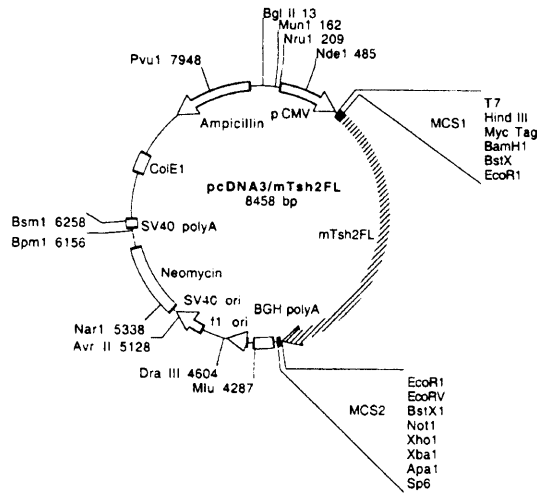
## A



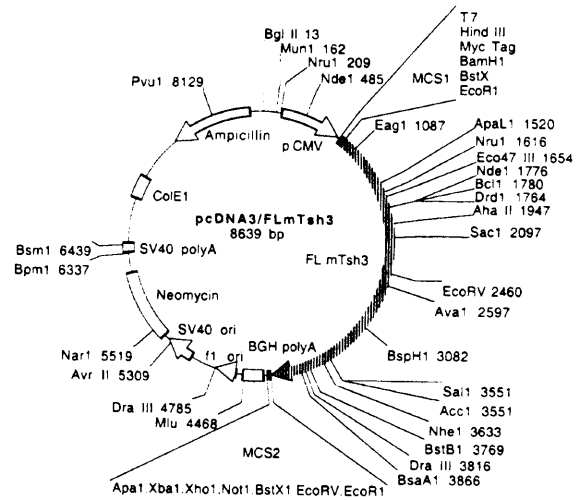
## B



## C



## D



To verify that the plasmids obtained contained the inserted DNA of interest 5 µl of plasmid DNA restriction digests were performed according to manufacturer's instructions on plasmid DNA using *EcoRI* (Invitrogen) for plasmids encoding Myc-tagged Tshzs and *BamHI* and *XbaI* (New England Biolabs, Ipswich, USA) for plasmids encoding Myc-tagged GFP. The digestion products were run on a 1 % agarose gel containing ethidium bromide (100 ng/ml) to check that the products were of the expected sizes.

If the expected products were seen, glycerol stocks of the bacteria were made (by adding 250 µl bacterial broth to 750 µl 50 % glycerol) and frozen at -80 °C for future use. The bacteria were also grown on a larger scale to allow harvesting of sufficient amounts of plasmid DNA for the transfection experiments. 1 ml of overnight bacterial culture was added to 250 ml LB broth (containing 50 µg/ml ampicillin) and incubated at 37 °C overnight in a shaking incubator. Plasmid DNA was prepared from the bacterial culture using a Maxiprep kit (Qiagen) according to manufacturer's instructions. The DNA was quantified using a spectrophotometer (by measuring the absorbance of diluted DNA at 260 nm).

#### ***Transfection of Myc-tagged Teashirts in HEK293 cells***

HEK293 cells were transfected with the plasmid DNA using Lipofectamine reagent (Invitrogen). Twenty-four hours prior to transfection,  $1 \times 10^6$  HEK293 cells were seeded into each well of a 6 well tissue culture plate in 2ml antibiotic free media (preliminary experiments had shown this to be the optimal seeding density for cells to reach 70-80 % after 24 hours incubation, which is an appropriate confluence for good transfection efficiency by Lipofectamine).

Immediately prior to transfection cells were washed in antibiotic and serum free media. Transfection was performed in antibiotic and serum free media according to manufacturers instructions using 1.5 µg plasmid DNA and 10 µl Lipofectamine in a total volume of 800 µl per well. Cells were incubated for 6 hours at 37 °C, 5% CO<sub>2</sub>, then transfection media was then replaced with 2 ml complete media (i.e. with serum and antibiotics) and cells incubated for a further 36 hours.

## **Western Blotting**

### ***Preparation of protein***

Protein was prepared from transfected HEK293 cells, 36 hours after transfection. After removal of media, cells were washed twice in ice cold, sterile PBS. PBS was removed and 100 µl Radioimmunoprecipitation assay (RIPA) buffer [150 mM sodium chloride, 1 % NP-40 (Calbiochem, EMD Chemicals Incorporated, Darmstadt, Germany), 0.5 % sodium deoxycholate, 1 % sodium dodecylsulphate, 50 mM Tris buffer pH 8] containing protease inhibitors (66 µg/ml aprotinin, 100 µg/ml phenylmethylsulfonylfluoride, 1 mM sodium orthovanadate) was added to each well of the six well plate, and the plate left on ice for 5 minutes. A cell scraper was used to disrupt cells and ensure their complete removal from the dish. The resulting mixture was then transferred to an eppendorf tube and sonicated on ice for 15 seconds.

Protein was also prepared from mouse urinary tract tissue. Tissues (approximately twelve E14 kidneys, eight E18 kidneys, six neonatal kidneys, an eighth of an adult kidney or twenty E18 ureters) were dissected from wild type outbred mouse (CD1)

embryos in Leibovitz's L15 media (+ L-glutamine + L-amino acids) using a Stemi SV6 dissection microscope. Protein was extracted by homogenising the tissue, on ice, in an appropriate amount of RIPA buffer (up to 250  $\mu$ l, depending on the quantity of tissue).

The cell or tissue containing mixture was centrifuged at 13000 rpm for 30 minutes at 4 °C, the pellet (containing cell debris) discarded and the supernatant (containing protein) transferred to a fresh eppendorf and stored at -70 °C or used immediately. Protein was quantified using a bicinchoninic acid (BCA) protein assay kit (Pierce Biotechnology, Rockford, USA) according to manufacturer's instructions.

### ***SDS-PAGE***

Proteins were separated on denaturing SDS-polyacramide gels. 1.5 mm thick vertical 8 % polyacramide gels (7.95 % polyacrylamide, 0.375 M Tris-HCl pH 8.8, 0.1 % SDS, 0.1 % ammonium persulphate and 0.06 % N,N,N-N-tetramethylethylenediamine (TEMED)) were prepared, with an upper layer of stacking gel containing wells for loading protein (5.1 % polyacramide, 0.125 M Tris-HCl pH 6.8, 0.1 % SDS, 0.1 % ammonium persulphate, and 0.1 % TEMED) using Mini-Protean II gel apparatus (Biorad) according to manufacturers instructions.

Protein was denatured by addition of an equal volume of 2x electrophoresis buffer (20 % glycerol, 10 %  $\beta$ -mercaptoethanol, 6 % SDS, 0.25 M Tris-HCl pH 6.8 and 0.2 mg/ml bromophenol blue) and heating to 98 °C for 10 minutes and then was held on ice for 5 minutes. Gels were placed in a vertical electrophoresis tank (Biorad) containing Running buffer (2.5 mM Trizma Base, 25 mM glycine and 0.01 % SDS),

and the desired amount of protein loaded. 20 µl Full range Rainbow Recombinant protein molecular weight marker (Amersham, Little Chalfont, UK) was loaded into one lane, so that protein sizes could be determined. Unused lanes were loaded with ddH<sub>2</sub>O plus 2x electrophoresis buffer. The gels were run at 80 V for 2 hours and 20 minutes.

### ***Electroblotting***

Protein was transferred from gels to protein transfer nitrocellulose membrane (Hybond C Nitrocellulose paper, 0.45 µm, Amersham) by semi-dry electroblotting. Firstly, nitrocellulose membrane (1 piece per gel) and 3MM Whatmann paper (6 pieces per gel) used for electroblotting were cut to size and soaked in transfer buffer (0.02 M Tris base, 0.15 M glycine, 0.0275 % SDS and 20 % methanol). Gels were removed from the electrophoresis apparatus and placed in transfer buffer. Then, the following were placed on the positively charged plate of the trans-blot semi-dry electroblotter (Biorad) in order; 3 sheets of 3MM paper, nitrocellulose membrane, gel, 3 sheets of 3MM paper. Care was taken that there were no air bubbles. To prevent short-circuiting that may occur if the upper and lower paper stacks contacted each other directly, saranwrap was placed between these two paper layers in areas that were not separated by the gel itself. The negative (upper) electrode was placed on top of the stacks and 12V applied for 1 hour in order to transfer the proteins from the gel to the nitrocellulose membrane. Nitrocellulose membranes were checked for protein by staining with Ponceau S for 5 minutes. Nitrocellulose membranes were then washed in PBS (Oxoid, Basingstoke, UK) before commencing the immunodetection protocol.

### ***Blocking and addition of antibodies***

The nitrocellulose membranes were then probed for the presence of the specific proteins using various antibodies. Blots were blocked (in 0.1 % PBS-Tween, 50 g/l dried milk, 1 g/litre bovine serum albumin) for 1 hour at room temperature, then incubated with primary antibody diluted to an appropriate concentration in block at 4 °C overnight with gentle mixing. See Table 2.6 for details of antibodies used.

Blots were washed twice in PBS-0.1 % Tween, blocked again for 20 minutes and incubated for 30 minutes at room temperature with an HRP conjugated secondary antibody diluted in block (see Table 2.6 for details). Blots were washed three times in PBS - 0.1 % Tween, and twice in PBS before bands were detected by chemiluminescence.

### ***Chemiluminescence***

Excess PBS was removed from the washed nitrocellulose membranes, and the membranes placed, face up, on saranwrap. Super Signal West Pico Chemiluminescent Substrate (Pierce Biotechnology) was added to the membranes. After three minutes the chemiluminescent substrate was removed and the membranes wrapped in fresh saranwrap and transferred to an X-ray cassette. Autoradiography film was placed onto the membranes in the X-ray cassette, in safe light conditions, and exposed for varying lengths of time to visualise the signal (up to one hour, depending on the strength of the signal). The film was then developed using a Compact X4 X-ray developing machine (Xograph, Tetbury, UK).

**Table 2.6 Antibodies used for Western blotting**

<b>Primary Antibody (concentration)</b>	<b>Raised in</b>	<b>Source of Primary Antibody</b>	<b>Antigen raised against</b>	<b>Secondary antibody (concentration)</b>
Anti-Tshz1 (1/1000 on cell extracts, 1/500 on tissue extracts)	chicken	Sigma Genosys	CMQERKIKEETEDAT (corresponding to residues 503-516 of Tshz1 protein)	rabbit anti-chicken HRP (Sigma Alrich Company Limited) (1/1000)
Anti-Tshz2 (1/200)	rabbit	Sigma Genosys	HQSSNDTGTDEELEC (corresponding to residues 111-124 of Tshz2 protein)	goat anti-rabbit HRP (Dako, Ely, UK) (1/2500), followed by a tertiary antibody step of rabbit anti-goat (Dako) (1/2500)
Anti-Tshz3 (1/500 on cell extracts, 1/250 on tissue extracts)	rabbit	Sigma Genosys	CKMKEPEGKLSPPKR (corresponding to residues 627-640 of Tshz3 protein)	HRP-labelled polymer anti-rabbit immunoglobins (Envision+ System, Dako) (1 drop per 10 ml block)

<p>Anti-Tshz3 (1/2500)</p>	<p>rabbit</p>	<p>A gift from L.Fasano. Antibody generated by A. Garrat (Max Delbruck Centre for Molecular Medicine, Berlin, Germany.</p>	<p>aa557-664 of mouse Tshz3 (a 108 amino acids peptide corresponding to a non-conserved region downstream of the N-terminal zinc finger motifs). The ability of this antibody to specifically recognise Tshz3 protein in mouse tissue by immunohistochemistry has been verified by Caubit et al. (submitted; Xavier Caubit and Laurent Fasano, personal communication).</p>	<p>HRP-labelled polymer anti-rabbit immunoglobins (Envision+ System, Dako) (1 drop per 10 ml block)</p>
<p>Anti-Tshz3 (1/5000)</p>	<p>guinea- pig</p>	<p>A gift from L.Fasano. Antibody generated by A. Garrat (Max Delbruck Centre for Molecular Medicine, Berlin, Germany.</p>	<p>aa557-664 of mouse Tshz3 (a 108 amino acids peptide corresponding to a non-conserved region downstream of the N-terminal zinc finger motifs). The ability of this antibody to specifically recognise Tshz3 protein in mouse tissue by immunohistochemistry has been verified by Caubit et al. (submitted; Xavier Caubit and Laurent Fasano, personal communication).</p>	<p>rabbit anti-guinea pig HRP (Dako) (1/1000)</p>



Anti-Myc (A14) (1/200)	rabbit	Santa Cruz Biotechnology Incorporated, Santa Cruz, USA	A peptide mapping near the C-terminus of c-Myc of human origin	HRP-labelled polymer anti-rabbit immunoglobins (Envision+ System, Dako) (1 drop per 10 ml block)
Monoclonal anti- $\beta$ actin (1/10000)	mouse	Sigma Alrich Company Limited	A slightly modified synthetic $\beta$ - cytoplasmic actin N-terminal peptide (16 amino acids in lengths)	HRP-labelled polymer anti-mouse immunoglobins (Envision+ System, Dako) (1 drop per 10 ml block)

### ***Control experiments to ensure specificity of antibody binding***

To ensure that any bands observed on western blots resulted from specific binding of the primary antibody to its target protein, negative controls experiments were carried out. In these experiments the primary antibody was pre-absorbed with an excess of its immunising peptide for 24 hours prior to the addition of the antibody to the blot, but otherwise the protocol remained unchanged. (When the final concentration of the antibody was known, 10x the concentration of peptide was used for pre-absorption. When antibodies were used in serum form, the final concentration of antibody was not known, and the amount of peptide recommended by Sigma-Genosys was used for pre-absorption; this was equivalent to 10 µg/ml of peptide for a 1/200 dilution of serum.)

### ***Stripping blots***

When required, blots were stripped and reprobed using a different antibody. Blots were washed twice for 5 minutes in PBS following exposure of autoradiography film, and were then placed in Restore Stripping Solution (Pierce Biotechnology) for 15-30 minutes, depending on the strength of the original signal. The blots were washed twice more for 5 minutes in PBS, before blocking and probing with the new antibody.

### **Immunocytochemistry of transfected HEK293 cells**

#### ***Growing and fixing of cells onto slides***

Thirty-six hours after transfection, cells were trypsinised and resuspended in media and  $1 \times 10^5$  cells, in a total volume of 800 µl media, were seeded into each well of plastic (permanox) four-well chamber slides (Nunc, Roskilde, Denmark). Following

twenty four hours incubation at 37°C (humidified environment, 5 % CO<sub>2</sub>) media was removed and cells washed in ice-cold sterile PBS, then fixed in 4 % paraformaldehyde for 15 minutes at room temperature, and washed twice more in PBS.

### ***Staining procedure***

Cells were permeabilised for 15 minutes in 0.25 % TritonX (in PBS), and then washed three times in 0.1 % Tween (in PBS). Cells were blocked (in 10 % fetal calf serum, 2 % bovine serum albumin, 0.1 % Tween in PBS) for 30 minutes at room temperature before incubation with primary antibody (rabbit anti-Myc 1/50 or rabbit anti-Tshz3 1/50 diluted in block) at 4 °C overnight in a humid chamber. The cells were then washed three times in 0.1 % Tween (in PBS) and incubated in FITC conjugated swine anti-rabbit (1/20 diluted in block) at room temperature in the dark. Cells were washed three times in 0.1 % Tween (in PBS) and then counterstained with Hoechst (2µg/ml) for 15minutes at room temperature in the dark. The cells were washed three times in PBS and then mounted in aqueous mountant (citifluor) and viewed using a Zeiss AxioImager.M1 microscope (Carl Zeiss) with ZeissPlan-NEOFLUAR objective lens (Carl Zeiss) with and a HBO100 ultraviolet light source (Carl Zeiss). Photographs were taken using an integrated AxioMRm camera and Axiovision4.4 software (Carl Zeiss).

### **Immunohistochemistry**

Immunohistochemistry was performed using a variety of antibodies on paraformaldehyde-fixed, paraffin-embedded renal tract tissue unless otherwise stated. Details of antibodies and antigen retrieval techniques used are outlined in Table 2.7.

**Table 2.7 Antibodies used for immunohistochemistry**

<b>Primary Antibody (concentration)</b>	<b>Raised in</b>	<b>Source of primary antibody</b>	<b>Antigen raised against</b>	<b>Reactive against</b>	<b>Antigen Retrieval</b>	<b>Secondary antibody (concentration)</b>
Anti-Tshz1 (different concentrations tested)	chicken	Sigma Genosys	CMQERKIKEETEDAT (corresponding to residues 503-516 of mouse Tshz1 protein)	Mouse (theoretical)	Different methods tested	Goat biotinylated anti-chicken (Vector Laboratories, Burlingame, USA) (1/200)
Anti-Tshz3 (different concentrations tested)	rabbit	Sigma Genosys	CKMKEPEGKLSPPKR (corresponding to residues 627-640 of mouse Tshz3 protein)	Mouse (theoretical)	Different methods tested	HRP labelled polymer anti-rabbit immunoglobins (Envision+ system, Dako) (neat)
EPOS™ monoclonal anti-alpha smooth muscle actin, HRP conjugated (neat)	mouse	Dako	N-terminal synthetic decapeptide of human $\alpha$ smooth muscle actin coupled to KLH	human, chicken, cow, rat	Citric acid, ten minutes	N/A

Polyclonal anti- $\beta$ galactosidase (1/1000)	rabbit	Cappel, MP Biomedicals Europe, Illkrich, France	$\beta$ -galactosidase from <i>Escherichia coli</i>	Product of <i>E.coli lacZ</i> gene	Citric acid, five minutes	HRP-labelled polymer anti-rabbit immunoglobins (neat)
Polyclonal anti-uroplakin1b (1/1000)	rabbit	gift from Tung-Tien Sun, Sackler Insitute, New York University Medical Centre, USA	Synthetic peptide corresponding to residues 160-173 of uroplakin1b (Liang et al., 2001).	rabbit, cows, others not reported	Citric acid, six minutes	HRP-labelled polymer anti-rabbit immunoglobins (neat)
Monoclonal anti-BMP4 (1/10)	mouse	Novacastra, VisionBiosystems (Europe), Newcastle- upon-Tyne, UK	Recombinant mouse BMP4	mouse, human	Citric acid, six minutes	HRP-labelled polymer anti-mouse immunoglobins (Envision+ system, Dako) (neat)
Monoclonal anti-PCNA (1/200)	mouse	Pharminagen, BD Biosciences, Oxford, UK	Epitope of human PCNA (exact epitope not reported)	Not reported	Protease, 15 minutes	HRP-labelled polymer anti-mouse immunoglobins (neat)
Polyclonal anti-pax2 (1/20)	rabbit	Zymed Laboratories Incorporated, San Francisco, USA	Fusion protein containing the C-terminal domain of the murine Pax2 protein	mouse, human, rat, Xenopus, zebrafish, sheep	Citric acid, ten minutes	HRP-labelled polymer anti-rabbit immunoglobins (neat)

Polyclonal anti-uromucoid (1/500)	sheep	Biodesign International, via AMS Biotechnology (Europe) Limited, Abingdon, UK	Human uromucoid, purified from human urine	Not reported	Citric acid, six minutes	Rabbit anti-sheep immunoglobins, HRP conjugated (Novus Biologicals, Littleton, USA) (1/100)
Polyclonal anti-aquaporin2 (1/400)	rabbit	Chemicon, Millipore, Chandlers Ford, UK	Purified peptide corresponding to residues 254-271 of rat or mouse aquaporin2	Mouse, rat, human, sheep	Citric acid, ten minutes	HRP-labelled polymer anti-rabbit immunoglobins (neat)
Monoclonal anti-podoplanin (1/250)	hamster	Abcam, Cambridge, UK	Murine thymic stromal cell line	mouse	Citric acid, ten minutes	Rabbit anti-hamster immunoglobins (Sigma Alrich Company Limited) (1/200) followed by HRP labelled polymer anti-rabbit immunoglobins (neat)

***Preparation of paraffin embedded sections of urinary tracts and treatments prior to blocking and the addition of antibodies***

Urinary tracts were dissected either fully, or partially, from surrounding tissue and were fixed in 4% paraformaldehyde (overnight at 4°C), washed in PBS and dehydrated through a graded alcohol series (30 % ethanol, 50 % ethanol, 70 % ethanol, 80 % ethanol, 95 % ethanol, 100 % ethanol, 100 % ethanol; 30 minutes each) to absolute ethanol. Tissue was cleared in HistoClear (30 minutes followed by 30 minutes in fresh HistoClear) and transferred to molten wax (30 minutes HistoClear/wax followed by 30 minutes in wax only, twice, at 70 °C). Tissue was then placed in moulds containing wax and allowed to set before cutting of five µm sections using a microtome and transferring of sections to slides.

Sections were dewaxed by briefly heating to 70 °C then placing in HistoClear (15 minutes). Slides were then rehydrated through graded alcohols (100 % ethanol, 100 % ethanol, 90 % ethanol, 80 % ethanol, 70 % ethanol, 50 % ethanol; 5 minutes each) and washed in tap water.

One of the following methods of antigen retrieval, or no antigen retrieval, was then carried out; incubation with Retrieval A (pH 6) or Retrieval B (pH 9.5) buffers (BD Pharmingen, BD Biosciences, San Jose, USA) at 95 °C for 10 minutes followed by cooling at room temperature for 20 minutes, incubation in 1 M citric acid pH 6 for 5-10 minutes in microwave (high) followed by cooling at room temperature for 20 minutes, incubation with 20 µg/ml protease (in PBS) for 15 minutes at room temperature, incubation with 20 µg/ml proteinase K (in PBS) for 15

minutes at room temperature or incubation with 1 mg/ml trypsin (in PBS) for 15 minutes at room temperature. Slides were then washed in tap water.

***Preparation of frozen sections of urinary tracts and treatments prior to blocking and the addition of antibodies***

Urinary tracts were dissected fully or partially from surrounding tissues and equilibrated in 30 % sucrose overnight at 4 °C before being embedded in Tissue Tek™ OCT (Tissue Tek™, Electron Microscopy Services, Hatfield, USA) (on dry ice) and were then stored at -80 °C. Eight µm sections were cut using a cryostat, mounted onto electrostatically charged glass slides, left at room temperature to dry for approximately 30 minutes and stored at -80 °C until the beginning of the staining procedure.

Prior to staining, sections were air dried for 30 minutes and were fixed either in methanol or acetone for 10 minutes at -20 °C, or left unfixed. Sections were washed in PBS (containing 100 mg/ml CaCl<sub>2</sub> and 100 mg/ml MgCl<sub>2</sub>), and then permeabilised in 0.5 % NP40 (in PBS containing 100 mg/ml CaCl<sub>2</sub> and 100 mg/ml MgCl<sub>2</sub>) and rinsed again in PBS (containing 100 mg/ml CaCl<sub>2</sub> and 100 mg/ml MgCl<sub>2</sub>).

***Quenching of endogeneous peroxidase activity and prevention of non-specific antibody binding***

Slides were incubated in 3 % hydrogen peroxidase (in water for paraffin sections; in PBS containing 100 mg/ml CaCl<sub>2</sub> and 100 mg/ml MgCl<sub>2</sub> for frozen sections) for 30 minutes at room temperature to block endogeneous peroxidase activity.



Paraffin embedded sections were then washed in tap water and rinsed in 0.1 % Tween (in PBS), whereas frozen sections were washed in PBS containing 100 mg/ml CaCl<sub>2</sub> and 100 mg/ml MgCl<sub>2</sub>.

When an avidin-biotin-HRP complex detection system was to be utilised (i.e. for Tshz1 immunohistochemistry) endogenous biotin was blocked by incubating slides in avidin (Dako) for 10 minutes, rinsing them, then incubating them in biotin (Dako) for 10 minutes.

To prevent non-specific binding of antibody, sections were incubated (for at least 30 minutes at room temperature in a humidity chamber) in blocking solution (10 % fetal calf serum, 2 % bovine serum albumin, 0.1 % Tween in PBS for paraffin sections; 1 % bovine serum albumin, 0.2 % triton X in PBS containing 100 mg/ml CaCl<sub>2</sub> and 100 mg/ml MgCl<sub>2</sub> for frozen sections).

### ***Application of antibodies***

Primary antibodies, diluted to an appropriate concentration in blocking solution, were applied to slides, which were then incubated overnight at 4 °C in a humidity chamber.

Slides were washed several times in 0.1 % Tween (in PBS) (paraffin sections) or PBS containing 100 mg/ml CaCl<sub>2</sub> and 100 mg/ml MgCl<sub>2</sub> (frozen sections) before addition of secondary antibody and incubated for 30 minutes at room temperature in a humidity chamber. For Tshz1 immunohistochemistry slides were washed again before incubation with HRP conjugated avidin-biotin complexes (ABC kit, Dako,

prepared according to manufacturers instructions) for 30 minutes at room temperature in a humidity chamber.

### ***Histochemical detection of HRP***

Slides were washed again and developed with diaminobenzidine. Slides were washed in tap water (paraffin sections) or PBS containing 100 mg/ml CaCl<sub>2</sub> and 100 mg/ml MgCl<sub>2</sub> (frozen sections), counterstained with periodic acid Schiff (PAS) and haematoxylin or haematoxylin alone, dehydrated through graded alcohols (50 % ethanol, 70 % ethanol, 80 % ethanol, 90 % ethanol, 100 % ethanol, 100 % ethanol; 5 minutes each), cleared in HistoClear (10 minutes) and mounted in DPX to be viewed with bright field microscopy.

### ***Photomicroscopy***

Slides were viewed, and photographs taken, using a Zeiss Axiophot2 upright microscope (Carl Zeiss) with Zeiss Plan-Neofluar objective lens (Carl Zeiss) and a ProgRes3012 scanning camera (Kontron Elektronik GmbH, Munich Germany). Images from the camera were imported from the camera directly into Photoshop (Version 5, Adobe Systems Europe, Edinburgh, UK) for image capturing and labelling.

### ***Control experiments to ensure specificity of antibody binding***

Negative control experiments to ensure that observed staining resulted from specific binding of the primary antibody its target protein were carried out for all antibodies used. When the immunising peptide for an antibody was available, negative control experiments in which the primary antibody was pre-absorbed with an excess (10x

concentration of antibody or, for Tshz3 antibody, as recommended by Sigma-Genosys; i.e. the equivalent of 10 µg/ml of peptide for a 1/200 dilution of serum) of its immunising peptide for 24 hours prior to the addition of the antibody to the slide were performed. When the immunising peptide for an antibody was not available, negative control experiments in which the primary antibody was omitted from the protocol were performed.

### ***Verification of observed staining patterns***

In addition to performing appropriate negative control experiments, where possible wildtype staining patterns observed were verified by comparison to published expression patterns in the literature. In almost all cases results were confirmed in more than one sample from genotype at each stage investigated. When this was the case, samples of each genotype were drawn from more than one litter.

### **Immunofluorescence**

Whole mount immunofluorescence was performed on embryonic ureters that had been dissected at E15 and cultured for six days. The method was based on the staining protocol published by Bush et al. (2006).

Ureters were fixed in 4 % paraformaldehyde for one hour, washed in PBS, then permeabilised in 0.25 % Triton X in PBS overnight. Ureters were incubated in 10 % fetal calf serum, 2 % bovine serum albumin, 0.1 % Tween (in PBS) for 24 hours prior to application of antibodies. Incubation with primary antibodies [rabbit anti-Up1b (gift from Tung Tien Sun) and anti- $\alpha$ SMA Cy3 conjugated (Sigma Aldrich Company Limited), both used at 1/100 dilution] was for two hours at room

temperature. Ureters were washed in PBS then incubated with secondary antibody for 1 hour (swine anti-rabbit, FITC conjugated, Dako, 1/20 dilution). Ureters were counterstained with Hoechst (2  $\mu\text{g}/\text{ml}$ ) and were imaged using a Leica DMRE microscope (Leica Microsystems) fitted with a TCS SP2 confocal head (Leica Microsystems) and Leica Confocal System imaging software (Leica Microsystems). Sequential scans (between frames) were used to image nuclei, Up1b and SMA. Optical sections were taken approximately every two  $\mu\text{m}$ . Sequential scans were utilised, and the imaging parameters chosen carefully, in order to help prevent bleed-through between signals. Details of imaging parameters can be found in Table 2.8.

**Table 2.8 Confocal Imaging Parameters**

<b>Fluorophore</b>	<b>Excitation wavelength (nm)</b>	<b>Collection wavelength range (nm)</b>	<b>Gain</b>	<b>Offset</b>
FITC	488	508-537	558	-3
Cy3	552	565-617	521	-4
Hoechst	UV light	400-462	508	-6

### **X-gal detection of $\beta$ -galactosidase activity**

Kidneys were dissected from *Tshz3*<sup>+/-</sup> adult mice and from wildtype outbred (CD1) adult mice (as negative controls). Kidneys were then washed in PBS and lightly fixed in 1 % paraformaldehyde for twenty minutes on ice. Kidneys were cut through the renal pelvis to give two halves, both of which contained cortex, medulla and papilla. The pieces of kidneys were washed three times in 2 mM MgCl<sub>2</sub>, 5 mM EGTA, 0.02 % Nonidet 40 (NP40) alternative, in calcium free (tissue culture grade) PBS for 30 minutes before incubating with X-gal staining solution for approximately 3 hours in the dark at 37 °C. X-gal staining solution comprised of 1 mg/ml 5-Bromo-4-chloro-3-indolyl- $\beta$ -galactopyranoside (X-gal), 5 mM K<sub>3</sub>Fe(CN)<sub>6</sub>, 5 mM K<sub>4</sub>(CN)<sub>6</sub>·3H<sub>2</sub>O, 2 mM MgCl<sub>2</sub>, 0.01 % sodium deoxycolate and 0.02 % NP40 which allows for optimal detection of the *lacZ* gene product whilst minimising background staining from endogenous galactosidase (Loughna et al., 1997; Loughna et al., 1998) (This is possible because endogenous galactosidases are active at acidic pHs, whereas *E.coli*  $\beta$ -galactosidase is active at neutral pHs (Weiss et al., 1997)).

Kidney pieces were then paraformaldehyde-fixed, paraffin embedded and sectioned as described for immunohistochemistry. Slides were either subject to immunohistochemistry using an anti- $\alpha$ SMA antibody (see Table 2.7) and counterstained with PAS, to compare the distribution of *Tshz3* positive cells with the expression of  $\alpha$ SMA. Slides were then viewed and photographed as described for immunohistochemistry.

### **Masson's trichrome histology**

Histological staining was performed on paraformaldehyde-fixed, paraffin-embedded tissue, which had been processed (in the same way as for immunohistochemistry) to produce 5 µm sections. Masson's trichrome staining was performed on these paraffin-embedded sections by Dyanne Rampling, Chief Biomedical Scientist, Department of Histopathology, Great Ormond Street Hospital, using the Gomoro one step trichrome (masson) method with Mayer's haematoxylin as a nuclear stain. This histological analysis allows the visualisation of red blood cells (light red), muscle and fibrin (red), collagen (blue/green) and nuclei (blue). Slides were then viewed and photographed as described for immunohistochemistry.

### **Phenotypic analysis of renal tracts from *Tshz3* null embryos**

The gross morphology of renal tracts of E18 *Tshz3*<sup>-/-</sup> embryos was investigated by viewing under a Stemi SV6 dissection microscope and whole-mount photographs were taken using a Olympus Camedia C-3030 zoom 3.3 megapixel camera mounted to this microscope, or photographs were taken of the renal tracts viewed under a Binocular Leica MZFL III dissecting microscope with a variable zoom lens (Leica Microsystems, Wetzlar, Germany) using a Nikon Dxm 1200 camera (Nikon, Tokyo, Japan).

### **Optical projection tomography**

Optical projection tomography imaging (OPT) of whole E18 kidneys was carried out by Julie Moss and Jane Armstrong in the laboratory of Jamie Davies (Centre of Integrative Physiology, University of Edinburgh), where this method of imaging biological specimens was first developed (Sharpe et al., 2002). In brief, visible light

was projected through a whole kidney, which had been embedded in transparent agarose gel. The kidney was rotated through 0.9 degrees and images of the projected light were recorded after each rotation of the specimen. After a total of 400 images were taken (i.e. after 360 degrees of rotation), a back-projection algorithm was used to reconstruct virtual sections through the specimen. The virtual sections could then be viewed individually, or used to create “fly-through” movies, by playing the virtual sections in sequence.

### **Injection of India ink into lumens of urinary tracts**

India ink was injected into the renal pelvis of E18 mice, which had their abdomens opened (after being dead for several hours) to reveal the kidneys, ureters and bladder (but which had not had the urogenital system itself disturbed) to visualise the urinary tract lumens. Several hundred  $\mu$ l of India Ink solution was injected using a pulled out Pasteur glass pipette, and gentle hydrostatic pressure was applied to push the ink through the ureter into the bladder. Photographs were taken of these renal tracts viewed under a Binocular Leica MZFL III dissecting microscope with a variable zoom lens, using a Nikon Dxm 1200 camera.

### **Detection and quantification of proliferating cells**

Proliferating cells were quantified *Tshz3*<sup>+/+</sup> and *Tshz3*<sup>-/-</sup> proximal ureters from E15 and E16 embryos by immunohistochemical staining for PCNA and counterstaining with haematoxylin. For each sample the number of PCNA positive cells, and the total number of cells were counted for each of the following cell populations in the proximal ureter: urothelium, condensing mesenchyme (the closely packed layer of mesenchymal cells, adjacent to the urothelium), loose mesenchyme (the loosely



packed mesenchymal cells, surrounding the condensing mesenchyme). The percentage of PCNA positive cells was calculated and SPSS was used to generate statistics.

### **Detection and quantification of apoptotic cells**

The number of apoptotic cells in *Tshz3*<sup>+/+</sup> and *Tshz3*<sup>-/-</sup> proximal ureters from E15 and E16 embryos was quantified using an *In-Situ* Death Detection kit (Roche, Basel, Switzerland), which utilises terminal deoxynucleotidyl transferase-mediated dUTP nick end labelling (TUNEL) technology.

TUNEL labelling was carried out on paraformaldehyde-fixed, paraffin-embedded tissue, which had been processed to produce five µm sections (as for immunohistochemistry) according to manufacturer's instructions using the trypsin pre-treatment method. Following the TUNEL labelling, sections were counterstained with Hoechst (2 µg/ml) and washed again in three times in PBS. Citifluor<sup>TM</sup> was added to the sections, and coverslips added and sealed with nail varnish. Sections were observed under an Zeiss AxioImager.M1 upright microscope with ZeissPlan-NEOFLUAR objective lens and a HBO100 ultraviolet light source. Photographs were taken using an integrated AxioMRm camera and Axiovision4.4 software.

Cells were identified as being apoptotic when they were TUNEL positive (fluorescence green) and had pyknotic nuclei (observed by characteristic morphology of nuclei stained blue with Hoesch). For each sample the number of apoptotic cells, and the total number of cells were counted for each of the following cell populations

in the proximal ureter: urothelium, condensing mesenchyme, loose mesenchyme.

Percentage of cells undergoing apoptosis was calculated and SPSS was used to perform statistical analyses.

## **Results Part I – Chapter Three**

### **Expression of *Tshz1*, 2 and 3, and *Larp* in kidneys and renal cell-lines**

#### **Introduction**

The aim of this first part of my thesis was to establish whether *Tshz* family genes, and one of their putative transcriptional targets, *Larp*, are expressed in the mouse kidney, and to characterise their expression patterns.

Initially I attempted to identify transcripts of these genes in RNA extracted from developing and mature kidneys and from renal cell lines, by reverse transcriptase PCR. I went on to compare the number of transcripts of these genes present at different developmental stages. This chapter details the results of these experiments and discusses them briefly.

#### **Results**

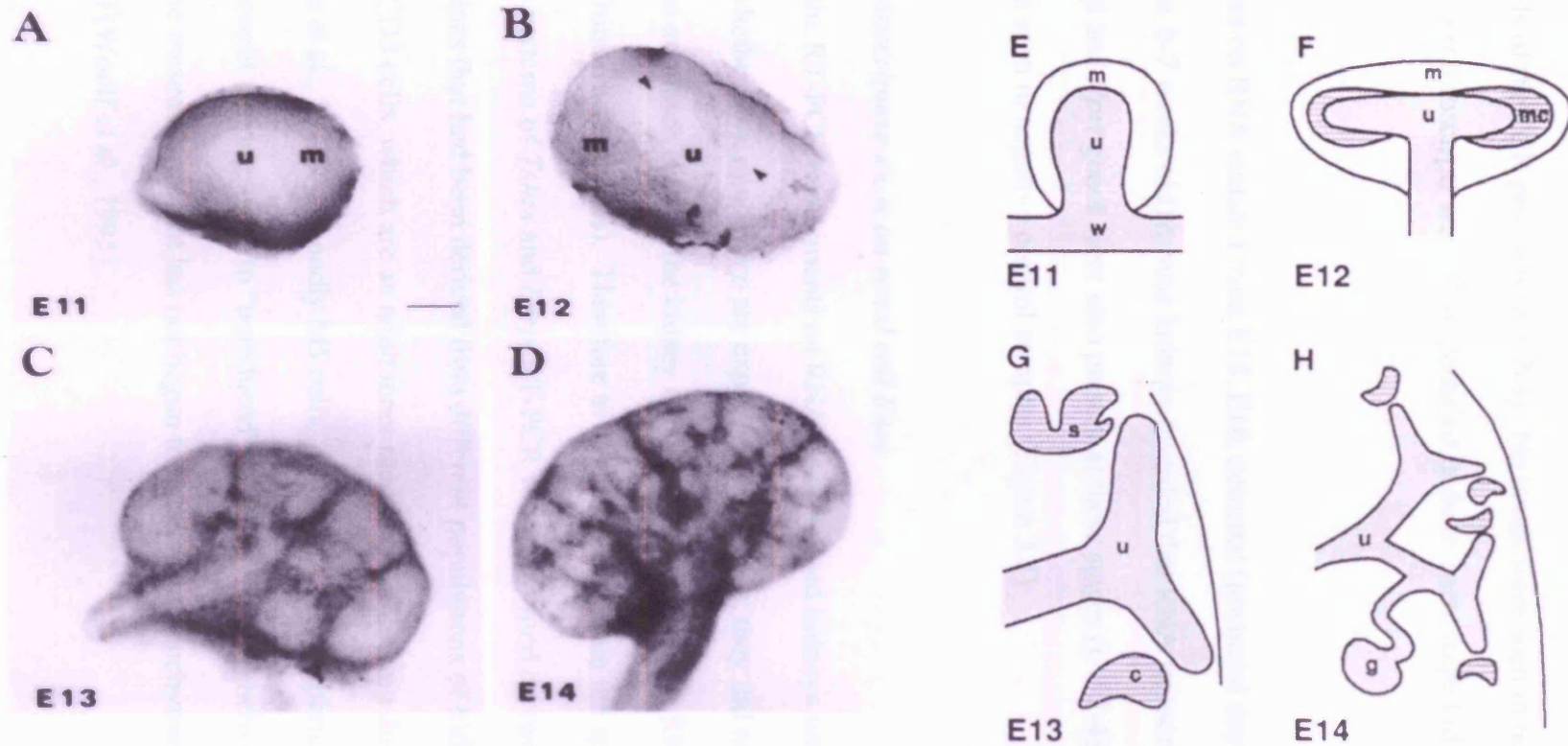
##### ***Reverse transcriptase PCR on embryonic and mature kidneys***

In order to investigate whether the *Tshz1*, 2 and 3, and *Larp* genes are expressed in mouse kidneys, and to investigate their temporal pattern of expression, I carried out reverse transcriptase Polymerase Chain Reaction (reverse transcriptase PCR, RT-PCR) on mouse metanephroi (kidneys; with ureters removed) isolated at different stages of development, ranging from embryonic day 11 (the day of inception of the metanephroi) to adult (mature kidneys from 6-7 week old male mice). Figure 3.1 illustrates the early stages of kidney development. Results were verified by carrying out each RT-PCR reaction on at least two independent samples of RNA (for each gene at each developmental stage).

### **Figure 3.1 Early development of the mouse kidney (metanephros)**

Reproduced from the **Journal of Cell Biology**, 1995: 128: 171-184. Copyright 1995 The Rockefeller University Press, with permission (Woolf et al., 1995). With thanks to the authors; A. Woolf, M. Kolatsi-Joannou, P. Hardman, E. Andermarcher, C. Moorby, L. Fine, P. Jat, M. Noble and E. Gherardi.

Stereomicroscopic images (**A-D**) and cross-sectional diagrams of the metanephros (**E-H**). E11 (**A** and **E**), E12 (**B** and **F**), E13 (**C** and **G**) and E14 (**D** and **H**) are shown. Note that the most primitive structures are located in the periphery of the E14 organ. Note also that the epithelial structures contained in developing kidneys after E14 (E15 – approximately postnatal day 14, not shown), are the same as at E14 (but they contain progressively a higher proportion of more developed structures as they grow, with primitive structures being restricted to the periphery). Arrowhead in **B** indicates the tips of the first branches of the ureteric bud. u – ureteric bud; m – mesenchyme; mc – mesenchymal condensate; c – comma-shaped body; s – S-shaped body; g – glomerulus; w – Wolffian duct. Scale bar - 50µm in **A-D**. **E-H** are not to scale.

**Figure 3.1**

Reproduced from the *Journal of Cell Biology*, 1995: 128: 171-184. Copyright 1995 The Rockefeller University Press

RNA transcripts of *Tshz1, 2 and 3* and *Larp* genes were detected in the metanephroi of E11 and E12 mice, as detected by the presence of bands of the predicted sizes on agarose gels of the PCR products (n = 2-3). No bands were seen in negative control samples. *Hprt* transcripts were also identified in these early stage kidneys (Figure 3.2).

Experiments on RNA isolated from E14, E18, neonatal (postnatal day zero, P0) and adult (male, 6-7 weeks old) mouse kidneys revealed that RNA transcripts of *Tshz1, 2 and 3, Larp* and *Hprt* genes were also present at these stages (n = 2-4). Again, no bands were seen in negative control samples (Figure 3.3).

#### ***Reverse transcriptase PCR on renal cell lines***

Although the RT-PCR experiments on RNA from isolated kidneys were useful to establish whether *Tshzs* and *Larp* are expressed in kidneys, they did not provide any information on which cells of the kidney expressed these genes (as RNA was extracted from whole organs). Therefore to begin to investigate the spatial expression patterns of *Tshzs* and *Larp*, RT-PCR was performed on two established renal cell lines that had been derived from different populations of kidney cells. Firstly IMCD3 cells, which are an adult inner medullary collecting duct cell line (Rauchman et al., 1993). Secondly M5 cells, which are a metanephric mesenchyme cell line thought to correspond to “uninduced” metanephric mesenchyme (that is metanephric mesenchyme that has not begun to undergo mesenchymal to epithelial transistion) (Woolf et al., 1995).

**Figure 3.2 Reverse transcriptase PCR for *Tshz1*, 2 and 3 and *Larp* on metanephric kidneys from E11 and E12 mice**

Agarose gels on which products from RT-PCR reactions have been run, along with a DNA ladder marker in the left-hand side lane of each gel. Bands are seen in RT+ (with reverse transcriptase) samples for each gene at E11 and E12, but not in RT- (without reverse transcriptase) samples (which served as negative controls). *Hprt* was used as a positive control. Bands were observed at the expected size for each primer set; 467bp of *Tshz1*, 418bp for *Tshz2*, 506bp for *Tshz3*, 296bp for *Larp* and 354bp for *Hprt*. Therefore *Tshz1-3* and *Larp* are expressed in kidneys of E11 and E12 mice.

Figure 3.2

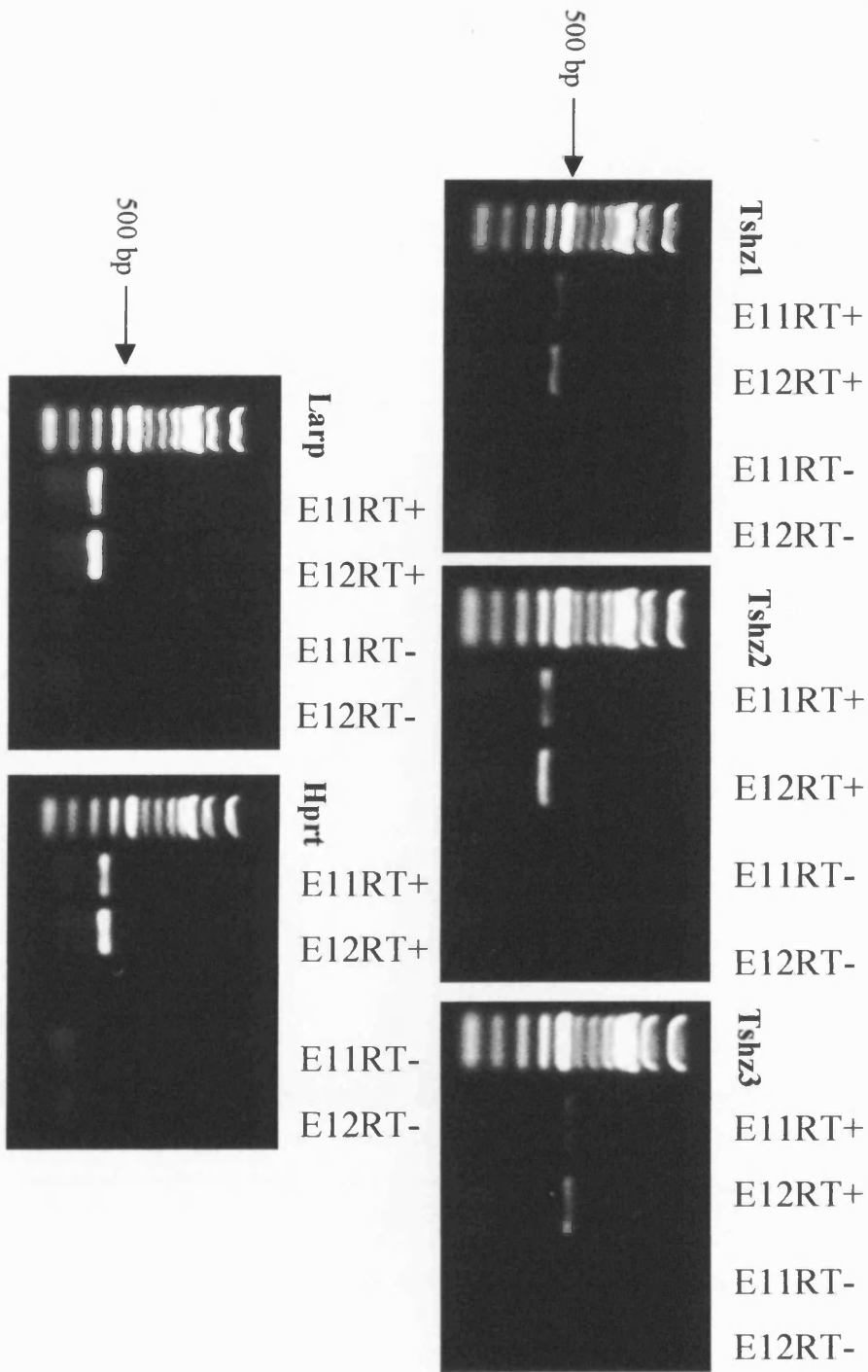




**Figure 3.3 Reverse transcriptase PCR for *Tshz1*, 2 and 3 and *Larp* on kidneys from E14, E18, neonatal and adult mice**

Agarose gels on which products from RT-PCR reactions have been run. Bands are seen in RT+ samples for each gene at E14, E18, neonatal and adult stages, but not in RT- samples (which served as negative controls). *Hprt* was used as a positive control. Bands were observed at the expected size for each primer set; 467bp of *Tshz1*, 418bp for *Tshz2*, 506bp for *Tshz3*, 296bp for *Larp* and 354bp for *Hprt*. Therefore *Tshz1-3* and *Larp* are expressed in kidneys of E14, E18, neonatal and adult mice.

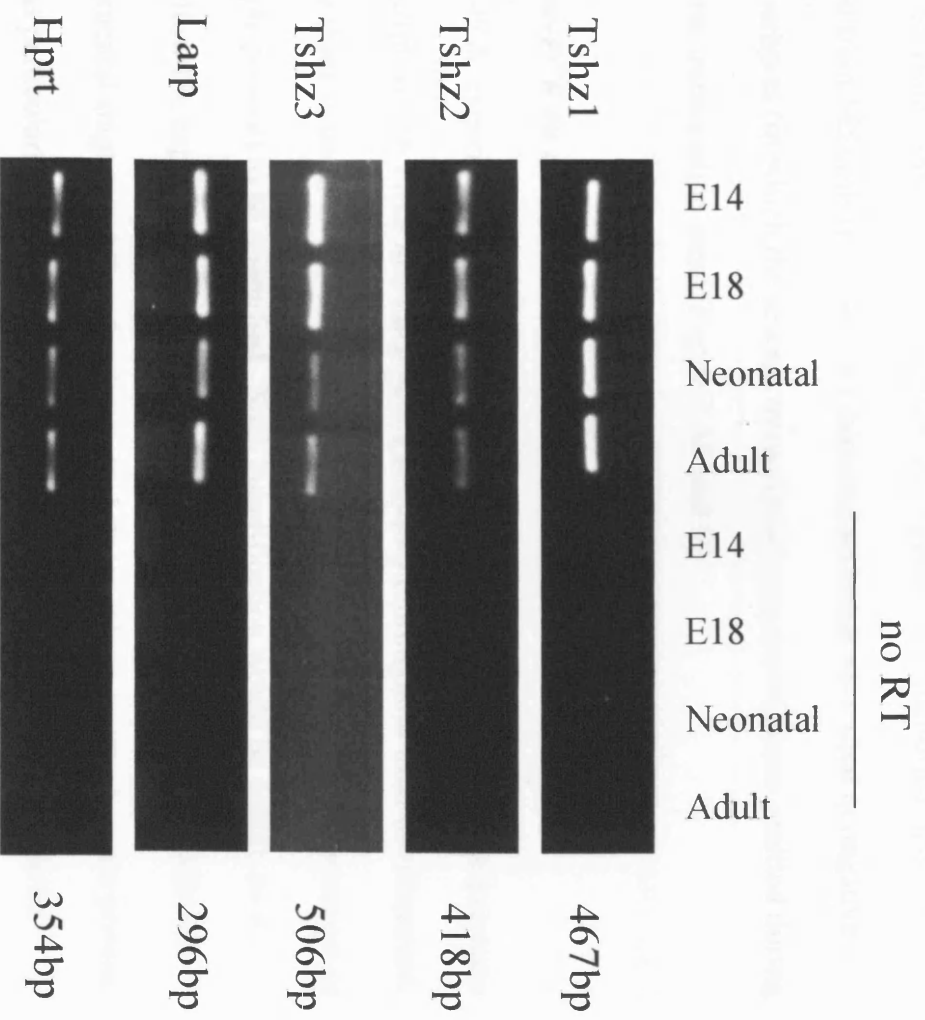


**Figure 3.3**

*Tshz1*, *Larp* and *Hprt* transcripts were identified in RNA extracted from IMCD3 cells, but no transcripts of *Tshz2* and *3* genes were identified (n= 2-3). As expected no bands were seen in negative control samples (in which the reverse transcriptase enzyme had been omitted during the reverse transcription step) (Figure 3.4A and C).

Transcripts from *Tshz1*, *2* and *3*, *Larp* and *Hprt* genes were identified in RNA extracted from M5 cells (n = 3-4). As expected no bands were seen in negative control samples (in which the reverse transcriptase enzyme had been omitted during the reverse transcription step) (Figure 3.4B and D).

#### ***Real time-PCR on embryonic and mature kidneys***

The RT-PCR experiments on RNA from isolated kidneys had revealed the presence of transcripts of the *Tshzs* and *Larp* genes in kidneys throughout their development, however these experiments did not allow the levels of expression (ie the numbers of transcripts present) to be quantified. Such quantification would be useful, as it would allow the expression levels of the genes to be compared between different developmental stages, and thus developmental stages where expression of a certain gene was particularly high to be identified, which may allow hypotheses to be formed as to the function of these genes.

**Figure 3.4 Reverse transcriptase PCR for *Tshz1*, 2 and 3 and *Larp* on renal cell lines**

**A** Phase contrast image of IMCD3 cells, note their typical epithelial morphology.

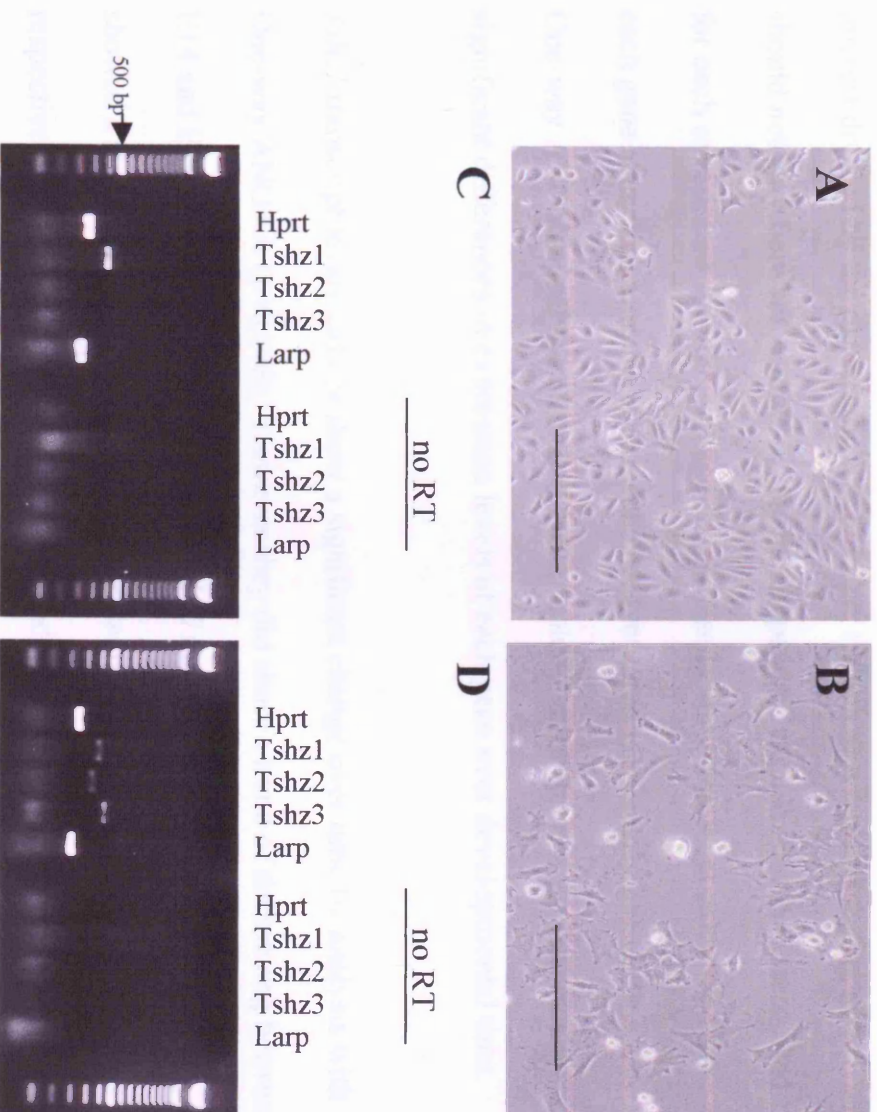
**B** Phase contrast image of M5 cells, note their typical mesenchymal morphology.

**C** and **D** Agarose gels on which products from RT-PCR reactions for *Tshz1-3* and *Larp* have been run, along with a DNA ladder marker in the left-hand side and right-hand side lanes of each gel. *Hprt* was used as a positive control. Samples without reverse transcriptase (no RT) were used as a negative control. Where bands were observed, they were seen at the expected size for each primer set; 467bp of *Tshz1*, 418bp for *Tshz2*, 506bp for *Tshz3*, 296bp for *Larp* and 354bp for *Hprt*.

**C** RT-PCR on RNA extracted from IMCD3 cells. Bands are observed for *Hprt*, *Tshz1* and *Larp*. Therefore IMCD3 cells express *Tshz1* and *Larp*, but not *Tshz2* or *Tshz3*. **D** RT-PCR on RNA extracted from M5 cells. Bands are observed for *Hprt*, *Tshz1*, *Tshz2*, *Tshz3* and *Larp*. Therefore M5 cells express *Tshz1*, *Tshz2*, *Tshz3* and *Larp*. Scale bars - 300µm.

to establish whether *Tshz1*, *Tshz2*, and *Tshz3* require a specific developmental signal for their expression. To address this question, we generated a *lacZ* reporter construct under the control of the *Tshz1* promoter and injected it into embryos at the blastula stage. The expression of the reporter was assessed by whole-mount in situ hybridization (WISH) in embryos at the blastula and gastrula stages. The results are shown in Figure 3.4. The *Tshz1* promoter-reporter construct was expressed in the blastula and gastrula stages of the embryo, indicating that the *Tshz1* promoter is active in these stages.

### Figure 3.4



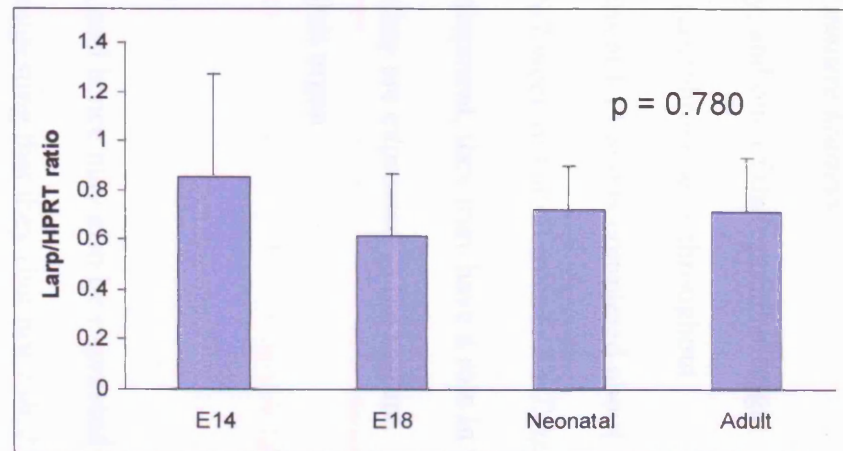
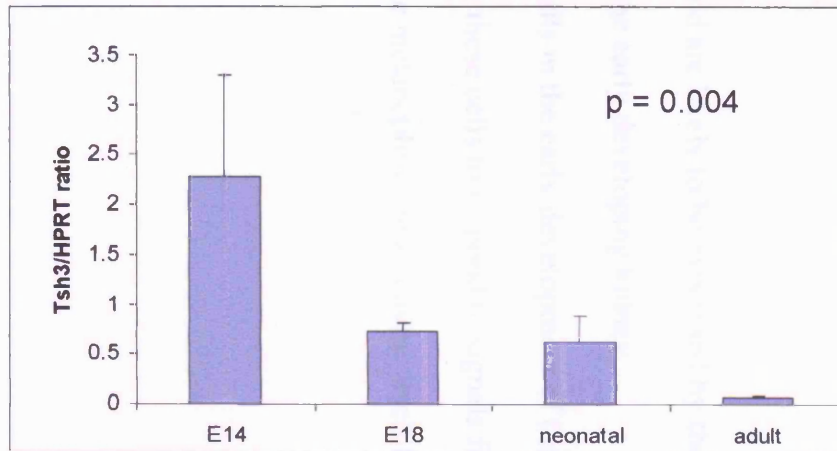
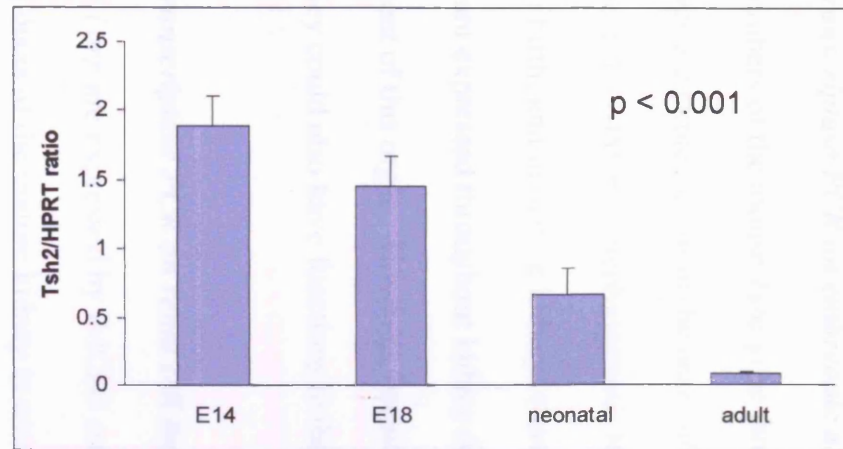
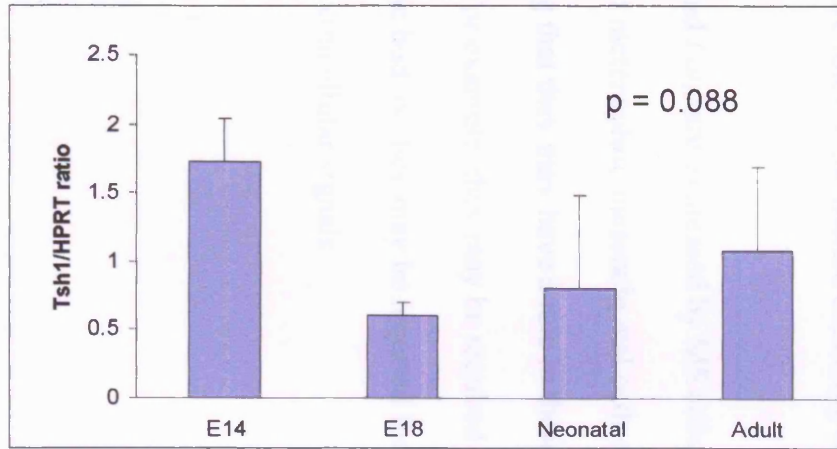
To establish whether *Tshz1*, 2 and 3, and *Larp* expression are developmentally regulated in the kidneys, I compared levels of expression of these genes between different developmental stages by performing Real Time-PCR for *Tshz1-3* and *Larp* on E14, E18, neonatal and adult kidneys. Expression levels were standardised for each sample, by being expressed as a ratio of the expression level of the gene of interest divided by the expression level of *Hprt* (which as a house-keeping gene should not vary between samples). Three independent samples of RNA were used for each experiment, and the average standardised expression level calculated for each gene at each timepoint. The results are presented graphically in Figure 3.5. One-way ANOVA analysis was used to ascertain whether there were statistically significant differences in expression levels of each gene over developmental time.

*Tshz1* transcript levels did not show a significant change over time by analysis with One-way ANOVA ( $p=0.088$ ). However they did show a trend of decreasing between E14 and E18, then increasing into adulthood. *Tshz2* and 3 transcript levels both showed a significant change over developmental time ( $p<0.001$  and  $p=0.004$  respectively), decreasing from E14 to adulthood. *Larp* expression levels do not vary significantly ( $p= 0.780$ ) over developmental time.

**Figure 3.5 Real Time PCR for *Tshz1*, 2 and 3 and *Larp* on kidneys from E14, E18, neonatal and adult mice**

Results of Real-Time PCR comparing average expression levels of each gene at different developmental stages. (Expression levels were standardised against Hprt expression.) P-values show the results of One Way Anova. Error bars show standard deviation. n=3 in each group. **A** Expression levels of *Tshz1* do not vary significantly over time, however there is a trend of decreasing expression levels during embryonic stages, followed by an increase in expression as kidneys mature. **B** Expression levels of *Tshz2* vary significantly over time ( $p < 0.001$ ), decreasing between E14 and adulthood. **C** Expression levels of *Tshz3* vary significantly over time ( $p = 0.004$ ), decreasing between E14 and adulthood. **D** Expression levels of *Larp* do not vary significantly over time. *Larp* expression levels appear to vary very little between different developmental stages.

**Figure 3.5**





## **Interpretation and Discussion**

### ***Reverse transcriptase PCR on embryonic and mature kidneys***

All the members of the mouse *Tshz* gene family, and one of their putative target genes, *Larp*, are expressed from the onset of metanephrogenesis throughout development (E11-P0; metanephrogenesis begins at E11 and is completed about 1 week after birth) and in mature kidneys (from 6-7 week old adult mice). As *Tshzs* and *Larp* are expressed throughout kidney development, they may have a role in the development of this organ. However, because they are expressed in the mature kidney, they could also have functions in the adult organ.

### ***Reverse transcriptase PCR on renal cell lines***

*Tshz1* and *Larp* are expressed by IMCD3 cells, and hence may also be expressed in collecting ducts of the mature kidney *in vivo*, suggesting that they (but not *Tshz2* and 3) may have roles in the mature collecting duct.

*Tshz1-3* and *Larp* are expressed by M5 cells, and are likely to be expressed by the uninduced metanephric mesenchymal cells of the early developing kidney, suggesting that they may have a role in these cells in the early development of the kidney. For example, they may be required for these cells to respond to signals from the ureteric bud, or they may be required for the metanephric mesenchyme itself to produce extracellular signals.

***Real time-PCR on embryonic and mature kidneys***

The trend of *Tshz1* transcript levels decreasing between E14 and E18, then increasing into adulthood suggests that this gene may be important both during development and in the mature kidney.

The significant decrease of *Tshz2* and *3* transcript levels from E14 to adulthood suggests that these genes may be required for development, and that expression levels in adults are very low and may not be biologically relevant.

The lack of variation of *Larp* expression is not suggestive of a developmental role for this gene; however neither does it exclude such a role.

### Summary of results in Chapter Three

1. *Tshz1*, 2 and 3, and *Larp* are expressed in mouse metanephric kidneys, at E11 (the day of their inception), throughout their development and in adulthood.
2. A renal cell line derived from uninduced mouse metanephric mesenchyme expresses *Tshz1*, 2 and 3, and *Larp*.
3. A renal cell line derived from adult mouse inner medullary collecting ducts expresses *Tshz1* and *Larp*.
4. The expression of *Tshz2* and *Tshz3* in the kidneys is developmentally regulated, with expression levels high in embryonic stages, and lower in neonatal and mature kidneys.

## Results part I - Chapter Four

### Raising and characterising antibodies against Tshz1, 2 and 3

#### Introduction

The aim of this first part of my thesis was to establish whether *Tshz* family genes, and one of their putative transcriptional targets, *Larp*, are expressed in the mouse kidney, and to characterise their expression patterns.

In the previous chapter, I showed that *Tshz1*, 2 and 3, and *Larp*, transcripts were expressed in the developing kidney. However the presence of a transcript does not necessarily mean that it is translated to produce protein (Mata et al., 2005), and therefore when investigating gene expression protein as well as mRNA should be analysed. In order to investigate expression of genes at the protein level, specific antibodies raised against the proteins the genes encode (or peptides components of the proteins) are required. When I began these experiments there were no antibodies available commercially against Tshz2 and Tshz3. There was one antibody available commercially (from Cemines, Golden, USA) against Tshz1, but it failed to demonstrate specific reactivity against Tshz1 protein in preliminary immunohistochemistry and western blotting experiments (as assessed by comparison of the reactivity of the antibody alone with the reactivity of the antibody pre-absorbed with the immunising peptide).

Therefore I decided to raise antibodies to epitopes of the Tshz1, Tshz2 and Tshz3 proteins. I then undertook experiments to characterise the specificity of the antibodies produced and attempted to use them to investigate the expression of the

*Tshz* gene family at the protein level. This chapter details the characterisation of the antibodies that I raised and describes ongoing attempts to use these antibodies to investigate the expression of Tshz proteins in the developing urinary tract.

## **Results**

### ***Design and generation of antibodies***

Antibodies against synthetic peptides corresponding to epitopes of the proteins encoded by the mouse *Tshz* gene family were raised by Sigma Genosys as described in the Methods of this thesis. For antibodies raised in rabbit, serum isolated from the final bleed was used in the subsequent experiments; whereas for the antibody raised in chicken, IgY purified from egg yolks was used.

### ***Characterising antibody reactivity and specificity***

To test the reactivity and specificity of the antibodies that had been raised, I overexpressed Tshz family proteins in HEK293 cells by transient transfection. These cells were used in western blotting and immunocytochemistry experiments. GFP was over-expressed in HEK293 cells to use as an over-expressed negative control protein in these experiments; additionally, untransfected HEK293 cells were used as a negative control. All the proteins that were overexpressed in HEK293 cells were tagged with a cMyc epitope (EQKLISEEDL; Myc tag), enabling the overexpressed proteins to be identified with an anti-(c)Myc antibody.

*Transfected HEK293 express Myc-tagged proteins, as determined by Western blotting*

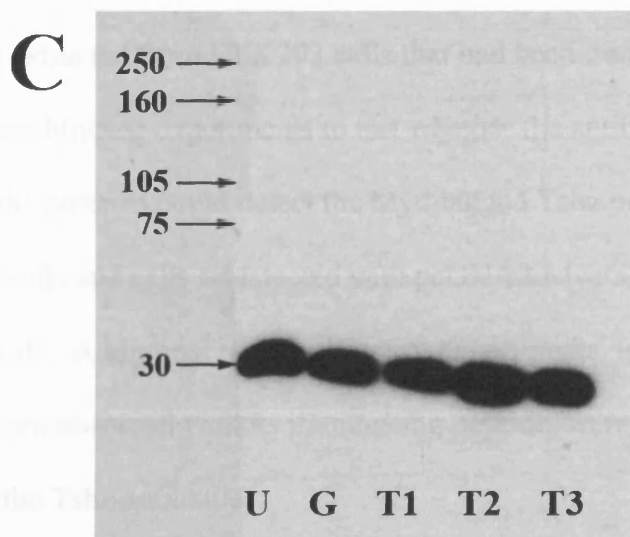
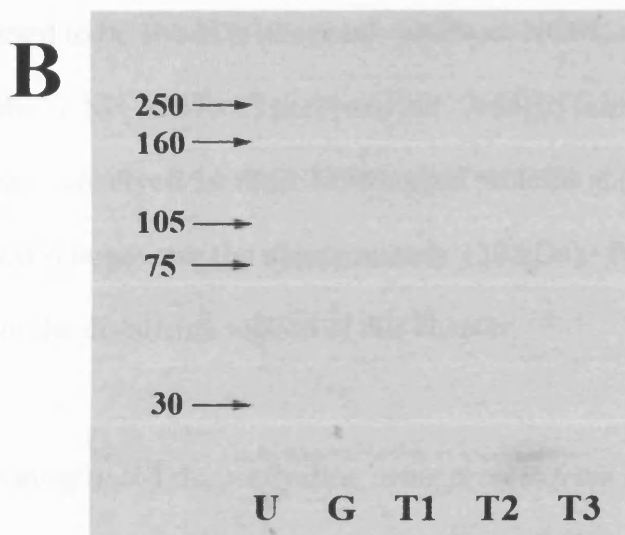
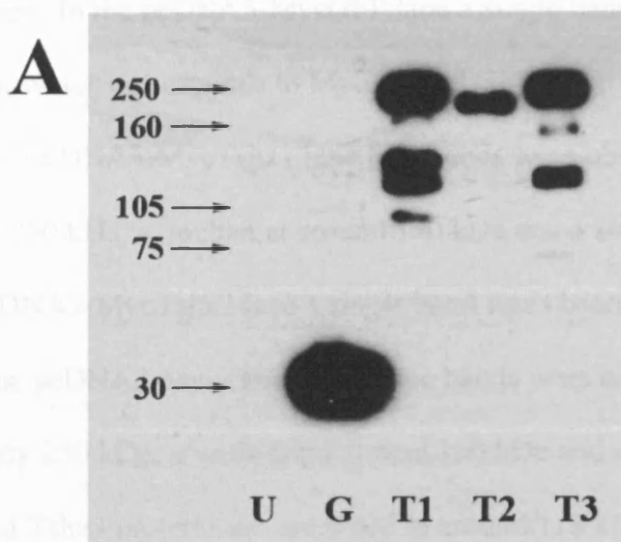
Protein extracted from HEK293 cells that had been transfected with the following plasmid DNAs were subjected to SDS-PAGE and transferred by electroblotting to nitrocellulose paper for western blot analysis; no plasmid, pcDNA3-MycGFP, pcDNA3-MycTshz1, pcDNA3-MycTshz2, pcDNA3-MycTshz3. I used anti-Myc antibody to detect whether Myc-tagged proteins were present in the cell extracts. A negative control experiment, in which the primary antibody was pre-absorbed with its immunising peptide, was run to check the specificity of the anti-Myc antibody.

When probed with anti-Myc antibody, bands were seen in lanes in which protein from pcDNA3-MycGFP, pcDNA3-MycTshz1, pcDNA3-MycTshz2, pcDNA3-MycTshz3 transfected cells had been loaded, but no bands were seen in the lane in which protein from untransfected cells had been loaded (Figure 4.1). No bands were observed when the anti-Myc antibody had been pre-absorbed with immunising peptide. Probing the blot with an anti- $\beta$  actin antibody verified loading of (at least approximately) equal amounts of protein in each lane (Figure 4.1).

#### **Figure 4.1 Transfected cells express Myc-tagged proteins**

Western blots showing that transfected HEK293 cells express Myc-tagged proteins. 20  $\mu\text{g}$  of protein was loaded in each lane. An indication of approximate protein sizes (in kDa) is given on the left-hand side of each blot. **A** Western blots using anti-Myc antibody show that Myc-tagged proteins (seen as bands) are present in extracts from pcDNA3-MycGFP (G), pcDNA3-MycTshz1 (T1), pcDNA3-MycTshz2 (T2) and pcDNA3-MycTshz3 (T3) transfected cells, but are not present in extracts from untransfected (U) cells. **B** No bands are seen in a western blot using anti-Myc antibody that has been pre-absorbed with immunising peptide (after 1 hour exposure time), indicating that bands seen in **A** are the result of specific binding of primary antibody to the Myc-tagged proteins. **C** Western blot probed with anti- $\beta$ -actin antibody demonstrates equal loading of protein in each lane.

**Figure 4.1**





These results indicate that the anti-Myc antibody is reactive against the Myc-tagged proteins, and that the transfections had been successful and had led to the expression of the transgenes. In the pcDNA3-MycGFP lane a single band was observed at around 30 kDa, which corresponds to Myc-tagged GFP (GFP is 27 kDa; Prasher et al. 1992). In the pcDNA3-MycTshz1 lane four bands were observed; a strong band at approximately 250 kDa, a doublet at around 130 kDa and a single band at around 90 kDa. In the pcDNA3-MycTshz2 lane a single band was observed between 160 and 250 kDa. In the pcDNA3-MycTshz3 lane three bands were observed; a strong band at approximately 250 kDa, a weak band around 160 kDa and a band at around 120 kDa. Tshz1 and Tshz3 proteins are predicted to around 118 kDa in size, whereas Tshz2 is predicted to be 108 kDa (Genbank database, NCBI; accession number NP\_001074769[Tshz1], NP\_536703[Tshz2] and NP\_758502[Tshz3]). However the major bands that I observed for these Myc-tagged proteins appeared to correspond to proteins of a much larger size (by approximately 130 kDa). Possible reasons for this are discussed in the discussion section of this chapter.

*Testing reactivity of anti-Tshz antibodies, using protein from transfected HEK293 cells*

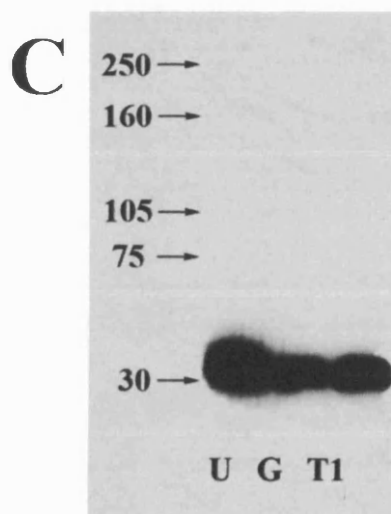
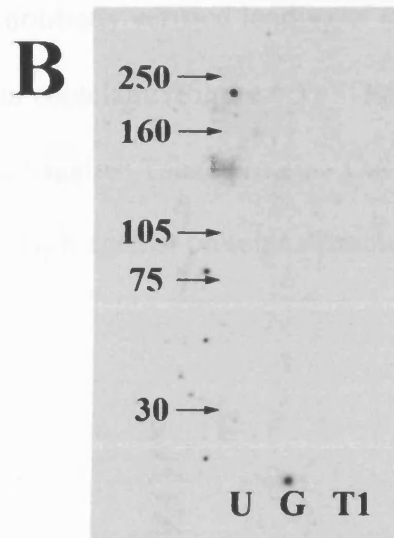
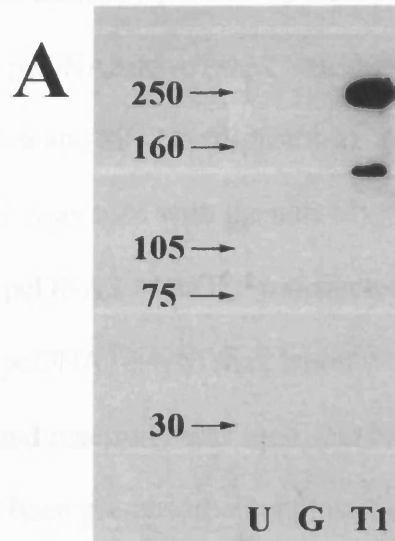
I used protein extracted from HEK293 cells that had been transfected with plasmid DNA in western blotting experiments to test whether the antibodies that I had raised against the Tshz proteins could detect the Myc-tagged Tshz proteins. Protein from untransfected cells and cells transfected with pcDNA3-MycGFP were used as negative controls. Additional negative control experiments, in which the primary antibody was pre-absorbed with its immunising peptide, were run to check the specificity of the Tshz antibodies.

The chicken anti-Tshz1 antibody shows strong reactivity against two proteins present in the extract from the pcDNA3-MycTshz1 transfected cells; one approximately 250 kDa in size, and the other (which was sometimes seen as a doublet; Figure 4.5) approximately 130 kDa in size (Figure 4.2). This banding pattern is very similar to that seen using the anti-Myc antibody (Figure 4.1), except that the doublet seen at around 130 kDa with the anti-Myc antibody is sometimes seen as a single band, and the band at 90 kDa is not seen. No bands were seen in lanes in which protein from untransfected or pcDNA3-MycGFP transfected cells had been run. No bands were observed when the anti-Tshz1 antibody had been pre-absorbed with immunising peptide. Probing the blot with an anti- $\beta$  actin antibody verified loading of (at least approximately) equal amounts of protein in each lane (Figure 4.2). These data indicate that the anti-Tshz1 antibody reacted against Tshz1 protein which is probably represented by the band seen at 250 kDa, but may also be represented by the band at 130 kDa.

**Figure 4.2 Anti-Tshz1 antibody is reactive against Myc-tagged Tshz1 protein**

Western blots showing that anti-Tshz1 antibody reacts against proteins extracted from pcDNA3-MycTshz1 transfected HEK293 cells. 50  $\mu$ g of protein was loaded in each lane. An indication of approximate protein sizes (in kDa) is given on the left-hand side of each blot. **A** Western blots using anti-Tshz1 antibody: bands are seen in the lane in which protein extracted from pcDNA3-MycTshz1 transfected cells has been run (T1), but not in lanes in which protein from pcDNA3-MycGFP transfected (G) and untransfected (U) cells have been run. **B** No bands are seen in a western blot probed with anti-Tshz1 antibody that has been pre-absorbed with immunising peptide (after 1 hour exposure time), indicating that bands seen in **A** are the result of specific binding of primary antibody to Myc-tagged Tshz1. **C** Western blot probed with anti- $\beta$ -actin antibody demonstrates equal loading of protein in each lane.

**Figure 4.2**

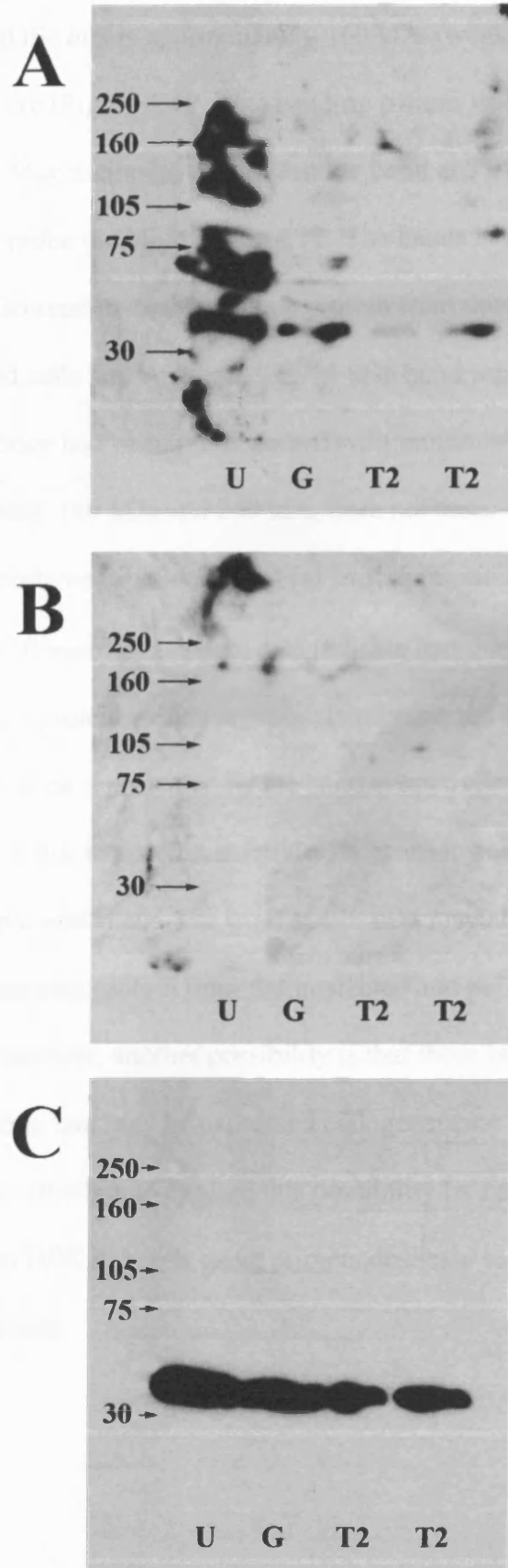


The rabbit anti-Tshz2 antibody showed no clear reactivity against proteins present in the extract from the pcDNA3-MycTshz2 transfected cells, although weak bands are seen at around 50 kDa and 80 kDa (Figure 4.3). No band at between 160 kDa and 250 kDa was seen, as was seen with the anti-Myc antibody (Figure 4.1). Lanes in which protein from pcDNA3-MycGFP transfected cells had been run gave similar banding patterns to pcDNA3-MycTshz2 lanes, whereas in the untransfected cells lane much background reactivity was seen. No bands were observed when the anti-Tshz2 antibody had been pre-absorbed with immunising peptide. Probing the blot with an anti- $\beta$  actin antibody verified loading of (at least approximately) equal amounts of protein in each lane (Figure 4.3). These data indicate that the anti-Tshz2 antibody did not react against Tshz2 protein. Only non-specific reactivity was seen, this was particularly high against proteins extracted from untransfected cells.

**Figure 4.3 Anti-Tshz2 antibody is not reactive against Myc-tagged Tshz2 protein**

Western blots showing that anti-Tshz2 antibody does not react against proteins extracted from pcDNA3-MycTshz2 transfected HEK293 cells. 80  $\mu$ g of protein was loaded in each lane. An indication of approximate protein sizes (in kDa) is given on the left-hand side of each blot. **A** Western blots using anti-Tshz2 antibody: no strong bands are seen in the lanes in which protein extracted from pcDNA3-MycTshz2 transfected cells has been run (T2), indicating that anti-Tshz2 antibody is not reactive against Myc-tagged Tshz2 protein. Some bands are seen in lanes in which protein from pcDNA3-MycGFP transfected (G) and untransfected (U) cells has been run, and are particularly strong for protein from untransfected cells, indicating that anti-Tshz2 antibody shows some non specific reactivity. **B** No bands are seen in a western blot probed with anti-Tshz2 antibody that has been pre-absorbed with immunising peptide (after 1 hour exposure time). **C** Western blot probed with anti- $\beta$ -actin antibody demonstrates equal loading of protein in each lane.

**Figure 4.3**



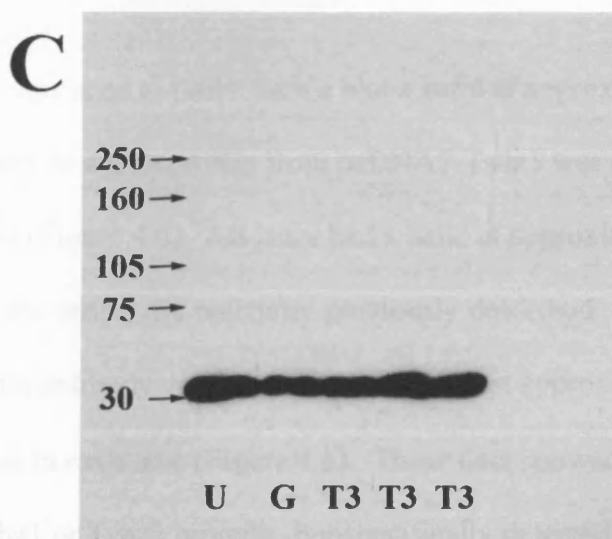
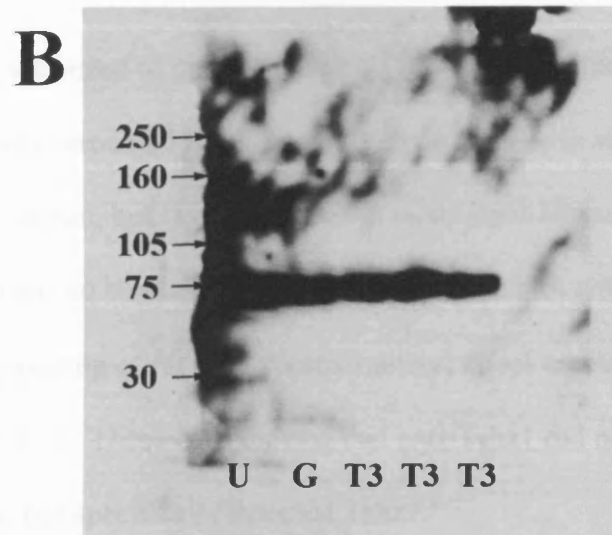
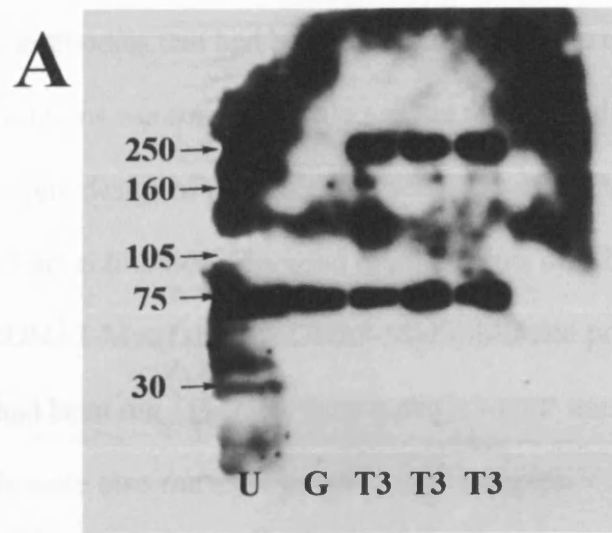
The rabbit anti-Tshz3 antibody showed reactivity against four proteins present in the extract from the pcDNA3-MycTshz3 transfected cells; one (strong) approximately 250 kDa in size, and the others approximately 160 kDa (weak) 120 kDa (weak) and 75 kDa (strong) in size (Figure 4.4). This banding pattern was very similar to that seen using the anti-Myc antibody, except that the band at 75 kDa was not seen when anti-Myc is used to probe the blot (Figure 4.1). The bands at approximately 120 kDa and 75 kDa were also seen in lanes in which protein from untransfected or pcDNA3-MycGFP transfected cells had been run. The 75 kDa band was also observed when the anti-Tshz3 antibody had been pre-absorbed with immunising peptide, but the bands at approximately 160 kDa and 250 kDa were not seen. Probing the blot with an anti- $\beta$  actin antibody verified loading of (at least approximately) equal amounts of protein in each lane (Figure 4.4). These data indicate that the anti-Tshz3 antibody reacted against Tshz3 protein, which is probably represented by the band at around 250 kDa and may also be represented by the band at approximately 160 kDa. The band at 75 kDa is not due to specific reactivity, because it was also seen when the antibody has been pre-absorbed. The band at 120 kDa may also not be specific, as it is seen in lanes containing protein from untransfected and pcDNA3-MycGFP transfected cells. However, another possibility is that these bands represented (human) Tshz3 protein that may be expressed endogeneously by these cells. In the future it would be worthwhile to explore this possibility by carrying out RT-PCR on RNA extracted from HEK293 cells using primers designed to specifically amplify human *Tshz3* transcripts.



#### **Figure 4.4 Anti-Tshz3 antibody is reactive against Myc-tagged Tshz3 protein**

Western blots showing that anti-Tshz3 antibody reacts against proteins extracted from pcDNA3-MycTshz3 transfected HEK293 cells. 50  $\mu$ g of protein was loaded in each lane. An indication of approximate protein sizes (in kDa) is given on the left-hand side of each blot. **A** Western blots using anti-Tshz3 antibody: bands are seen at approximately 160 kDa and 250 kDa in the lane in which protein extracted from pcDNA3-MycTshz3 transfected cells has been run (T3; note protein from three separate batches of pcDNA3-MycTshz3 transfected cells was run in three separate lanes), but not in lanes in which protein from pcDNA3-MycGFP transfected (G) and untransfected (U) cells have been run. Additionally bands at approximately 75 kDa and 120 kDa are seen in all lanes. **B** Bands at approximately 75 kDa are seen in a western blot probed with anti-Tshz3 antibody that has been pre-absorbed with immunising peptide (after 1 hour exposure time), indicating that bands at 75 kDa seen in **A** are the result of specific non specific binding. No bands are seen at around 160 kDa or 250 kDa, indicating that these bands seen in **A** are the result of specific binding of primary antibody to Myc-tagged Tshz3. **C** Western blot probed with anti- $\beta$ -actin antibody demonstrates equal loading of protein in each lane.

**Figure 4.4**



*Anti-Tshz1 and Anti-Tshz3 antibodies are specifically reactive against the Tshz of interest, they do not react with other Tshz protein family members*

To ensure that the antibodies that had been found to be capable of detecting the presence of Tshz proteins were reactive only against the particular Tshz family member that they were designed to detect, I performed western blotting experiments in which the anti-Tshz antibodies were used to probe blots on which protein extracted from pcDNA3-MycTshz1, pcDNA3-MycTshz2 and pcDNA3-MycTshz3 transfected cells had been run. Extracts from pcDNA3-GFP transfected and untransfected cells were also run as negative control samples.

When anti-Tshz1 was used to probe such a blot a band at approximately 250 kDa, and a doublet band at around 130 kDa were seen in the lane in which protein from pcDNA3-Tshz1 was run, but it was not seen in other lanes (Figure 4.5). In fact, all other lanes contained no bands whatsoever. Probing the blot with an anti- $\beta$  actin antibody verified loading of (at least approximately) equal amounts of protein in each lane (Figure 4.5). These data showed that anti-Tshz1 did not react with Tshz2 or Tshz3 proteins, but specifically detected Tshz1.

When anti-Tshz3 was used to probe such a blot a band at approximately 250 kDa was seen in the lane in which protein from pcDNA3-Tshz3 was run, but it was not seen in other lanes (Figure 4.6). All lanes had a band at approximately 75 kDa, corresponding to the unspecific reactivity previously described. Probing the blot with an anti- $\beta$  actin antibody verified loading of (at least approximately) equal amounts of protein in each lane (Figure 4.6). These data showed that anti-Tshz3 did not react with Tshz1 or Tshz2 proteins, but specifically detected Tshz3.

**Figure 4.5 Anti-Tshz1 antibody does not react against Tshz2 and Tshz3 proteins**

Western blots showing that anti-Tshz1 antibody reacts specifically against Myc-tagged Tshz1 protein, but does not detect Myc-tagged Tshz2 or Myc-tagged Tshz3 proteins. 50  $\mu$ g of protein was loaded in each lane. An indication of approximate protein sizes (in KDa) is given on the left-hand side of each blot. **A** Western blot probed with anti-Tshz1 antibody. Bands are seen in the lane in which protein extracted from pcDNA3-MycTshz1 transfected cells has been run (T1), but not in lanes in which protein from pcDNA3-MycTshz2 (T2), pcDNA3-MycTshz3 (T3), pcDNA3-MycGFP transfected (G) or untransfected (U) cells has been run. **B** Western blot probed with anti- $\beta$ -actin antibody demonstrates equal loading of protein in each lane.

**Figure 4.5**

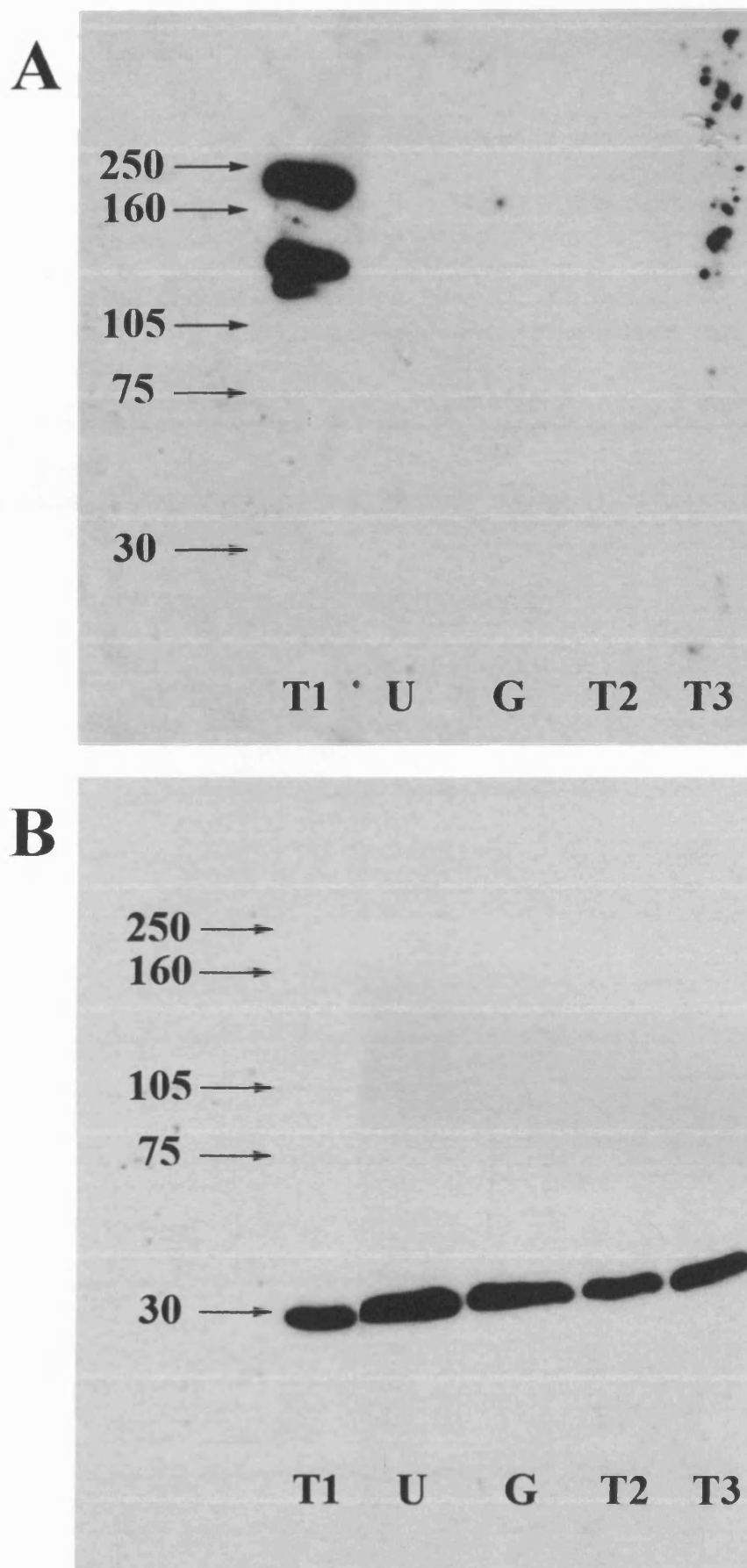
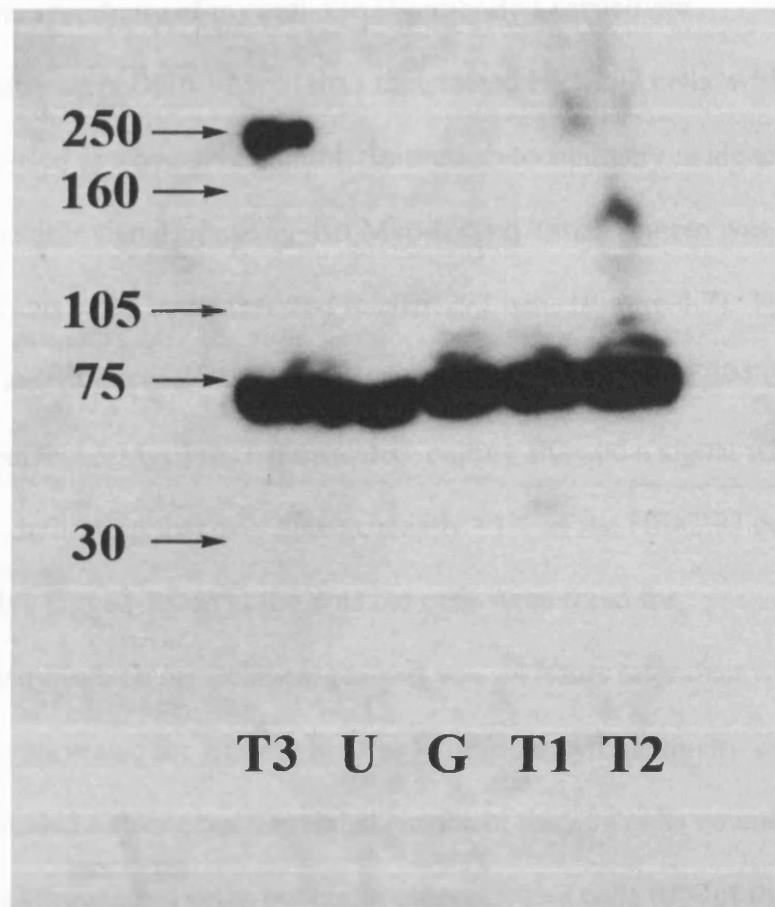


**Figure 4.6 Anti-Tshz3 antibody does not react against Tshz1 and Tshz2 proteins**

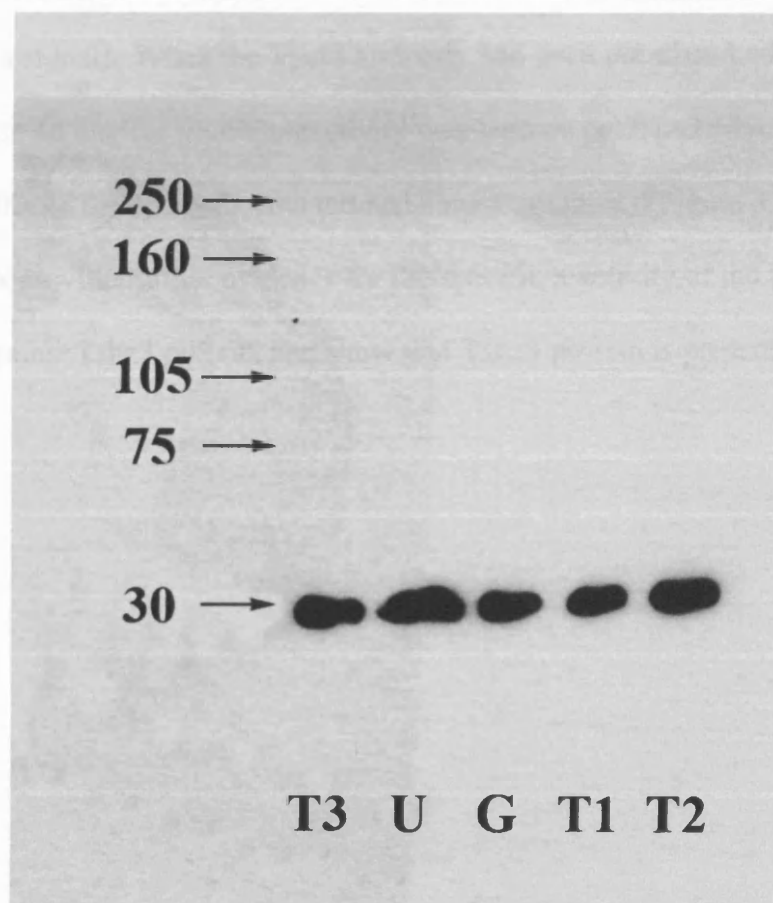
Western blots showing that anti-Tshz3 antibody reacts specifically against Myc-tagged Tshz3 protein, but does not detect Myc-tagged Tshz1 or Myc-tagged Tshz2 proteins. 50  $\mu$ g of protein was loaded in each lane. An indication of approximate protein sizes (in KDa) is given on the left-hand side of each blot. **A** Western blot probed with anti-Tshz3 antibody. A specific band at approximately 250 kDa is seen in the lane in which protein extracted from pcDNA3-MycTshz3 transfected cells has been run (T3), but not in lanes in which protein from pcDNA3-MycTshz1 (T1), pcDNA3-MycTshz2 (T2), pcDNA3-MycGFP transfected (G) or untransfected (U) cells has been run. **B** Western blot probed with anti- $\beta$ -actin antibody demonstrates equal loading of protein in each lane.

**Figure 4.6**

**A**



**B**



### *Testing reactivity of anti-Tshz3 antibody in immunocytochemistry experiments*

To further verify the specificity of my anti-Tshz3 antibody I carried out immunocytochemistry on pcDNA3-MycTshz3 transfected HEK293 cells, with untransfected cells used as a negative control. Immunocytochemistry using anti-Myc revealed a strong nuclear signal, showing that Myc-tagged Tshz3 protein was localised in the nucleus when overexpressed in HEK293 cells (Figure 4.7). No signal was seen in any of the 450 untransfected cells counted. 45 out of 394 cells counted from the pcDNA3-MycTshz3-transfected culture showed a signal with the anti-Myc antibody, indicating that only approximately 11% of the HEK293 cells were expressing Myc tagged Tshz3 at the time the cells were fixed for immunocytochemistry (which for technical reasons was 24 hours later than when protein was usually harvested for western blotting). Immunocytochemistry using anti-Tshz3 also revealed a strong nuclear signal (in 4% of the 304 cells counted) in pcDNA3-MycTshz3 transfected cells, but not in untransfected cells (0% of the 458 cells counted had a signal). When the Tshz3 antibody had been pre-absorbed with immunising peptide no nuclear immunoreactivity was seen on pcDNA3-Myc Tshz3 transfected cells (0% of the 459 cells counted had a nuclear signal) (Figure 4.7). These experiments provide further evidence for the specific reactivity of the anti-Tshz3 antibody against Tshz3 protein, and show that Tshz3 protein is present in the nucleus.

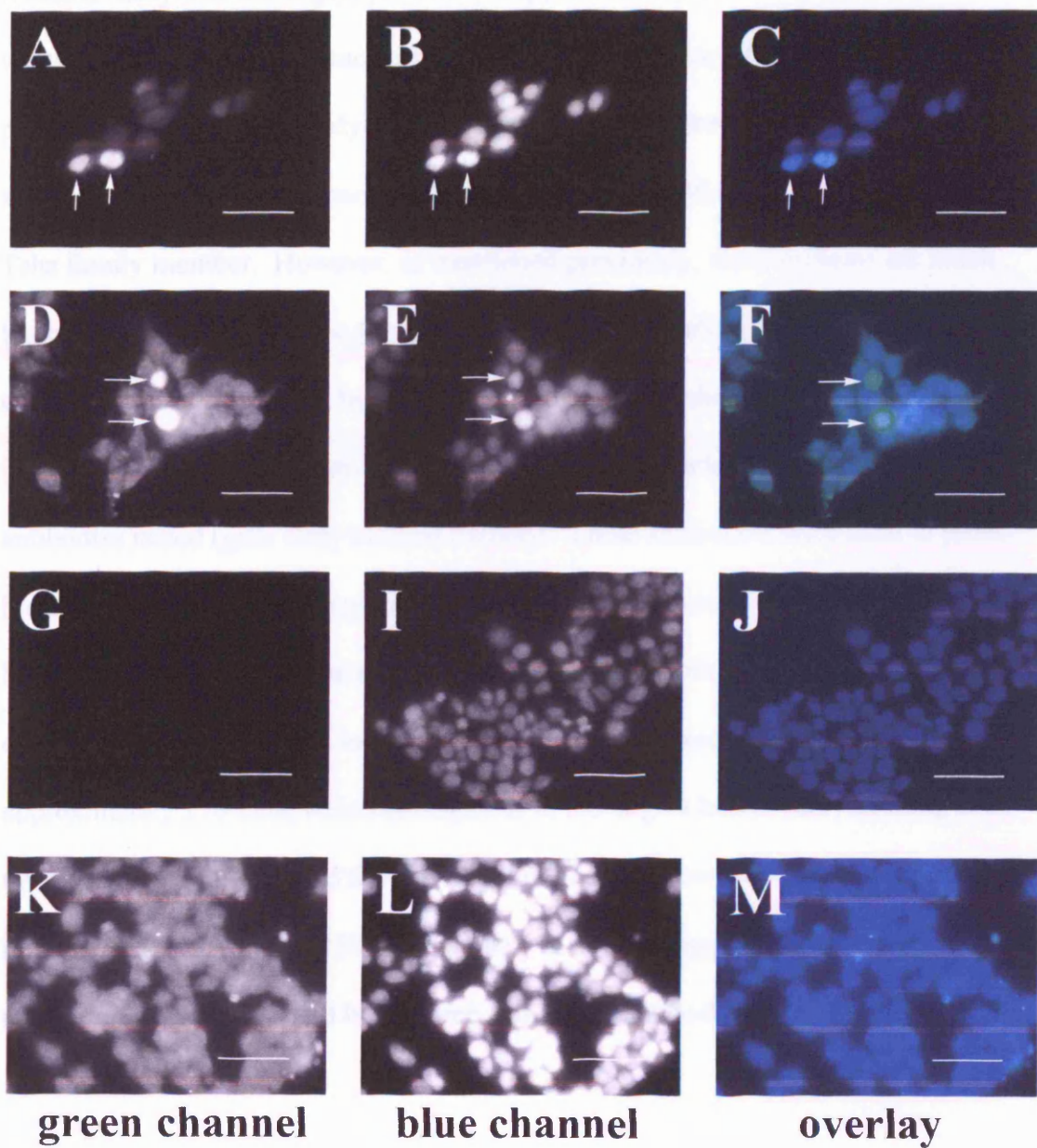


#### **Figure 4.7 Immunocytochemistry on cells transfected with pcDNA3-MycTshz3**

HEK293 cells were transfected with pcDNA-MycTshz3 and used for immunocytochemistry, with anti-Myc and anti-Tshz3 primary antibodies, and FITC (green) conjugated secondary antibodies. Untransfected cells were used as a negative control. Hoeschst was used to stain all nuclei blue. Cells were observed using a UV microscope with a x40 objective lens. **A, D, G** and **K** Cells viewed using filters to allow observation of FITC (green) signal. **B, E, I** and **L** Cells viewed using filters to allow observation of Hoechst (blue) signal. **C, F, J** and **M** Overlay of green and blue signals. **A-C** Cells transfected with pcDNA3-MycTshz3 stained using anti-Myc primary antibody. Two of the cells show green nuclear staining (arrows) indicating that these cells express Myc-tagged Tshz3 protein. **D-F** Cells transfected with pcDNA3-MycTshz3 stained using anti-Tshz3 primary antibody. Two of the cells show green nuclear staining (arrows) indicating that these cells express Myc-tagged Tshz3 protein, which can be detected by the anti-Tshz3 antibody (N.B. the bright cell in **E**, indicated by the lower arrow, shows some bleed-through from the green to the blue channel). **G-J** Untransfected stained using anti-Tshz3 primary antibody. No FITC signal is observed as the untransfected cells do not contain Tshz3 protein. **K-M** Cells transfected with pcDNA3-MycTshz3 stained using anti-Tshz3 primary antibody that has been pre-absorbed with immunising peptide. No green nuclear staining is seen, indicating that green nuclear signal seen in **D-F** is the result of anti-Tshz3 antibody binding specifically to Myc-tagged Tshz3 protein.

Scale bars - 50µm.

**Figure 4.7**



***Tshz3 protein is approximately 250 kDa in size, as observed by western blotting using three different antibodies***

It seems likely that the largest proteins (of approximately 250 kDa) observed on western blots of protein extracted from cells overexpressing Myc-tagged Tshz proteins correspond to the Myc tagged Tshz proteins, as these bands are the strongest, and are the only band observed (with the anti-Myc antibody) for every Tshz family member. However, as mentioned previously, these proteins are much larger than the predicted size for the Tshz proteins. Therefore I sought verification of the size of Tshz3 protein by using two different anti-Tshz3 antibodies, one raised in rabbit and the other in guinea-pig, that had become available since I had had my antibodies raised (gifts from Laurent Fasano). These antibodies were used to probe blots on which protein from pcDNA3-MycTshz3 transfected cells (and pcDNA3-MycGFP transfected cells as a control) had been run. Both of these antibodies detected several proteins of various sizes, and notably detected a protein of approximately 250 kDa, which corresponds to the largest band observed using both my anti-Tshz3 antibody and the anti-Myc antibody (Figure 4.8) Therefore, this protein (of approximately 250 kDa) is likely to be Myc-tagged Tshz3, as it is the only protein that is detected by all three anti-Tshz3 antibodies.

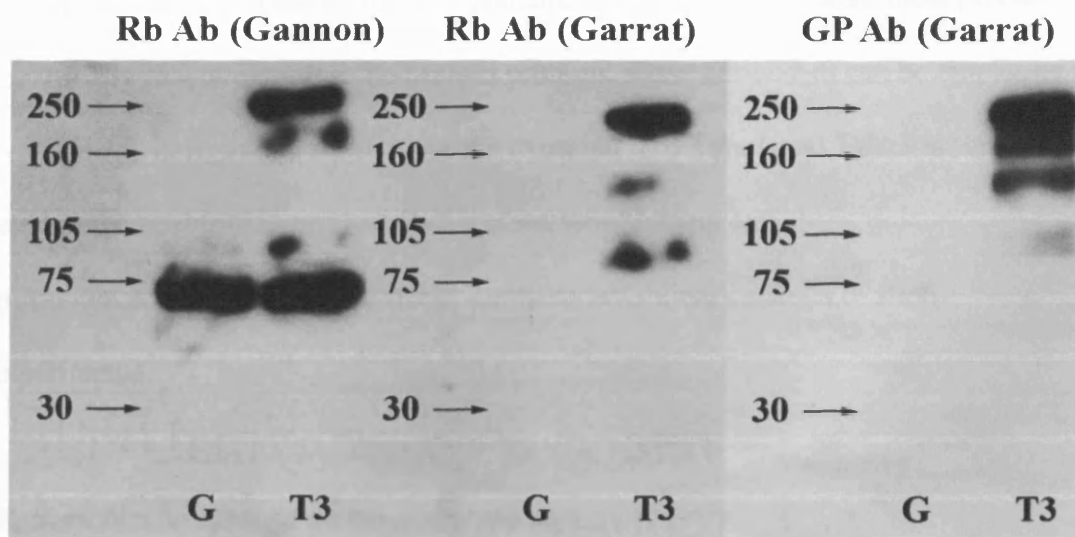
**Figure 4.8 Western blotting for Tshz3 using three different anti-Tshz3 antibodies**

Western blots using three different anti-Tshz3 antibodies, showing that all anti-Tshz3 antibodies react against a protein, of approximately 250 kDa in size. 50  $\mu$ g of protein was loaded in each lane. An indication of approximate protein sizes (in kDa) is given on the left-hand side of each blot. **A** Western blots using three different anti-Tshz3 antibodies. With all antibodies a band is seen at approximately 250 kDa in the lane in which protein extracted from pcDNA3-MycTshz3 transfected cells has been run (T3), but not in lanes in which protein from pcDNA3-MycGFP transfected (G) has been run. All antibodies also detect smaller proteins in the lane in which pcDNA3-MycTshz3 has been run, but antibodies do not give the same banding pattern as one another. **B** Western blots probed with anti- $\beta$ -actin antibody demonstrates equal loading of protein in each lane.

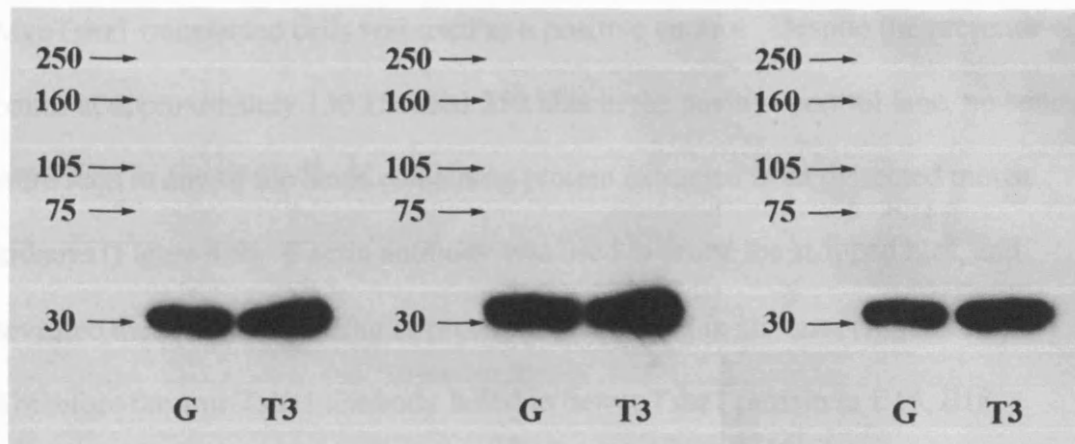
Rb (Gannon); rabbit anti-Tshz3 generated by Sigma-Genosys. Rb (Garrat); rabbit anti-Tshz3 generated by A. Garrat and obtained from L. Fasano. GP (Garrat); rabbit anti-Tsh3 generated by A. Garrat and obtained from L. Fasano. For details of epitopes against which these antibodies were raised see Figure 4.4 (in methods).

# Figure 4.8

## A



## B



***Using anti-Tshz1 and anti-Tshz3 antibodies to investigate the expression of Tshz proteins in urinary tract tissue***

Because characterisation of the antibodies that I had raised against epitopes of Tshz proteins revealed that the anti-Tshz1 and anti-Tshz3 antibodies were most probably specifically reactive against their target proteins, these antibodies can be employed in experiments designed to investigate the expression of Tshz1 and Tshz3 at the protein level in the developing urinary tract (by western blotting and immunohistochemistry). This thesis contains preliminary results of such experiments.

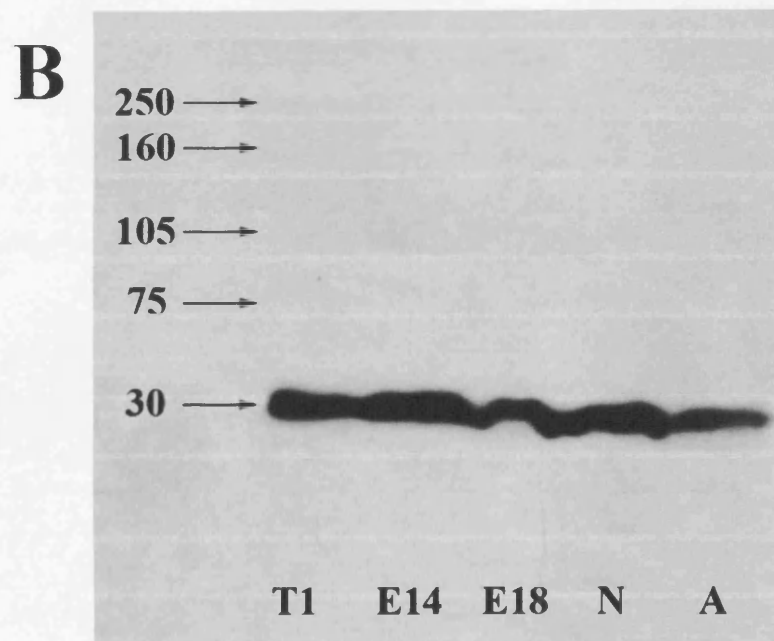
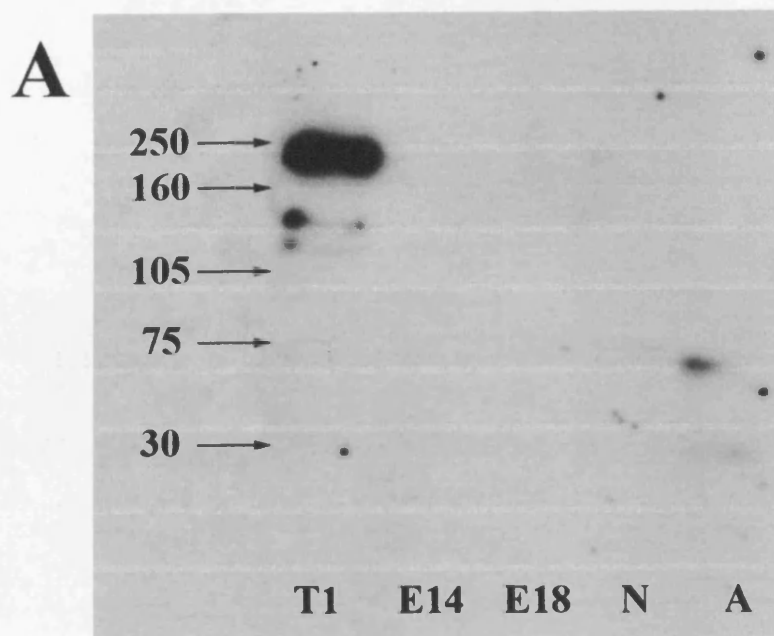
***Western blots on mouse urinary tract tissue***

I used anti-Tshz1 antibody to probe western blots on which protein extracted from E14, E18, neonatal and adult kidneys had been run. Protein from pcDNA3-MycTshz1 transfected cells was used as a positive control. Despite the presence of bands at approximately 130 kDa and 250 kDa in the positive control lane, no bands were seen in any of the lanes containing protein extracted from dissected mouse kidneys (Figure 4.9).  $\beta$  actin antibody was used to probe the stripped blot, and revealed that efficient loading of protein had occurred in all lanes (Figure 4.9). Therefore the anti-Tshz1 antibody failed to detect Tshz1 protein in E14, E18, neonatal or adult kidneys (despite high amounts, 200  $\mu$ g, of protein being loaded in each lane).

**Figure 4.9 Western blot for Tshz1 on kidney tissue**

200  $\mu$ g of protein extracted from dissected kidneys from mice of various ages (E14, E18, neonatal and adult) was run on a western blot. Protein from HEK293 transfected with pcDNA3-MycTshz1 was used as a positive control. An indication of approximate protein sizes (in kDa) is given on the left-hand side of each blot. **A** No bands are detected in lanes in which protein extracted from E14, E18, neonatal (N) or adult (A) kidneys has been run, although bands are seen in the lane in which positive control protein (T1) has been run. Therefore Tshz1 protein is undetectable by this method in kidneys from E14, E18, neonatal or adult mice. **B** Western blot probed with anti- $\beta$ -actin antibody demonstrates equal loading of protein in each lane.

**Figure 4.9**



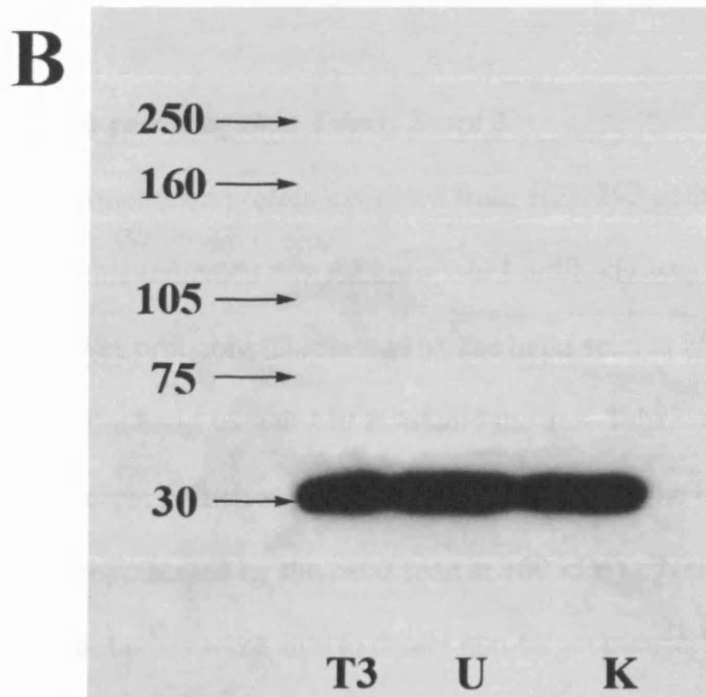
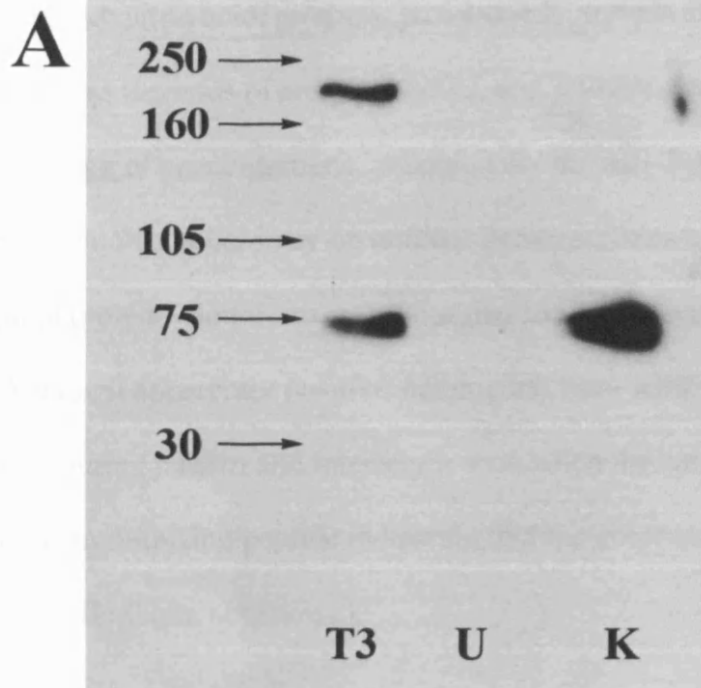


I used anti-Tshz3 antibody to probe western blots on which protein extracted from E14 kidneys and E18 ureters had been run. E14 kidneys were chosen, as Real Time-PCR experiments had shown that Tshz3 transcripts were expressed most highly in kidneys at this stage of development. E18 ureters were chosen as experiments using a *lacZ* reporter mouse suggested that Tshz3 is expressed highly in this tissue (see Chapter Five). Protein from pcDNA3-MycTshz3 transfected cells was used as a positive control. Despite the presence of bands at approximately 75 kDa and 250 kDa in the positive control lane, no bands were seen in the lane containing protein from E18 ureters, and only a band at approximately 75 kDa was seen in the lane containing protein from E14 kidneys (Figure 4.10). It seems likely that the band at 75 kDa in the E14 kidney lane represents non-specific binding, since I have shown (earlier in this chapter) that the anti-Tshz3 antibody reacts unspecifically to a protein of approximately this size. However, confirmation that this is the case is required (by using the anti-Tshz3 antibody pre-absorbed with the immunising peptide as a negative control).  $\beta$  actin antibody was used to probe the stripped blot, and revealed that efficient loading of protein had occurred in all lanes (Figure 4.10). Therefore the anti-Tshz3 antibody probably failed to detect Tshz3 protein in E14 kidneys or E18 ureters (despite high amounts of protein being loaded in each lane: 300  $\mu$ g of protein from E14 kidneys and 200  $\mu$ g of protein from E18 ureters) although the possibility that the band seen at approximately 75 kDa in the E14 kidney lane may be specific requires further investigation.

**Figure 4.10 Western blot for Tshz3 on kidney and ureter tissue**

300  $\mu\text{g}$  of protein extracted from kidneys of E14 mice and 200  $\mu\text{g}$  of protein extracted from ureters of E18 mice was run on a western blot. Protein from HEK293 transfected with pcDNA3-MycTshz3 was used as a positive control. An indication of approximate protein sizes (in kDa) is given on the left-hand side of each blot. **A** No bands are detected in lanes in which protein extracted from E14 kidneys (K) or E18 ureters (U) has been run (except for a band at approximately 75 kDa in lane K, which is likely to be non-specific as this antibody has been shown to react in a non-specific manner to a protein of this size, see Figure 6.4), although bands are seen in the lane in which positive control protein (T3) has been run. Therefore Tshz3 protein is undetectable by this method in kidneys from E14 mice or ureters from E18 mice. **B** Western blot probed with anti- $\beta$ -actin antibody demonstrates equal loading of protein in each lane.

**Figure 4.10**



### *Immunohistochemistry on mouse urinary tract tissue*

I have also used anti-Tshz1 and anti-Tshz3 antibodies for immunohistochemistry on paraffin embedded E14 and E18 kidneys and proximal ureters. A variety of protocols have been tried: citric acid, protease, proteinase K, trypsin and retreivagen buffers have been tried as methods of antigen retrieval, and primary antibodies have been used at a wide range of concentrations. Additionally the anti-Tshz3 antibody has been used for immunohistochemistry on unfixed frozen sections of E14 and E18 kidneys and proximal ureters. So far, no specific signal has been detected using either antibody. Although apparently positive staining has been seen with some protocols, the same staining pattern and intensity is seen when the antibody has been pre-absorbed with the immunising peptide indicating that the observed staining patterns were not specific (Data not shown).

## **Discussion**

### ***Reactivity of antibodies raised against Tshz1, 2 and 3***

Western blotting experiments on protein extracted from HEK293 cells expressing Myc-tagged Tshz proteins indicated that the anti-Tshz1 antibody was able to detect Tshz1 protein (which was probably represented by the band seen at 250 kDa, may also be represented by the band seen at 130 kDa) and the anti-Tshz3 antibody was able to detect Tshz3 protein (which was probably represented by the band seen at 250 kDa, may also be represented by the band seen at 160 kDa). Neither the anti-Tshz1 or anti-Tshz3 antibodies were able to detect non-target mouse Tshz proteins in western blotting experiments, and therefore these antibodies should provide useful tools for the specific detection of Tshz1 and Tshz3 proteins.

When using the anti-Tshz3 antibody in western blotting experiments a band was seen at 120 kDa in lanes containing protein from untransfected and pcDNA3-MycGFP transfected cells as well as those containing protein from pcDNA3-MycTshz3 transfected cells. This band may represent endogenous (human) Tshz3 protein that may be expressed by HEK293 cells. In order to gain insight into this possibility an RT-PCR could be performed on RNA extracted from untransfected HEK293 cells to see whether they do indeed express *Tshz3*. Whether or not HEK293 cells do express *Tshz3*, the ability of the anti-Tshz3 antibody to detect human Tshz3 should be investigated further, as if the antibody is reactive against human Tshz3 protein it could provide a useful tool for investigating *Tshz3* expression in human samples. Indeed, the epitope of Tshz3 against which the anti-Tshz3 antibody was raised is highly conserved between mouse and human (the human protein sequence can be found in Genbank, NCBI; accession number Q63HK5), with only one out of fourteen amino acids being different between the species. Therefore there is high probability that the anti-Tshz3 antibody would be reactive against human Tshz3 protein. In contrast the epitope against which the anti-Tshz1 antibody was raised is not well conserved between mouse and humans, with only seven out of the fourteen amino-acids being identical (the human protein sequence can be found in Genbank, NCBI; accession number NP\_005777). Therefore it is very unlikely that the anti-Tshz1 antibody would be reactive against human Tshz1 protein.

The anti-Tshz2 antibody did not display reactivity against Tshz2 protein, as no band was seen at the size identified by the anti-Myc antibody to correspond to Myc-tagged Tshz2. Lack of observed reactivity was despite loading high amounts (80 µg) of protein in each lane and using the antibody at a high concentration (1/200 dilution).

Non-specific reactivity was seen, particularly against proteins extracted from untransfected cells. As the anti-Tshz2 antibody that I raised does not detect Tshz2 protein in order to investigate whether Tshz2 is present in the developing mouse urinary tract (or indeed elsewhere in the mouse) another antibody should be designed, raised and characterised.

### ***Tshz3 is a nuclear protein***

Immunocytochemistry experiments using anti-Myc and anti-Tshz3 antibody to probe HEK293 cells that had been transfected with pcDNA3-MycTshz3 showed that Tshz3 protein is localised to the nucleus. As discussed in the introduction of this thesis Tshz3 is a protein that contains zinc-finger motifs and a homeodomain, and therefore is a putative transcription factor (Manfroid et al., 2004). Furthermore, it has been shown to be able to act as a transcriptional repressor in mammalian cell culture (Manfroid et al., 2004) and its homologue in *Drosophila* has been shown to bind to DNA (Alexandre et al., 1996).

### ***Western blot banding patterns and size of Tshz proteins***

Tshz1 and Tshz3 proteins are predicted to be around 118 kDa in size, whereas Tshz2 is predicted to be 108 kDa (Genbank database, NCBI; accession number NP\_001074769[Tshz1], NP\_536703[Tshz2] and NP\_758502[Tshz3]), but no western blot data of endogeneous mouse Tshz protein has been published leaving the actual sizes of these proteins unknown. The major bands that I observed for these Myc-tagged proteins (when using either anti-Myc or the anti-Tshz1 or anti-Tshz3 antibodies that I had raised) appeared to correspond to proteins of a much larger size than predicted (approximately 250 kDa), but as predicted Tshz2 (when probed with

anti-Myc antibody) does appear to be marginally smaller than the other Tshzs. Additionally I used two different anti-Tshz3 antibodies (gifts from Laurent Fasano) to verify the observed size of Tshz3. Both of these antibodies detected a protein of approximately 250 kDa, which corresponds to the major specific band observed using both my anti-Tshz3 antibody and the anti-Myc antibody. This is the only band that is detected by all three anti-Tshz3 antibodies, and is therefore highly likely to be Myc-tagged Tshz3 protein. As Tshz1 and Tshz2 are highly similar to Tshz3 both in size and structure it is therefore likely that they are also represented by the bands observed at approximately 250 kDa.

The large observed size of the Myc-tagged Tshz proteins in comparison to the predicted size of the Tshz proteins cannot be explained by the presence of the Myc tag which is only 10 amino acids, approximately 1 kDa, in size. There is no published information on the actual size of mouse Tshz proteins, and the larger observed size than expected may be explained in several different ways. Firstly; although proteins were reduced prior to SDS-page for western blotting, to break disulphide bonds, and denatured further by the SDS itself (SDS is an anionic detergent that disrupts nearly all non-covalent bonds) and therefore the Tshz proteins should have been separated from any other proteins that they were in complexes with, the observed size of the Tshz proteins is roughly twice the expected size so it is tempting to speculate that the Tshz proteins detected on the western blots at approximately 250 kDa represent Tshz dimers (or protein complexes containing Tshz), and this possibility cannot be excluded (as the denaturing process may not have dissociated other proteins that were tightly bound to Tshz3). Secondly; Tshz proteins may undergo extensive post-translational modification (such as

glycosylation) so may be larger than predicted. In addition to adding to the size of the proteins some post-translational modifications (e.g. glycosylation) may cause the proteins to run through the gel anomalously (i.e. their mobility not being a linear functional of the logarithm of their molecular weight), as presence of sugars in proteins can cause this to happen (Stryer, 1995), and so this may help to explain the particularly large observed size of major bands on the western blots. In the future, proteomic analysis of the protein contained in the band by peptide mass fingerprinting (which involves digestion of the protein into peptides followed by mass spectrometry of the peptides) should allow the protein to be positively identified (Pappin et al., 1993).

A variety of smaller bands were also seen for Tshz1 and Tshz3, and at least some of these bands appeared to be specific. Indeed the guinea-pig anti-Tshz3 antibody detected a band between 160 and 250 kDa, which is sometimes also seen when using my anti-Tshz3 antibody, providing an argument that this is more than just an unspecific band. The presence of these additional bands for Tshz1 and Tshz3 may indicate that these proteins are present in the cell in a variety of modified states, or the additional bands may represent degradation products of Tshz proteins. Indeed, if the Tshz proteins exist in a variety of post-translationally modified states, this would provide an argument that Tshz function is regulated by post-translational modification. Indeed, post-translational modification is known to be important in the control of transcription factor activity, with many types of modification, in addition to the well recognised phosphorylation, now thought to play a role (including glycosylation, acetylation, sumoylation and ubiquitination) (Tootle and Rebay,



2005). Therefore the investigation into the post-translational modifications present on the Teashirt protein would be very worthwhile.

### *Using the antibodies to detect endogeneous Tshz proteins*

The use of both the anti-Tshz1 and anti-Tshz3 antibodies to detect endogeneous Tshz proteins in protein extracts from mouse urinary tract tissue have so far been unsuccessful. The anti-Tshz1 antibody failed to detect Tshz1 protein in E14, E18, neonatal or adult kidneys and the anti-Tshz3 antibody failed to detect Tshz3 protein in E14 kidneys or E18 ureters. This apparent lack of expression of Tshz1 and Tshz3 is in contrast to RT-PCR results which indicated that Tshz1 and Tshz3 transcripts were present in kidneys at all developmental stages tested, and that Tshz3 is expressed at relatively high levels in E14 kidneys compared to adulthood (which is why protein from E14 kidneys was used in Western blots where the anti-Tshz3 antibody was used). The failure to detect Tshz1 and Tshz3 protein could be explained by a failure of the transcripts to be translated to produce protein. However, the detection of a  $\beta$ -galactosidase-Tshz3 fusion protein in kidneys and ureters (described in Chapter Five) suggest that Tshz3 transcripts are indeed translated in kidneys and ureters, therefore it seems likely that the anti-Tshz3 antibody is not sensitive enough to detect the levels of Tshz3 protein expressed in E14 kidneys and E18 ureters by this western blotting protocol. It is also possible that Tshz1 transcripts are translated in the kidney, and that the anti-Tshz1 antibody is not sensitive enough to detect the Tshz1 protein in kidneys using this protocol.

Attempts to use the anti-Tshz1 and anti-Tshz3 antibodies to detect Tshz1 and Tshz3 proteins in urinary tract tissue by immunohistochemistry have also so far been

unsuccessful. In conclusion further optimisation of protocols will be required in order to detect endogeneous Tshz1 and Tshz3 proteins, by either western blotting or immunohistochemistry, using the antibodies that I have raised.

## Summary of Results in Chapter Four

1. The anti-Tshz1 and anti-Tshz3 antibodies that I had raised are reactive against Myc-tagged Tshz1 and Tshz3 respectively. The anti-Tshz2 does not exhibit any specific reactivity.
2. Tshz3 protein is approximately 250 kDa in size, and other Tshz family members are likely to be of a similar size. This is much larger than predicted and suggests that Tshz proteins undergo extensive post-translational modification.
3. The anti-Tshz1 and anti-Tshz3 antibodies that I had raised do not cross react with other Tshz proteins.
4. Attempts to use anti-Tshz1 and anti-Tshz3 antibodies to detect Tshz proteins in tissue, either by western blotting or immunohistochemistry have so far been unsuccessful.

## Results Part II - Chapter Five

### The expression of *Tshz3* in the developing mouse urinary tract

#### Introduction

In this second part of the thesis, the specific aim was to investigate the expression and function of *Tshz3* in the development of the urinary tract using *Tshz3/lacZ* mice, to which I had access to through a collaboration with Laurent Fasano (Institute of Developmental Biology Marseilles-Luminy, Marseilles, France).

*Tshz3/lacZ* mice can be used to investigate *Tshz3* expression patterns. *Tshz3/lacZ* mice were generated by replacing most of the second exon of *Tshz3* with a *lacZ* gene. The *LacZ* insertion was in frame with the remaining *Tshz3* coding sequence, resulting in the expression of a *Tshz3*/βgalactosidase fusion protein (which contains only a short fragment of the *Tshz3* protein fused to β-galactosidase). This fusion protein can be detected either with anti-β-galactosidase antibodies or using the X-Gal reaction (which detects β-galactosidase activity). Analyses of X-Gal staining showed patterns of β-galactosidase activity in *Tshz3/lacZ* +/- embryos reliably reported endogenous *Tshz3* expression as assessed by *in-situ* hybridisation (Caubit et al., submitted). Therefore *Tshz3/lacZ* +/- mice can be used to investigate *Tshz3* expression patterns, by following the expression of the *lacZ* reporter gene. However it is important to note that these mice might have defects resulting from the loss of one of their two copies of the native *Tshz3* gene.

From here onwards *Tshz3/lacZ* mice are referred to as *Tshz3* mice, for simplicity.

This Chapter details experiments undertaken to investigate the expression of *Tshz3* in grossly normal urinary tracts by following *lacZ* expression in *Tshz3*<sup>+/-</sup> mice.

Experiments included X-gal staining and immunohistochemistry using an anti- $\beta$ -galactosidase antibody.

## **Results**

### ***Tshz3 is expressed in the embryonic kidney***

Using immunohistochemistry for  $\beta$ -galactosidase on sections of E15-18 kidneys from *Tshz3*<sup>+/-</sup> mice, I characterised the expression pattern of *Tshz3* in the embryonic kidney. A signal was seen in the nuclei of some of the medullary, and corticomedullary stromal cells of the *Tshz3*<sup>+/-</sup> kidneys (Figure 5.1.1), but was not seen in *Tshz3*<sup>+/+</sup> kidneys (which lack the *Tshz3*/ $\beta$ -galactosidase fusion protein, and were thus used as a control to ensure staining specificity) or in sections of kidneys in which the primary antibody had been omitted during the staining procedure (Figure 5.1.2). The stromal expression of *Tshz3* in the kidney was confirmed in three samples at E15, one sample at E16, four samples at E17 and seven samples at E18.

**Figure 5.1.1 Immunohistochemistry for  $\beta$ -galactosidase in kidneys from E15 – E18 *Tshz3*<sup>+/-</sup> mice**

Sections were stained using an anti- $\beta$ -galactosidase antibody and developed with DAB to give a brown colour. Sections were counterstained with haematoxylin to colour the nuclei blue, and periodic acid Schiffs (pink). **A** and **B** E15 kidneys. **C** and **D** E16 kidneys. **E** and **F** E17 kidneys. **G** and **H** E18 kidneys.  $\beta$ -galactosidase staining can be seen in the nuclei of interstitial (stromal) cells of the kidney, in the medulla and cortico-medullary regions. **A**, **C**, **E** and **G** kidneys and proximal ureters. **B** cortico-medullary junction region of **A** at higher power. **D** and **F** inner medullary region of **C** and **E** respectively, at higher power. **H** outer medullary region of **G** at higher power. Scale bars - 500 $\mu$ m (**A**), 1000 $\mu$ m (**C**, **E** and **G**) or 100 $\mu$ m (**B**, **D**, **F** and **H**).

L. Fasano provided the dissected mouse urinary tracts used in this experiment.

D. Rampling embedded and sectioned some of the mouse urinary tracts used in this experiment.

**Figure 5.1.1**

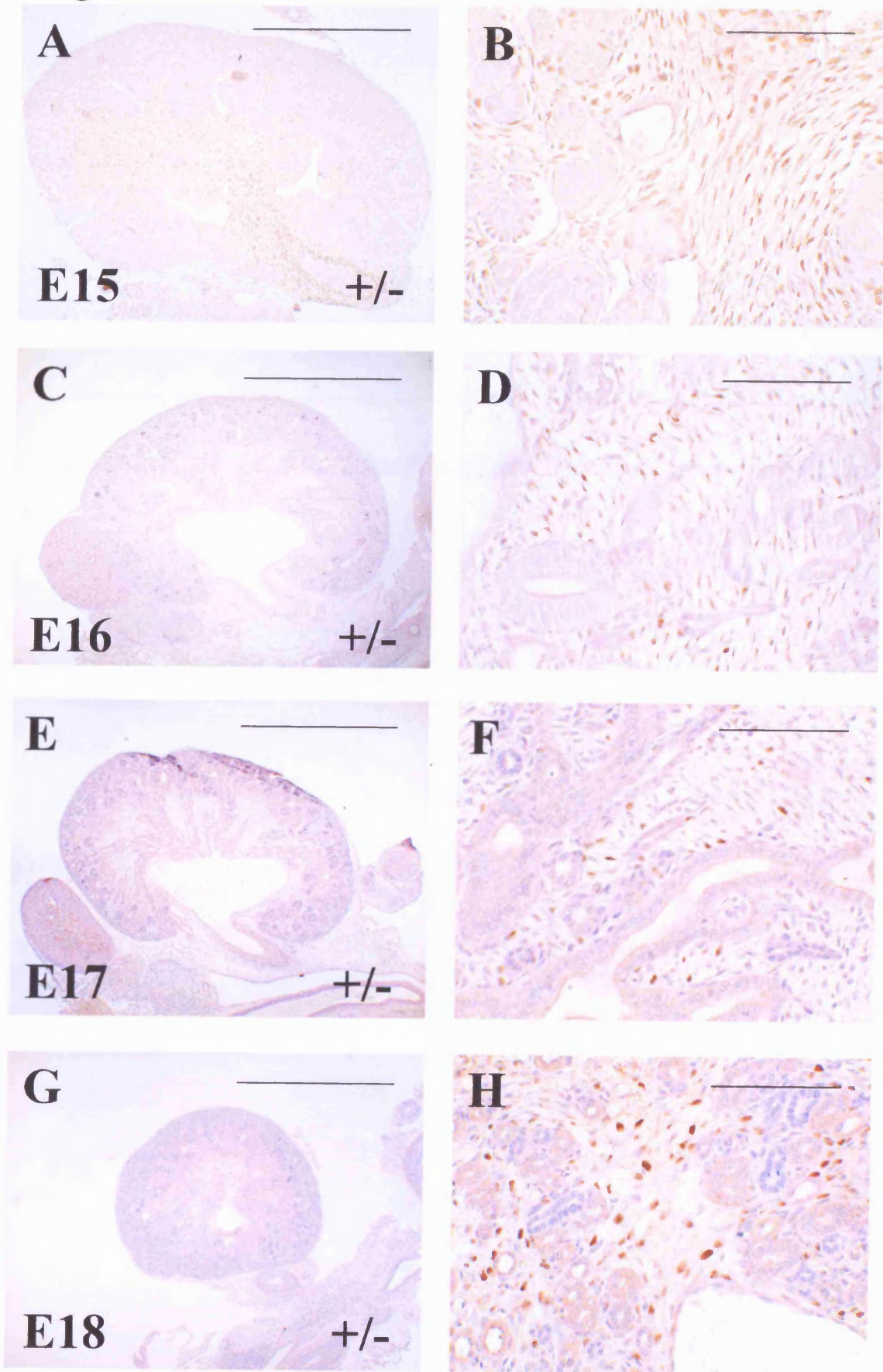


**Figure 5.1.2 Negative control immunohistochemistry for  $\beta$ -galactosidase in kidneys from E15–E18 *Tshz3*<sup>+/-</sup> and *Tshz3*<sup>+/+</sup> mice**

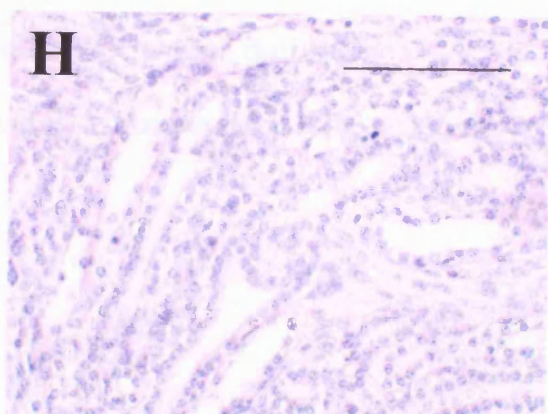
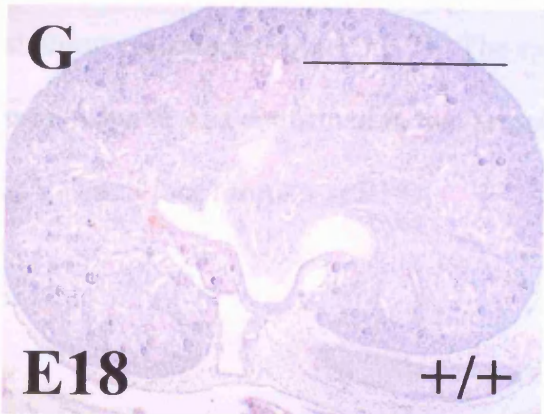
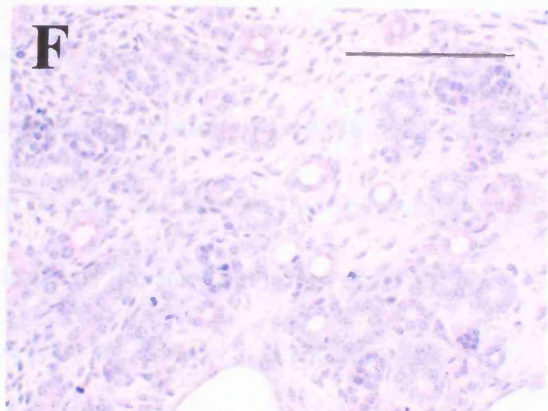
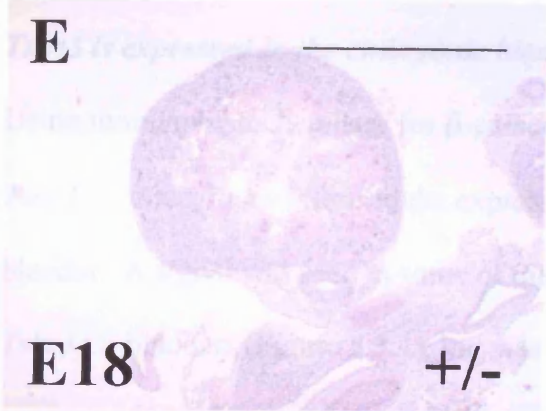
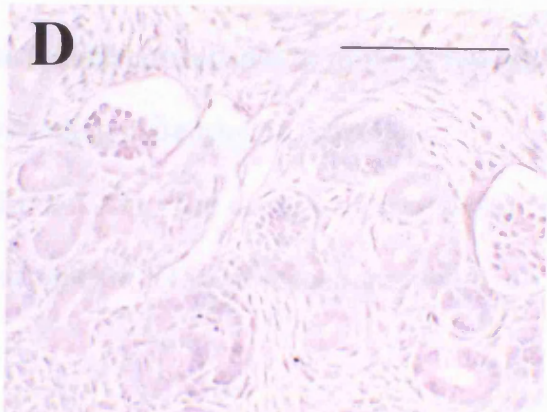
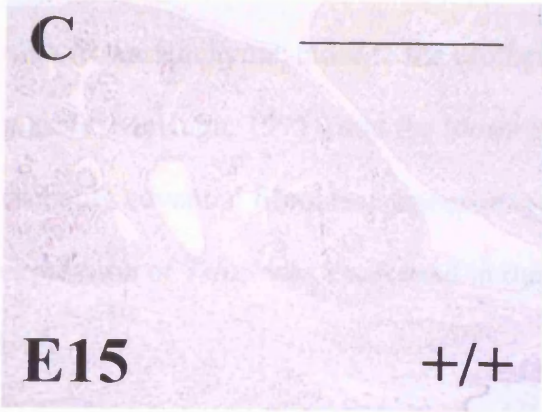
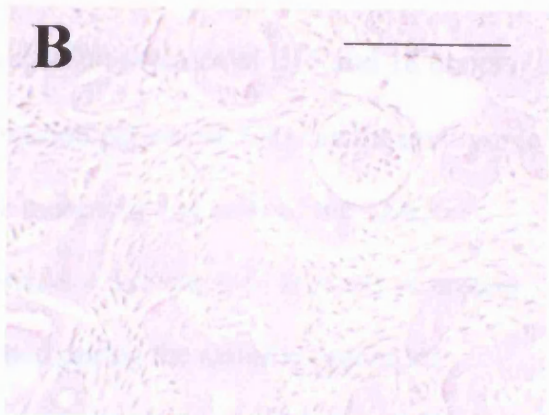
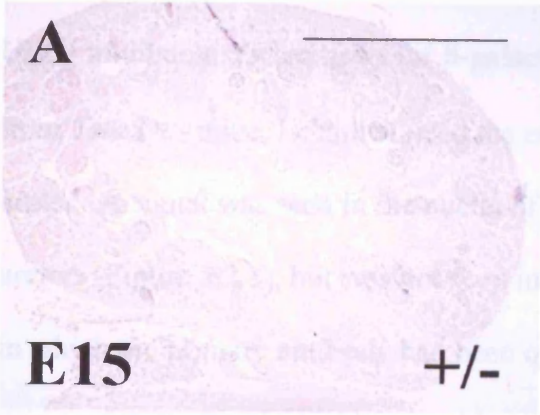
**A, B, E and F** Sections of *Tshz3*<sup>+/-</sup> kidneys were stained using the same method as in Figure 5.1.1, except the anti- $\beta$ -galactosidase antibody was omitted. **C, D, G and H** Sections of *Tshz3*<sup>+/+</sup> kidneys (which lack the *Tshz3/lacZ* reporter gene) were stained using an anti- $\beta$ -galactosidase antibody and developed with DAB to give a brown colour. Sections were counterstained with haematoxylin to colour the nuclei blue, and periodic acid Schiffs (pink). **A-D** E15 kidneys. **E-H** E18 kidneys. No nuclear  $\beta$ -galactosidase staining can be seen indicating that the staining patterns shown in Figure 5.1.1 are specific. **A, C, E and G** kidneys and proximal ureters. **B and D** corticomedullary region of kidneys in **A** and **C** respectively, at higher power. **F** outer medullary region of **E** at higher power. **H** inner medullary region of **G** at higher power. Scale bars - 500 $\mu$ m (**A** and **C**), 1000 $\mu$ m (**E** and **G**) or 100 $\mu$ m (**B, D, F** and **H**).

L. Fasano provided the dissected mouse urinary tracts used in this experiment.

D. Rampling embedded and sectioned some of the mouse urinary tracts used in this experiment.



**Figure 5.1.2**



### ***Tshz3 is expressed in the embryonic ureter***

Using immunohistochemistry for  $\beta$ -galactosidase on sections of E15 and 18 ureters from *Tshz3*<sup>+/-</sup> mice, I characterised the expression pattern of *Tshz3* in the embryonic ureter. A signal was seen in the nuclei of the mesenchymal cells of the *Tshz3*<sup>+/-</sup> ureters (Figure 5.2.1), but was not seen in *Tshz3*<sup>+/+</sup> ureters or in sections of ureters in which the primary antibody had been omitted during the staining procedure (Figure 5.2.2).  $\beta$ -galactosidase positive cells were present in both the condensing ureteric mesenchyme, close to the urothelium (which corresponds to forming smooth muscle (McHugh, 1995)) and the looser surrounding mesenchyme (which are probably adventitial fibroblast precursors) (Figure 5.2.1). The ureteric mesenchymal expression of *Tshz3* was confirmed in three samples at E15 and seven samples at E18.

### ***Tshz3 is expressed in the embryonic bladder***

Using immunohistochemistry for  $\beta$ -galactosidase on sections of E15-18 ureters from *Tshz3*<sup>+/-</sup> mice, I characterised the expression pattern of *Tshz3* in the embryonic bladder. A signal was seen in some of the nuclei of the mesenchymal cells of the *Tshz3*<sup>+/-</sup> bladders (Figure 5.3.1), but was not seen in *Tshz3*<sup>+/+</sup> bladders or in sections of bladders in which the primary antibody had been omitted during the staining procedure (Figure 5.3.2). The expression of *Tshz3* in the bladder mesenchyme was confirmed in two samples at E15, one sample at E16, two samples at E17 and four samples at E18.

**Figure 5.2.1 Immunohistochemistry for  $\beta$ -galactosidase in ureters from E15 and E18 *Tshz3*<sup>+/-</sup> mice**

Sections were stained using an anti- $\beta$ -galactosidase antibody and developed with DAB to give a brown colour. Sections were counterstained with haematoxylin to colour the nuclei blue, and periodic acid Schiffs (pink). **A** and **B** E15 kidney and proximal ureter. **C** and **D** E18 kidney and proximal ureter.  $\beta$ -galactosidase staining can be seen in nuclei of mesenchymal cells surrounding the urothelium of the proximal ureter.  $\beta$ -galactosidase positive cells are observed with the condensing and loose mesenchymal layers at both stages. **A** and **C** kidneys and proximal ureters. **B** and **D** proximal ureters at higher power. u – urothelium, cm – condensed mesenchyme (smooth muscle precursor cells), lm – loose mesenchyme. Scale bars - 500 $\mu$ m (**A**), 1000 $\mu$ m (**C**) or 100 $\mu$ m (**B** and **D**).

L. Fasano provided the dissected mouse urinary tracts used in this experiment.

**Figure 5.2.1**

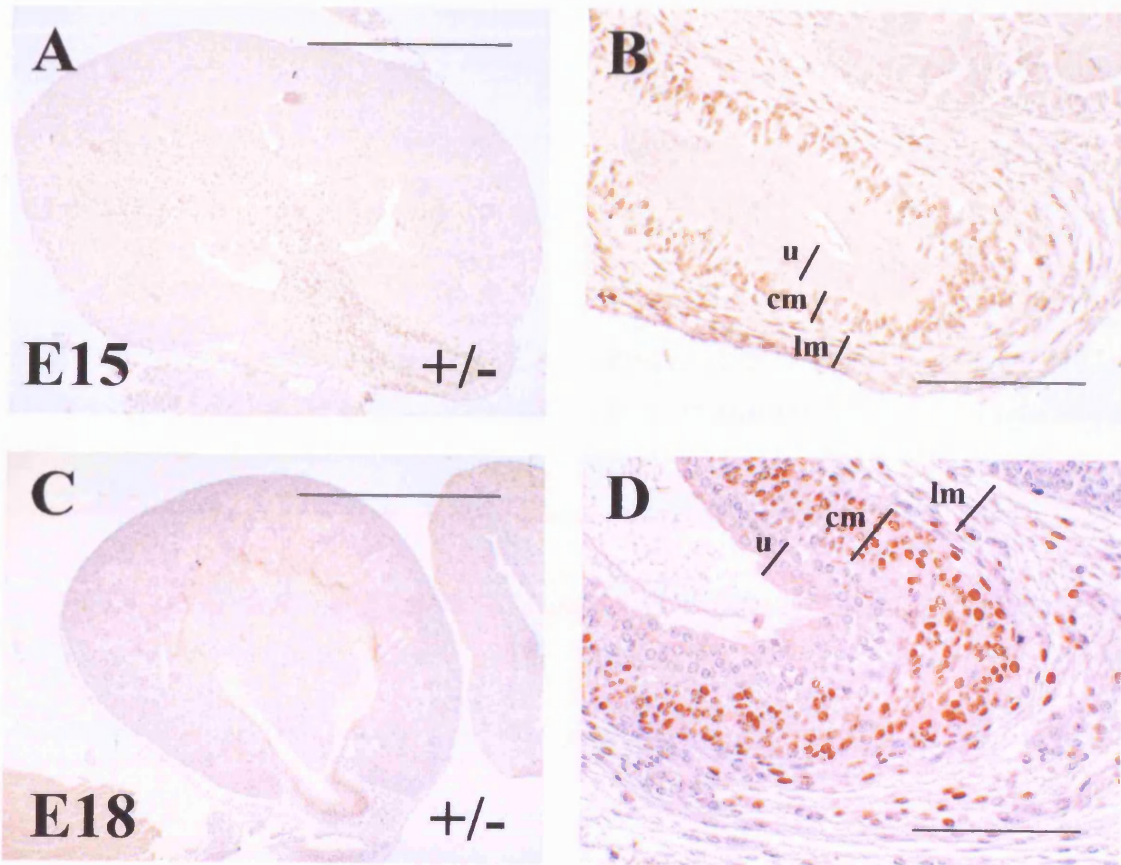


**Figure 5.2.2 Negative control immunohistochemistry for  $\beta$ -galactosidase in ureters from E15 and E18 *Tshz3*<sup>+/-</sup> and *Tshz3*<sup>+/+</sup> mice**

**A** and **B** Sections of *Tshz3*<sup>+/-</sup> kidneys and proximal ureters were stained using the same method as in Fig5.2.1, except the anti- $\beta$ -galactosidase antibody was omitted. **C - F** Sections of *Tshz3*<sup>+/+</sup> kidneys and proximal ureters (which lack the *Tshz3/lacZ* reporter gene) were stained using an anti- $\beta$ -galactosidase antibody and developed with DAB to give a brown colour. Sections were counterstained with haematoxylin to colour the nuclei blue, and periodic acid Schiff's (pink). **A-D** E15 kidneys and proximal ureters. **E** and **F** E18 kidney and proximal ureter. No nuclear  $\beta$ -galactosidase staining can be seen indicating that the staining patterns shown in Figure 5.2.1 are specific. **A, C** and **E** kidneys and proximal ureters. **B, D** and **F** proximal ureters at higher power. Scale bars - 500 $\mu$ m (**A** and **C**), 1000 $\mu$ m (**E**) or 100 $\mu$ m (**B, D** and **F**).

L. Fasano provided the dissected mouse urinary tracts used in this experiment.

**Figure 5.2.2**

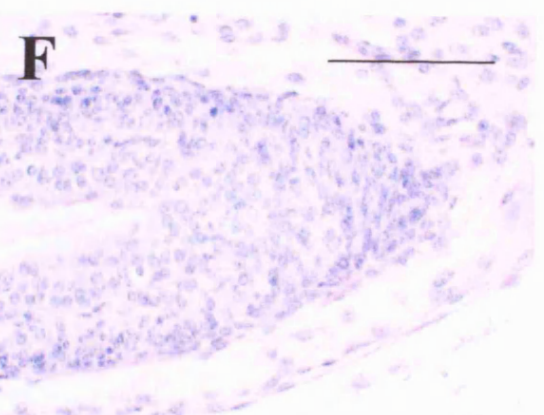
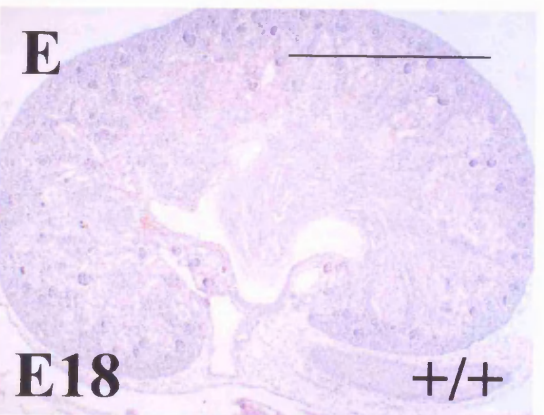
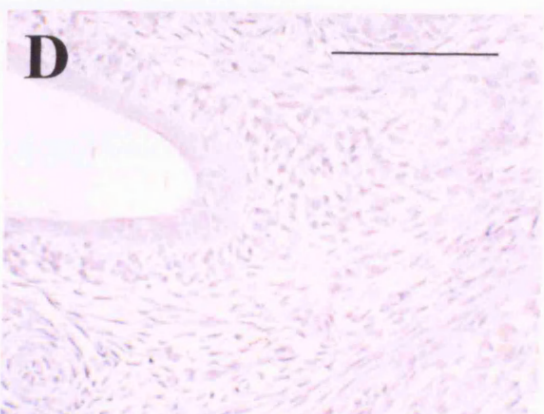
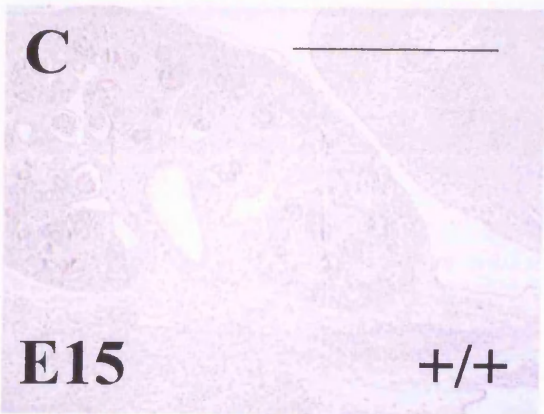
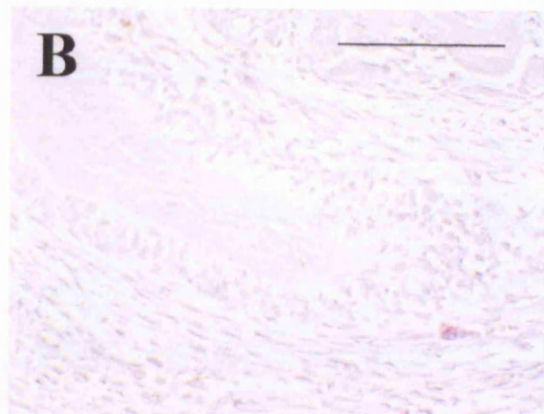
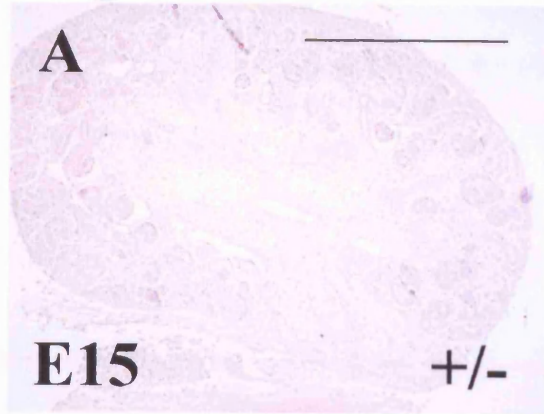


**Figure 5.3.1 Immunohistochemistry for  $\beta$ -galactosidase in bladders from E15 – E18 *Tshz3*<sup>+/-</sup> mice**

Sections were stained using an anti- $\beta$ -galactosidase antibody and developed with DAB to give a brown colour. Sections were counterstained with haematoxylin to colour the nuclei blue, and periodic acid Schiffs (pink). **A** and **B** E15 bladder. **C** and **D** E16 bladder. **E** and **F** E17 bladder. **G** and **H** E18 bladder.  $\beta$ -galactosidase staining can be seen in nuclei of mesenchymal cells of the bladder.  $\beta$ -galactosidase positive cells are seen in the lamina propria and smooth muscle layers at E15 (**B**), and are most prominent in the lamina propria. At later stages  $\beta$ -galactosidase positive cells are more readily observable in the detrusor smooth muscle layers (**D**, **F** and **H**), but are sometimes also seen in the lamina propria (arrow in **H**). **A**, **C**, **E** and **G** bladders. **B**, **D**, **F** and **H** parts of bladders (including mesenchymal cell layers) at higher power. sm – smooth muscle, lp – lamina propria, u – urothelium. Scale bars - 500 $\mu$ m (**A**), 1000 $\mu$ m (**C**, **E** and **G**) or 100 $\mu$ m (**B**, **D**, **F** and **H**).

L. Fasano provided the dissected mouse urinary tracts used in this experiment.

**Figure 5.3.1**

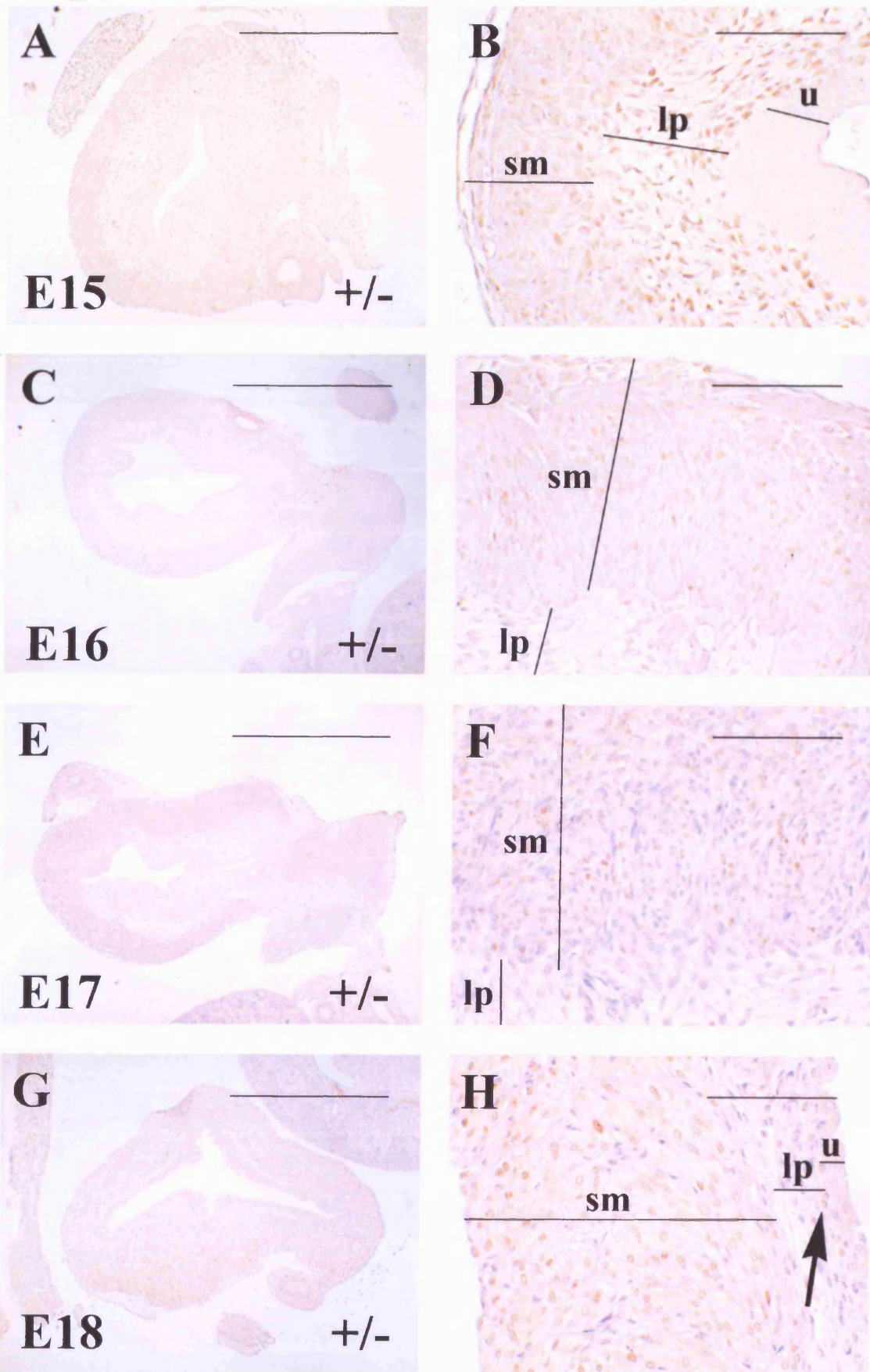


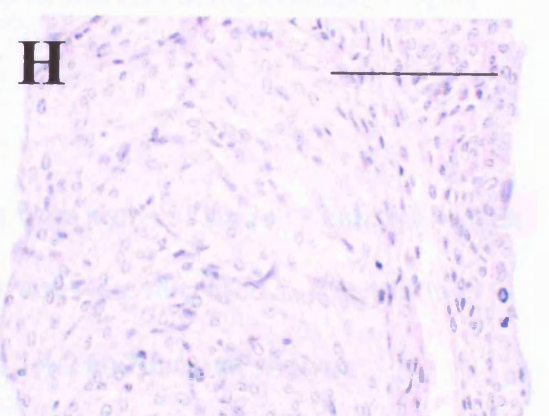
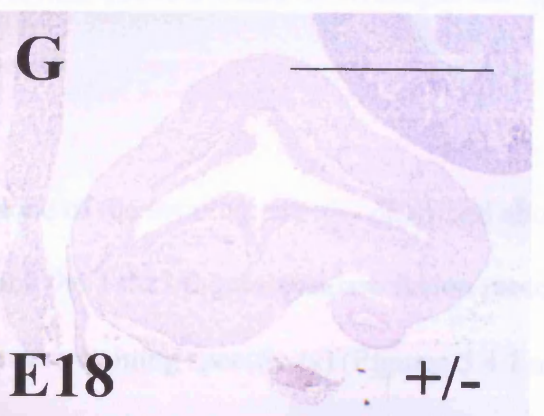
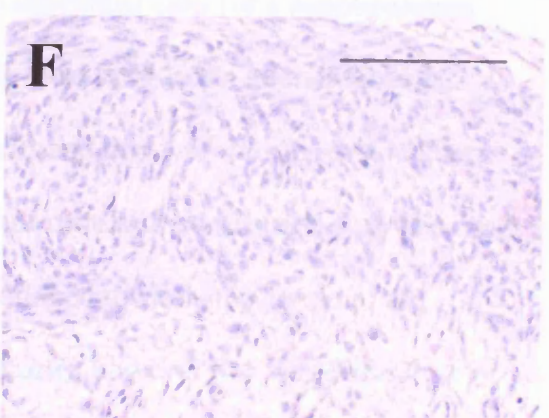
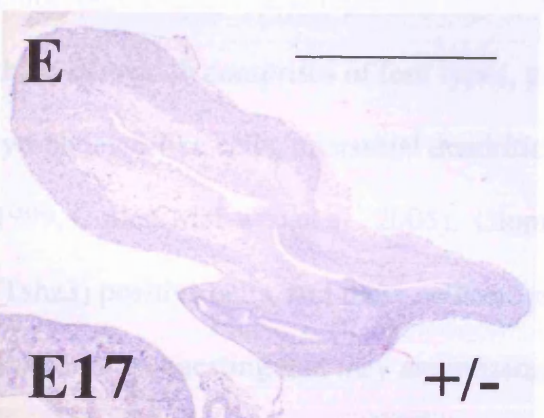
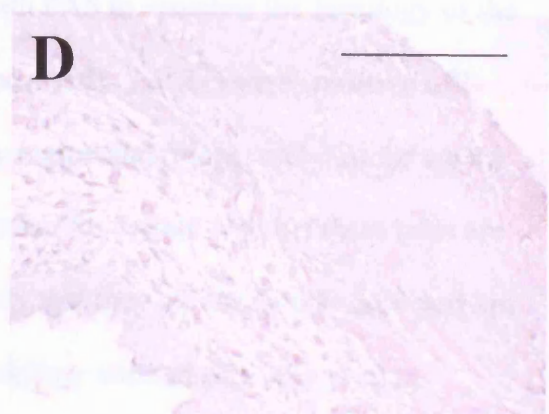
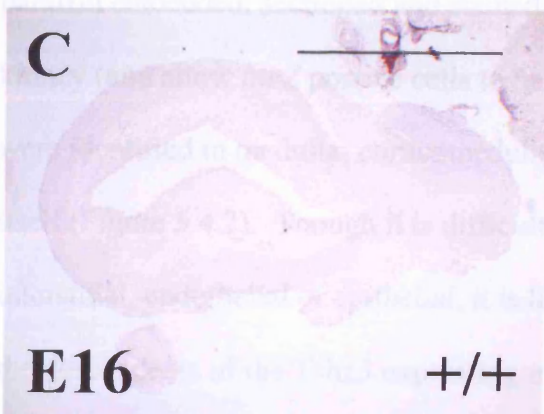
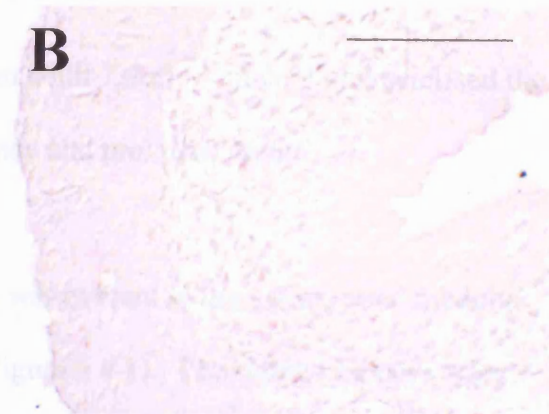
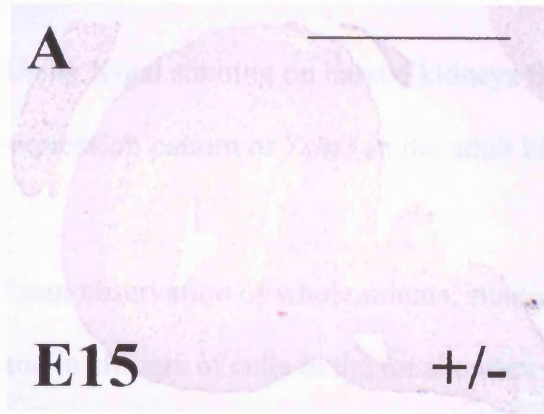


**Figure 5.3.2 Negative control immunohistochemistry for  $\beta$ -galactosidase in bladders from E15 – E18 *Tshz3*<sup>+/-</sup> and *Tshz3*<sup>+/+</sup> mice**

All sections were counterstained with haematoxylin to colour the nuclei blue, and periodic acid Schiffs (pink). (**A and B; E-H**) Sections of *Tshz3*<sup>+/-</sup> bladders were stained using the same method as in Fig 5.3.1, except the anti- $\beta$ -galactosidase antibody was omitted. (**C and D**) Sections of *Tshz3*<sup>+/+</sup> bladders (which lack the *Tshz3/lacZ* reporter gene) were stained using an anti- $\beta$ -galactosidase antibody and developed with DAB to give a brown colour. **A and B** E15 bladder. **C and D** E16 bladder. **E and F** E17 bladder. **G and H** E18 bladder. No nuclear  $\beta$ -galactosidase staining can be seen indicating that the staining patterns shown in Figure 5.3.1 are specific. **A, C, E and G** bladders. **B, D, F and H** parts of bladders (including mesenchymal cell layers) at higher power. Scale bars - 500 $\mu$ m (**A**), 1000 $\mu$ m (**C, E and G**) or 100 $\mu$ m (**B, D, F and H**).

L. Fasano provided the dissected mouse urinary tracts used in this experiment.

**Figure 5.3.2**



### **Tshz3 is expressed in the adult kidney and ureter**

Using X-gal staining on halved kidneys from adult *Tshz3*<sup>+/-</sup> mice, I characterised the expression pattern of *Tshz3* in the adult kidney and proximal ureter.

From observation of wholemounts, staining was evident in the ureter, renal medulla and in clusters of cells in the renal cortex (Figure 5.4.1). The stained kidneys were paraffin embedded, sectioned and stained with PAS to visualise the histology of the kidney (and allow *lacZ* positive cells to be localised). *LacZ* (*Tshz3*) positive cells were identified in medulla, corticomedullary region and (more rarely) in the cortex itself (Figure 5.4.2). Though it is difficult to say for certain whether these cells are interstitial, endothelial or epithelial, it is likely that they are the former (and perhaps the descendants of the *Tshz3* expressing medullary stromal cells observed in embryonic kidneys) and represent medullary interstitial cells (or a subpopulation there-of) which comprises of four types; prominent lipid-laden interstitial cells, lymphocyte-like cells, interstitial dendritic cells and pericytes (Grupp and Müller; 1999, Cullen-McEwen et al., 2005). Glomeruli were also confirmed to contain *lacZ* (*Tshz3*) positive cells, and these cells are positioned towards the centre of the glomeruli, suggesting that they are mesangial cells, however this was difficult to confirm due to the lack of mesangial cell specific markers being available (Figure 5.4.2).

None of the staining patterns described above were seen in *Tshz3*<sup>+/+</sup> kidneys (which lack the *Tshz3*/β-galactosidase fusion protein, and were thus used as a control to ensure staining specificity) (Figures 5.4.1 and 5.4.2 and data not shown).

**Figure 5.4.1 X-gal staining of *Tshz3*<sup>+/-</sup> kidneys and *Tshz3*<sup>+/+</sup> controls**

A wholemount X-gal (blue) staining of a half adult *Tshz3*<sup>+/-</sup> kidney and proximal ureter (which has been cut down its midline to reveal the medullary region and lumen of the proximal ureter). Prominent staining is seen in the ureter and the medulla, and small spots of staining are seen in the cortex, which can be seen more clearly at higher magnification (**B**). These photomicrographs were taken on a dissecting microscope with a variable zoom, and therefore no scale bars can be provided.

This figure was kindly provided by L. Fasano.

**Figure 5.4.1**

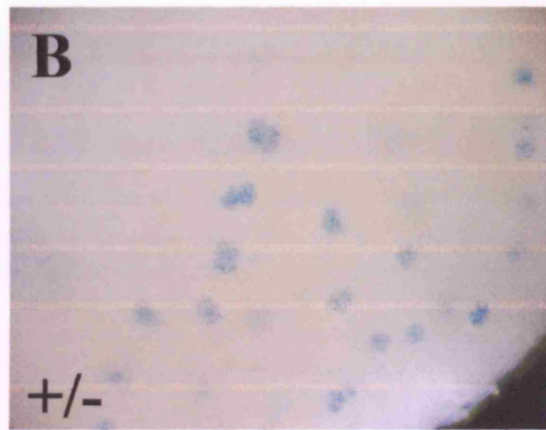
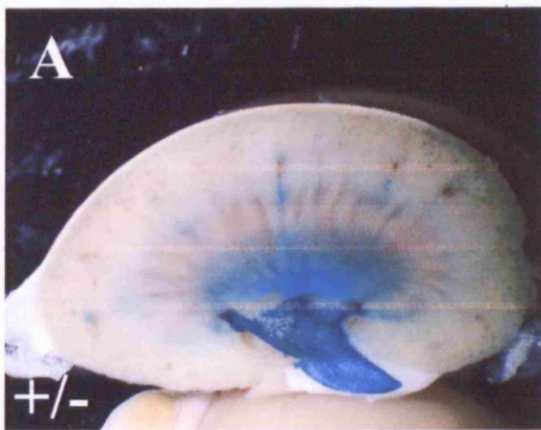
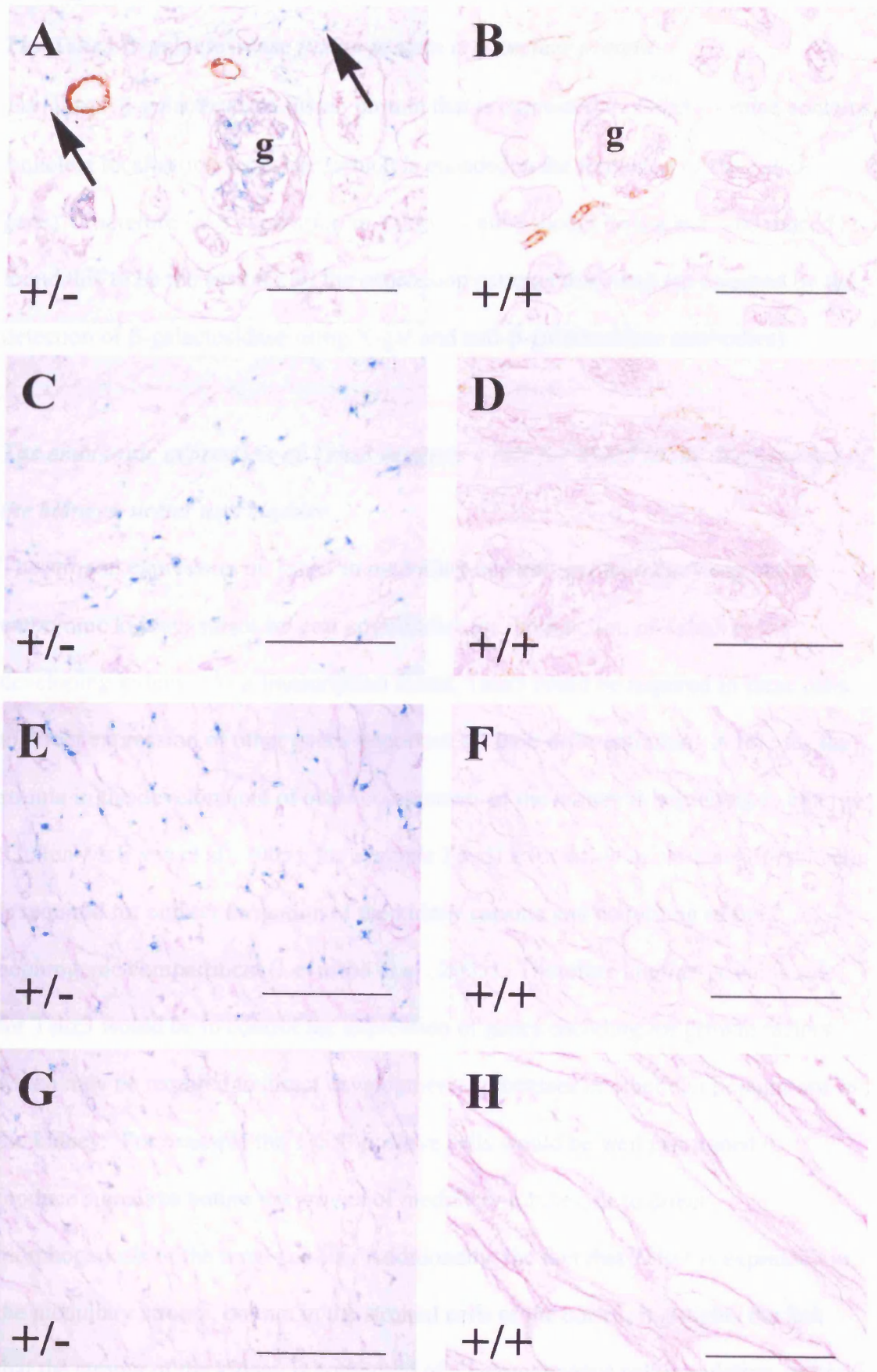


**Figure 5.4.2 Double  $\alpha$ SMA and X-gal staining of *Tshz3*<sup>+/-</sup> kidneys and *Tshz3*<sup>+/+</sup> controls**

X-gal stained kidneys were embedded and sectioned. Sections were then stained using an anti- $\alpha$ SMA antibody and developed with DAB to give a brown colour and counterstained periodic acid Schiff's (pink). **A, C, E and G** sections through a *Tshz3*<sup>+/-</sup> kidney. **B, D, F and H** sections through a *Tshz3*<sup>+/+</sup> kidney, which was used as a negative control, since it lacks the *Tshz3/lacZ* reporter gene. **A-B** sections through the cortex. **C-D** sections through the corticomedullary region. **E-F** sections through the outer medulla. **G-H** sections through the inner medulla. In **A** X-gal positive cells are seen in the glomerulus (*g*), and also in a few nearby cells (arrow). In **C, E and G**, scattered X-gal positive cells are seen. These (and the none glomerular cells in **A**) are probably interstitial cells. No blue staining is seen in **B, D, F or H** indicating that staining observed in other panels is specific. Scale bars - 100 $\mu$ m.

L. Fasano provided the dissected mouse urinary tracts used in this experiment.

**Figure 5.4.2**



## **Discussion**

### ***The Tshz3- $\beta$ -galactosidase fusion protein is a nuclear protein***

The Tshz3- $\beta$ -galactosidase fusion protein that is expressed in *Tshz3*<sup>+/-</sup> mice contains a nuclear localisation sequence (which is encoded in the first exon of the *Tshz3* gene). Therefore *lacZ* expression in *Tshz3*<sup>+/-</sup> mice should be nuclear, and indeed I found this to be the case for all the expression patterns described (as assessed by the detection of  $\beta$ -galactosidase using X-gal and anti- $\beta$ -galactosidase antibodies).

### ***The embryonic expression of Tshz3 suggests a role for Tshz3 in the development of the kidneys, ureter and bladder***

The stromal expression of Tshz3 in medullary and corticomedullary regions of embryonic kidneys raises several possibilities for the function of Tshz3 in the developing kidney. As a transcription factor, Tshz3 could be required in these cells to direct expression of other genes important for their differentiation. A role for the stroma in the development of other components of the kidney is beginning to emerge (Cullen-McEwen et al., 2005), for example Foxd1 expression in cortical stromal cells is required for correct formation of the kidney capsule and patterning of the nephrogenic compartment (Levinson et al., 2005). Therefore another possible role for Tshz3 would be to control the expression of genes encoding for growth factors, which may be required to direct developmental processes in other cell populations in the kidney. For example the Tshz3 positive cells would be well positioned to produce signals to nurture the growth of medullary tubules, or to direct morphogenesis of the renal papilla. Additionally, the fact that Tshz3 is expressed in the medullary stroma, but not in the stromal cells of the cortex, highlights the fact that the stroma of the kidney is composed of a heterogeneous cell population, as has



been previously commented upon in the literature (Cullen-McEwen et al., 2005; Marxer-Meier et al., 1998; Maric et al., 1997).

The expression of *Tshz3* in the embryonic ureter, indicates that it may be involved in its development. The ureter develops from the stalk of the ureteric bud (which becomes the urothelium) and the surrounding mesenchymal cells (which will form the lamina propria, smooth muscle and adventitial layers). Differentiation of these components depends upon reciprocal signalling both between and within the epithelium and the mesenchyme (Raatikainen-Ahokas et al., 2000; Yu et al., 2002; Miyazaki et al., 2003; Airik et al., 2006). Therefore although *Tshz3* is expressed in the mesenchymal cells of the ureter, and as a transcription factor is likely to be important for their differentiation; it may also be required for the differentiation of the urothelium, via the control of production of extracellular signals.

As *Tshz3* is expressed in the embryonic bladder, it may be required for aspects of its development. In a similar way to the ureter, bladder development depends upon mesenchymal-epithelial interactions (Baskin et al., 1997). *Tshz3* positive cells were detected in the mesenchyme, in both the lamina propria and smooth muscle layers, and therefore may be required for their development. Alternatively, or additionally, *Tshz3* may be required in the mesenchyme to enable it to produce growth factors that will influence the development of the urothelium. It is intriguing that at E15 *Tshz3* positive cells were more readily observable in the lamina propria than the smooth muscle layer, but at later stages *Tshz3* positive cells were more prominent in the smooth muscle layer. This observation suggests that *Tshz3* may have temporally

distinct roles in the development of the lamina propria and the smooth muscle of the bladder.

***Tshz3 is expressed in the adult kidney and ureter, suggesting additional roles for Tshz3 in the mature urinary tract***

Tshz3 is expressed in dispersed cells in the medulla and corticomedullary region (and rarely in the cortex) of the adult kidney. The cells in which Tshz3 is expressed are probably interstitial cells. Interstitial cells have important roles in the adult kidney, including maintaining the structural integrity of the kidney by secreting extracellular matrix and providing cellular support for capillaries and loops of Henle and erythropoetin synthesis (Lemley and Kriz, 1991; Maxwell et al., 1993).

Therefore Tshz3 may be required in adult renal interstitial cells to promote expression of genes required for these functions. The renal papilla has been identified as a niche for adult kidney stem cells, as it contains large numbers of BrdU-retaining cells (whereas BrdU-retaining cells were very rare in other parts of the kidney) that were mainly of an interstitial phenotype (Oliver et al., 2004).

Considering the spatial distribution of the Tshz3 positive interstitial cells (which were most abundant in the renal medulla, the inner portion of which makes up the papilla) it is also possible that Tshz3 is a marker of adult renal stem cells, and may act to maintain these cells in a (relatively) undifferentiated state. This possibility could be investigated by administering BrdU to *Tshz3*<sup>+/-</sup> mice, and then, after an appropriate “chase” using immunohistochemistry and/or X-gal staining to establish whether BrdU retaining cells express Tshz3.

Tshz3 is also expressed in a subset of cells of the glomerulus, which probably represent mesangial cells (which are smooth muscle-like cells that help to maintain the structure of the glomerulus), and may be required for the correct function of these cells. Unfortunately no specific markers of mesangial cells have been identified, but investigation of whether Tshz3 positive cells also express markers of podocytes (e.g. Wt1 (Mundlos et al., 1993)) or endothelial cells (e.g. VEGFR2/Flk1 (Neufeld et al., 1999)) should help to identify which type of glomerular cell expresses Tshz3, and so help to define the role for Tshz3 in the adult glomerulus.

Tshz3 is also expressed in the adult ureter, though the identity of the Tshz3 expressing cells has not been identified. As Tshz3 is expressed in the mesenchymal cells of the developing ureter, including the smooth muscle precursors, the Tshz3 positive cells of the adult could correspond to smooth muscle cells. This hypothesis could be tested by investigating whether the Tshz3 positive cells express smooth muscle markers such as smooth muscle actin. A possible function of Tshz3 in adult ureteric smooth muscle would be the maintenance of the smooth muscle phenotype through promotion of continued expression of smooth muscle specific genes.

### **Summary of results in Chapter Five**

1. *Tshz3* is expressed in some of the medullary and cortico-medullary stromal cells of the embryonic mouse kidney.
2. *Tshz3* is expressed in the mesenchymal cells of the embryonic ureter; in both the condensing and loose mesenchymal cell layers.
3. *Tshz3* is expressed in the mesenchymal cells of the embryonic bladder; in both the lamina propria early on and later in smooth muscle layers.
4. *Tshz3* is expressed in the adult kidney; in interstitial cells, in the mesangial cells of the glomeruli and in the smooth muscle cells of the renal pelvis. *Tshz3* is also expressed in the adult ureter.

## Results Part II - Chapter Six

### The function of *Tshz3* in the developing urinary tract; *in vivo* studies

#### Introduction

In this second part of the thesis, the specific aim was to investigate the expression and function of *Tshz3* in the development of the urinary tract using *Tshz3* mice. In the previous chapter I demonstrated that *Tshz3* is expressed in the developing mouse urinary tract using *Tshz3*<sup>+/-</sup> mice. *Tshz3*<sup>-/-</sup> mice can be used to investigate the function of *Tshz3*. *Tshz3*<sup>-/-</sup> mice have two copies of the *Tshz3*/β-galactosidase fusion protein gene (which contains only a very small fragment of the native *Tshz3* protein; this fragment is devoid of DNA binding motifs required for transcription factor function) and a lack full-length *Tshz3* protein gene and can be considered null mutants. Therefore phenotypic analysis of *Tshz3*<sup>-/-</sup> mice can be used to help reveal *Tshz3* function.

This chapter details the *in vivo* studies undertaken to explore the phenotype of *Tshz3*<sup>-/-</sup> mice. Experiments included studies of gross anatomy and histology, investigation of the expression of specific cell markers and growth factors, and quantification of proliferative and apoptotic cells. Note *Tshz3*<sup>-/-</sup> mice die shortly after birth, thus the phenotypic analyses of these mice (described in this chapter) could only be performed on embryonic mice.

## Results

### *Gross anatomy by external examination*

Initially, to identify whether there were abnormalities in the urinary tract of *Tshz3*<sup>-/-</sup> mice, E18 *Tshz3*<sup>-/-</sup> mice, and their littermates were dissected and their urinary tracts (including kidneys, ureters and bladders) examined under a dissecting microscope. In the first litter, which was observed in a blinded manner (the observers being unaware of the genotypes of the samples at the time of observation), the urinary tracts from homozygous *Tshz3*<sup>-/-</sup> mice were identified as displaying bilateral hydroureter and hydronephrosis. This is defined as an abnormal distension of both ureters and of the pelvic cavity of both kidneys, caused by an accumulation of urine. The other urinary tracts (which included both wildtype and heterozygous littermates) were normal in appearance. The affected urinary tracts had dilatation of the ureters and a translucent area in the kidneys close to where the ureter attached to the kidney, indicative of urine accumulation in the renal pelvis, which leads to stretching of the kidney tissue. The hydroureter was noted to be particularly severe in the part of the ureter closest to the kidney (hereafter referred to as the proximal ureter, whilst the end closest to the bladder is referred to as the distal ureter.) Figure 6.1 A-C shows representative pictures of whole mount renal tracts from *Tshz*<sup>+/+</sup> and *Tshz3*<sup>-/-</sup> E18 mice.

**Figure and Movies 6.1 *Tshz3*<sup>-/-</sup> develop hydroureter and hydronephrosis**

**A-C** Wholemout E18 urinary tracts showing paired kidneys and ureters, and the bladder. (These photomicrographs were taken on a dissecting microscope with a variable zoom, and therefore no scale bars can be provided.) Compared to wild-type littermates (**A**), *Tshz3*<sup>-/-</sup> kidneys had bilateral hydronephrosis and hydroureter (**B**). (**C**) Higher magnification view of hydroureter shown in boxed area of **B**. **D-E** Optical projection tomography single optical sections through the middle of the E18 kidneys. Compared to heterozygote (**D**), *Tshz3*<sup>-/-</sup> kidneys (**E**) have an enlarged pelvic space, lack a papilla and have a dilated proximal ureter. b, bladder; k, kidney; u (in **A-C**) arrows (in **D** and **E**), ureter; ut, uterus; p, papilla.

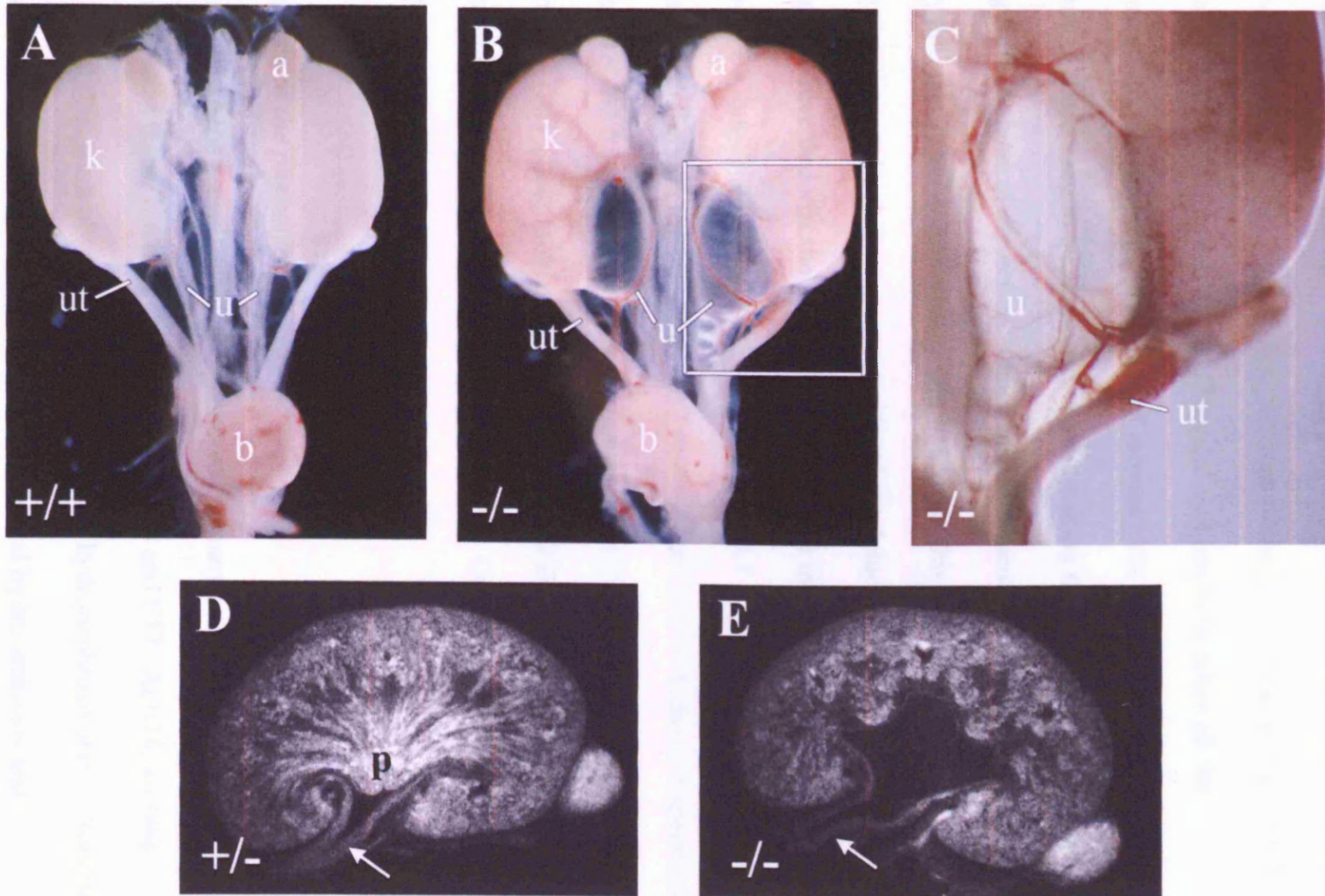
**F** and **G** Movies showing a “fly-through” view of the kidneys, generated by sequential optical sections generated by Optical Projection Tomography. Compared to heterozygote (**F**), *Tshz3*<sup>-/-</sup> kidneys (**G**) have an enlarged pelvic space, lack a papilla and have a dilated proximal ureter. (NB These movies are provided on a CD in MPEG format, you may need to download Quicktime, in order to view them. Quicktime is available at <http://www.apple.com/quicktime/download/>).

L. Fasano provided the dissected mouse urinary tracts used in this experiment.

J. Moss and J. Armstrong carried out the Optical Projection Tomography.

Part of this figure appears in Caubit et al. (submitted).

**Figure 6.1**





### ***Gross anatomy of the kidney by optical projection tomography***

To aid the investigation of the gross anatomy of the kidneys, OPT was performed. This technique utilises the light-absorbing properties of a tissue to image it in three dimensions, without physically making sections of the tissue (Sharpe et al., 2002). Optical projection tomography allowed optical sections to be taken all the way through the kidney, and “fly-through” movies to be made, allowing the internal anatomy of the kidney to be examined without risking the damage that may occur during further physical dissection. One *Tshz3*<sup>+/-</sup> (phenotypically-normal) E18 kidney and one *Tshz3*<sup>-/-</sup> E18 kidney was imaged in this way. Results confirmed that in *Tshz3*<sup>-/-</sup> the renal pelvis was very much enlarged due to urine accumulation, and additionally revealed that the papilla did not protrude into the pelvic space as it did in the *Tshz3*<sup>+/-</sup>, but appeared to be “missing”. Figure 6.1 D and E show single optical sections taken through the middle of the *Tshz3*<sup>+/-</sup> and *Tshz3*<sup>-/-</sup> kidneys respectively. Movie 6.1F and 6.1G show fly-through movies of the *Tshz3*<sup>+/-</sup> and *Tshz3*<sup>-/-</sup> kidneys respectively (NB These movies are provided on a CD in MPEG format, you may need to download Quicktime, in order to view them. Quicktime is available at <http://www.apple.com/quicktime/download/>).

### ***Prevalance of the phenotype***

To characterise the prevalence of the phenotype, urinary tracts were dissected from several (at least three) litters of embryos at both E18 and E17. At E18; all nine *Tshz3*<sup>-/-</sup> embryos were observed to display bilateral hydronephrosis and hydroureter, one out of thirteen *Tshz3*<sup>+/-</sup> displayed severe bilateral hydronephrosis and hydroureter (and had a dilated bladder) and none of eight *Tshz3*<sup>+/+</sup> had hydronephrosis or hydroureter (however one had a partial duplex kidney in which the

renal pelvis was observed to be split into two sections). At E17; all eleven *Tshz3*<sup>-/-</sup> displayed bilateral hydronephrosis and hydroureter, three out of eight *Tshz3*<sup>+/-</sup> displayed mild hydroureter and none of four *Tshz3*<sup>+/+</sup> were abnormal.

Therefore at E17 and E18 the urinary tract hydronephrosis/hydroureter phenotype was completely penetrant in *Tshz3*<sup>-/-</sup>, and there appeared to be an element of haploinsufficiency, as some *Tshz3*<sup>+/-</sup> also displayed a phenotype (which is usually milder).

### ***Ontogeny of the phenotype***

To determine at what stage of embryogenesis hydronephrosis and hydroureter was first observed, urinary tracts dissected from E15 and E16 *Tshz3*<sup>-/-</sup> mice, and their littermates, were paraffin-embedded, sectioned and stained with Masson's trichrome so that their histology could be examined. Histology was used to observe the phenotype of urinary tracts from E15 and E16 mice, because it was difficult to reliably identify the phenotype in whole mount samples due to the small size and fragility of the tissue.

Sections of all E15 *Tshz3*<sup>-/-</sup> (Figure 6.2.1 I-J) and *Tshz3*<sup>+/-</sup> (Figure 6.2.1E-F) kidneys and ureters were grossly normal, with the diameter of ureters being indistinguishable between *Tshz3*<sup>+/+</sup> (Figure 6.2.1 A-B) and *Tshz3*<sup>-/-</sup>. In total, six *Tshz3*<sup>-/-</sup>, four *Tshz3*<sup>+/+</sup> and five *Tshz3*<sup>+/-</sup> embryos were examined. Note that at this stage of the development the papilla has yet to form, even in wildtype kidneys.

By E16, bilateral hydronephrosis and hydroureter was already evident on sections of two out three *Tshz3*<sup>-/-</sup> embryos, as identified by the abnormally large diameter of their proximal ureters, enlarged pelves and lack of papilla. (Figure 6.2.2 I-J) The remaining *Tshz3*<sup>-/-</sup> embryo had mild unilateral hydroureter (minor enlargement of the diameter of the proximal ureter, without kidney abnormalities). One out of six *Tshz3*<sup>+/-</sup> embryos displayed unilateral hydroureter (Figure 6.2.2 E-F). The other five *Tshz3*<sup>+/-</sup> and all the six *Tshz3*<sup>+/+</sup> embryos had normal urinary tracts (Figure 6.2.2 A-B).

### ***Histology***

Masson's trichrome stained histological sections were also used to characterise the phenotype in more detail from E12-18.

At E12 the histology of this early stage of kidney development appeared normal on sections made from paraffin embedded, whole *Tshz3*<sup>-/-</sup> embryos, and their littermates (Figure 6.3). The mesonephric duct was identifiable and normally positioned. One ureteric bud per kidney could be observed to be invading, and branching within, the metanephric mesenchyme.

From E16 onwards (Figure 6.2.2, 6.2.3. and 6.2.4), *Tshz3*<sup>-/-</sup> metanephric kidneys did not have papilla that protruded into the renal pelvis (which confirmed observations made by OPT). Otherwise the histology of the mutant kidneys appeared grossly normal. From E15 to E18 *Tshz3*<sup>-/-</sup> kidneys (Figure 6.2.1, 6.2.2, 6.2.3, 6.2.4 and 6.4) had distinct nephrogenic zones (containing branching termini of the ureteric bud tree, condensing mesenchyme, renal vesicles, S-shaped bodies and developing glomeruli),

which were grossly similar in thickness to nephrogenic zones in kidneys from wildtype and heterozygote embryos of the same stage. By E18 *Tshz3*<sup>-/-</sup> kidneys had several layers of vascularised glomeruli, as did wildtype and heterozygous kidneys (Figure 6.4).

Despite the normal diameter of the proximal ureters of E15 *Tshz3*<sup>-/-</sup>, closer inspection revealed subtle abnormalities at this stage (Figure 6.5). The ureteric mesenchymal cells were not normally arranged in their proximal ureters. In wildtype (and heterozygous), a well organised layer of condensing mesenchymal cells (the presumed precursors of the smooth muscle layers (McHugh, 1995)) was clearly identifiable immediately surrounding the urothelium; the nuclei of these cells are arranged in a line, and there is a “clear zone” devoid of nuclei between this line of nuclei and the urothelium (Figure 6.5A and B). This clear zone also appears to contain little cytoplasm (as there is little red staining). In *Tshz3*<sup>-/-</sup> the condensed mesenchymal cells surrounding the urothelium, are present, but appear disorganised and lack the “clear zones” described above (Figure 6.3C).

From E16 onwards, homozygous null urinary tracts that displayed the typical phenotype had proximal ureters that were dilated and thin-walled (Figure 6.2.2, 6.2.3 and 6.2.4). Although it was possible to identify a layer of condensed mesenchyme, this was thinner than in wildtype, and remained disorganised. The urothelium was also thinner than in wildtypes.

**Figure 6.2.1 Histology of the urinary tracts from E15 *Tshz3*<sup>-/-</sup> mice and their littermates**

Sections were stained with Masson's trichrome and haematoxylin which stains muscle and cytoplasm red/pink, collagen blue/green and nuclei dark blue. Sections from *Tsh3*<sup>+/+</sup> (**A-D**), *Tshz3*<sup>+/-</sup> (**E-H**), and *Tshz3*<sup>-/-</sup> (**I-L**) mice are shown. **A, E and I** kidneys and proximal ureters; **B, F and J** proximal ureters, at a higher magnification; **C, G and K** transverse sections of distal ureters; **D, H and L** bladders. k, kidney; u, ureter, ur, urothelium; cm, condensing mesenchyme; lm, loose mesenchyme; b, bladder; lp, lamina propria; sm, smooth muscle. Scale bars - 1000µm (**A, D, E, H, I** and **L**), 200µm (**B, F and J**) or 100µm (**C, G and K**).

L. Fasano provided the dissected mouse urinary tracts used in this experiment.

D. Rampling performed the Masson's Trichrome staining.

Part of this figure appears in Caubit et al. (submitted).

**Figure 6.2.1**

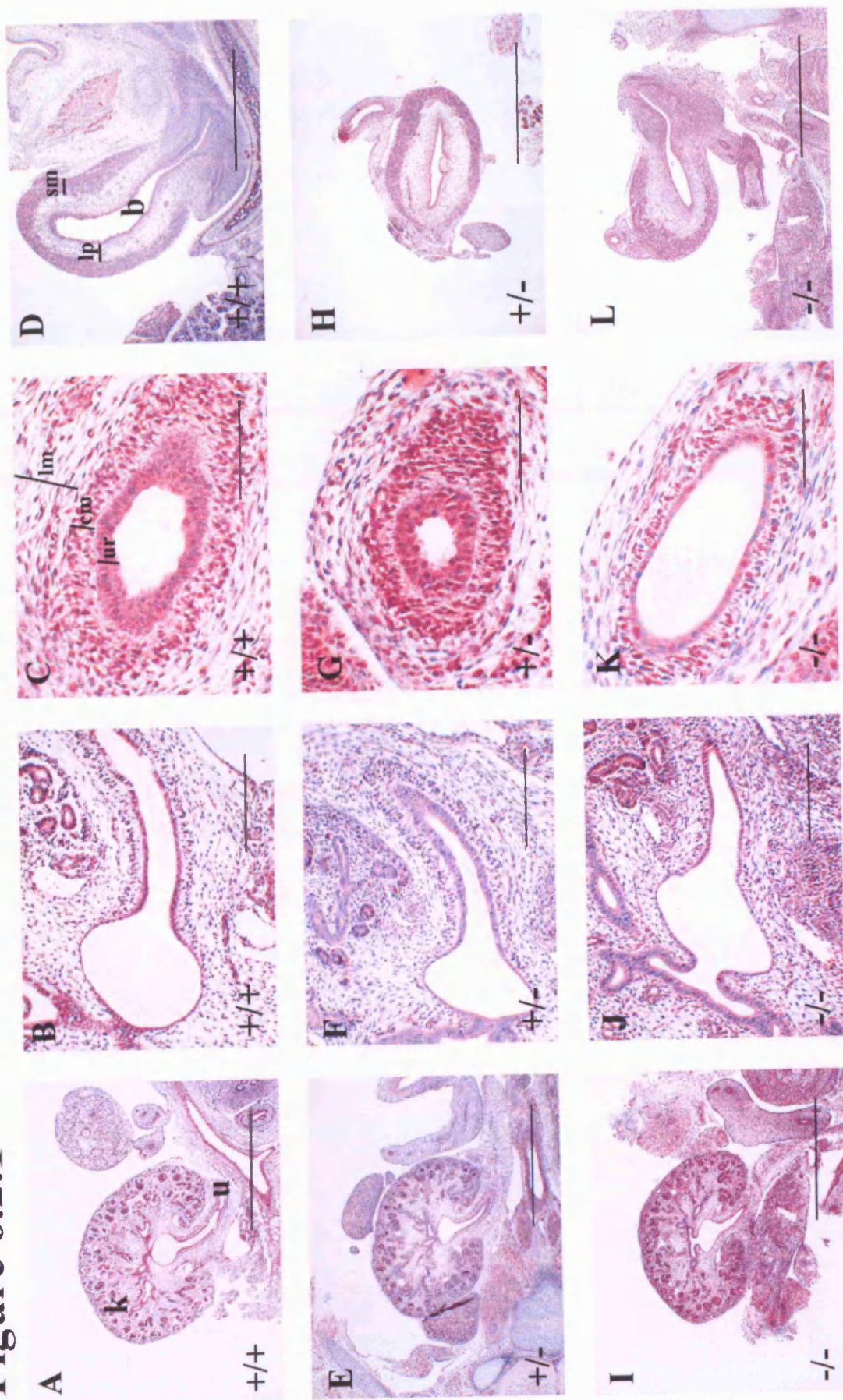


**Figure 6.2.2 Histology of the urinary tracts from E16 *Tshz3*<sup>-/-</sup> mice and their littermates**

Sections were stained with Masson's trichrome and haematoxylin which stains muscle and cytoplasm red/pink, collagen blue/green and nuclei dark blue. Sections from *Tshz3*<sup>+/+</sup> (**A-D**), *Tshz3*<sup>+/-</sup> (**E-H**), and *Tshz3*<sup>-/-</sup> (**I-L**) mice are shown. **A, E and I** kidneys and proximal ureters; **B, F and J** proximal ureters, at a higher magnification. Note thin, disorganised layer of condensed mesenchyme in *Tshz3*<sup>-/-</sup> (arrows in **J**), compared to thicker, organised layer of condensed mesenchyme in *Tshz3*<sup>+/+</sup> (arrowheads in **B**). **C, G and K** transverse sections of distal ureters; **D, H and L** bladders. p, papilla; pel, pelvis. Scale bars - 1000µm (**A, D, E, H, I and L**), 200µm (**B, F and J**) or 50µm (**C, G and K**).

L. Fasano provided the dissected mouse urinary tracts used in this experiment.

D. Rampling performed the Masson's Trichrome staining.

Part of this figure appears in Caubit et al. (submitted).

**Figure 6.2.2**

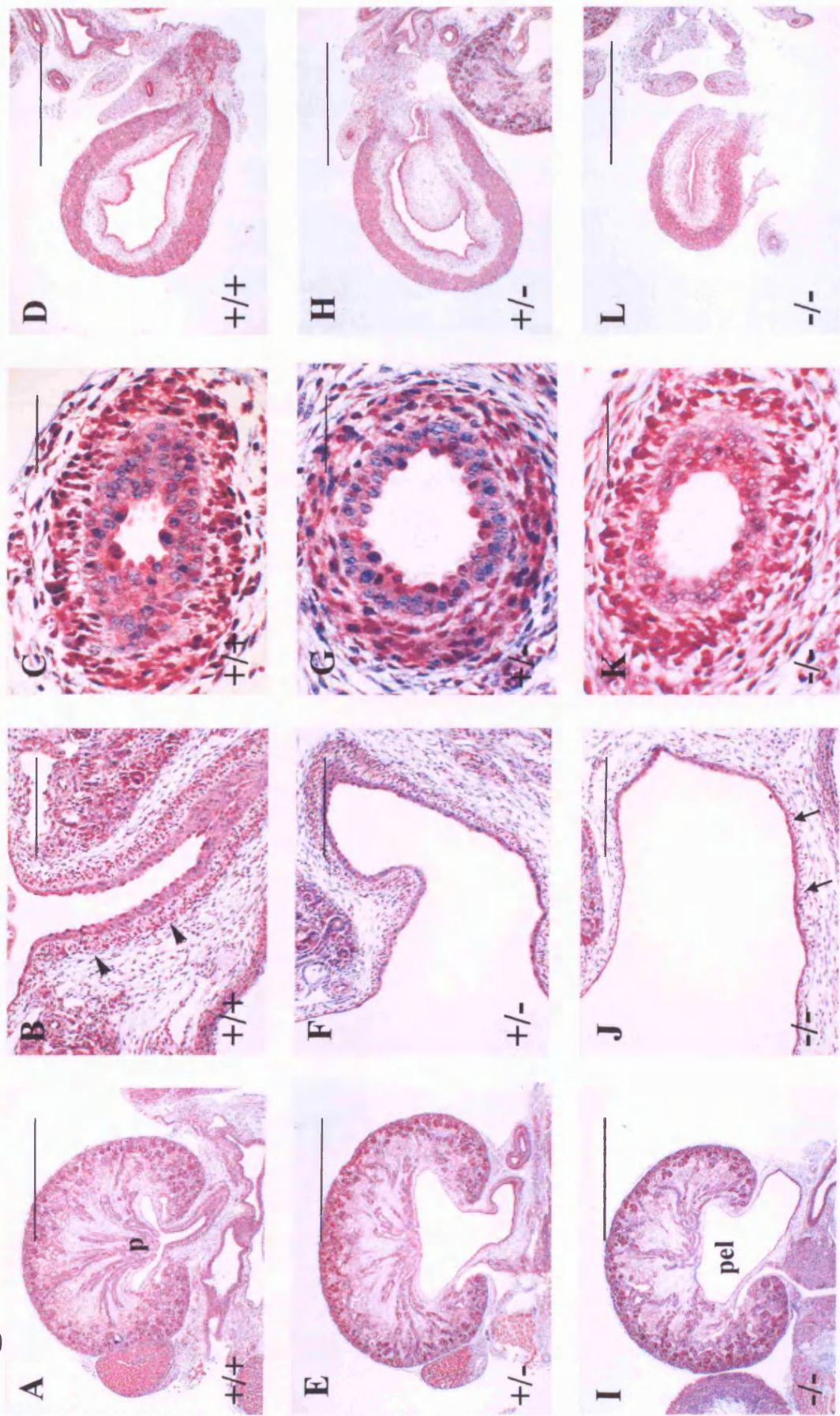




**Figure 6.2.3 Histology of the urinary tracts from E17 *Tshz3*<sup>-/-</sup> mice and their littermates**

Sections were stained with Masson's trichrome and haematoxylin which stains muscle and cytoplasm red/pink, collagen blue/green and nuclei dark blue. Sections from *Tshz3*<sup>+/+</sup> (**A-D**), *Tshz3*<sup>+/-</sup> (**E-H**), and *Tshz3*<sup>-/-</sup> (**I-L**) mice are shown. **A, E and I** kidneys and proximal ureters. (Note; in **A** no papilla is observed as the section was not taken through the very centre of the kidney); **B, F and J** proximal ureters, at a higher magnification (Note thin, disorganised layer of condensed mesenchyme in *Tshz3*<sup>-/-</sup>, compared to thicker, organised layer of condensed mesenchyme in *Tshz3*<sup>+/+</sup>); **C, G and K** transverse sections of distal ureters; **D, H and L** bladders. Arrows in **D** and **L** indicate the position of the vesicoureteric junctions. u, ureter. Scale bars - 1000µm (**A, D, E, H, I and L**), 200µm (**B, F and J**) or 50µm (**C, G and K**).

L. Fasano provided the dissected mouse urinary tracts used in this experiment.

D. Rampling performed the Masson's Trichrome staining.

Part of this figure appears in Caubit et al. (submitted).

**Figure 6.2.3**

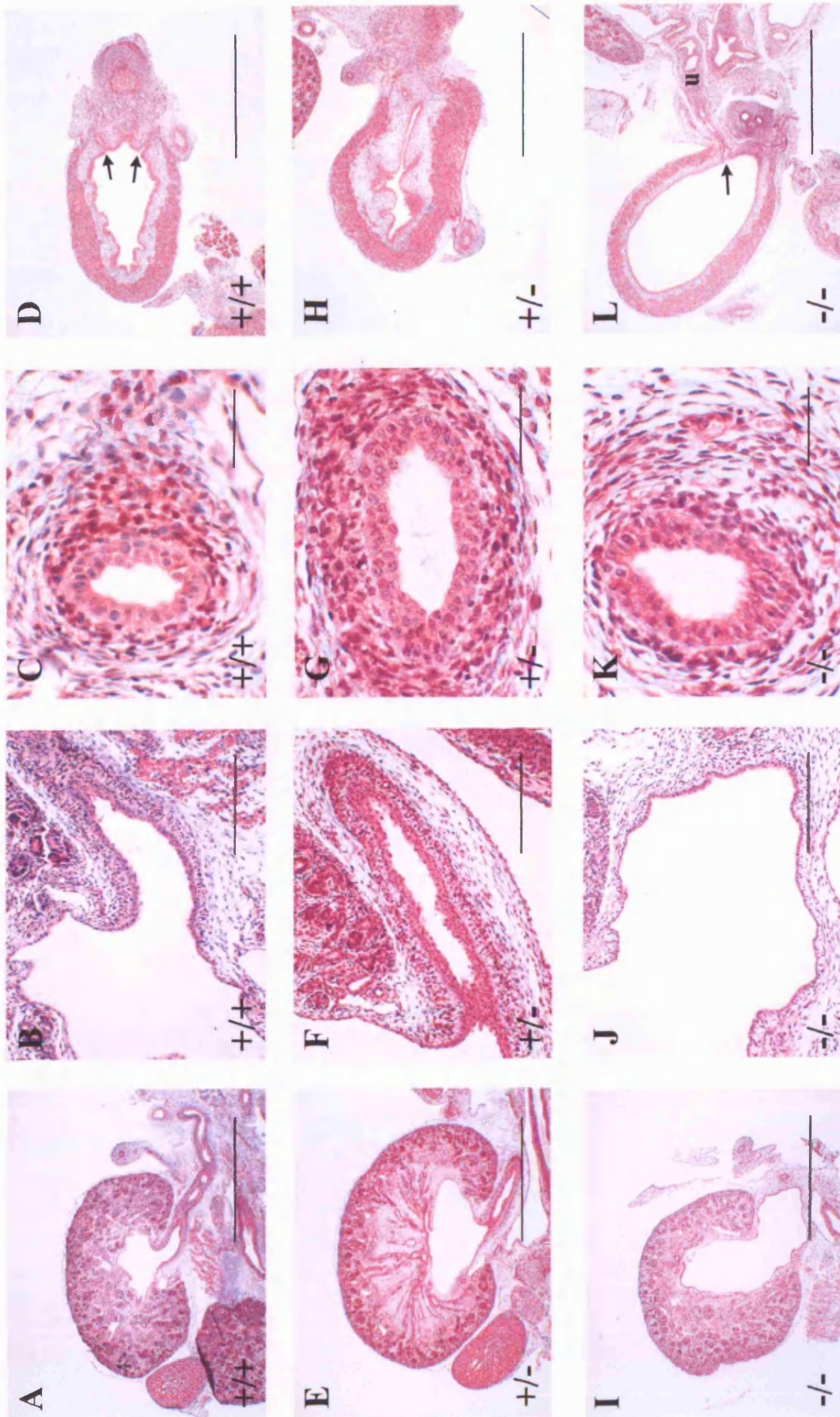


**Figure 6.2.4 Histology of the urinary tracts from E18 *Tshz3*<sup>-/-</sup> mice and their littermates**

Sections were stained with Masson's trichrome and haematoxylin which stains muscle and cytoplasm red/pink, collagen blue/green and nuclei dark blue. Sections from *Tshz3*<sup>+/+</sup> (**A-D**), *Tshz3*<sup>+/-</sup> (**E-H**), and *Tshz3*<sup>-/-</sup> (**I-L**) mice are shown. **A, E and I** kidneys and proximal ureters; **B, F and J** proximal ureters, at a higher magnification. (Note thin, disorganised layer of condensed mesenchyme in *Tshz3*<sup>-/-</sup>, compared to thicker, organised layer of condensed mesenchyme in *Tshz3*<sup>+/+</sup>); **C, G and K** transverse sections of distal ureters; **D, H and L** bladders. Scale bars - 1000µm (**A, D, E, H, I and L**), 200µm (**B, F and J**) or 100µm (**C, G and K**).

L. Fasano provided the dissected mouse urinary tracts used in this experiment.

D. Rampling performed the Masson's Trichrome staining and embedded and sectioned some of the mouse urinary tracts used in this experiment.

Part of this figure appears in Caubit et al. (submitted).

**Figure 6.2.4**

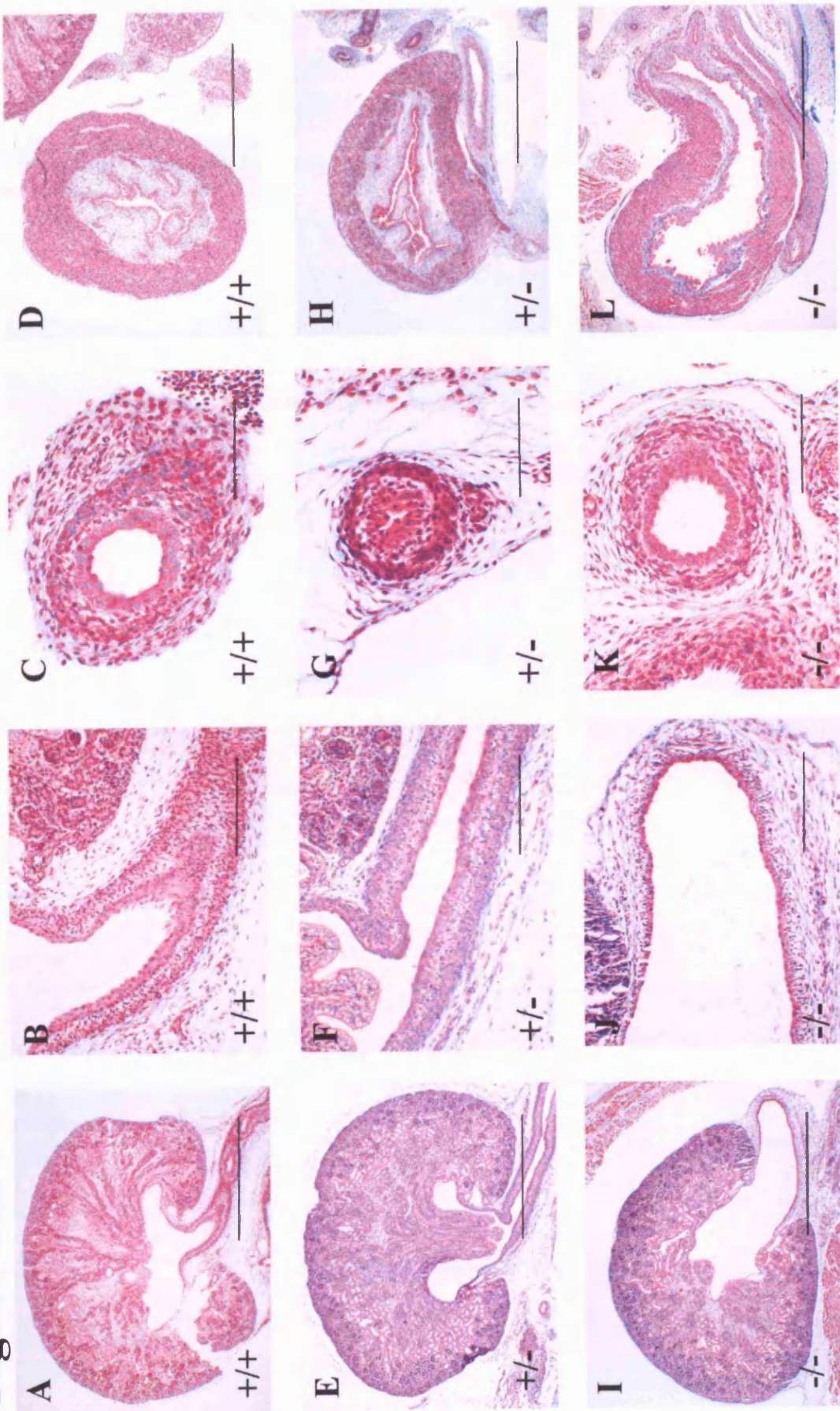


**Figure 6.3 Histology of the metanephric region of E12 *Tshz3*<sup>-/-</sup> mice and their littermates**

Sections were stained with Masson's trichrome and haematoxylin which stains muscle and cytoplasm red/pink, collagen blue/green and nuclei dark blue. Sections from *Tshz3*<sup>+/+</sup> (**A,B**), *Tshz3*<sup>+/-</sup> (**C,D**), and *Tshz3*<sup>-/-</sup> (**E,F**) mice are shown. **A, C** and **E** frontal sections through the region containing the forming kidneys (k) (or metanephri). The mesonephric ducts (which the ureteric buds bud from) can also be seen. Note one of the metanephri in each of **A, C** and **E** have sheared during processing. **B, D** and **F** metanephri at higher magnification; in all genotypes ureteric buds (ub) can be seen to have invaded the metanephric mesenchyme (mm) and branched. Scale bars - 500µm (**A, C** and **E**) or 100µm (**B, D** and **F**).

L. Fasano provided the dissected mouse urinary tracts used in this experiment.

D. Rampling performed the Masson's Trichrome staining.

**Figure 6.3**

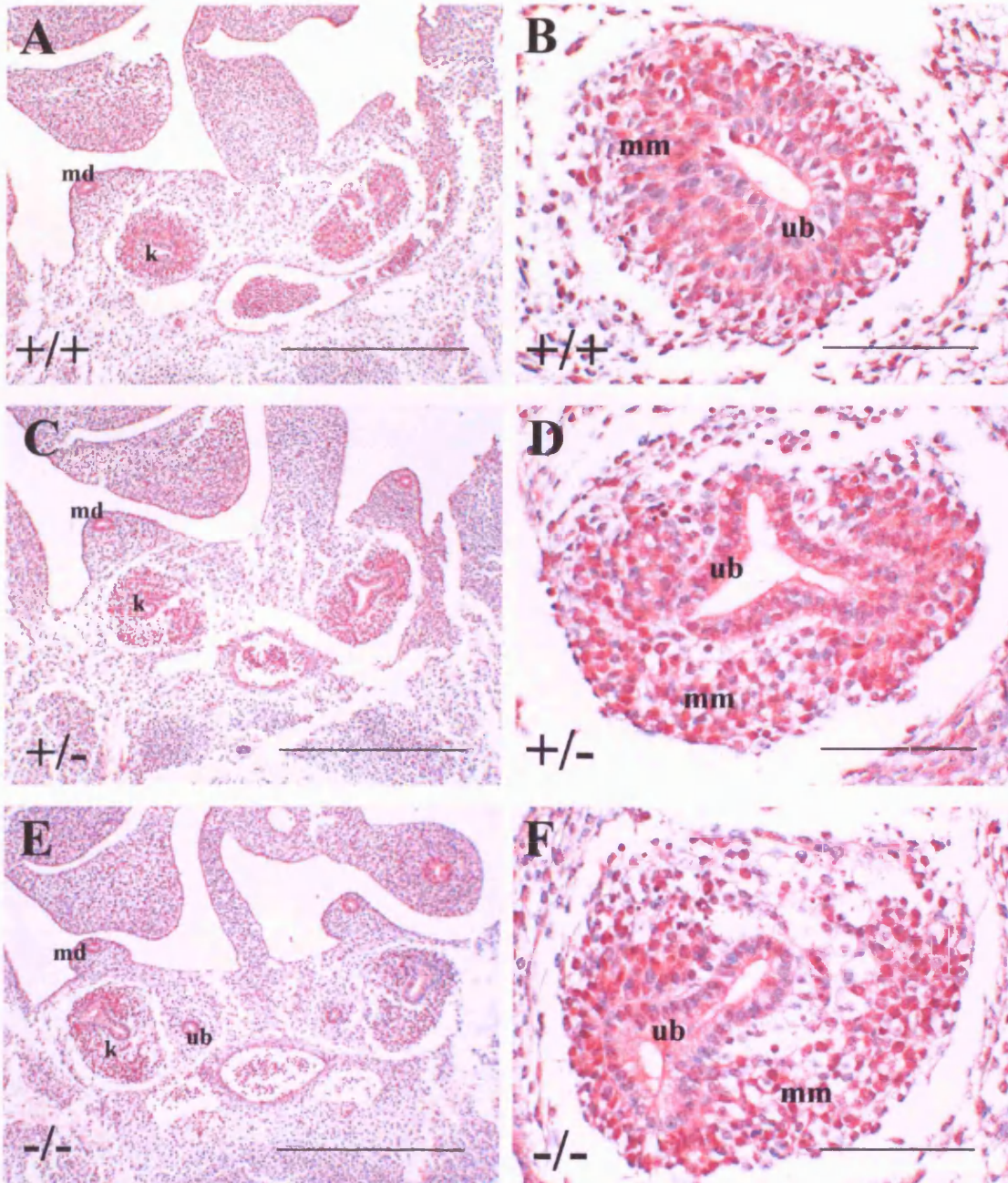


**Figure 6.4 Histology of the nephrogenic zones of kidneys from E18 *Tshz3*<sup>-/-</sup> mice and their littermates**

Sections were stained with Masson's trichrome and haematoxylin which stains muscle and cytoplasm dark red/pink, collagen blue/green and nuclei dark blue. Red blood cells appear light red/pink. Sections from *Tshz3*<sup>+/+</sup> (**A, B**), *Tshz3*<sup>+/-</sup> (**C, D**) and *Tshz3*<sup>-/-</sup> (**E,F**) kidneys are shown. **A, C and E** Nephrogenic zones from all genotypes appear normal containing ureteric buds (ub) surrounded by condensing mesenchyme, s-shaped bodies (s) and glomeruli (g). **B, D and F** Higher magnifications of glomeruli reveal that glomeruli are vascularised, and contain red blood cells (arrows). Scale bars - 200µm (**A, C and E**) or 50µm (**B, D and F**).

L. Fasano provided the dissected mouse urinary tracts used in this experiment.

D. Rampling performed the Masson's Trichrome staining.

Part of this figure appears in Caubit et al. (submitted).

**Figure 6.4**

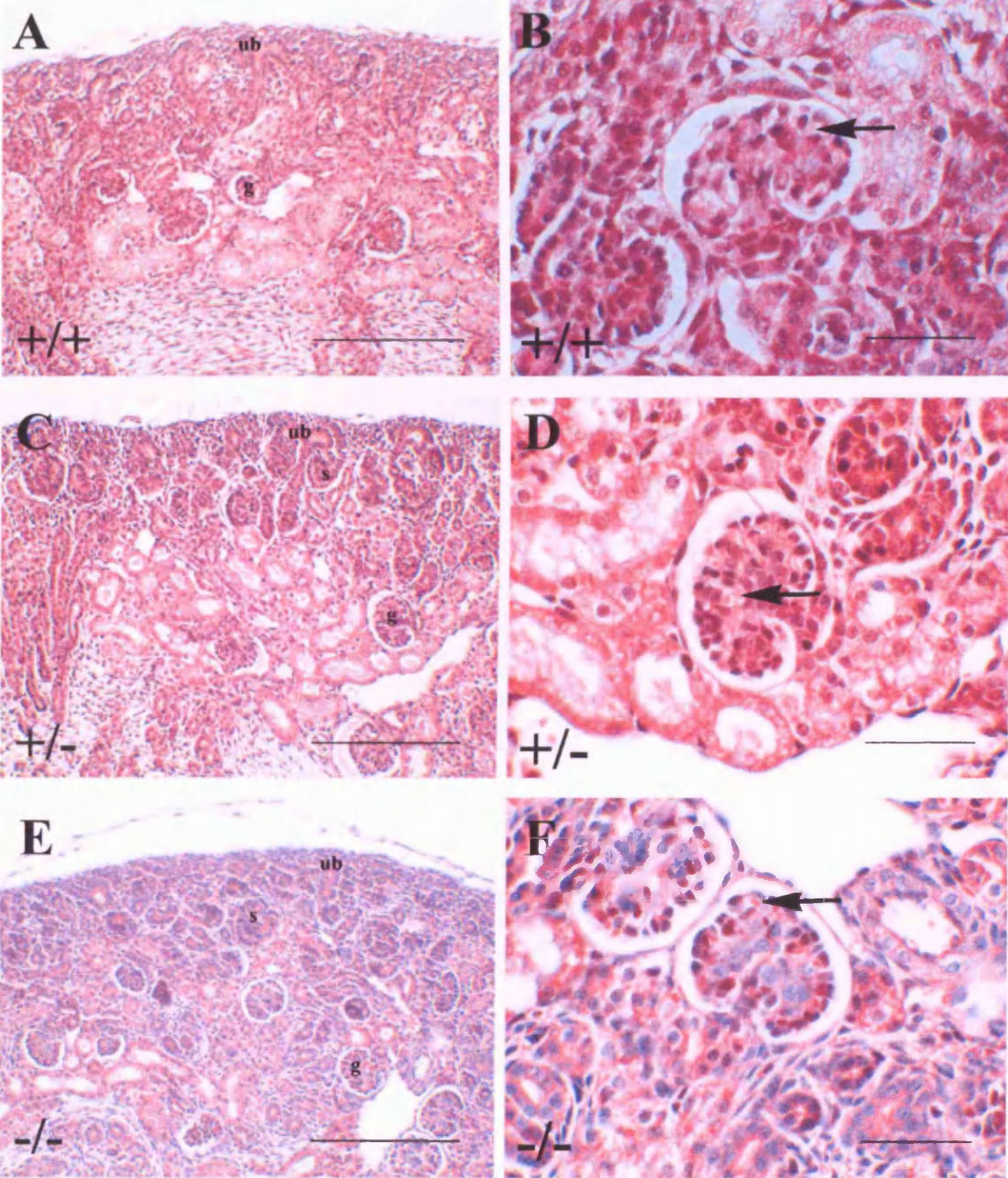




**Figure 6.5 High magnification view of histology staining of E15 proximal ureters from *Tshz3*<sup>-/-</sup> mice and their littermates**

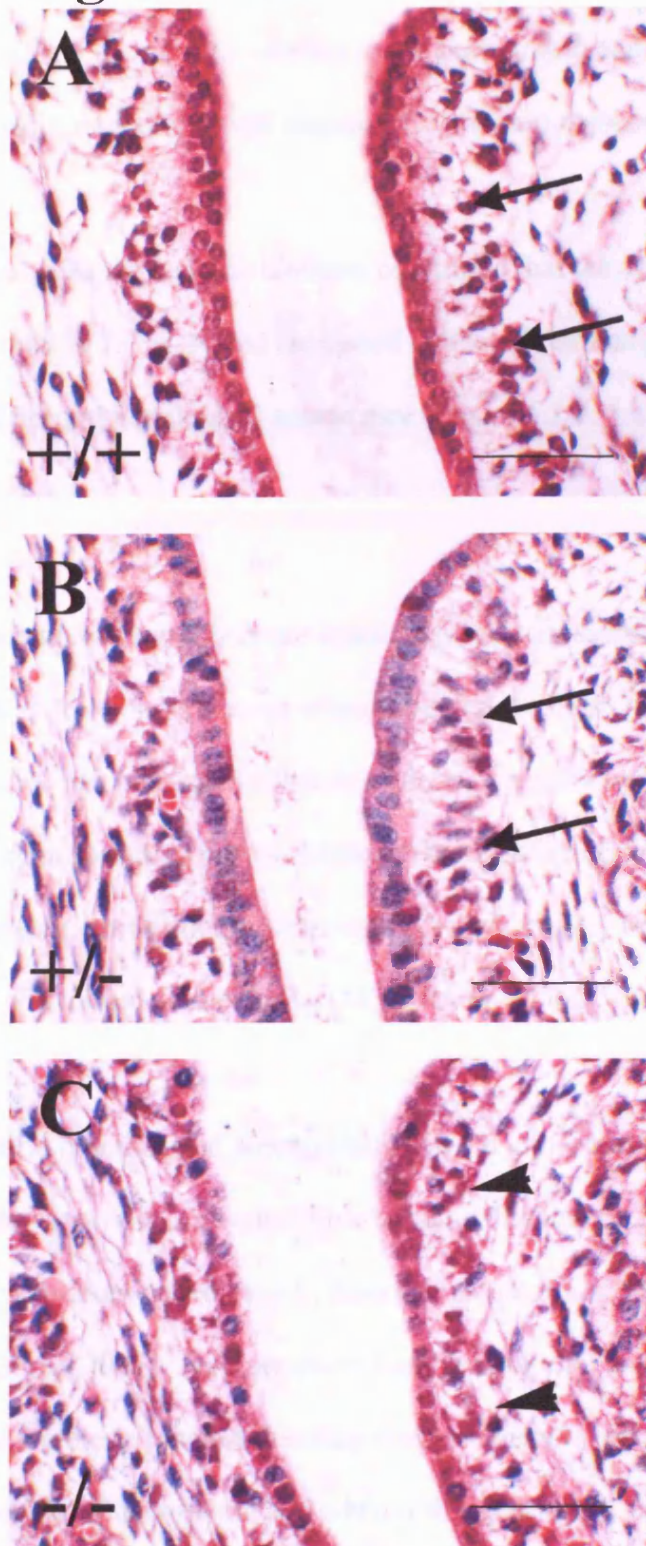
Sections were stained with Masson's trichrome and haematoxylin which stains muscle and cytoplasm red/pink, collagen blue/green and nuclei dark blue. Note in *Tshz3*<sup>+/+</sup> (A), *Tshz3*<sup>+/-</sup> (B) condensed mesenchymal cells (arrows) are organised in a line, with their nuclei a little way away from the urothelium, where in *Tshz3*<sup>-/-</sup> (C) condensed mesenchymal cells (arrowheads) are present, but some of their nuclei lie immediately adjacent to the urothelium. Scale bars - 50µm.

L. Fasano provided the dissected mouse urinary tracts used in this experiment.

D. Rampling performed the Masson's Trichrome staining.

Part of this figure appears in Caubit et al. (submitted).

**Figure 6.5**



Histological sections through distal ureters of E15 to E18 (Figure 6.2.1, 6.2.2, 6.2.3 and 6.2.4) *Tshz3*<sup>-/-</sup> embryos confirmed that they had relatively normal diameter lumens (in comparison to *Tshz3*<sup>+/+</sup> ureters at the same stage) and morphologically grossly normal walls, containing well organised condensed mesenchymal cell layers.

Observation of sections through the bladders confirmed that they were grossly anatomically normal in *Tshz3*<sup>-/-</sup>, and contained urothelial, lamina propria and smooth muscle layers of normal histological appearance (Figure 6.2.1, 6.2.2, 6.2.3 and 6.2.4).

***Hydronephrosis and hydroureter is not caused by overt anatomical obstruction***

Hydroureter and hydronephrosis occur when urine fails to drain to the bladder. Such a failure of drainage can be caused either by a physical obstruction in the ureter (or at the junction between the ureter and the bladder; the vesicoureteric junction), or a failure in the peristaltic movements of the ureter (which usually act to propel urine down the ureter and towards the bladder) (Mendelsohn, 2004; Mendelsohn, 2006).

If the vesicoureteric junction (the junction between the ureter and the bladder) fails to form during development, a physical obstruction will occur at the ends of the ureters, leading to hydronephrosis and hydroureter (Mackie and Stephens, 1975; Murawski and Gupta, 2006). Hydronephrosis and hydroureter can also occur as a result of the vesicoureteric junction forming at an ectopic site, which may result from abnormal positioning of the ureteric bud when it forms from the mesonephric duct. It has been proposed that if the ureteric bud forms too cranially along the ureteric bud the ureter will attach to the urethra, rather than the bladder. If the ureteric bud

develops more caudally than usual then the ureteric orifice will be situated in the bladder, but laterally to the bladder trigone. (Mackie and Stephens, 1975; Schwarz et al., 1981). Histological sections of the vesicoureteric junctions revealed that ureters attach to the bladder normally in *Tshz3* null mice, and vesicoureteric junctions are normally situated as compared to wildtype (Figure 6.2.3 D and L).

To confirm that there was no physical obstruction at the vesicoureteric junction, and to test whether a physical obstruction was present in the ureter itself, India ink was injected into the renal pelvis of an E18 *Tshz3*<sup>-/-</sup>. Upon exerting gentle pressure, the ink flowed down the ureter into the bladder, thus excluding complete intrinsic anatomical obstruction (Figure 6.6).

It has been reported that abnormally arranged blood vessels (Hoffer and Lebowitz, 1985; Rooks and Lebowitz, 2001; Simforoosh et al., 2005), or aneurysm (Miyagawa et al., 2001) can constrict the ureter, and so lead to an extrinsic physical obstruction of the ureter. At autopsy no blood vessels were observed to “cross over” the ureter at the termini of dilated segments, and no aneurysms were observed (Figure 6.6).

Therefore urine flow was not impeded due to constriction of the ureter by abnormally arranged blood vessels.

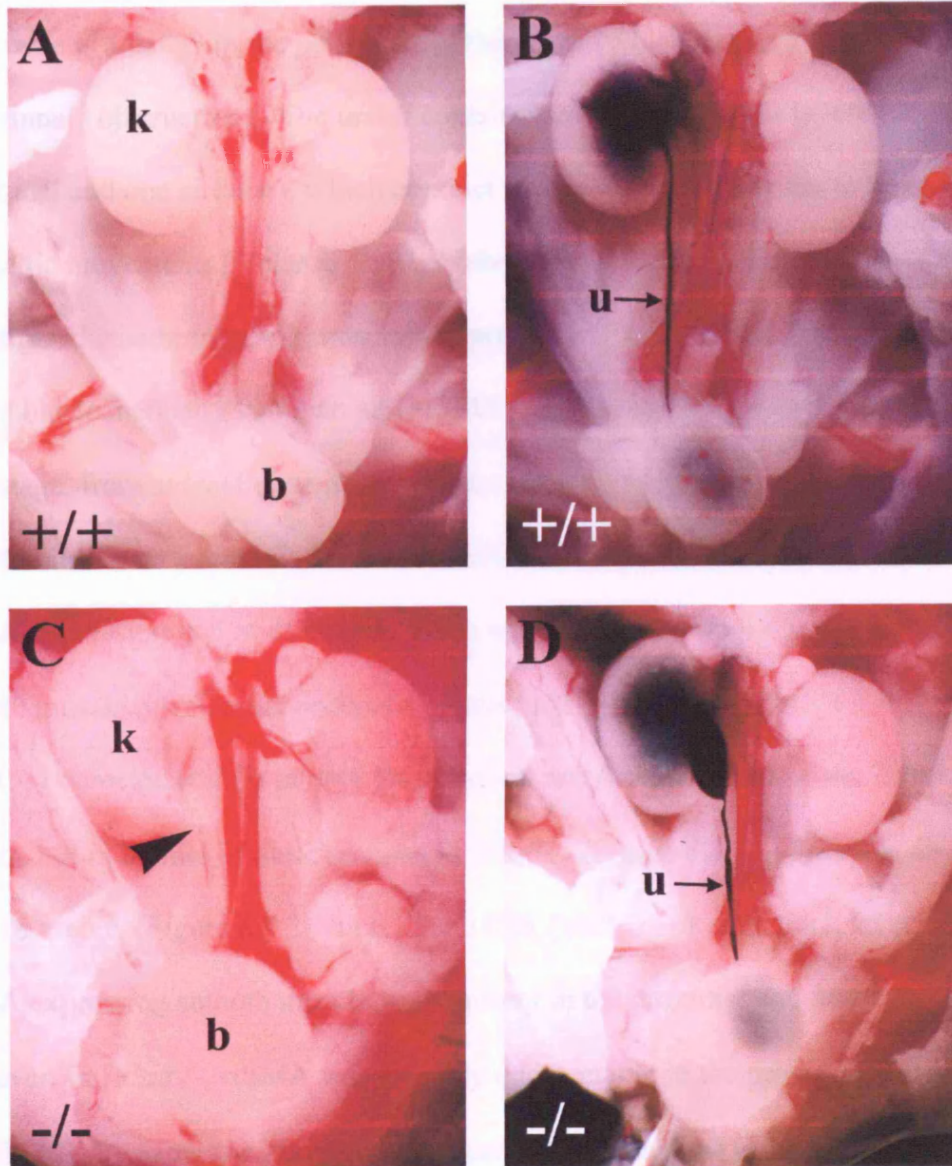
### **Figure 6.6 Injection of ink into renal pelves of *Tshz3*<sup>-/-</sup> mice**

Wildtype (**A, B**) and homozygous mutant (**C, D**) E18 mice were partially dissected to reveal the kidneys, ureters and bladders. Urinary tracts were not fully dissected, to prevent inadvertently relieving an obstruction. India ink was then injected into the renal pelvis of one kidney from each genotype with a pulled out Pasteur pipette, and the kidney gently tapped to encourage the flow of ink. **A** and **C** urinary tracts prior to the injection of India ink. The arrangement of blood vessels close to the kidneys appears similar in the wildtype and mutant. In particular, crossing vessels cannot be seen constricting the ureter at the distal end of the highly hydronephrotic section (arrowhead). **B** and **D** urinary tracts after the injection of India ink. In both wildtype and mutant the ink has travelled down the ureter and can be seen to have entered the bladder, indicating that there is no physical obstruction within the urinary tract. k, kidney; b, bladder; u, ureter. Note; frame **C** is at a slightly higher magnification to other frames. These photomicrographs were taken on a dissecting microscope with a variable zoom, and therefore no scale bars can be provided.

The partial dissections and India ink injections were performed by L. Fasano and myself.

Part of this figure appears in Caubit et al. (submitted).

**Figure 6.6**



### ***Defects in ureteric smooth muscle in *Tshz3*<sup>-/-</sup> mice***

The absence of intrinsic and extrinsic physical obstructions in the urinary tracts of *Tshz3*<sup>-/-</sup> mice, indicated that the likely cause of hydroureter and hydronephrosis in these mice is a defect in the peristalsis of the ureter (which causes a so called “functional” obstruction). The ureter contains two smooth muscle layers (one longitudinal and one circular), which contract in a co-ordinated manner to bring about peristaltic movements (Velardo, 1981; Mahoney et al., 2006). Therefore I investigated whether smooth muscle was present in the ureters of *Tshz3* null mice, by immunohistochemistry using an anti- $\alpha$ SMA antibody (n=2-5 for each genotype at each stage, from at least three different litters at each stage), which is an early smooth muscle differentiation marker (McHugh, 1995). It has been reported that  $\alpha$ SMA expression is first detectable in the wildtype ureter at E14.5, and ureteric smooth muscle development occurs in a proximal to distal direction (Yu et al., 2002). At E15, I detected  $\alpha$ SMA in both the proximal and distal sections of the *Tshz3*<sup>+/+</sup> ureters, but in neither of these sections in *Tshz3*<sup>-/-</sup> (Figure 6.7.1). This was also true for E16 ureters (Figure 6.7.2). In E17 and E18 *Tshz3*<sup>+/+</sup> ureters thick layers of  $\alpha$ SMA expressing smooth muscle were present in the proximal and distal ureters. However, in *Tshz3*<sup>-/-</sup>,  $\alpha$ SMA was virtually undetectable in the proximal ureters and distally  $\alpha$ SMA expressing layers were apparently not as thick as in wildtype (Figure 6.7.3 and 6.7.4). Some sections stained for  $\alpha$ SMA included the junction between the distended and relatively normal parts of the ureter. Here it was observed that lack of expression of SMA correlated with the severity of the distension: that is SMA was not expressed in the highly distended section of ureter but was expressed in the part of ureter immediately below the distended part (Figure 6.7.3G).

**Figure 6.7.1 Immunohistochemistry for  $\alpha$ SMA in kidneys and ureters from E15 *Tshz3*<sup>-/-</sup> mice and their littermates.**

Sections were stained using an anti- $\alpha$ SMA antibody and developed with DAB to give a brown colour. Sections were counterstained with haematoxylin, to colour the nuclei blue, and PAS. Sections from *Tshz3*<sup>+/+</sup> (**A-C**), *Tshz3*<sup>+/-</sup> (**D-F**), and *Tshz3*<sup>-/-</sup> (**G-I**) mice are shown. Note at this stage *Tshz3*<sup>-/-</sup> mice have not developed hydronephrosis and hydroureter. **A, D and G** kidneys and proximal ureters; **B, E and H** proximal ureters, at a higher magnification (proximal ureter sections are longitudinal, except **B**, which is transverse); **C, F and I** transverse sections of distal ureters.  $\alpha$ SMA staining can be seen in mesenchymal cells surrounding the urothelium of the proximal and distal ureter in *Tshz3*<sup>+/+</sup> and *Tshz3*<sup>+/-</sup>, but not in *Tshz3*<sup>-/-</sup>.  $\alpha$ SMA staining can also be seen in the arteries of all genotypes. Scale bars - 1000 $\mu$ m (**A, D and G**), 200 $\mu$ m (**B, E and H**) or 100 $\mu$ m (**C, F and I**).

L. Fasano provided the dissected mouse urinary tracts used in this experiment.



**Figure 6.7.1**

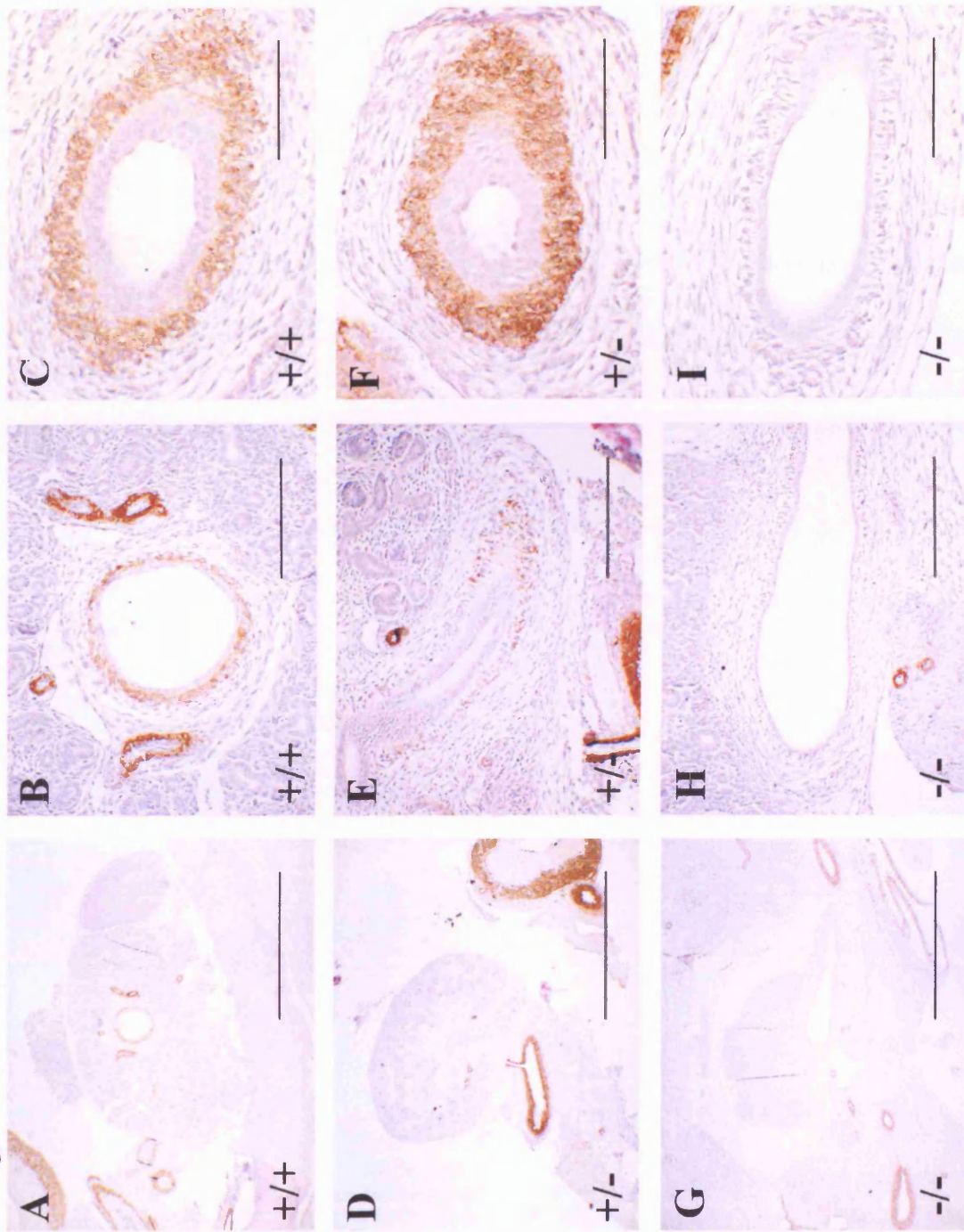


**Figure 6.7.2 Immunohistochemistry for  $\alpha$ SMA in kidneys and ureters from E16 *Tshz3*<sup>-/-</sup> mice and their littermates.**

Sections were stained using an anti- $\alpha$ SMA antibody and developed with DAB to give a brown colour. Sections were counterstained with haematoxylin, to colour the nuclei blue, and PAS. Sections from *Tshz3*<sup>+/+</sup> (**A-C**), *Tshz3*<sup>+/-</sup> (**D-F**), and *Tshz3*<sup>-/-</sup> (**G-I**) mice are shown. Note by this stage *Tshz3*<sup>-/-</sup> mice have developed hydronephrosis and hydroureter. **A, D** and **G** kidneys and proximal ureters; **B, E** and **H** proximal ureters, at a higher magnification; **C, F** and **I** transverse sections of distal ureters.  $\alpha$ SMA staining can be seen in a thick layer of mesenchymal cells surrounding the urothelium of the proximal and distal ureter in *Tshz3*<sup>+/+</sup> and *Tshz3*<sup>+/-</sup>, but not in *Tshz3*<sup>-/-</sup>.  $\alpha$ SMA staining can also be seen in the arteries and renal stroma of all genotypes. Scale bars - 1000 $\mu$ m (**A, D** and **G**), 200 $\mu$ m (**B, E** and **H**) or 50 $\mu$ m (**C, F** and **I**).

L. Fasano provided the dissected mouse urinary tracts used in this experiment.

Part of this figure appears in Caubit et al. (submitted).

**Figure 6.7.2**

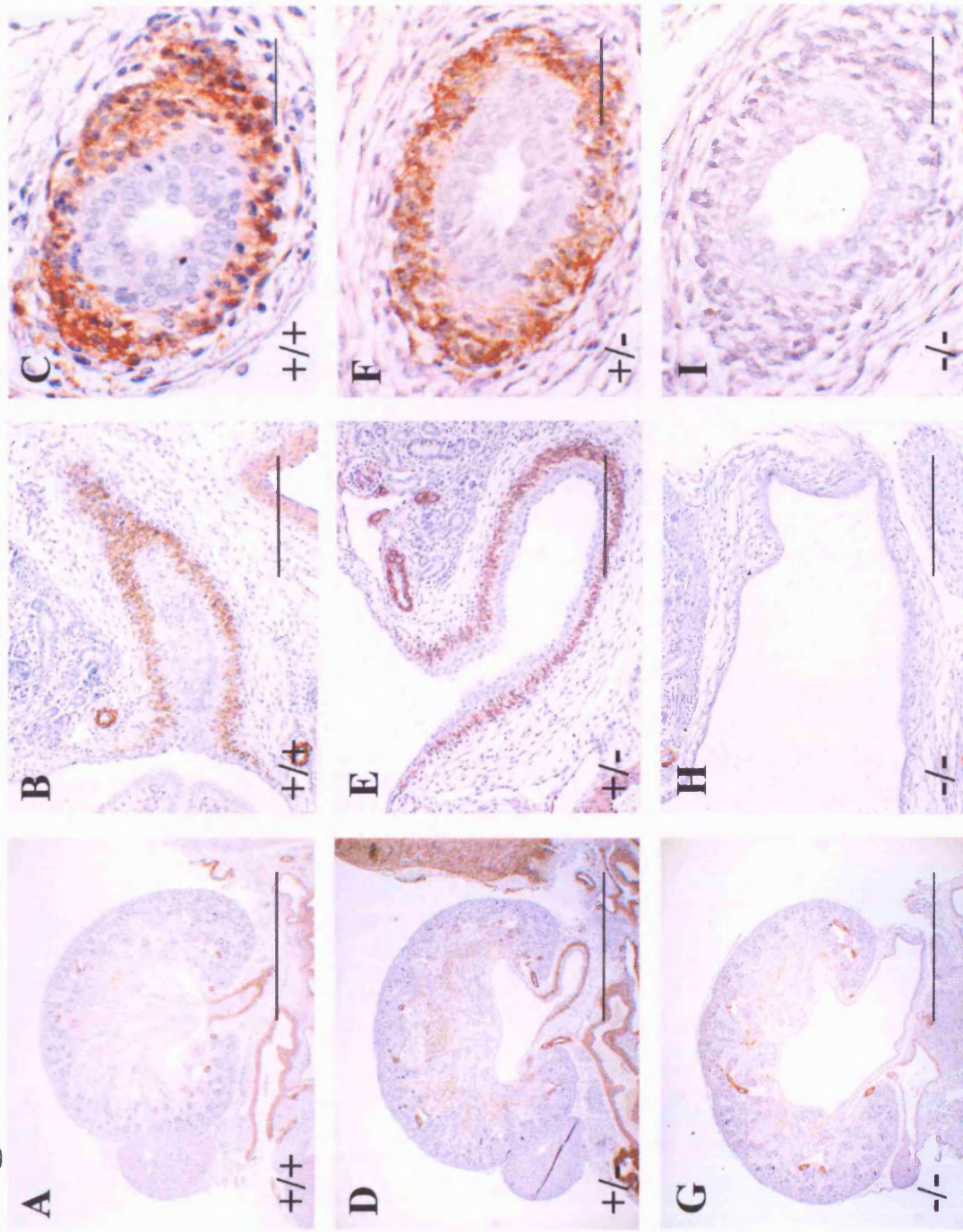


**Figure 6.7.3 Immunohistochemistry for  $\alpha$ SMA in kidneys and ureters from E17 *Tshz3*<sup>-/-</sup> mice and their littermates.**

Sections were stained using an anti- $\alpha$ SMA antibody and developed with DAB to give a brown colour. Sections were counterstained with haematoxylin, to colour the nuclei blue, and PAS. Sections from *Tshz3*<sup>+/+</sup> (**A-C**), *Tshz3*<sup>+/-</sup> (**D-F**), and *Tshz3*<sup>-/-</sup> (**G-I**) mice are shown. Note the *Tshz3*<sup>-/-</sup> mice has severe hydronephrosis and hydroureter, and the *Tshz3*<sup>+/-</sup> mouse has mild hydroureter. **A, D** and **G** kidneys and proximal ureters; **B, E** and **H** proximal ureters, at a higher magnification; **C, F** and **I** transverse sections of distal ureters.  $\alpha$ SMA staining can be seen in a thick layer of mesenchymal cells surrounding the urothelium of the proximal and distal ureter in *Tshz3*<sup>+/+</sup> and *Tshz3*<sup>+/-</sup>. In the *Tshz3*<sup>-/-</sup> proximal ureter no  $\alpha$ SMA positive cells can be seen in the mesenchyme of the highly dilated section of the ureter; however  $\alpha$ SMA staining is seen in the ureteric mesenchyme of the relatively unaffected (more distal) part of the ureter seen on this section (arrow). In the *Tshz3*<sup>-/-</sup> distal ureter only a few  $\alpha$ SMA positive cells can be seen.  $\alpha$ SMA staining can also be seen in the arteries and renal stroma of all genotypes. Scale bars - 1000 $\mu$ m (**A, D** and **G**), 200 $\mu$ m (**B, E** and **H**) or 50 $\mu$ m (**C, F** and **I**).

L. Fasano provided the dissected mouse urinary tracts used in this experiment.

Part of this figure appears in Caubit et al. (submitted).

**Figure 6.7.3**

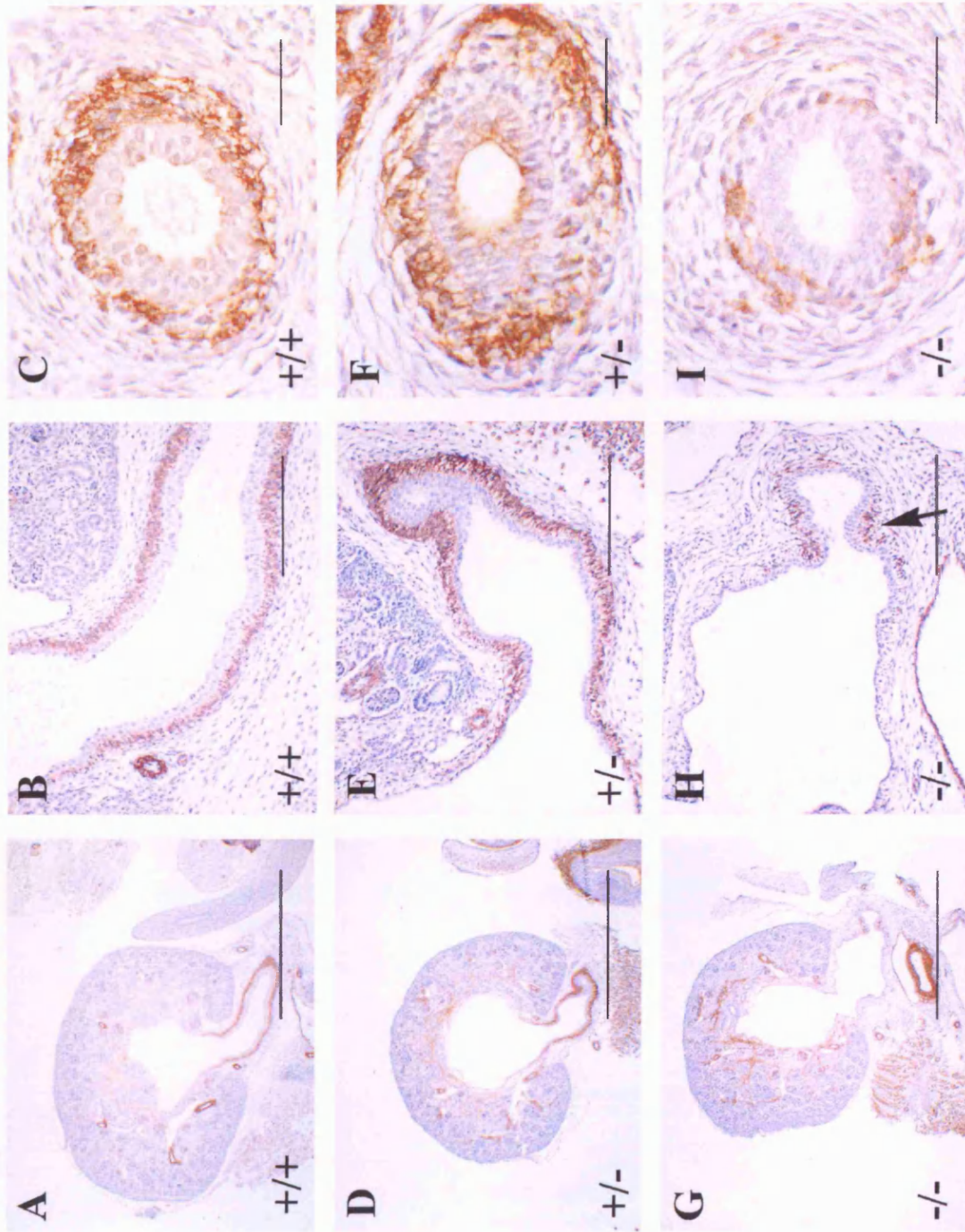


## Figure 6.7.4 Immunohistochemistry for $\alpha$ SMA in kidneys and ureters from E18

### *Tshz3*<sup>-/-</sup> mice and their littermates

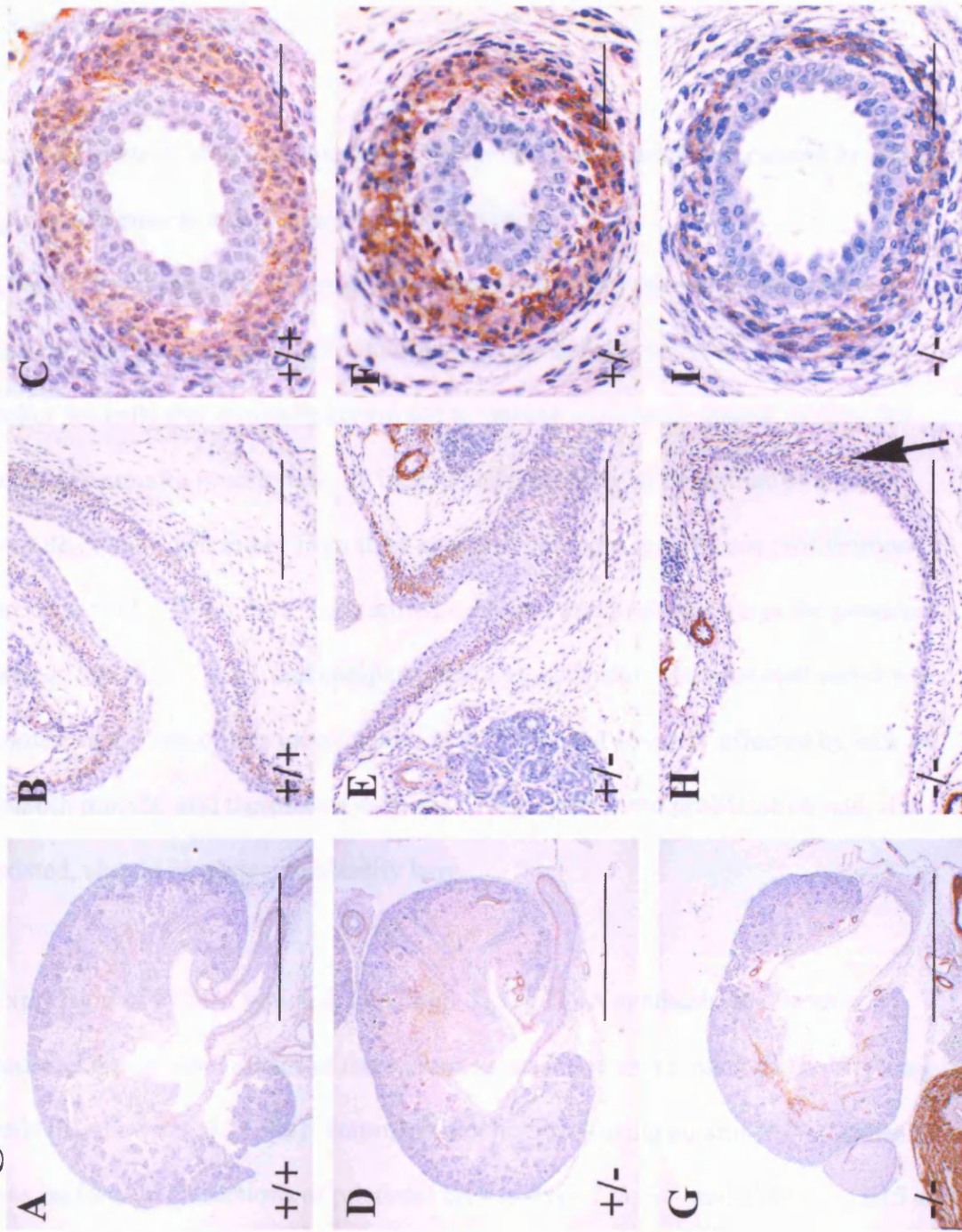
Sections were stained using an anti- $\alpha$ SMA antibody and developed with DAB to give a brown colour. Sections were counterstained with haematoxylin, to colour the nuclei blue, and PAS. Sections from *Tshz3*<sup>+/+</sup> (**A-C**), *Tshz3*<sup>+/-</sup> (**D-F**), and *Tshz3*<sup>-/-</sup> (**G-I**) mice are shown. Note the *Tshz3*<sup>-/-</sup> mouse has severe hydronephrosis and hydroureter. **A, D** and **G** kidneys and proximal ureters; **B, E** and **H** proximal ureters, at a higher magnification; **C, F** and **I** transverse sections of distal ureters.  $\alpha$ SMA staining can be seen in a thick layer of mesenchymal cells surrounding the urothelium of the proximal and distal ureter in *Tshz3*<sup>+/+</sup> and *Tshz3*<sup>+/-</sup>. In the *Tshz3*<sup>-/-</sup> proximal ureter only few  $\alpha$ SMA positive cells can be seen in the mesenchyme of the more distal part of this section of ureter (arrow). In the *Tshz3*<sup>-/-</sup> distal ureter a ring of  $\alpha$ SMA positive cells can be seen, but the ring is not as thick as in *Tshz3*<sup>+/+</sup> and *Tshz3*<sup>+/-</sup>.  $\alpha$ SMA staining can also be seen in the arteries and renal stroma of all genotypes. Scale bars - 1000 $\mu$ m (**A, D** and **G**), 200 $\mu$ m (**B, E** and **H**) or 50 $\mu$ m (**C, F** and **I**).

L. Fasano provided the dissected mouse urinary tracts used in this experiment.

D. Rampling embedded and sectioned some of the mouse urinary tracts used in this experiment.

Part of this figure appears in Caubit et al. (submitted).

**Figure 6.7.4**



The defect in the smooth muscle is apparent at E15, and therefore precedes the gross phenotype. Therefore the smooth muscle deficiency cannot be explained by damage that may be caused to the ureter by the pressure from accumulated urine, and must have a developmental cause.

***Lack of ureteric smooth muscle in *Tshz3*<sup>-/-</sup> mutants is probably caused by a failure of smooth muscle cell precursor differentiation***

There are two possible causes of the absence of smooth muscle in the proximal ureters (and attenuation of smooth muscle in the distal ureters) of *Tshz3*<sup>-/-</sup> mice; either the cells that normally contribute to smooth muscle are absent, or they fail to adopt a smooth muscle fate. A lack of cells available to contribute to smooth muscle could result either from their apoptosis, or from insufficient proliferation of precursor cells. Therefore, I quantified apoptosis and proliferation in the proximal ureters of *Tshz3*<sup>-/-</sup> mice and compared them to wildtype. The proximal ureter was chosen as the site of this investigation as it is the most severely affected by lack of smooth muscle, and therefore a difference in apoptosis and proliferation rate, if it existed, should be easiest to identify here.

Expression of PCNA, which is very high during DNA synthesis, and is almost undetectable at other stages of the cell cycle, was used as a marker of proliferating cells (Mathews et al., 1984). Immunohistochemistry using an anti-PCNA antibody was performed on sections of proximal ureters from *Tshz3*<sup>-/-</sup> and *Tshz3*<sup>+/+</sup> E15 and E16 mice (n=4 for each genotype at E15, n=3 for each genotype at E16), and the number of PCNA positive cells quantified as a percentage of total nuclei present for the following populations of cells; urothelia, condensing mesenchyme (presumptive



smooth muscle cells) and loose mesenchyme. No statistically significant differences in proliferation rates were observed between *Tshz3*<sup>+/+</sup> and *Tshz3*<sup>-/-</sup> in any of the cell populations at either E15 (before hydronephrosis) or E16 (when hydronephrosis was present). However, at E15 there was a tendency for decreased proliferation in the condensing mesenchyme (presumptive smooth muscle layer) of *Tshz3*<sup>-/-</sup> ureters compared with *Tshz3*<sup>+/+</sup> ureters. Table 6.1 shows a summary of the results of this experiment. Figures 6.8.1 and 6.8.2 show graphical representations of the quantification of proliferative cells. Figure 6.8.3 shows representative PCNA immunohistochemistry.

**Table 6.1 Proliferation of Cells in the Proximal Ureter**

**Percentage of PCNA positive cells**

Percentages are given as; Average percentage  $\pm$  standard error of the mean

P-values refer to independent samples T-test (equal variance not assumed).

<b>E15</b>	<b>Urothelium</b>	<b>Condensing Mesenchyme</b>	<b>Loose Mesenchyme</b>
Tshz3+/+	13.2 $\pm$ 4.3	7.9 $\pm$ 3.8	9.5 $\pm$ 1.3
Tshz3-/-	9.92 $\pm$ 6.0	4.3 $\pm$ 1.9	11.3 $\pm$ 2.9
T-test P=	0.67	0.44	0.61

<b>E16</b>	<b>Urothelium</b>	<b>Condensing Mesenchyme</b>	<b>Loose Mesenchyme</b>
Tshz3+/+	11.7 $\pm$ 4.8	2.1 $\pm$ 1.5	6.4 $\pm$ 3.3
Tshz3-/-	6.3 $\pm$ 0.62	2.3 $\pm$ 0.64	4.9 $\pm$ 1.3
T-test P=	0.38	0.93	0.70

**Total number of cells counted per sample**

Numbers given refer to the range, median of the number of cells counted per sample

<b>E15</b>	<b>Urothelium</b>	<b>Condensing Mesenchyme</b>	<b>Loose Mesenchyme</b>
Tshz3+/+	109-489, 180.5	261-857, 358	165-769, 451
Tshz3-/-	94-753, 136.5	52-1095, 245.5	32-986, 334

<b>E16</b>	<b>Urothelium</b>	<b>Condensing Mesenchyme</b>	<b>Loose Mesenchyme</b>
Tshz3+/+	279-339, 317	326-597, 594	423-737, 494
Tshz3-/-	113-671, 227	143-404, 168	363-679, 378

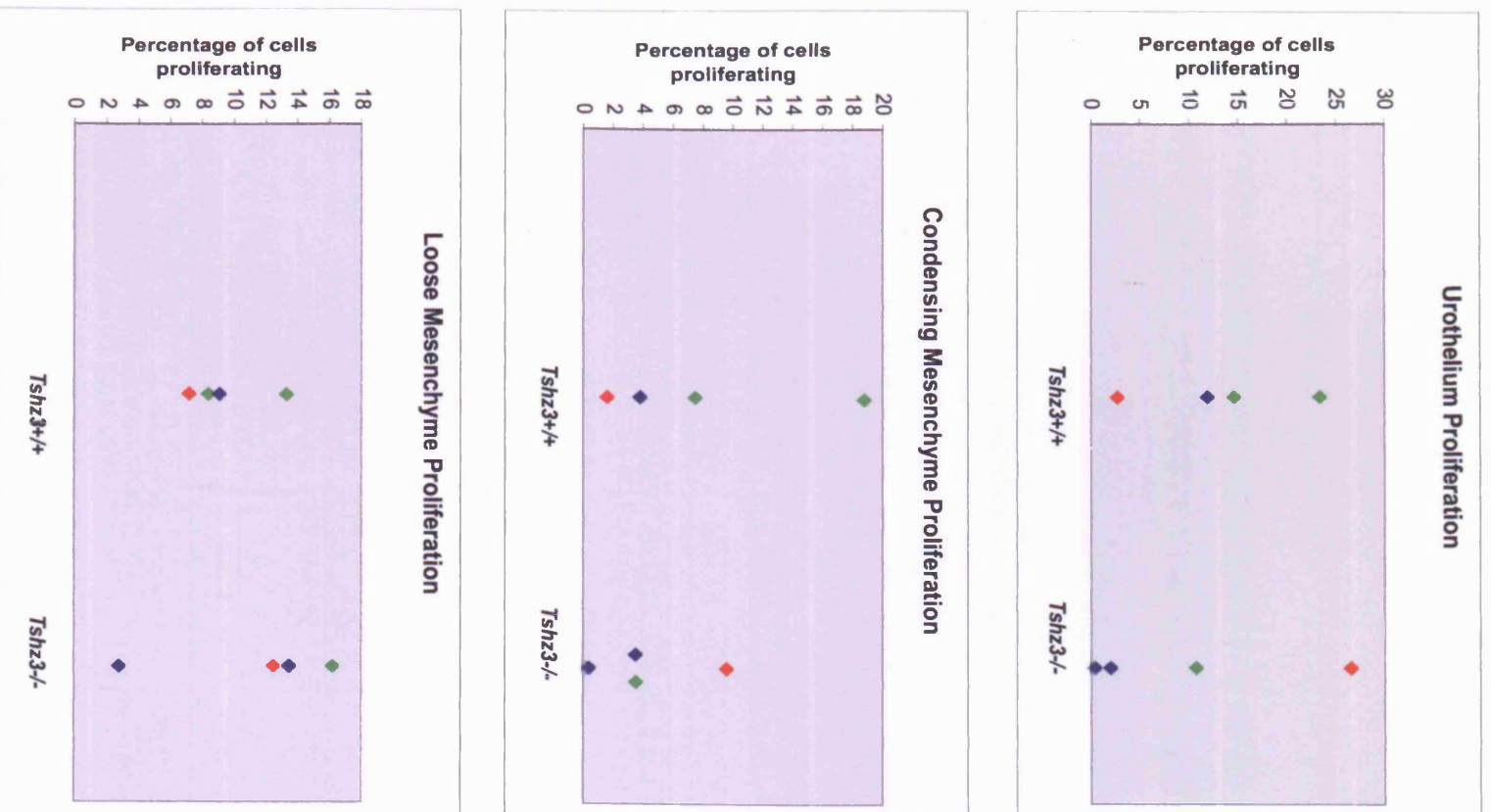
**Figure 6.8.1 Scatter plots showing the percentage of proliferative cells in E15**

***Tshz3*<sup>-/-</sup> and *Tshz3*<sup>+/+</sup> proximal ureters**

Proliferative cells were quantified in three distinct cell populations in the proximal ureter; the urothelium, the condensing mesenchyme and the loose mesenchyme.

Separate scatter plots are shown for each cell population. The number of proliferative cells, expressed as a percentage of total number of cells, is shown for each *Tshz3*<sup>-/-</sup> and *Tshz3*<sup>+/+</sup> sample analysed. Although there is variation in the percentage of proliferative cells between samples, no reproducible differences were observed between *Tshz3*<sup>+/+</sup> and *Tshz3*<sup>-/-</sup> samples in any cell population. Samples taken from different litters are shown in different colours. There is no reproducible difference in proliferation rates between samples taken from different litters in any cell population.

**Figure 6.8.1 - E15 Proliferation**



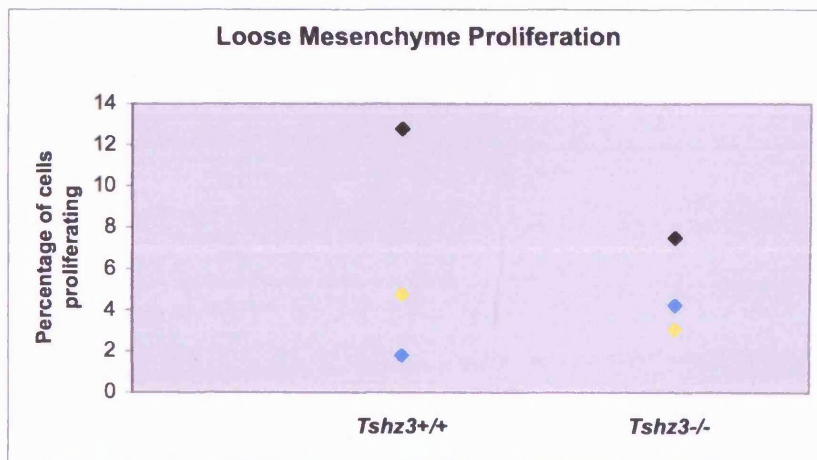
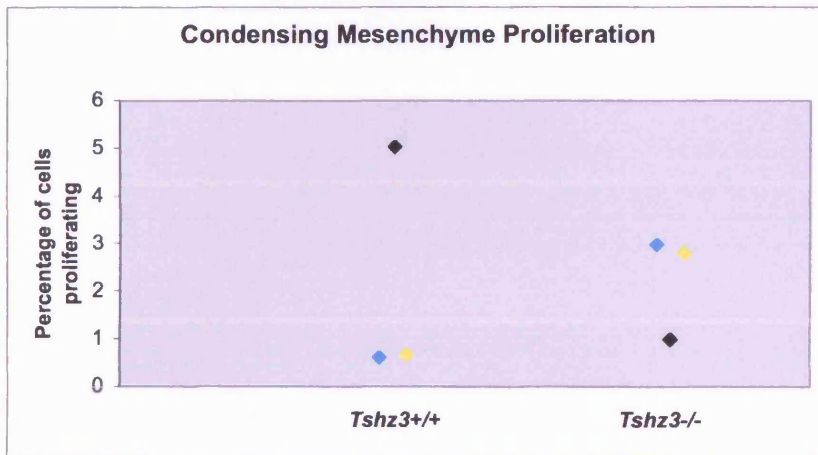
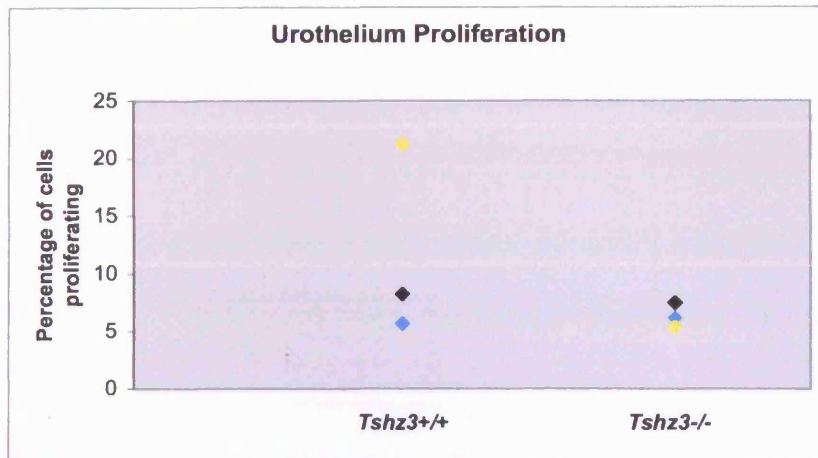
Samples from the same litter are shown in the same colour

**Figure 6.8.2 Scatter plots showing the percentage of proliferative cells in E16 *Tshz3*<sup>-/-</sup> and *Tshz3*<sup>+/+</sup> proximal ureters**

Proliferative cells were quantified in three distinct cell populations in the proximal ureter; the urothelium, the condensing mesenchyme and the loose mesenchyme.

Separate scatter plots are shown for each cell population. The number of proliferative cells, expressed as a percentage of total number of cells, is shown for each *Tshz3*<sup>-/-</sup> and *Tshz3*<sup>+/+</sup> sample analysed. Although there is variation in the percentage of proliferative cells between samples, no reproducible differences were observed between *Tshz3*<sup>+/+</sup> and *Tshz3*<sup>-/-</sup> samples in any cell population. Samples taken from different litters are shown in different colours. There is no reproducible difference in proliferation rates between samples taken from different litters in any cell population.

# Figure 6.8.2 - E16 Proliferation



Samples from the same litter are shown in the same colour

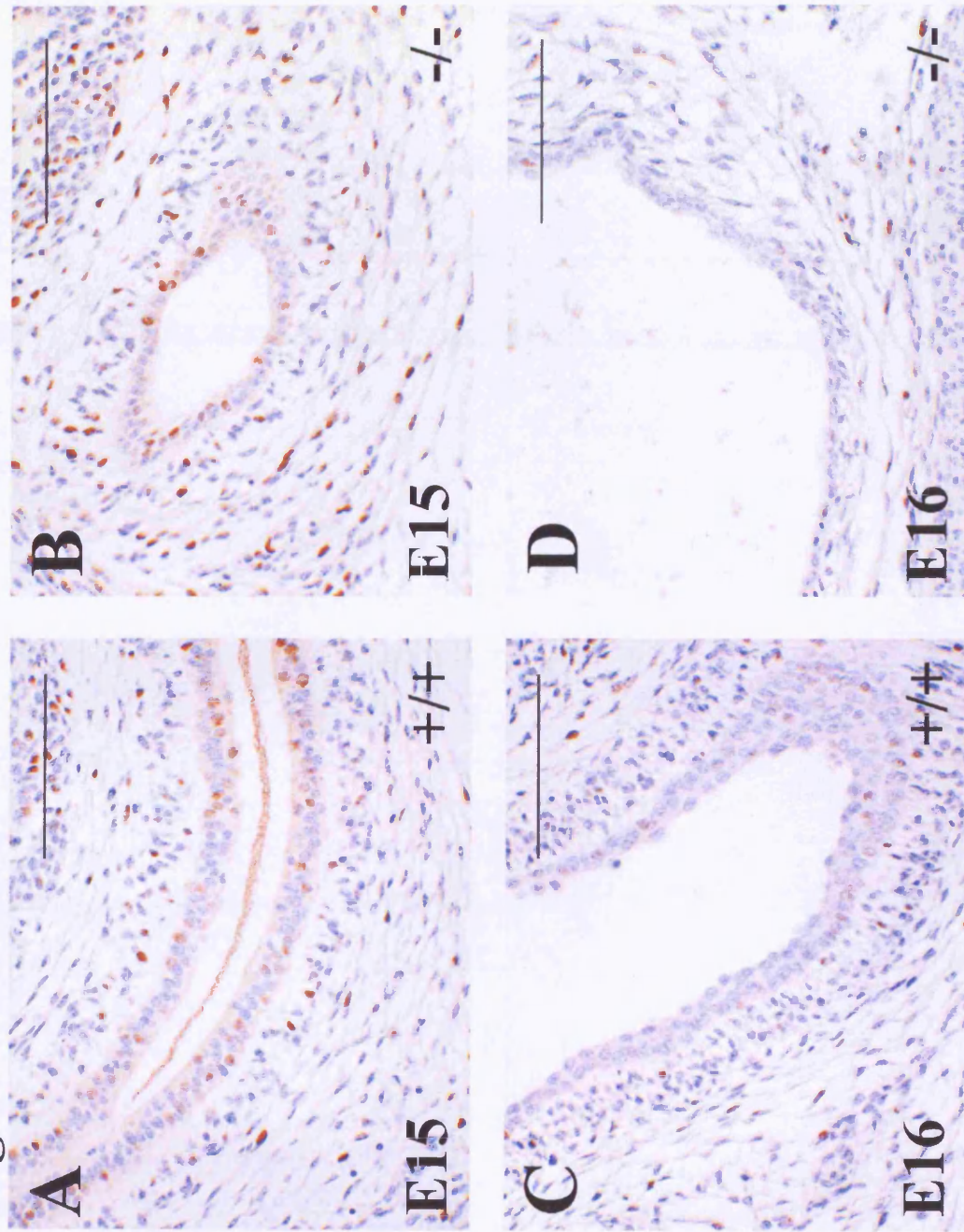
**Figure 6.8.3 Representative PCNA staining of proximal ureters *Tshz3*<sup>-/-</sup> and *Tshz3*<sup>+/+</sup> mice**

Sections were stained using an anti-PCNA antibody and developed with DAB to give a brown colour. Sections were counterstained with haematoxylin to colour the nuclei blue. Views from proximal ureters of *Tshz3*<sup>+/+</sup> (**A** and **C**) and *Tshz3*<sup>-/-</sup> (**B** and **D**) mice are shown. **A** and **B** Similar point prevalence of PCNA positive cells can be seen in the urothelium, condensing mesenchyme and loose mesenchyme of E15 wildtype and mutant mice. **C** and **D** Similar point prevalence of PCNA positive cells can be seen in the urothelium (u), condensing mesenchyme (cm) and loose mesenchyme (lm) of E16 wildtype and mutant mice. Scale bars – 100µm.

L. Fasano provided the dissected mouse urinary tracts used in this experiment.

Part of this figure appears in Caubit et al. (submitted).

**Figure 6.8.3**





Apoptosis was assessed by TUNEL, which utilises terminal deoxynucleotidyl transferase to identify DNA strand breaks (which are present characteristically in apoptotic cells) and label their free 3'-OH ends with fluorescein labelled nucleotides. Labelling of apoptotic cells was carried out on sections of proximal ureters from *Tshz3<sup>-/-</sup>* and *Tshz3<sup>+/+</sup>* E15 and E16 mice (n=4 for each genotype at E15, n=3 for each genotype at E16), and the number of TUNEL positive cells quantified as a percentage of total nuclei present for the following populations of cells; urothelia, condensing mesenchyme (presumptive smooth muscle cells) and loose mesenchyme. No statistically significant differences in apoptotic rates were observed between *Tshz<sup>+/+</sup>* and *Tshz3<sup>-/-</sup>* in any of the cell populations at either E15 (before hydronephrosis) or E16 (when hydronephrosis was present). Table 6.2 shows a summary of the results of this experiment. Figures 6.9.1 and 6.9.2 show graphical representations of the quantification of apoptotic cells. Figure 6.9.3 shows representative TUNEL staining, along with positive and negative control experiments. It is noteworthy that apoptosis was never detected in the condensed mesenchymal layer of cells (presumptive smooth muscle cells), whereas a low prevalence of apoptosis was observable in other cell layers.

**Table 6.2 Apoptosis of Cells in the Proximal Ureter**

**Percentage of TUNEL positive cells**

Percentages are given as; Average percentage  $\pm$  standard error of the mean

P-values refer to independent samples T-test (equal variance not assumed).

<b>E15</b>	<b>Urothelium</b>	<b>Condensing Mesenchyme</b>	<b>Loose Mesenchyme</b>
Tshz3+/+	0.47 $\pm$ 0.33	0 $\pm$ 0	0.12 $\pm$ 0.07
Tshz3-/-	0.09 $\pm$ 0.09	0 $\pm$ 0	0.16 $\pm$ 0.16
T-test P=	0.34	NA	0.81

<b>E16</b>	<b>Urothelium</b>	<b>Condensing Mesenchyme</b>	<b>Loose Mesenchyme</b>
Tshz3+/+	0.42 $\pm$ 0.42	0 $\pm$ 0	0 $\pm$ 0
Tshz3-/-	0.09 $\pm$ 0.09	0 $\pm$ 0	0.053 $\pm$ 0.053
T-test P=	0.52	NA	0.42

**Total number of cells counted per sample**

Numbers given refer to the range, median of the number of cells counted per sample.

<b>E15</b>	<b>Urothelium</b>	<b>Condensing Mesenchyme</b>	<b>Loose Mesenchyme</b>
Tshz3+/+	130-407, 217	310-738, 593.5	200-1081, 643
Tshz3-/-	92-516, 208	119-765, 433	156-1348, 911.5

<b>E16</b>	<b>Urothelium</b>	<b>Condensing Mesenchyme</b>	<b>Loose Mesenchyme</b>
Tshz3+/+	254-319, 288	217-288, 283	227-387, 363
Tshz3-/-	56-794, 242	94-322, 193	138-739, 608

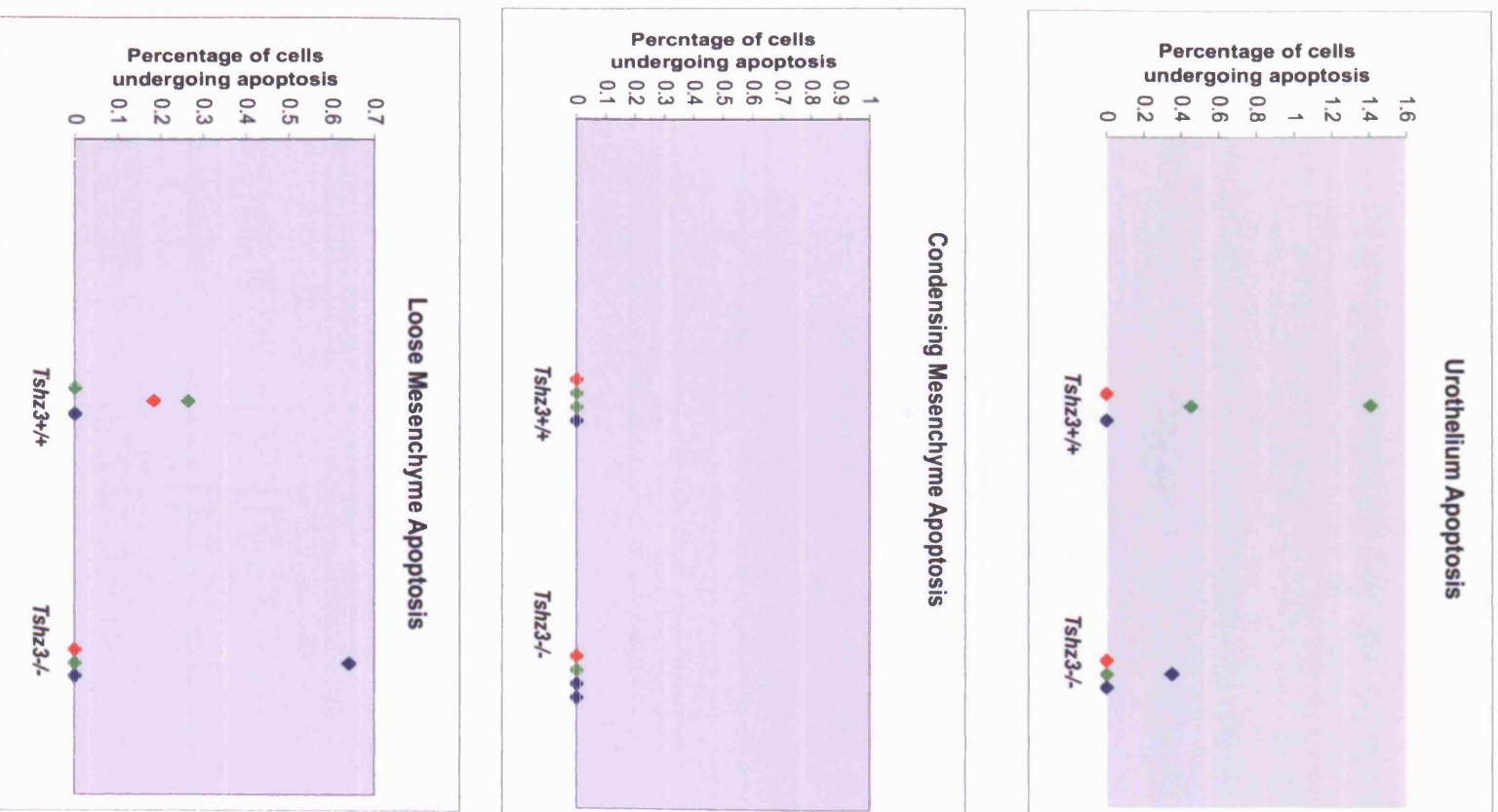
**Figure 6.9.1 Scatter plots showing the percentage of apoptotic cells in E15**

***Tshz3*<sup>-/-</sup> and *Tshz3*<sup>+/+</sup> proximal ureters**

Apoptotic cells were quantified in three distinct cell populations in the proximal ureter; the urothelium, the condensing mesenchyme and the loose mesenchyme.

Separate scatter plots are shown for each cell population. The number of apoptotic cells, expressed as a percentage of total number of cells, is shown for each *Tshz3*<sup>-/-</sup> and *Tshz3*<sup>+/+</sup> sample analysed. Although there is variation in the percentage of apoptotic cells between samples, no reproducible differences were observed between *Tshz3*<sup>+/+</sup> and *Tshz3*<sup>-/-</sup> samples in any cell population. Samples taken from different litters are shown in different colours. There is no reproducible difference in apoptotic rates between samples taken from different litters in any cell population.

**Figure 6.9.1 - E15 Apoptosis**



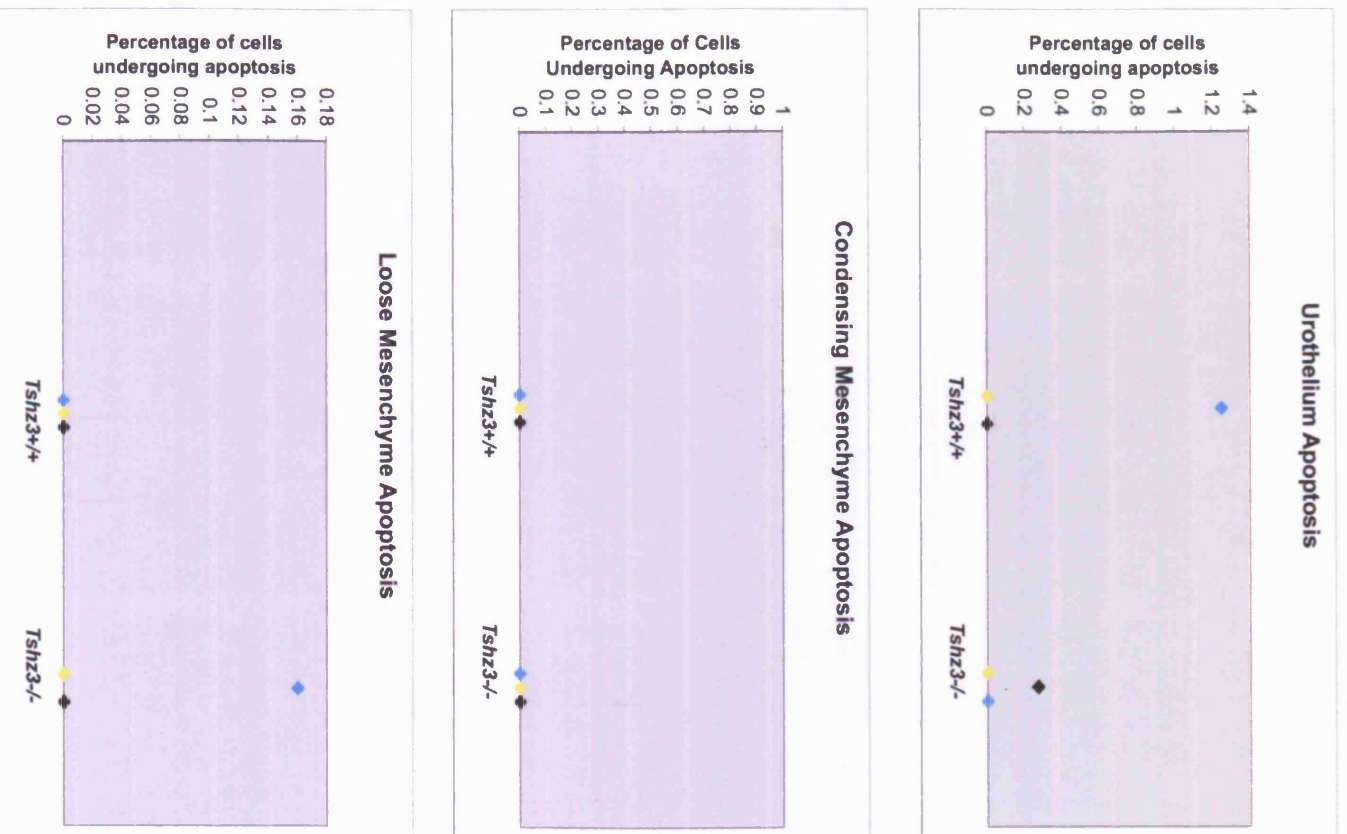
Samples from the same litter are shown in the same colour

**Figure 6.9.2 Scatter plots showing the percentage of apoptotic cells in E16**

***Tshz3*<sup>-/-</sup> and *Tshz3*<sup>+/+</sup> proximal ureters**

Apoptotic cells were quantified in three distinct cell populations in the proximal ureter; the urothelium, the condensing mesenchyme and the loose mesenchyme. Separate scatter plots are shown for each cell population. The number of apoptotic cells, expressed as a percentage of total number of cells, is shown for each *Tshz3*<sup>-/-</sup> and *Tshz3*<sup>+/+</sup> sample analysed. Although there is variation in the percentage of apoptotic cells between samples, no reproducible differences were observed between *Tshz3*<sup>+/+</sup> and *Tshz3*<sup>-/-</sup> samples in any cell population. Samples taken from different litters are shown in different colours. There is no reproducible difference in apoptotic rates between samples taken from different litters in any cell population.

**Figure 6.9.2 - E16 Apoptosis**



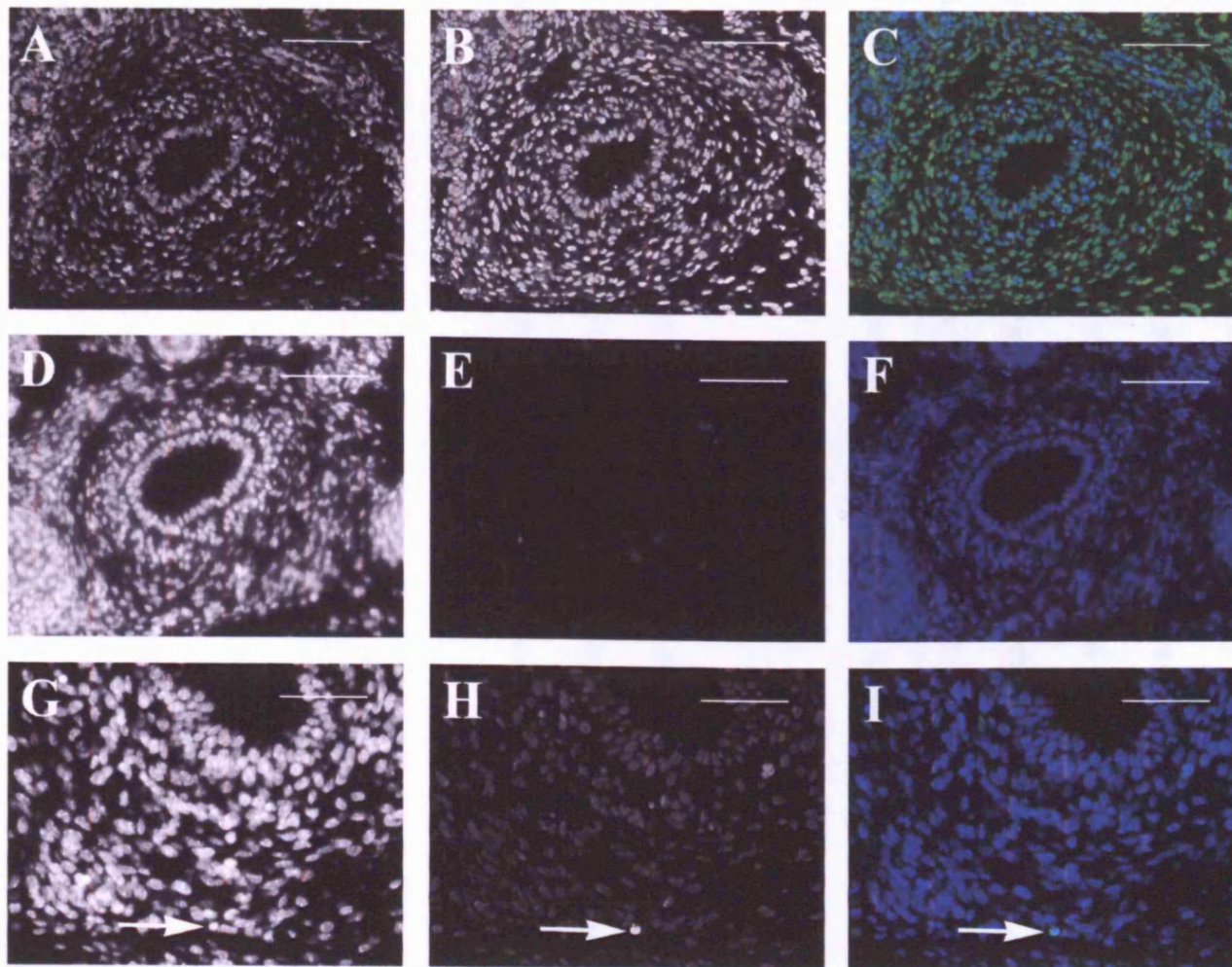
Samples from the same litter are shown in the same colour

### Figure 6.9.3 TUNEL staining of proximal ureters

Sections from proximal ureters of E15 and E16 *Tsh3*<sup>+/+</sup> and *Tshz3*<sup>-/-</sup> mice were stained using a TUNEL kit to label apoptotic cells with fluorescein. The fluorescein signal is shown in panels **B**, **E** and **H**. Nuclei were counterstained with Hoechst (33342), which is shown in panels **A**, **D** and **G**. Overlays of the fluorescein (green) and Hoechst (blue) staining is shown in panels **C**, **F** and **I**. **A-C** DNase treated positive control sample (DNase breaks up the DNA of the cells causing them to be detected by the TUNEL procedure). All nuclei are fluorescein positive, indicating that the TUNEL procedure was working. **D-E** Negative control sample (in which the enzyme component of the solution was omitted, leaving only the label component). Only very faint non-specific signal is seen (**E**). **G-H** An example of an apoptotic cell (arrow) detected in the loose mesenchyme of a test sample. The apoptotic cell is TUNEL positive, as observed by the strong fluorescein signal (**H**), and can be observed as a pyknotic nucleus with the Hoechst stain (**G**). Scale bars - 100µm.

L. Fasano provided the dissected mouse urinary tracts used in this experiment.

**Figure 6.9.3**





No statistically significant differences in proliferation or apoptosis rates between *Tshz3*<sup>-/-</sup> and *Tshz3*<sup>+/+</sup> were observed in the condensing mesenchyme of proximal ureters. This suggests that *Tshz3* is not essential for SMC precursor proliferation or survival. Additionally immunohistochemistry for  $\beta$ -galactosidase in E18 *Tshz3*<sup>-/-</sup> mice (n=2) showed that *lacZ* expressing cells are present (Figure 6.10). Therefore the “*Tshz3* expressing” cell population is not lost in mutants, despite the lack of functional *Tshz3* protein, which also suggests that *Tshz3* is not essential for SMC precursor proliferation or survival. However, my data does not exclude the possibility that small differences (which may not be found to be significant in statistical analyses, unless large numbers of samples were tested) in proliferation and apoptosis rates between *Tshz3*<sup>+/+</sup> and *Tshz3*<sup>-/-</sup> exist.

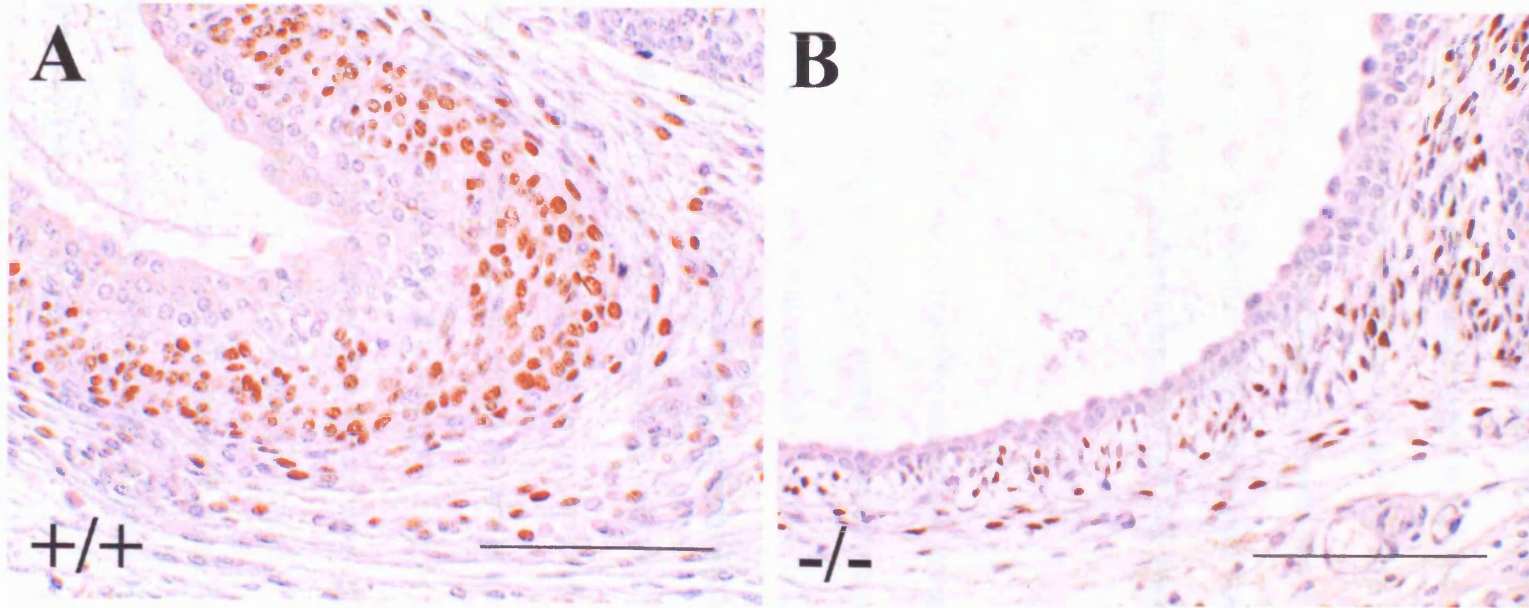
As I have shown that SMC precursors are not absent from the proximal ureters of *Tshz3*<sup>-/-</sup> mice, the lack of SMCs is likely to be due to a failure of SMC precursors to differentiate. However small deficiencies in SMC precursor numbers may also contribute to the lack of SMCs.

**Figure 6.10 Immunohistochemistry for  $\beta$ -galactosidase in proximal ureters from E18 *Tshz3*<sup>-/-</sup> and *Tshz*<sup>+/-</sup> mice**

Sections were stained using an anti- $\beta$ -galactosidase antibody and developed with DAB to give a brown colour. Sections were counterstained with haematoxylin, to colour the nuclei blue, and PAS. Proximal ureters of *Tshz3*<sup>+/-</sup> (**A**) and *Tshz3*<sup>-/-</sup> (**B**) E18 mice are shown.  $\beta$ -galactosidase positive cells are present in the condensing and loose mesenchyme of the ureters of both *Tshz3*<sup>+/-</sup> and *Tshz*<sup>-/-</sup> mutant mice, indicating that population of cells that would usually express wildtype *Tshz3* protein are present in both samples. Scale bars – 100 $\mu$ m.

L. Fasano provided the dissected mouse urinary tracts used in this experiment.

**Figure 6.10**



***The expression of Bmp4 in the ureter, which is important for the development of ureteric smooth muscle, is unaffected in Tshz3<sup>-/-</sup> mice***

Bmp4, which is expressed in the mesenchymal cells of the ureter under the control of Shh (which is expressed in the urothelium) signalling via Patched1 (Miyazaki et al., 2000; Yu et al., 2002) has been shown to play an important role in the development of ureteric smooth muscle (Raatikainen-Ahokas et al., 2000; Miyazaki et al., 2003). Therefore I investigated whether Bmp4 expression was affected in ureters of E15 *Tshz3<sup>-/-</sup>* mice, by immunohistochemistry (n=2 for both *Tshz3<sup>+/+</sup>* and *Tshz3<sup>-/-</sup>*) (Figure 6.11).

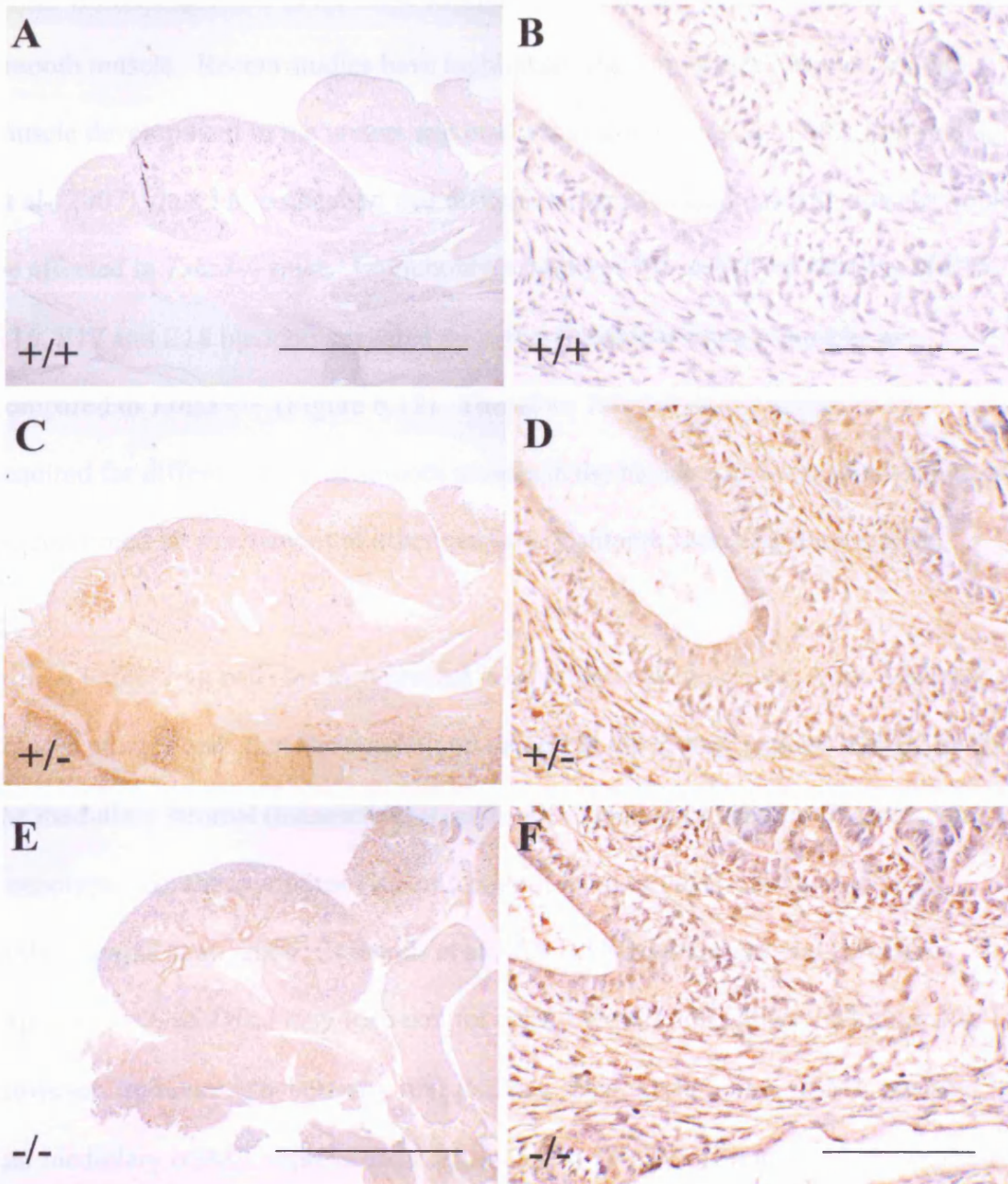
I showed that Bmp4 immuno-reactive material is present in the ureteric mesenchyme and also in the urothelium, but no signal is seen in negative control experiments where the primary antibody was omitted (Figure 6.11). Expression was also observed in the kidney itself in a similar, although broader pattern to that reported by Miyazaki et al. (2000) and Yu et al. (2002). The apparent broader expression of Bmp4 that I observed is not surprising; as my method detects Bmp4 protein, rather than transcripts of the *Bmp4* gene. Bmp4 protein is a secreted growth factor and is therefore likely to diffuse into the urothelium from its source in the mesenchyme; indeed Bmp type I receptor genes have been shown by *in-situ* hybridisation to be expressed in the epithelium of the ureter (and kidney) as well as the ureteric mesenchyme (Miyazaki et al., 2000), indicating that Bmp4 signalling is likely to occur in both these cell populations. Expression of Bmp4 in the ureter of *Tshz3<sup>-/-</sup>* was similar to that of *Tshz3<sup>+/+</sup>* (Figure 6.11).

**Figure 6.11 Immunohistochemistry for Bmp4 in kidneys and proximal ureters from E15 *Tshz3*<sup>-/-</sup> and *Tshz3*<sup>+/-</sup> mice**

**A, C and E** show kidneys and proximal ureters from E15 mice. **B, D and F** show proximal ureters at higher magnification. **A and B** negative control on *Tshz3*<sup>+/+</sup>, in which the primary antibody was omitted, no brown signal is seen, indicating that signal seen in other panels is due to binding of primary antibody. **C-F** Sections were stained using an anti-Bmp4 antibody and developed with DAB to give a brown colour. Sections were counterstained with haematoxylin to colour the nuclei blue. Bmp4 is detected in mutant kidneys and ureters of both genotypes. Staining is observed throughout the ureter, and in the stroma and some (but not all) epithelia of the kidney. Scale bars - 1000µm (**A, C and E**) or 100µm (**B, D and F**).

L. Fasano provided the dissected mouse urinary tracts used in this experiment.

**Figure 6.11**



***Other populations of  $\alpha$ SMA expressing cells in the urinary tracts of *Tshz3*<sup>-/-</sup> mice appear to be unaffected***

*Tshz3* is also expressed in the mesenchyme of the bladder, which contains layers of smooth muscle. Recent studies have highlighted the similarities between smooth muscle development in the ureters and bladders (Haraguchi et al., 2007; Shiroyanagi et al., 2007), thus I hypothesised that differentiation of bladder smooth muscle would be affected in *Tshz3*<sup>-/-</sup> mice. Immunohistochemistry for  $\alpha$ SMA on sections of E15, E16, E17 and E18 bladders revealed no defect in bladder smooth muscle, as compared to *Tshz3*<sup>+/+</sup> (Figure 6.12). Therefore *Tshz3* does not appear to be required for differentiation of smooth muscle in the bladder, however this remains to be confirmed by assessment of other markers of smooth muscle differentiation.

$\alpha$ SMA expressing cells are also present in other parts of the urinary tract. Vascular smooth muscle cells that surround blood vessels in the kidney express  $\alpha$ SMA, as do the medullary stromal (mesenchymal) cells of the kidney (which are fibromuscular in phenotype, like the myofibroblasts of the adult interstitium (Iwano and Neilson, 2004; Itaranta et al., 2006; Bascands et al., 2007). Medullary stromal cells also express *Tshz3*, so *Tshz3* may help control  $\alpha$ SMA expression within the kidney itself. However, immunohistochemistry revealed that renal arteries were  $\alpha$ SMA positive, and medullary  $\alpha$ SMA expression is unaffected in *Tshz3*<sup>-/-</sup>. (Figure 6.13 shows these results in E18 kidneys. The same results are also observable in Figures 6.7.1, 6.7.2, 6.7.3 and 6.7.4).

## Figure 6.12 Immunohistochemistry for $\alpha$ SMA in bladders from E15-E18

### *Tshz3*<sup>-/-</sup> mice and their littermates

Sections were stained using an anti- $\alpha$ SMA antibody and developed with DAB to give a brown colour. Sections were counterstained with haematoxylin, to colour the nuclei blue, and PAS. Sections from *Tshz3*<sup>+/+</sup> (**A-D**), *Tshz3*<sup>+/-</sup> (**E-F**), and *Tshz3*<sup>-/-</sup> (**I-J**) mice are shown. **A, E and I** E15; **B, F and J** E16; **C, G and K** E17; **D, H and L** E18.  $\alpha$ SMA staining can be seen in a layer of mesenchymal cells in the periphery of the bladders (surrounding the lamina propria layer) in *Tshz3*<sup>+/+</sup> and *Tshz3* the +/- and *Tshz3*<sup>-/-</sup> at all stages. The thickness of the  $\alpha$ SMA appears comparable between all genotypes at each embryonic stage. Scale bars - 1000 $\mu$ m.

L. Fasano provided the dissected mouse urinary tracts used in this experiment.



**Figure 6.12**

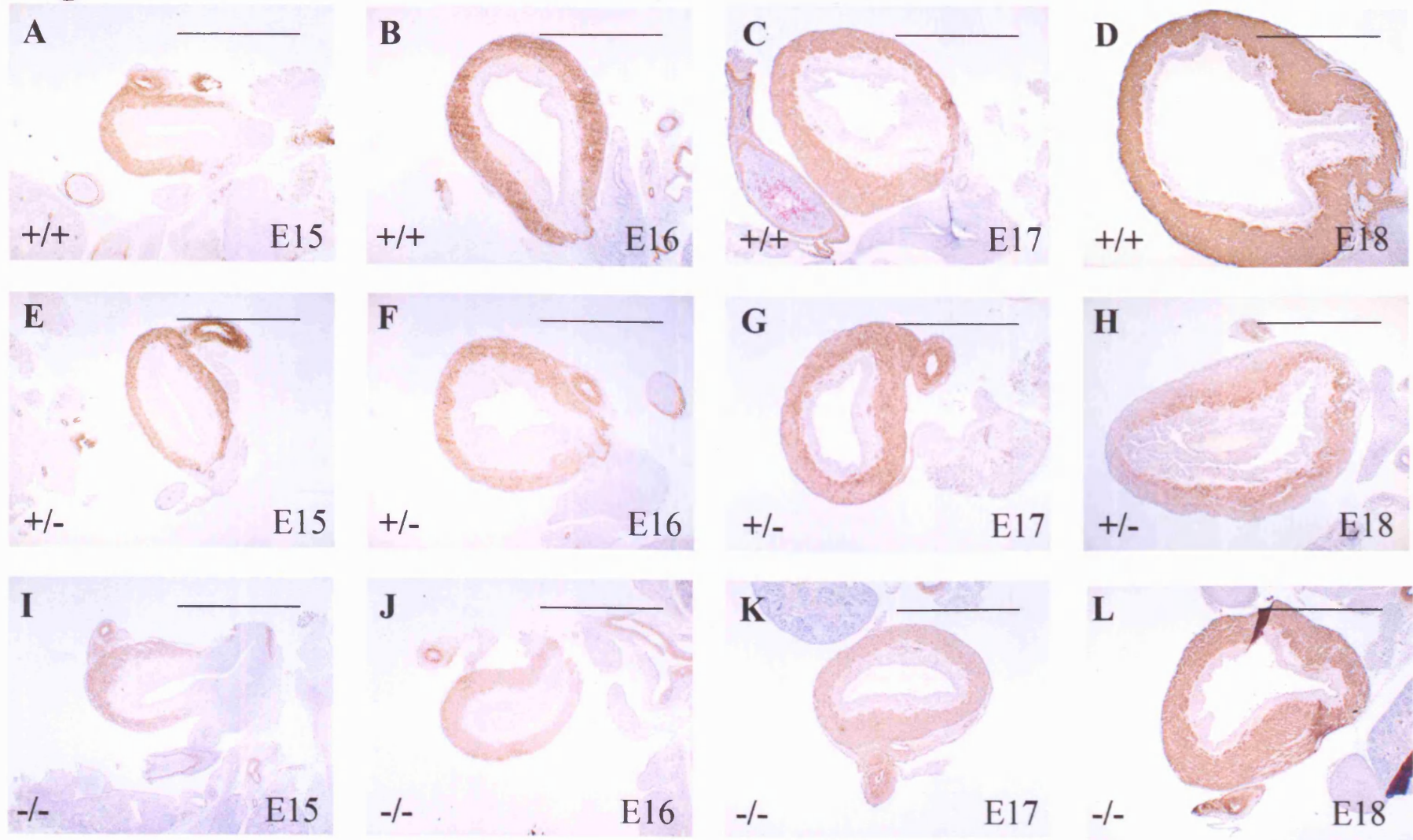
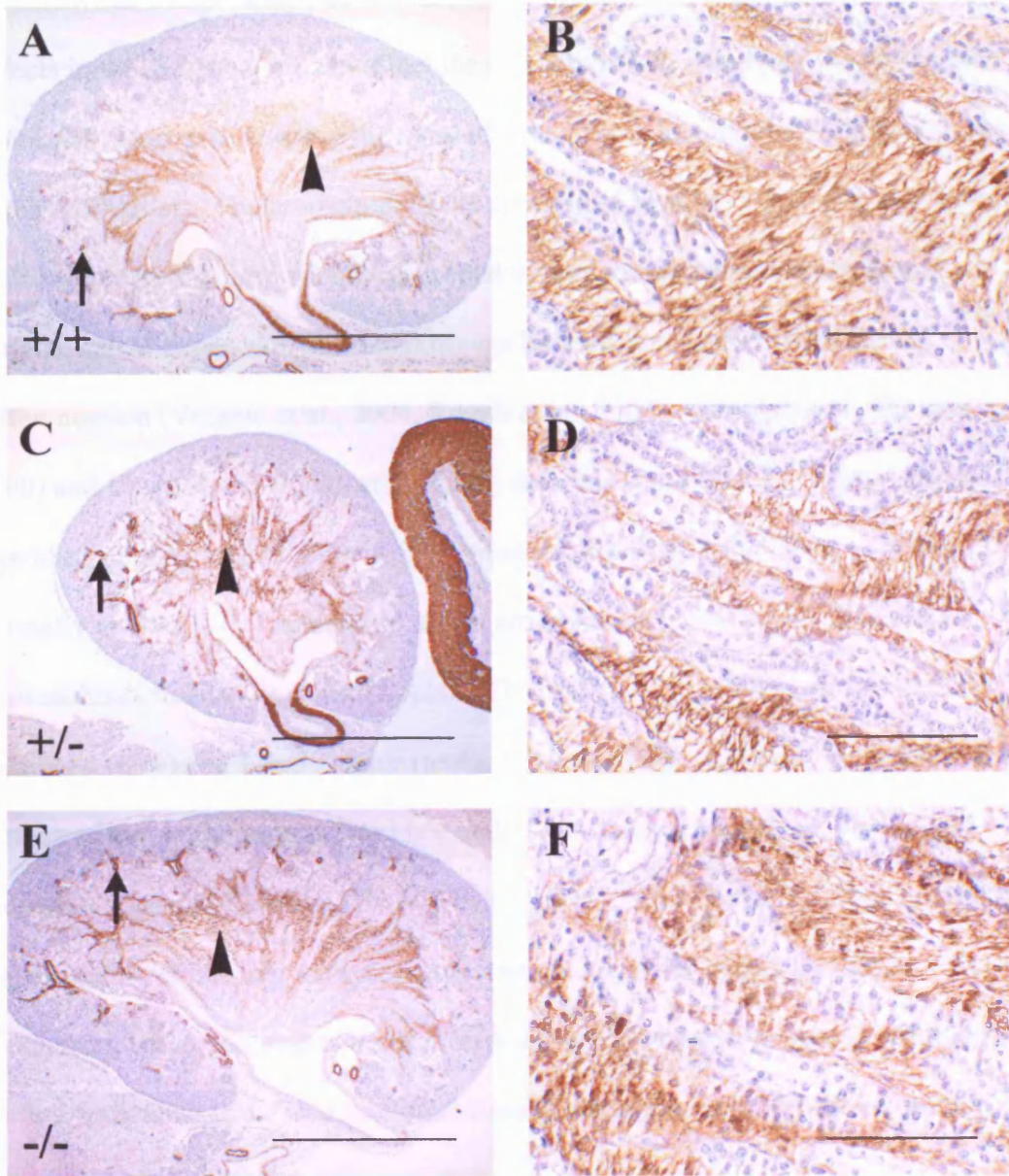


**Figure 6.13 Immunohistochemistry for  $\alpha$ SMA in kidneys from E18 *Tshz3*<sup>-/-</sup> mice and their littermates**

Sections were stained using an anti- $\alpha$ SMA antibody and developed with DAB to give a brown colour. Sections were counterstained with haematoxylin, to colour the nuclei blue, and PAS. Sections from *Tshz3*<sup>+/+</sup> (**A-B**), *Tshz3*<sup>+/-</sup> (**C-D**), and *Tshz3*<sup>-/-</sup> (**E-F**) mice are shown. Note (**E**) the *Tshz3*<sup>-/-</sup> mice had hydronephrosis and hydroureter, but the urine was drained from the renal pelvis on autopsy, and the papilla was able to resume its natural pointed position (as pressure from the accumulating urine had been revealed). **A, C** and **E** kidneys and proximal ureters. Strong  $\alpha$ SMA staining can be seen in the arteries (arrows) and renal stroma (arrowheads) of all genotypes. **B, D** and **F** renal medulla (containing  $\alpha$ SMA positive stromal cells) at higher magnification. Scale bars - 1000 $\mu$ m (**A, C** and **E**) or 100 $\mu$ m (**B, D** and **F**).

L. Fasano provided the dissected mouse urinary tracts used in this experiment.

**Figure 6.13**



### ***Urothelial differentiation is unaffected in *Tshz3*<sup>-/-</sup> mutant mice***

The differentiation of the ureter depends upon crosstalk between the epithelial and mesenchymal components (Airik et al., 2006; Mendelsohn et al., 2006), so molecular defects in the mesenchyme can affect the urothelium and visa versa. Therefore lack of normal *Tshz3* expression in the mesenchyme may cause abnormal differentiation of the urothelium. The urothelium of the ureter (and bladder) is a highly specialised multilayered epithelium, which has uroplakin-containing plaques on its apical surface: apical expression of uroplakins can be used as a marker of urothelial differentiation (Veranic et al., 2004; Romih et al., 2005). *Uroplakin III* (Hu et al., 2000) and *Uroplakin II* (Kong et al., 2004) deficient mice develop hydronephrosis, providing another reason to investigate whether urothelial differentiation occurs normally in *Tshz3*<sup>-/-</sup>. Therefore to assess urothelial differentiation, I performed immunohistochemistry against Uroplakin1b (Up1b), in proximal ureters from E18 *Tshz3*<sup>+/+</sup> (n=4) and *Tshz3*<sup>-/-</sup> mice (n=4). Up1b staining was observed on the apical surface of the urothelium in *Tshz3*<sup>+/+</sup> and *Tshz3*<sup>-/-</sup> ureters, although the layer of uroplakin appeared flatter in *Tshz3*<sup>-/-</sup> (Figure 6.14). This flattening of the uroplakin-expressing layer is likely to be due to the distension of the ureters in *Tshz3*<sup>-/-</sup>. In conclusion, Up1b was expressed in mutant ureters in a similar pattern to wildtype ureters, indicating that *Tshz3* (and, incidentally smooth muscle cell differentiation) is not required for urothelial differentiation.

**Figure 6.14 Immunohistochemistry for Up1b in the proximal ureters of *Tshz3*<sup>+/+</sup> and *Tshz3*<sup>-/-</sup> mice**

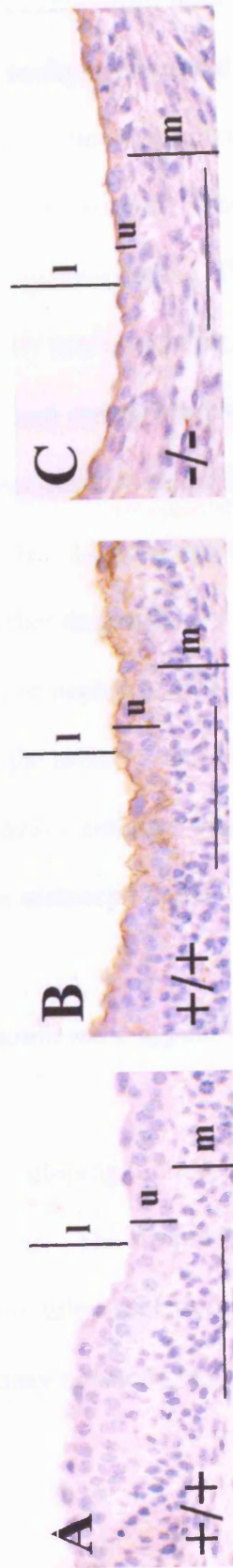
Sections from *Tshz3*<sup>+/+</sup> (**A** and **B**) and *Tshz3*<sup>-/-</sup> (**C**) E18 mice are shown. Epithelium (urothelium; u), and some underlying mesenchyme (m), of proximal ureters at high magnification are shown. l indicates lumen. Sections were counterstained with haematoxylin, to colour the nuclei blue, and PAS. **A** negative control on *Tshz3*<sup>+/+</sup>, in which the primary antibody was omitted, no brown signal is seen, indicating that signal seen in other panels is due to binding of primary antibody. **B** and **C** Sections were stained using an anti-Up1b antibody and developed with DAB to give a brown colour. Brown staining, indicating Up1b expression, is seen in the epithelium of the proximal ureter of both *Tshz3*<sup>+/+</sup> and *Tshz3*<sup>-/-</sup> mice at the apical surface. No brown staining is seen in the negative control sample, where primary antibody was omitted. Scale bars - 50µm.

L. Fasano provided the dissected mouse urinary tracts used in this experiment.

D. Rampling embedded and sectioned some of the mouse urinary tracts used in this experiment.

Part of this figure appears in Caubit et al. (submitted).

**Figure 6.14**



***The expression of Pax2, a gene that is important for controlling early events in nephrogenesis, is normal in Tshz3<sup>-/-</sup> null mice***

*Tshz3* is expressed in the mesenchyme surrounding the stalk of the ureteric bud at E11 and E12, and is expressed in the mesenchyme around the mesonephric ducts (Laurent Fasano, personal communication). Therefore it may play a role in regulating the events of early nephrogenesis. The expression of several genes is known to be important for early nephrogenesis, one of these is Pax2, which is expressed in the ureteric bud and metanephric mesenchyme and is essential for the expression of Gdnf (in the metanephric mesenchyme), which triggers ureteric bud outgrowth (Brophy et al., 2001). I carried out immunohistochemistry using a Pax2 antibody, to investigate whether its expression was normal in the developing metanephri of *Tshz3<sup>-/-</sup>* early in nephrogenesis (n=1 for each genotype). Pax2 expression was observed in the ureteric buds and metanephric mesenchyme at E12 in *Tshz3<sup>+/+</sup>*, *Tshz3<sup>+/-</sup>* and *Tshz3<sup>-/-</sup>* embryos (Figure 6.15). Thus there is no apparent defect in Pax2 expression in metanephri of E12 *Tshz3<sup>-/-</sup>* mice.

***The kidneys of Tshz3<sup>-/-</sup> mutant mice appear normal, other than they are hydronephrotic***

*Tshz3* is expressed in the developing kidney, in the stromal cells of the medullary and cortico-medullary regions. The stroma has been shown to play a role in the development of the kidney (Cullen-McEwen et al., 2005), thus I hypothesised that there may be defects in kidney development in *Tshz3<sup>-/-</sup>* mice.

**Figure 6.15 Immunohistochemistry for Pax2 in the metanephric region of E12**

***Tshz3*<sup>-/-</sup> mice and their littermates**

Sections from *Tshz3*<sup>+/+</sup> (**A, B**), *Tshz3*<sup>+/-</sup> (**C, D** and **G, H**), and *Tshz3*<sup>-/-</sup> (**E, F**) E12 mice are shown. **A-F** Sections were stained using an anti-Pax2 antibody and developed with DAB to give a brown colour. Sections were counterstained with haematoxylin to colour the nuclei blue. **G-H** negative control on *Tshz3*<sup>+/-</sup>, in which the primary antibody was omitted, no brown signal is seen, indicating that signal seen in other panels is due to binding of primary antibody. **A, C, E** and **G** show frontal sections through the region containing the forming kidneys (k) or metanephroi. **B, D, F** and **H** show metanephroi at higher magnification. Pax2 protein is present in the ureteric bud and metanephric mesenchymal cells of all genotypes. N.B. sections of metanephroi were taken in slightly different planes for each genotype: this explains apparent differences in ureteric bud branching pattern observed between the different genotype. k, kidney (metanephros); ub, ureteric bud; mm, metanephric mesenchyme. Scale bars - 500µm (**A, C, E** and **G**) or 100µm (**B, D, F** and **H**).

L. Fasano provided the dissected mouse urinary tracts used in this experiment.

Part of this figure appears in Caubit et al. (submitted).



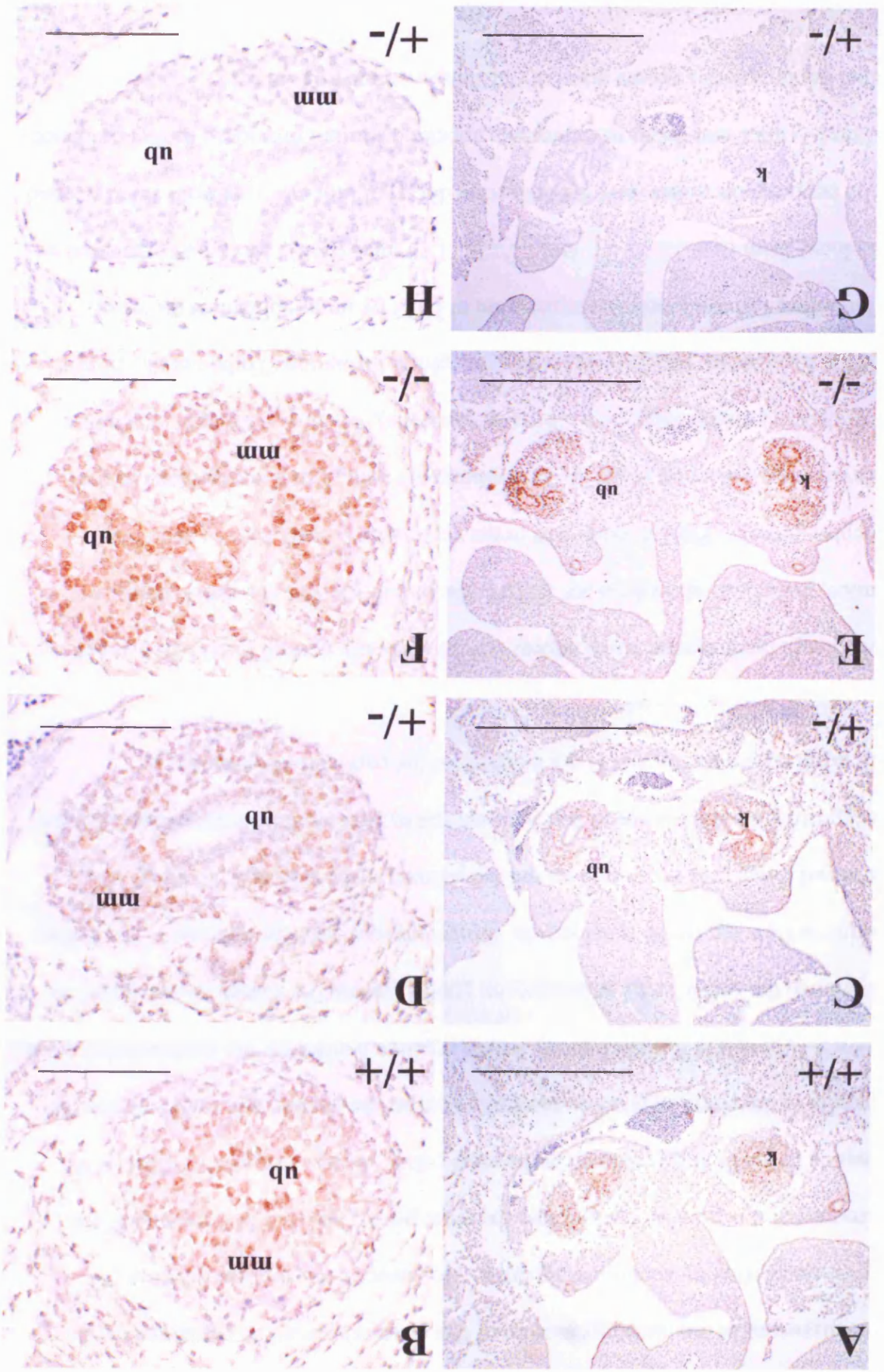


Figure 6.15

The abnormalities in the kidneys observed in histological sections of *Tshz3*<sup>-/-</sup> mice (as discussed in the histology section of this chapter) *can* all be explained by the pressure exerted by accumulating urine. However, it was unclear whether the absence of a papilla protruding into the renal pelvis, was due to flattening of the papilla tissue by high pressure in the renal pelvis, or was a result of failure of the papilla to develop. In order to ascertain whether the papilla fails to develop in the *Tshz3*<sup>-/-</sup>, or if it is flattened solely due to pressure exerted by the accumulating urine, I drained the pelvic urine at autopsy by gently tapping the kidney to encourage the urine to flow out of the renal pelvis. Observation of paraffin sections of this kidney showed the papilla recovered its normal pointed shape (Figure 6.13 and 6.19), suggesting that the flattened papilla is caused by increased hydrostatic pressure due to urine accumulation and is not a failure of the papilla to develop per se.

Although nephrogenic zones appear morphologically normal in E15-E18 *Tshz3*<sup>-/-</sup> mice, this observation does not exclude the possibility that is a subtle defect in nephrogenesis. Pax2 is expressed in the nephrogenic zone, as well as in the developing collecting ducts. In the nephrogenic zone, Pax 2 is expressed in the condensing mesenchyme (and forming nephrons), where it is thought to activate Wnt4 expression, which is essential for nephron formation (Torban et al., 2006). Therefore I investigated that expression of Pax2 by immunohistochemistry of kidneys from both *Tshz3*<sup>+/+</sup> and *Tshz3*<sup>-/-</sup> E18 mice (n=2). Pax2 was expressed in the nephrogenic zones (and the collecting ducts) of kidneys from both *Tshz3*<sup>+/+</sup> and *Tshz3*<sup>-/-</sup> mice and levels of expression appeared similar, providing further evidence that nephrogenesis occurs normally in *Tshz3*<sup>-/-</sup> mice (Figure 6.16).

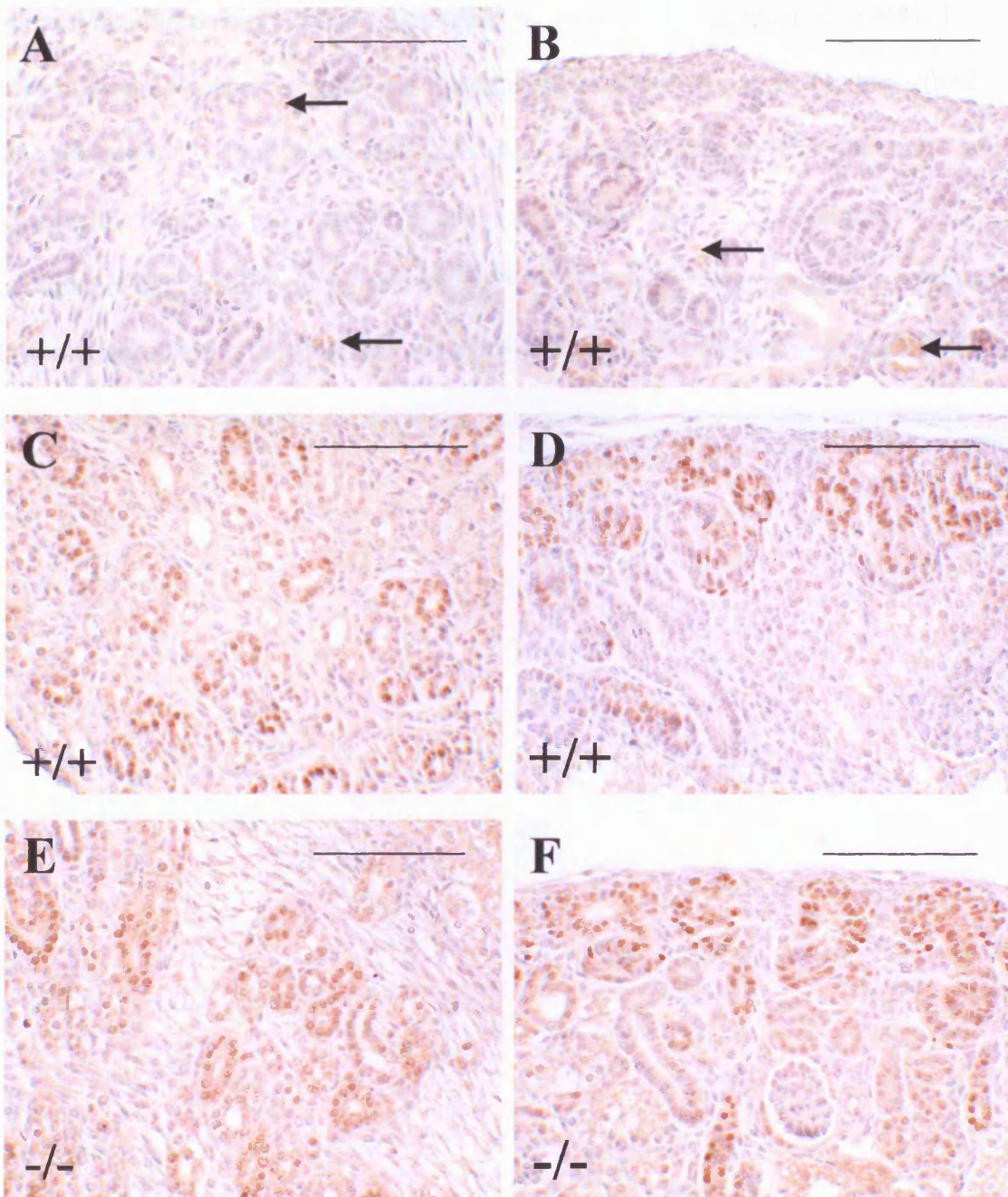
**Figure 6.16 Immunohistochemistry for Pax2 in the kidneys of E18 *Tshz3*<sup>-/-</sup> and *Tshz3*<sup>+/+</sup> kidneys**

Sections from kidneys of *Tshz3*<sup>+/+</sup> (A-D) and *Tshz3*<sup>-/-</sup> (E, F) E18 mice are shown. **A-B** negative control on *Tshz3*<sup>+/+</sup>, in which the primary antibody was omitted, no brown signal is seen, indicating that signal seen in other panels is due to binding of primary antibody. Light brown cells observed in these sections are red blood cells, which sometimes stain with DAB due to high levels of endogenous peroxidase (arrows). **C-F** Sections were stained using an anti-Pax2 antibody and developed with DAB to give a brown colour. Sections were counterstained with haematoxylin to colour the nuclei blue. **A, C** and **E** medullary regions of kidneys containing collecting ducts; **B, D** and **F** nephrogenic zones of kidneys. Pax2 protein is present in the nuclei of collecting ducts and in the nuclei of cells within the nephrogenic zone in both genotypes. Scale bars - 100µm.

L. Fasano provided the dissected mouse urinary tracts used in this experiment.

D. Rampling embedded and sectioned some of the mouse urinary tracts used in this experiment.

**Figure 6.16**



Histological sections also showed that by E18 *Tshz3*<sup>-/-</sup> kidneys had several layers of vascularised glomeruli (as did wildtype) (Figure 6.4). Podoplanin is a 43KDa integral membrane protein that is expressed by podocytes (Matsui et al., 1998). I used immunohistochemistry against podoplanin on sections from E18 kidneys (n=2 for each genotype) to investigate whether these glomeruli contained podocytes. Results revealed that glomeruli of *Tshz3*<sup>-/-</sup>, as well as *Tshz3*<sup>+/+</sup>, contained podoplanin expressing podocytes and that these podocytes were arranged in a typical fashion, surrounding the Bowman's capsule (Figure 6.17). Therefore glomeruli of *Tshz3*<sup>-/-</sup> mice appear normal, containing both podocytes and vascular components.

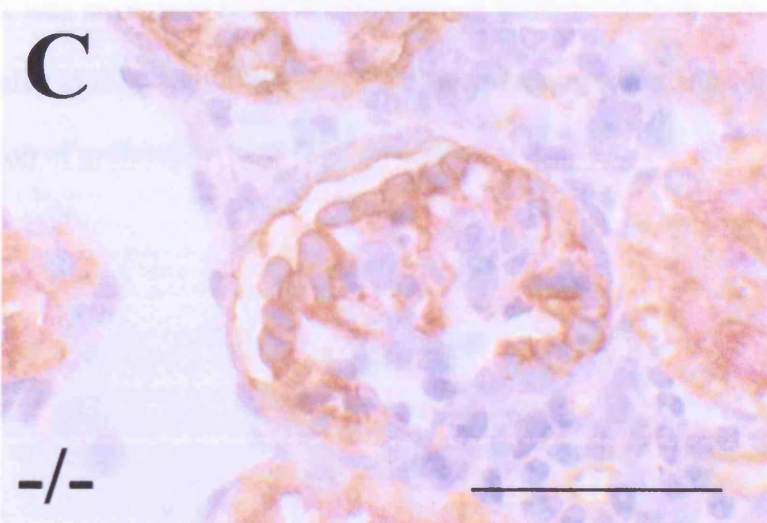
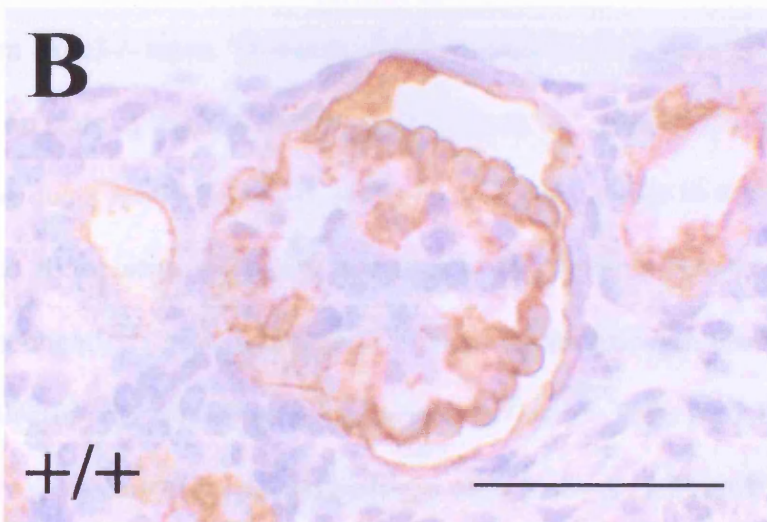
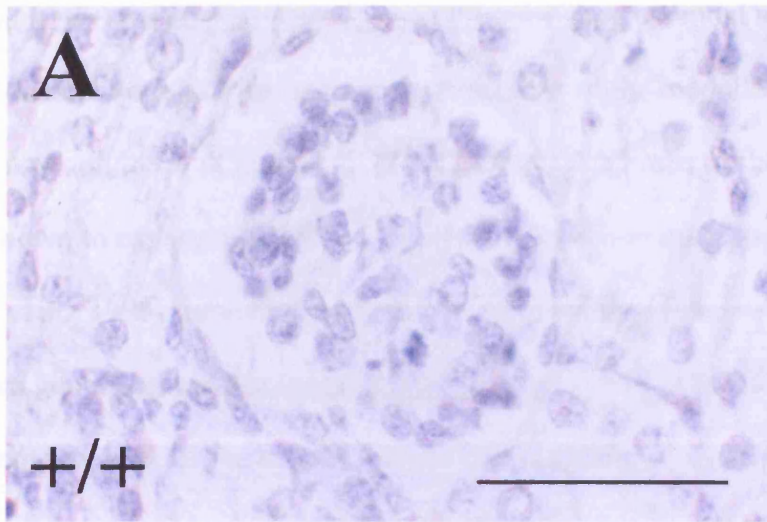
**Figure 6.17 Immunohistochemistry for podoplanin in the kidneys of *Tshz3*<sup>+/+</sup> and *Tshz3*<sup>-/-</sup> mice**

Sections showing representative glomeruli from kidneys of *Tshz3*<sup>+/+</sup> (**A** and **B**) and *Tshz3*<sup>-/-</sup> (**C**) E18 mice, at high magnification. **A** and **B** Sections were stained using an anti-podoplanin antibody and developed with DAB to give a brown colour. Sections were counterstained with haematoxylin, to colour the nuclei blue, and PAS. **C** negative control on *Tshz3*<sup>+/+</sup>, in which the primary antibody was omitted, no brown signal is seen, indicating that signal seen in other panels is due to binding of primary antibody. Brown staining, indicating podoplanin expression, is seen in the podocytes of glomeruli in both *Tshz3*<sup>+/+</sup> and *Tshz3*<sup>-/-</sup> mice. Note some non-specific staining outside the glomeruli is also seen. No brown staining is seen in the negative control sample, where primary antibody was omitted. Scale bars - 50µm.

L. Fasano provided the dissected mouse urinary tracts used in this experiment.

D. Rampling embedded and sectioned some of the mouse urinary tracts used in this experiment.

**Figure 6.17**



As *Tshz3* is expressed in the medullary stroma of the kidney, it is possible to envisage that it has special functions here such as providing essential signals for the growth and differentiation of the epithelial components of the medulla (i.e the collecting ducts and loops of Henle). The ascending thick limbs of the loops of Henle are known to express uromodulin, and it is absent from other kidney epithelia (Bachmann et al., 1990) Immunohistochemistry revealed that *Tshz3*<sup>-/-</sup> E18 kidneys (n=3 for each genotype) contain loops of Henle (Figure 6.18). Therefore *Tshz3* is apparently not required for the development or differentiation of loops of Henle. Pax2 immunohistochemistry had confirmed that collecting ducts were present in kidneys from *Tshz3*<sup>-/-</sup> mice. However, Pax2 expression does not indicate the differentiation state of these observed “collecting ducts”. Aquaporin 2 is expressed by collecting ducts and is important for their physiological role in water re-absorption to allow urine concentration (Rojek et al., 2006) therefore immunohistochemistry using an antibody against aquaporin2 was used to investigate whether collecting ducts differentiate normally in *Tshz3*<sup>-/-</sup> mice (n=2 for each genotype. Negative control was antibody pre-absorbed with immunising peptide). Aquaporin 2 was expressed in collecting ducts of kidneys of both *Tshz3*<sup>-/-</sup> and *Tshz3*<sup>+/+</sup> mice at E18, indicating that *Tshz3* is not required for the correct differentiation of collecting ducts (Figure 6.19).



**Figure 6.18 Immunohistochemistry for uromodulin in the kidneys of E18 *Tshz3*<sup>-/-</sup> and *Tshz3*<sup>+/+</sup> kidneys**

Sections from kidneys of *Tshz3*<sup>+/+</sup> (**A-B**) and *Tshz3*<sup>-/-</sup> (**C**) E18 mice are shown. **A** and **C** Sections were stained using an anti-uromodulin antibody and developed with DAB to give a brown colour. Sections were counterstained with haematoxylin to colour the nuclei blue. **B** is also stained with PAS (pink). **B** negative control on *Tshz3*<sup>+/+</sup>, in which the primary antibody was omitted, no brown signal is seen, indicating that signal seen in other panels is due to binding of primary antibody. **A** and **C** Uromodulin staining is observed as an apical signal in the loops of Henle of both genotypes (arrows). Scale bars - 100µm.

L. Fasano provided the dissected mouse urinary tracts used in this experiment.

D. Rampling embedded and sectioned some of the mouse urinary tracts used in this experiment.

Part of this figure appears in Caubit et al. (submitted).

**Figure 6.18**

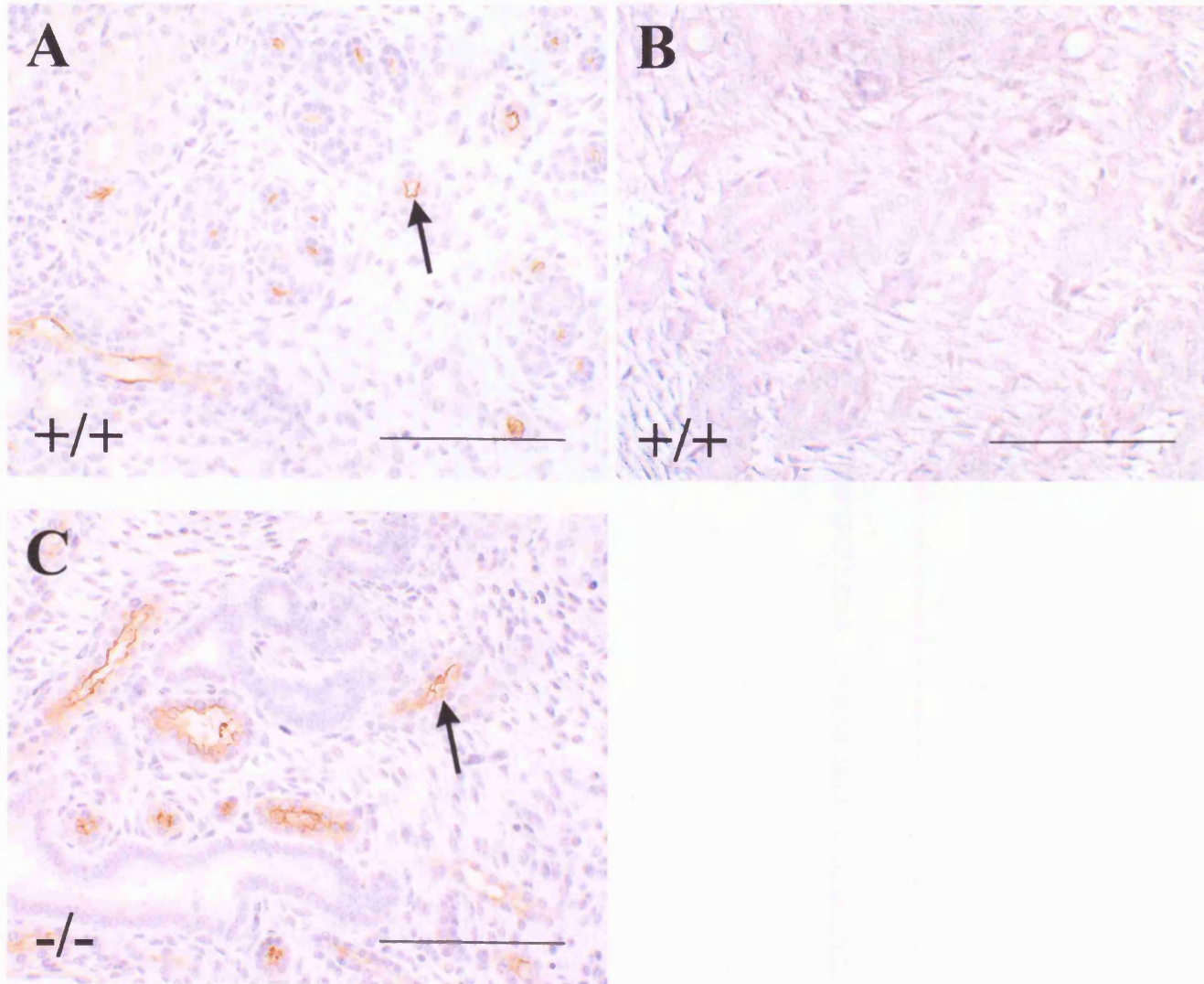


**Figure 6.19 Immunohistochemistry for aquaporin 2 in the kidneys of E18 *Tshz3*<sup>-/-</sup> and *Tshz3*<sup>+/+</sup> kidneys**

Sections from kidneys of *Tshz3*<sup>+/+</sup> (A-F) and *Tshz3*<sup>-/-</sup> (G-I) E18 mice are shown.

A, D and E E18 kidneys. Double boxed areas (cortex) are shown in B, E and H, respectively. Single boxed areas (medulla) are shown in C, F and I, respectively.

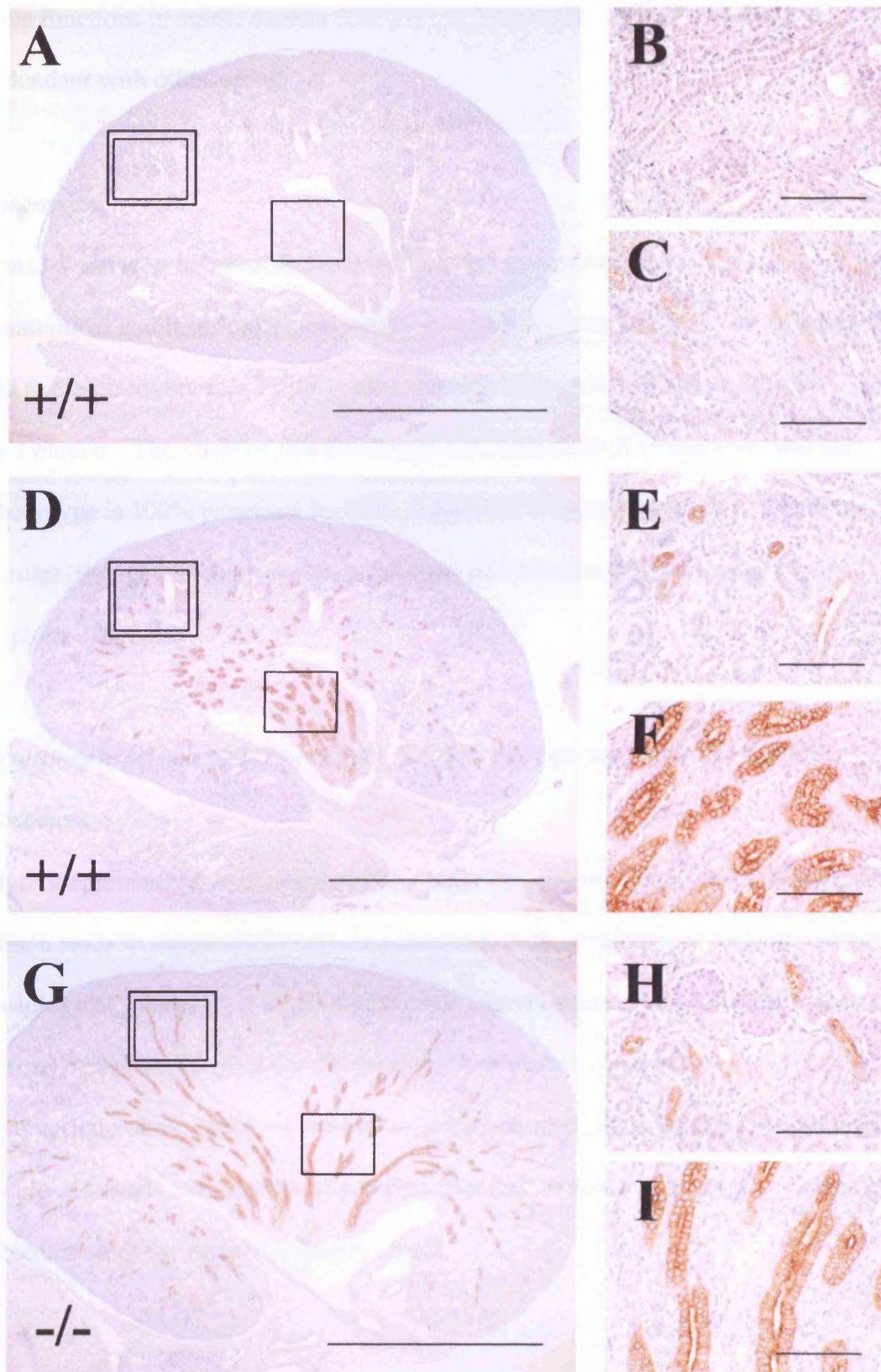
Note (G) the *Tshz3*<sup>-/-</sup> mice had hydronephrosis and hydroureter, but the urine was drained from the renal pelvis on autopsy, and the papilla was able to resume its natural pointed position (as pressure from the accumulating urine had been relieved). A-C negative control on *Tshz3*<sup>+/+</sup>, in which the primary antibody was pre-absorbed with the immunising peptide. Only very weak staining is seen, indicating that signal seen in other panels is due to specific binding of primary antibody to aquaporin2 protein.

D-I Sections were stained using an anti-aquaporin2 antibody and developed with DAB to give a brown colour. Sections were counterstained with haematoxylin, to colour the nuclei blue, and PAS. Aquaporin 2 is observed in both cortical and medullary collecting ducts in kidneys from both wildtype and homozygous mutant mice. Scale bars - 1000µm (A, D and G) or 100µm (B, C, E, F, H and I).

L. Fasano provided the dissected mouse urinary tracts used in this experiment.

Part of this figure appears in Caubit et al. (submitted).

**Figure 6.19**



In conclusion, no evidence could be found that supported the hypothesis that *Tshz3* is important for the anatomical development of the kidney itself. However, *Tshz3* may have functions in subtle aspects of kidney development, or functions that are redundant with other genes.

## **Discussion**

### ***Tshz3*<sup>-/-</sup> develop bilateral hydronephrosis and hydroureter**

Anatomical and histological examinations of urinary tracts from *Tshz3*<sup>-/-</sup> embryos led to the discovery that *Tshz3*<sup>-/-</sup> mice develop bilateral hydronephrosis and hydroureter. The onset of this phenotype occurs between E15 and E16, and the phenotype is 100% penetrant by E18. Additionally some heterozygotes develop a similar (though usually less severe) phenotype, indicating that there is a degree of haploinsufficiency.

### ***Hydronephrosis and hydroureter in Tshz3*<sup>-/-</sup> *mice do not result from physical obstruction***

Hydronephrosis and hydroureter can be caused by physical obstruction of the ureter, which leads to accumulation of urine upstream of the obstruction. Examination of histological sections and India ink injection experiments revealed that there was no intrinsic obstruction either in the ureter itself or at the vesicoureteric junction, and that vesicoureteric junctions were normally positioned. Additionally, no aneurysms or blood vessels crossing the ureter were observed at autopsy, so there is no extrinsic obstruction of the ureters in *Tshz3*<sup>-/-</sup> mice.

***Ureters from *Tshz3*<sup>-/-</sup> mice lack smooth muscle in their proximal portions, and have attenuated smooth muscle distally***

Hydronephrosis and hydroureter can also result from failure of/abnormal peristalsis of the ureter. As peristalsis requires smooth muscle, I decided to investigate whether the ureteric smooth muscle was normal in *Tshz3*<sup>-/-</sup> embryos. From E15 a severe defect in ureteric smooth muscle is observable in *Tshz3*<sup>-/-</sup> mice, as assessed by immunohistochemistry against the smooth muscle marker,  $\alpha$ SMA:  $\alpha$ SMA expression was almost entirely missing in proximal portions of *Tshz3*<sup>-/-</sup> ureters, and  $\alpha$ SMA expressing layers were thinner than those seen in wildtype in the more distal parts of the ureter. Similar observations have been made for other markers of smooth muscle differentiation (SM-MHC and SM-22a) and have been confirmed for  $\alpha$ SMA (by *in-situ* hybridisation), by members of Laurent Fasano's laboratory (Caubit et al., submitted). Therefore where I have reported a lack of  $\alpha$ SMA expression, this is due to smooth muscle is not being present, rather than the alternative possible explanation that smooth muscle was present, but was not expressing  $\alpha$ SMA.

The defect in the smooth muscle precedes the gross phenotype, and therefore cannot be explained by damage that may be caused to the ureter by the pressure from accumulated urine. Thus the lack of smooth muscle in mutant ureters must be the result of a failure of the smooth muscle to form. This defect in smooth muscle is likely to be the cause of the hydronephrosis and hydroureter, and this hypothesis is investigated further in Chapter Seven.

***The attenuation of smooth muscle in *Tshz3*<sup>-/-</sup> ureters is probably due to a failure of smooth muscle differentiation***

Comparison of numbers of proliferative and apoptotic cells between *Tshz3*<sup>-/-</sup> and wildtype ureters failed to reveal any statistically significant differences, suggesting that the failure of smooth muscle development in *Tshz3*<sup>-/-</sup> ureters is not due to a lack of smooth muscle precursor cells but is caused by the failure of these cells to differentiate appropriately. However, I observed a large amount of variation in both proliferation and apoptosis rates between individual mice of the same genotype, so large numbers of samples would be required for quantification of apoptosis and proliferation in order to identify whether there are small (but potentially biologically important) defects in cell turnover in the presumptive smooth muscle layer in *Tshz3*<sup>-/-</sup> ureters. Thus, although SMC precursors are not absent from the proximal ureters of *Tshz3*<sup>-/-</sup> mice, and the deficiency in smooth muscle is likely to be due to a failure of SMC precursors to differentiate, paucity in SMC precursor numbers may also contribute to the lack of SMCs. In order to clarify this point in future the quantification of proliferating and apoptotic cells in *Tshz3*<sup>-/-</sup> and wildtype ureters using anti-PCNA antibodies and TUNEL, respectively, could be repeated with larger sample sizes. Additionally this quantification could be verified using independent techniques. For example incorporation of the thymidine analogue bromodeoxyuridine (BrdU) could be used to identify (and quantify) cells in S-phase (Morstyn et al., 1983) and anti-activated caspase 3 (a key executioner of apoptosis (Cohen, 1997)) antibodies to detect cells in which the apoptotic pathway has been activated.

***Bmp4 expression, which is required for ureteric smooth muscle development, is not affected in Tshz3<sup>-/-</sup> ureters***

I compared the expression of Bmp4 in *Tshz3<sup>-/-</sup>* ureters to that of wildtype, as *Tshz3<sup>-/-</sup>* ureters lack smooth muscle, and Bmp4 is known to be important for ureteric smooth muscle development (Raatikainen-Ahokas et al., 2000; Miyazaki et al., 2003). I found similar patterns of Bmp4 expression in wildtype and mutant ureters (by immunohistochemistry), and these results have been confirmed by Xavier Caubit by *in-situ* hybridisation, which showed *Bmp4* transcripts to be present in the ureteric mesenchyme of both wildtype and *Tshz3* null mice at E15 (Caubit et al., submitted). Additionally Xavier Caubit has shown by *in-situ* that *Shh* and *Patched1* (which lie upstream of Bmp4 expression; (Yu et al., 2002)) transcript expression is not affected in the ureters of *Tshz3* null mice (Caubit et al., submitted). Therefore the failure of smooth muscle development in the proximal ureters of *Tshz3<sup>-/-</sup>* mice is not due to defects in this signalling cascade that has previously been shown to be important in the control of ureteric development.

***Abnormalities in cell shape may be the cause of the failure of smooth muscle differentiation***

Elongation of SMC precursors has been observed to precede SMC differentiation (Thelier, 1989; Roman and McDonald, 1992), and more recently this cell shape change has been shown to be vital for smooth muscle differentiation (Yang et al., 1999). Yang et al. (1999) demonstrated, by culturing cells on different microspheres to control cell shape, that mesenchymal cells from different origins could be induced to/prevented from differentiating into smooth muscle when forced to adopt an elongated/round cell shape. These observations were found to be independent of the



cells' natural fate, and could not be overcome by treatment with growth factors known to either stimulate (RA, TGF- $\beta$ 1) or inhibit (PDGF-BB) smooth muscle differentiation (Holycross et al., 1992; Desmouliere et al., 1993; Orlandi et al., 1994; Blank et al., 1995; Hirschi et al., 1998; Yang et al., 1999). The histological appearance (described in the histology section of this chapter, see Figure 6.5) of the condensing mesenchyme in *Tshz3*<sup>+/+</sup> E15 ureters appear to represent a line of spindle shaped (i.e. elongated) cells orientated perpendicular to the urothelium (and therefore a "clear zone", representing the elongated cell bodies, is seen between the nuclei of the mesenchyme and the urothelium). As no "clear zone" is observable on sections of *Tshz3*<sup>-/-</sup> ureter, and cells appear disorganised, this suggests that although smooth muscle cell precursors do "condense" (i.e. become more closely packed) around the urothelium, they fail to adopt the correct cell shape and organisation. From the results of Yang et al. (1999) it seems likely that their failure to adopt the correct cell shape means that they are unable to subsequently differentiate into smooth muscle. The exact mechanism by which cell elongation and smooth muscle differentiation are linked has not been fully elucidated. However in the lung epithelial laminin  $\alpha$ 1 is required for initial elongation of mesenchymal cells (Schuger et al., 1997). Mesenchymal cells upregulate MAPK38 synthesis and phosphorylation (Yang et al., 1999) and laminin 2 in response to elongation, and laminin 2 has been shown to be important for further cell elongation and upregulation of smooth muscle specific gene expression (Relan et al., 1999). To conclude, in *Tshz3*<sup>-/-</sup> ureters smooth muscle precursor cells appear by histology to fail to adopt the usual shape, and correct cell shape has been implicated in other contexts to be required for differentiation of smooth muscle (although the mechanisms involved have not been fully elucidated). Therefore the failure of

smooth muscle development in *Tshz3*<sup>-/-</sup> ureters may be due to the precursor cells being the wrong shape. This possibility could be investigated further by the use of transmission electron microscopy to compare shapes of smooth muscle precursor cells in *Tshz3*<sup>-/-</sup> and wildtype ureters.

***Other than in the ureter, expression of  $\alpha$ SMA is not affected in urinary tracts of *Tshz3*<sup>-/-</sup> mice.***

The bladder contains smooth muscle, as does the kidney (which contains blood vessels surrounded by vascular smooth muscle cells). Additionally the medullary stromal cells of the embryonic kidney express  $\alpha$ SMA. *Tshz3* is expressed in both the bladder and the kidney, and is required for smooth muscle development in the ureter. Bladder detrusor smooth muscle development is known to depend (at least in part) on a pathway that regulates ureteric smooth muscle development: urothelial Shh having been implicated as playing an important role (Shiroyanagi et al., 2007). The expression of  $\alpha$ SMA in the kidney has been postulated to depend on Bmp4 (downstream of Wnt4 (Itaranta et al., 2006)), highlighting similarities between regulation of development of  $\alpha$ SMA expressing populations of cells in the ureter and kidney. Therefore I decided to investigate the expression of  $\alpha$ SMA in the bladders and kidneys of *Tshz3*<sup>-/-</sup> embryos. I found no abnormalities in  $\alpha$ SMA expression in either bladders or kidneys of *Tshz3*<sup>-/-</sup> embryos.

These observations show that the expression of  $\alpha$ SMA does not depend on *Tshz3* expression in all circumstances within the urinary tract. This observation can be explained in two ways; either when no defect  $\alpha$ SMA expression is observed in *Tshz3*<sup>-/-</sup> mice it is because *Tshz3* play no role in control of  $\alpha$ SMA expression, or in

these regions redundant genes are expressed which are able to compensate for the lack of *Tshz3*. Either way; these results emphasise the fact that different populations of  $\alpha$ SMA expressing cells have different requirements for their expression of  $\alpha$ SMA (despite also having some similar requirements, which are discussed above).

***Other than the defect in ureteric smooth muscle development, leading to hydronephrosis and hydroureter, no abnormalities could be found in the development of urinary tracts***

The development of the ureter is known to involve reciprocal signalling between the epithelium and the mesenchyme (Airik et al., 2006; Mendelsohn et al., 2006).

Therefore the observed abnormalities in mesenchymal development (smooth muscle development) could be associated with abnormalities of epithelial development. I assessed epithelial (urothelial) development by observation of the expression of Up1b, a marker of urothelial differentiation. No abnormalities in Up1b expression was observed in *Tshz3*<sup>-/-</sup> ureters, indicating that urothelial differentiation is not affected in *Tshz3*<sup>-/-</sup> embryos. Additionally, no statistically significant differences in the numbers of proliferating or apoptosing cells in the urothelium were observed, although small changes in the rate of cell division and/or apoptosis cannot be excluded. In conclusion, I found no defects in urothelial development in *Tshz3*<sup>-/-</sup> embryos, however I cannot exclude the possibility that subtle abnormalities of the development of the ureteric epithelium occur.

*Tshz3* is expressed in the mesenchyme surrounding the stalk of the ureteric bud at E11 and E12, and is expressed in the mesenchyme around the mesonephric ducts (Laurent Fasano, personal communication) indicating that it may play a role in

regulating the early events of kidney development; for example regulation of ureteric bud formation from the mesonephric ducts or elongation of the ureteric bud and invasion of the metanephric mesenchyme. However, histological sections taken of E12 *Tshz3*<sup>-/-</sup> mice from the region containing the metanephros revealed that metanephri were morphologically normal at this early stage of their development (as detailed in the histology of this chapter; Figure 6.3). Additionally, expression of Pax2 (a gene important for the regulation of early kidney development) was normal in *Tshz3*<sup>-/-</sup> embryos at this stage. Therefore a role for *Tshz3*<sup>-/-</sup> in the regulation of the early events of kidney development is unlikely.

As detailed in Chapter Five *Tshz3* is expressed in the developing kidney and bladder, so may be involved in regulating their development. However, no evidence to support such a hypothesis was found. Both kidneys and bladders were morphologically and histologically normal. Additionally the expression of Pax2, a gene important for kidney development, and the expression of markers of various components of the kidney were normal in *Tshz3*<sup>-/-</sup> embryonic kidneys. Therefore if *Tshz3* has functions in the development of the kidney or bladder they are either very subtle and/or are redundant with other genes.

## Summary of results in Chapter Six

1. *Tshz3*<sup>-/-</sup> mice develop bilateral hydronephrosis and hydroureter. The phenotype is completely penetrant, and is first observable at E16.
2. The phenotype is not a result of physical obstruction, but is probably a result of functional obstruction resulting from a deficiency in ureteric smooth muscle.
3. The deficiency in ureteric smooth muscle observed in *Tshz3*<sup>-/-</sup> mice is a result of failure of smooth muscle precursor cells to differentiate.
4. Other populations of smooth muscle in the urinary tract are unaffected in *Tshz3*<sup>-/-</sup> mice.
5. Other aspects of urinary tract development appear unaffected in *Tshz3*<sup>-/-</sup> mice; in particular no defects in kidney development were observed.

## Results Part II - Chapter Seven

### The function of *Tshz3* in the developing urinary tract; *in vitro* studies

#### Introduction

This chapter details the *in vitro* embryonic organ culture studies undertaken to explore the phenotype of *Tshz3*<sup>-/-</sup> mice. These experiments were undertaken to complement the *in vivo* experiments detailed in Chapters Five and Six, with an overall aim to discover the function of *Tshz3* in the developing urinary tract.

In Chapter Six I showed that *Tshz3*<sup>-/-</sup> mice developed hydronephrosis and hydroureter in utero with 100% penetrance by E17. Hydroureter and hydronephrosis can be caused by either physical or functional obstruction (Mendelsohn, 2004; Mendelsohn, 2006). In the case of *Tshz3*<sup>-/-</sup> mice, no physical obstruction could be found (injection of India Ink into the renal pelvis and analysis of serial sections revealed the urinary tract lumen to be patent from the renal pelvis to the bladder), suggesting that functional obstruction (that is, failure of the peristaltic movements of the ureter) could well be the cause of the phenotype. Indeed, smooth muscle differentiation was found to be impaired, particularly in the proximal part of the ureter (which was the most highly distended part). This defect in differentiation preceded the onset of the hydronephrosis by approximately one day, thus was well placed to be its cause, because functional smooth muscle is required for peristalsis.

It has previously been reported that when ureters are isolated from E15 mouse embryos and cultured at the air/medium interface they spontaneously begin to undergo unidirectional peristaltic contractions after three days (David et al., 2005).

In order to test the hypothesis that *Tshz3*<sup>-/-</sup> embryos have functionally-obstructed ureters, culture experiments were performed in order to assess their peristaltic activity, utilising a method based on the one described in David et al. (2005). Additionally, the growth of the ureters (as assessed by their change in length) in culture and their expression of  $\alpha$ SMA was assessed.

## **Results**

Ureters were dissected from E15 mice, prior to the onset of the gross phenotype, so that any observed defects in *Tshz3*<sup>-/-</sup> ureters could not be attributed to damage secondary to the hydroureter. They were cultured either with serum or in serum free conditions (three litters of *Tshz3* mice were used for each culture condition). In agreement with David et al. (2005), I found that the ureters began to contract after three days in culture (in both culture conditions).

### ***Quality of peristalsis***

To assess the quality of peristaltic contractions, ureters were imaged by timelapse videomicroscopy on the fifth day of the culture period (n=36 *Tshz3*<sup>+/+</sup> and n=35 *Tshz3*<sup>-/-</sup> ureters). From observation of the movies recorded, it was noted that in *Tshz3*<sup>+/+</sup> ureters peristalsis usually initiated about a fifth of the way down the ureter from the proximal end, though the exact position of the initiation site sometimes varied between contractions. The contraction propagated distally to produce a peristaltic wave along the ureter. Additionally, immediately after initiation the proximal fifth of ureter also contracted in *Tshz3*<sup>+/+</sup> ureters. In *Tshz3*<sup>-/-</sup> ureters peristalsis initiated and propagated distally in the same way as it did in *Tshz3*<sup>+/+</sup> ureters, however contraction of the proximal fifth of the ureter did not

occur. Movies 7.1A and B show timelapse recordings of representative peristalses of a *Tshz3*<sup>+/+</sup> and *Tshz3*<sup>-/-</sup> ureter respectively. Both these movies show ureters that were cultured with serum-free media. Similar results were observed when ureters were cultured with serum (data not shown).

Videos recordings of ureters cultured with serum-free media were analysed by measuring the diameter of the ureter at specific points over time during a contraction. The diameter of each point along the ureter, expressed as a percentage of its relaxed diameter, provided a quantitative measure of how much that point of the ureter had contracted. Figure 7.1 illustrates this analysis for a representative peristaltic wave of a *Tshz3*<sup>+/+</sup> and a *Tshz3*<sup>-/-</sup> ureter cultured with serum-free media. This analysis confirms the previous observation that in *Tshz3*<sup>-/-</sup> ureters the proximal part of the ureter is acontractile, but other aspects of their peristalsis appeared normal.

### ***Frequency of peristalsis***

In addition to assessing the quality of peristalsis, I assessed the frequency of peristalsis. Each ureter was observed under a dissecting microscope twice a day, the number of times it contracted counted and the average number of peristalses per minute over a two-day period (the third and fourth day of culture) was calculated. This “frequency of peristalsis” was then compared between *Tshz3*<sup>+/+</sup> and *Tshz3*<sup>-/-</sup> ureters.



### **Movies 7.1 Timelapse movies of ureters cultured for five days in serum free conditions**

Ureters were imaged using a phase contrast timelapse microscope, after five days in serum free culture. The movies show the duration of one peristaltic wave. In both movies the proximal ureter is on the right hand side. Movies are played at approximately 4x actual speed. **A** *Tshz3*<sup>+/+</sup> ureter. Peristalsis initiates approximately one fifth of the way down the ureter. Following the contraction at the initiation site, the most proximal part contracted and the peristaltic wave was propagated distally. **B** *Tshz3*<sup>-/-</sup> ureter. Peristalsis initiates approximately one fifth of the way down the ureter. Following the contraction at the initiation site the peristaltic wave was propagated distally. Significantly, however, the proximal ureter completely failed to contract. (Note: These movies are provided on a CD in Quicktime Movie format, you may need to download Quicktime, in order to view them. Quicktime is available at <http://www.apple.com/quicktime/download/>).

These movies appear in Caubit et al. (submitted).

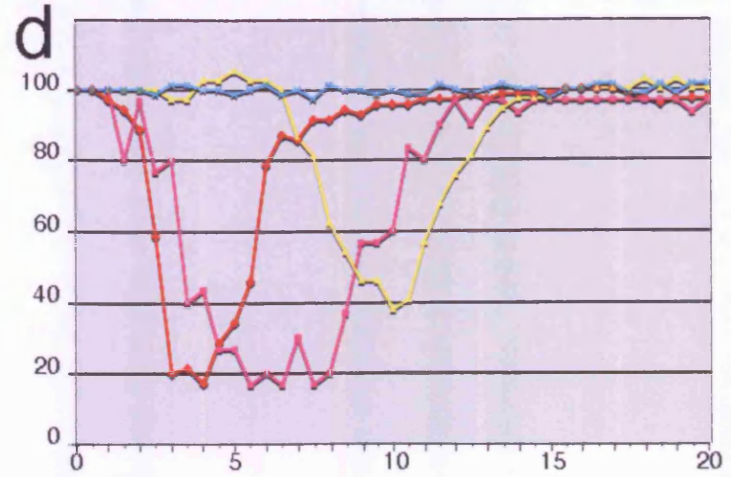
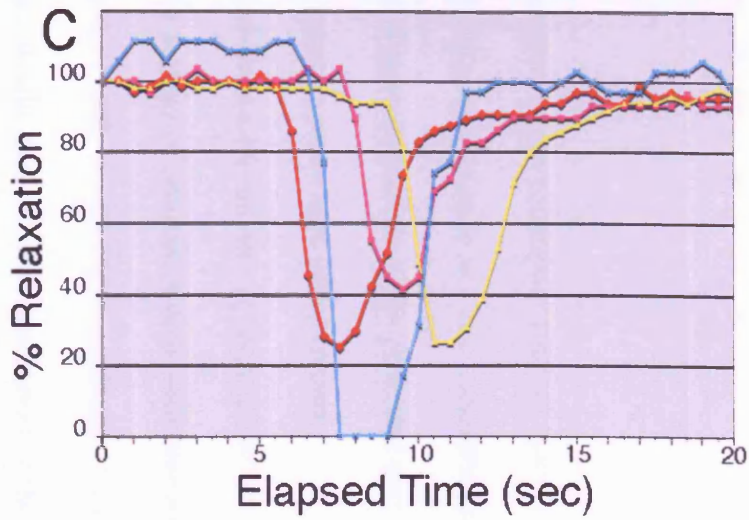
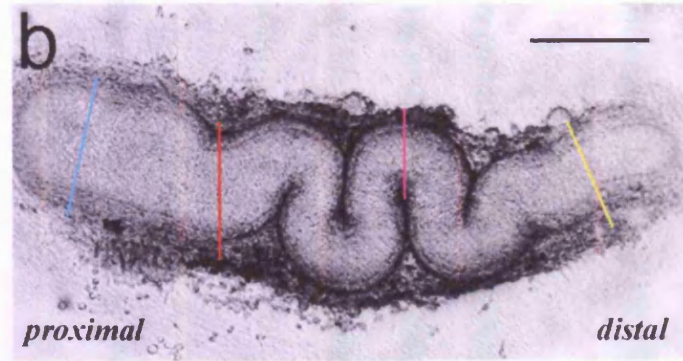
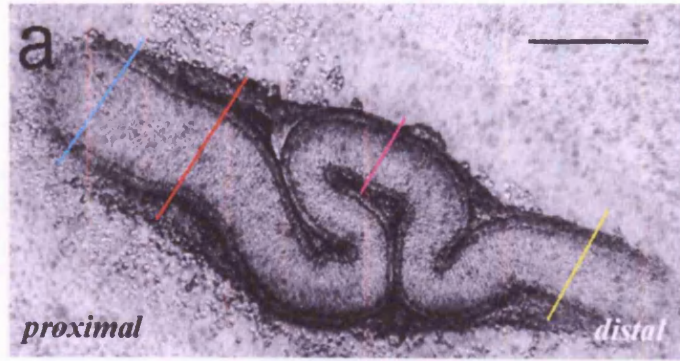
**Figure 7.1 Analysis of movies of ureters cultured in serum free conditions for five days**

Ureters were imaged using a phase contrast timelapse microscope, after five days in serum free culture, and analysis using metamorph software. **A** and **C** *Tshz3*<sup>+/+</sup> ureter; **B** and **D** *Tshz3*<sup>-/-</sup> ureter. **A** and **B** Phase contrast views of ureters after five days culture: the proximal end of the ureter is shown on the right. Scale bars - 200µm. **C** and **D** Graphs illustrating peristaltic contractions of cultured ureters shown above. Measurements of luminal diameters were made at four different positions from their proximal to distal ends from a 20 second digital recording of contracting ureters (**Movies 9.1A** and **B**). Data are presented as the percent of the relaxed diameter. In the trace from the *Tshz3*<sup>+/+</sup> ureter (**C**) the contraction (downward motion from baseline) initiates about one fifth of the way down (red line) the ureter; this is rapidly followed by both contraction of the more proximal segment (blue line) and also by distal propagation (pink and yellow lines). The trace from the *Tshz3*<sup>-/-</sup> ureter (**D**) shows absent proximal segment contraction (blue line), but contractions at other sites along the ureter are comparable to wildtype (red, pink and yellow lines).

L. Fasano performed the computer aided analysis of the ureter culture movies and kindly provided this figure.

Part of this figure appears in Caubit et al. (submitted).

**Figure 7.1**



For ureters cultured in serum free conditions *Tshz3*<sup>+/+</sup> ureters peristalsed 0.81 times/min (SEM= 0.13, n=13) and *Tshz3*<sup>-/-</sup> ureters peristalsed 1.43 times/min (SEM= 0.17, n=23). An independent samples two tailed T-test, revealed that there was a significant difference (P<0.05).

For ureters cultured with serum *Tshz3*<sup>+/+</sup> ureters peristalsed 1.08 times/min (SEM=0.14, n=25) and *Tshz3*<sup>-/-</sup> ureters peristalsed 1.94 times/min (SEM= 0.16, n=12). An independent samples two tailed T-test, revealed that there was a significant difference (P<0.001).

In conclusion, explanted *Tshz3*<sup>-/-</sup> ureters peristalse more frequently than ureters of their wildtype littermates (but the proximal section of the ureter fails to contract in *Tshz3*<sup>-/-</sup> mutants).

### ***Differentiation of ureters in vitro***

Because smooth muscle fails to differentiate in the proximal ureter of *Tshz3*<sup>-/-</sup> *in vivo*, and the proximal part of the ureter was acontractile *in vitro*, I hypothesised that there were defects in the development of smooth muscle in the proximal part of the ureters of *Tshz3*<sup>-/-</sup> mice *in vitro*. Therefore, I performed whole mount immunofluorescence on ureters that had been cultured for six days to analyse expression of  $\alpha$ SMA, which is an early marker of smooth muscle differentiation (McHugh, 1995). I also stained the ureters with an anti-Up1b antibody. Up1b is a marker of urothelial differentiation, and would thus allow visualisation of the urothelial layer of the ureter. The stained ureters were analysed by confocal microscopy.

Ureters cultured both with and without serum were examined in this way. Note that ureters in which either the  $\alpha$ SMA or Up1b primary antibodies had been omitted during the staining procedure were used as negative controls, and verified that staining observed was specific. By observation of serial optical sections through whole-mount ureters, I noted that the urothelium was surrounded by a layer of  $\alpha$ SMA expressing cells; no differences were observed between ureters that had been grown with or without serum. Figure 7.2.1 shows an example of a ureter stained with anti- $\alpha$ SMA and anti-Up1b antibodies, as well as negative control ureters, viewed at low power. No gross difference was seen in expression of  $\alpha$ SMA (or Up1b) between *Tshz3*<sup>+/+</sup> and *Tshz3*<sup>-/-</sup> ureters, at any position along the ureter (n=3 *Tshz3*<sup>+/+</sup> and n=4 *Tshz3*<sup>-/-</sup>). Figure 7.2.2 shows proximal ureter, Figure 7.2.3 shows middle ureter and Figure 7.2.4 shows distal ureter. Therefore, *in vitro*, *Tshz3* is not required for the expression of  $\alpha$ SMA in the ureter, even though null mutant ureters do show striking aberrations of contractile function.

### ***Elongation of ureters in vitro***

In order to assess whether ureters grew during their period of culture, the length of ureters was measured on the first and last day of culture, and percentage change in length was calculated for each ureter.

### **Figure 7.2.1 Expression of $\alpha$ SMA and Up1b in cultured ureters**

All panels show ureters that have been cultured for six days, then stained using immuno-fluorescence, and viewed by confocal microscopy. All panels show single longitudinal optical sections through the centre of a wildtype ureter, at low magnification. **A** ureter stained to visualize  $\alpha$ SMA (red) and Up1b (green), shows the presence of a urothelium at the centre of the ureter, surrounded by a layer of smooth muscle. Note that the proximal end of the ureter is at the top of this frame, and has some urothelium from the renal pelvis attached (which is not surrounded by smooth muscle). **B** negative control staining to show that  $\alpha$ SMA staining is specific. The ureter was stained and imaged in the same as in **A**, except that the  $\alpha$ SMA antibody was omitted. Note that the proximal end of the ureter is at the left of this frame. No red signal is seen, indicating that the  $\alpha$ SMA signal in **A** and **C** (and in **Figures 7.2.2, 7.2.3 and 7.2.4**) is specific. **C** negative control staining to show that Up1b staining is specific. The ureter was stained and imaged in the same as in **A**, except that the Up1b antibody was omitted. Note that the proximal end of the ureter is at the left of this frame. No green signal is seen, indicating that the Up1b signal in **A** and **C** (and in **Figures 7.2.2, 7.2.3 and 7.2.4**) is specific. Scale bars - 300 $\mu$ m.

**Figure 7.2.1**

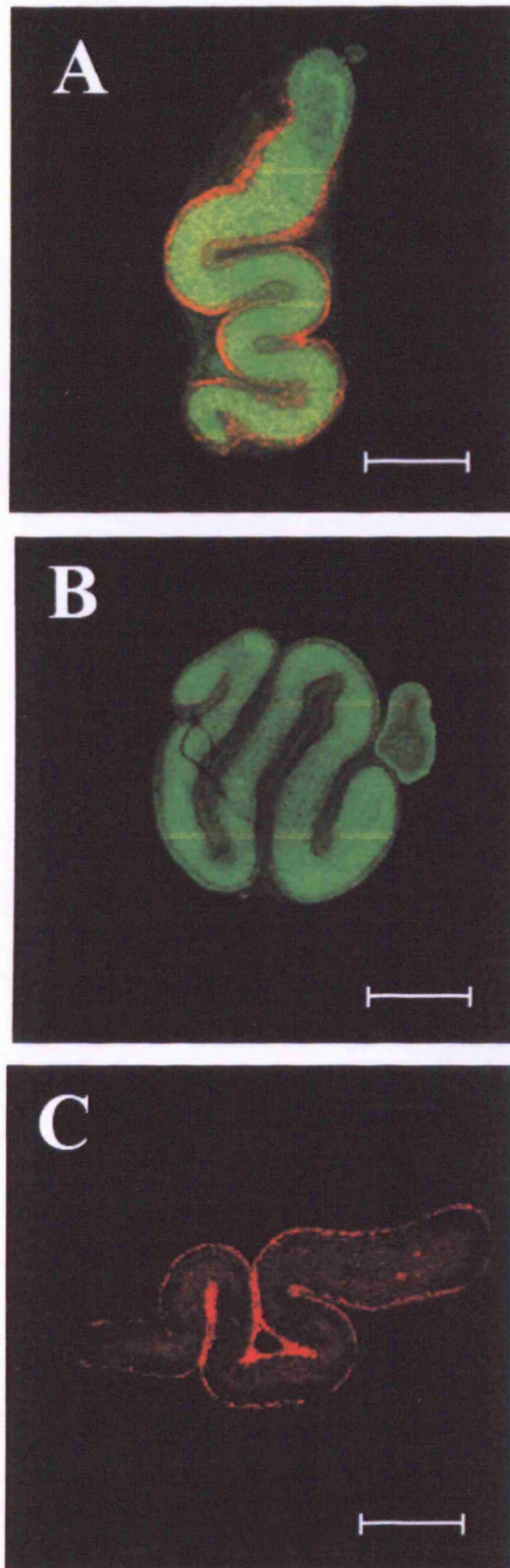


**Figure 7.2.2 Expression of  $\alpha$ SMA and Up1b in the proximal section of cultured ureters**

All panels show proximal sections of ureters that have been cultured for six days, then stained using immunofluorescence to visualize  $\alpha$ SMA (red) and Up1b (green), and viewed by confocal microscopy at high magnification. **A** and **B** *Tshz3*<sup>+/+</sup> ureters; **C** and **D** *Tshz3*<sup>-/-</sup> ureters. **A** and **C** Single longitudinal optical sections through the smooth muscle layer; **B** and **D** Single longitudinal optical sections through the centre of the ureter (the urothelial layer). No differences are observed in either  $\alpha$ SMA (red) or Up1b (green) expression between *Tshz3*<sup>+/+</sup> and *Tshz3*<sup>-/-</sup> ureters, in their proximal sections. Note in **C** and **D** the ureter has been damaged by handling with forceps during the staining procedure, leading to the patch of non  $\alpha$ SMA expressing tissue in the smooth muscle layer (**C**), and the patch of  $\alpha$ SMA expressing tissue in the urothelial layer (**D**). Scale bars - 75 $\mu$ m.



**Figure 7.2.2**

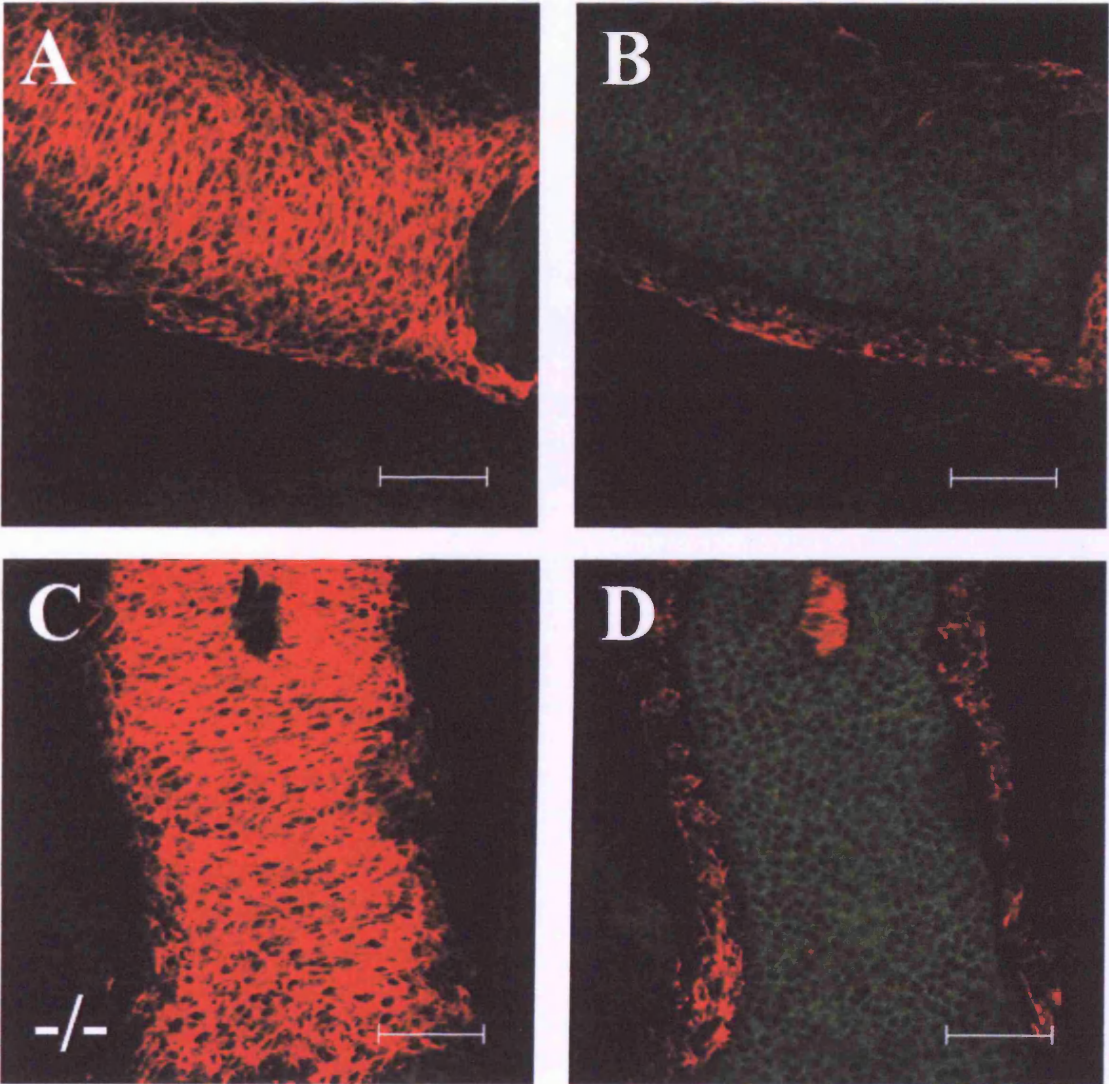


**Figure 7.2.3 Expression of  $\alpha$ SMA and Up1b in the middle section of cultured ureters**

All panels show middle (ie neither proximal nor distal) sections of ureters that have been cultured for six days, then stained using immuno- fluorescence to visualize  $\alpha$ SMA (red) and Up1b (green), and viewed by confocal microscopy at high magnification. **A** and **B** *Tshz3*<sup>+/+</sup> ureters; **C** and **D** *Tshz3*<sup>-/-</sup> ureters. **A** and **C** Single longitudinal optical sections through the smooth muscle layer. **B** and **D** Single longitudinal optical sections through the centre of the ureter (the urothelial layer). No differences are observed in either  $\alpha$ SMA (red) or Up1b (green) expression between *Tshz3*<sup>+/+</sup> and *Tshz3*<sup>-/-</sup> ureters, in their middle sections. Scale bars - 75 $\mu$ m.

**Figure 7.2.3**

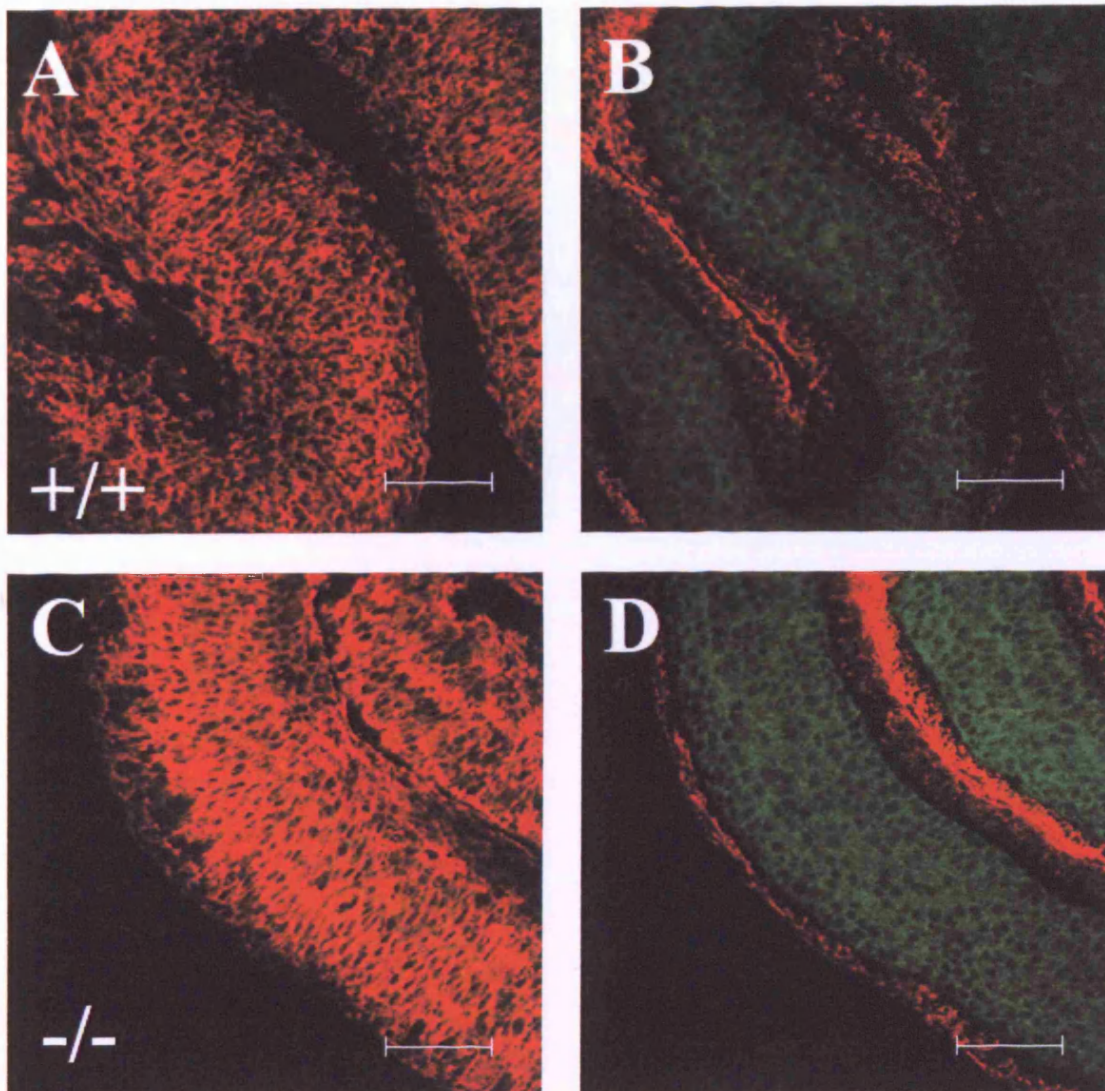
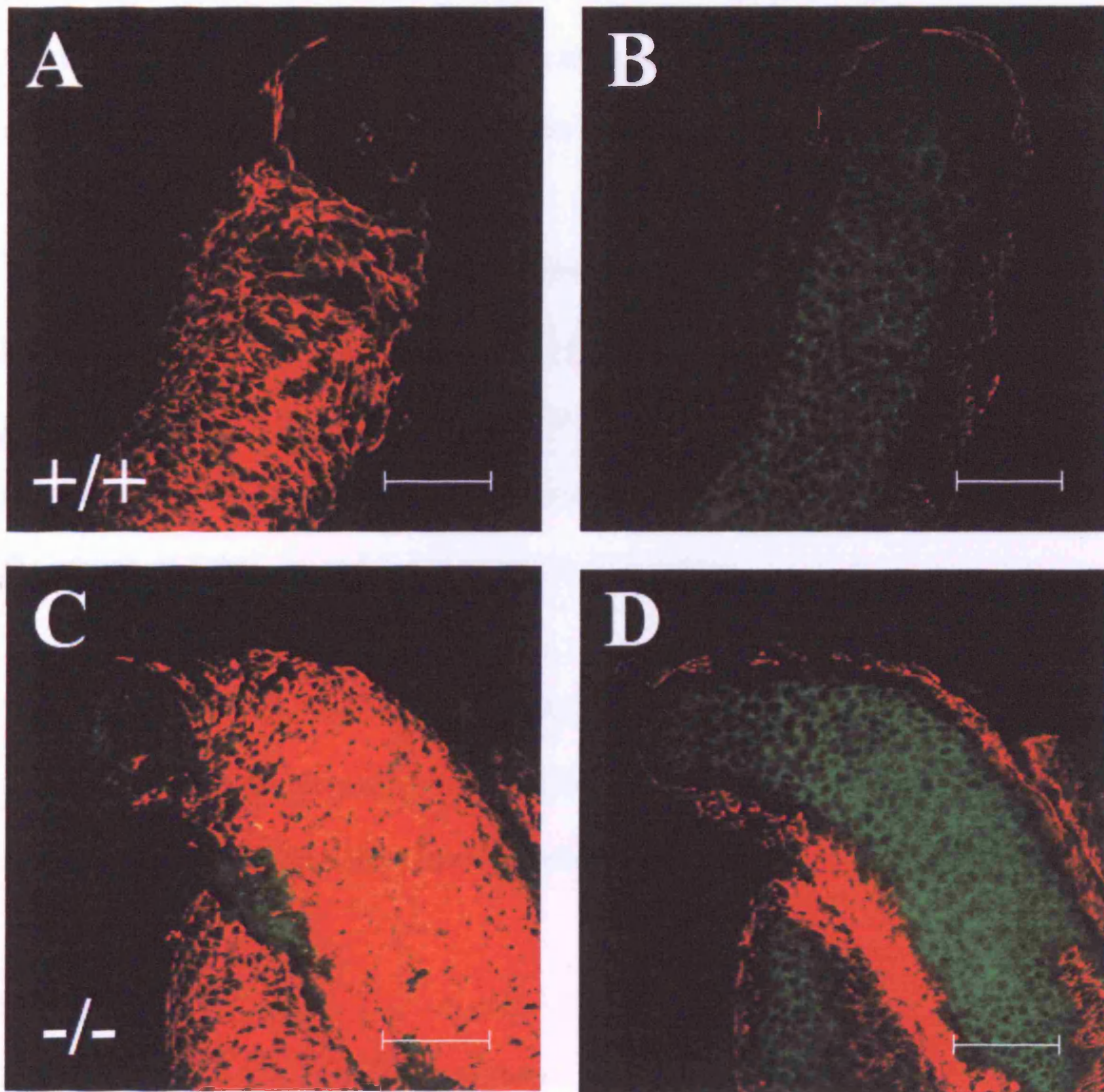


**Figure 7.2.4 Expression of  $\alpha$ SMA and Up1b in the distal section of cultured ureters**

All panels show distal sections of ureters that have been cultured for six days, then stained using immuno- fluorescence to visualize  $\alpha$ SMA (red) and Up1b (green), and viewed by confocal microscopy at high magnification. **A** and **B** *Tshz3*<sup>+/+</sup> ureters; **C** and **D** *Tshz3*<sup>-/-</sup> ureters. **A** and **C** Single longitudinal optical sections through the smooth muscle layer. **B** and **D** Single longitudinal optical sections through the centre of the ureter (the urothelial layer). No differences are observed in either  $\alpha$ SMA (red) or Up1b (green) expression between *Tshz3*<sup>+/+</sup> and *Tshz3*<sup>-/-</sup> ureters, in their distal sections. Scale bars - 75 $\mu$ m.

**Figure 7.2.4**



In serum-free culture conditions *Tshz3*<sup>+/+</sup> ureters had an average percentage length increase of 61.7% (SEM=3.6%, n=13), whereas *Tshz3*<sup>-/-</sup> ureters had an average percentage change increase of 34.2% (SEM=3.3%, n=23). An independent samples two tailed T-test indicated that there was a significant difference between the elongation of *Tshz3*<sup>+/+</sup> and *Tshz3*<sup>-/-</sup> ureters (P < 0.001).

When ureters were cultured with serum *Tshz3*<sup>+/+</sup> ureters had an average percentage length increase of 52.7% (SEM=4.0%, n=24), whereas *Tshz3*<sup>-/-</sup> ureters had an average percentage change increase of 18.4% (SEM=1.7%, n=8). An independent samples two tailed T-test indicated that there was a significant difference between the growth of *Tshz3*<sup>+/+</sup> and *Tshz3*<sup>-/-</sup> ureters (P < 0.001)

Therefore, although both wildtype and null mutant ureters increase in length during the culture period, the percentage increase in length is significantly less in *Tshz3*<sup>-/-</sup>, indicating that mutant ureters grow relatively less than *Tshz3*<sup>+/+</sup> in culture.

## **Discussion**

### ***Peristalsis is defective in Tshz3<sup>-/-</sup> ureters***

In *Tshz3*<sup>-/-</sup> ureters I have found that there is a defect in peristalsis *in vitro*, hence these ureters are most probably functionally obstructed *in vivo*. The functional obstruction described here is localised but severe, with the proximal part of the ureter completely failing to contract. The localisation of the acontractile part of the ureter in culture correlates strikingly with the most severely affected part of the ureter *in vivo*; as it is the proximal part of the ureter *in vivo* which almost completely lacks smooth muscle cells and becomes highly distended (whilst some smooth muscle

develops in the more distal ureter, and the diameter of its lumen is comparable with wildtype) (see Chapter Six).

Therefore, the hydronephrosis and hydroureter that develops in *Tshz3*<sup>-/-</sup> embryos can be explained by the failure of smooth muscle function in their proximal ureters, leading to an inability of this part of the ureter to contract during peristalsis. Thus urine is not propelled from the kidney through the proximal part of the ureter, to the distal ureter and bladder, causing urine to accumulate in this acontractile part of the ureter, and further “upstream” in the kidney.

Additionally I have found, unexpectedly, that *Tshz3*<sup>-/-</sup> ureters peristalse more frequently than wildtype ureters, suggesting that the timing between peristaltic contractions is mis-regulated in mutants. Such mis-regulation of contraction timings might be explained by a defect in the pacemaker cells of the ureter. These pacemaker cells have been shown to be c-kit positive, and culture experiments utilising inhibitory antibodies have shown that they are important for co-ordinated, unidirectional peristalsis (David et al., 2005). I observed no problems in directionality or co-ordination of peristaltic movements, so a severe defect in this cell population seems unlikely in *Tshz3*<sup>-/-</sup> ureters, however it remains a possibility that there is a subtle abnormality in the activity of these cells. The increased frequency could also be explained by a compensatory mechanism. I have described that *Tshz3*<sup>-/-</sup> ureters are functionally obstructed in their proximal sections; perhaps these ureters attempt to compensate for this obstruction by peristalsing more frequently. If this compensation occurs *in vivo*, it must not be sufficient to allow clearance of urine

from the functionally obstructed section of the ureter (as urine does accumulate within it).

***αSMA expression is not affected in Tshz3<sup>-/-</sup> ureters in vitro***

The observation that αSMA was expressed overtly normally throughout the length of cultured *Tshz3<sup>-/-</sup>* ureters was unexpected, and is in contrast to *in vivo* observations (see Chapter Six). However, it is important to note that αSMA is not only expressed by smooth muscle cells: for example it is expressed in myofibroblasts of the renal interstitium, which are particularly numerous during fibrosis (Iwano and Neilson, 2004; Bascands et al., 2007), and in mesangial cells during glomerulonephritis (Ichimura et al., 2006). Therefore, this expression of αSMA in *Tshz3<sup>-/-</sup>* ureters *in vitro* does not necessarily indicate that smooth muscle development occurs normally in *Tshz3<sup>-/-</sup>* ureters in culture. Further experiments, such as observation of other smooth muscle differentiation markers (such as SM-MHC) or transmission electron microscopy, are therefore required to clarify this point.

If smooth muscle differentiation was found to be unaffected in *Tshz3<sup>-/-</sup>* ureters *in vitro*, this may be explained by the culture media containing a factor capable of rescuing the defect in smooth muscle differentiation seen *in vivo*. For the ureters cultured with fetal calf serum, a variety of hormones and growth factors may have been present that could have caused a rescue of the smooth muscle defect. The serum-free culture medium contained insulin and transferrin, which are capable of signalling to cells, and it is possible that one of these could have activated a signalling pathway capable of rescuing smooth muscle development as both of these factors have been implicated in embryonic development. Transferrin is an iron



binding serum protein and has been shown to be required for the proliferation and differentiation of induced metanephric mesenchyme in cultured embryonic kidneys, by delivering iron to the cells via the transferrin receptor (Ekblom et al., 1983; Landschulz et al., 1984; Thesleff et al., 1985). Insulin-like growth factor I and II have been found to be produced in the metanephros, and to play a role in the growth and differentiation of this organ *in vitro* (Rogers et al., 1991). High concentrations of insulin may mimic insulin-like growth factor signalling. Significantly, insulin and insulin like growth factor are both known to promote smooth muscle cell differentiation via the PI3K/Akt signalling pathway (Hayashi et al., 1998). In the future it would be interesting to culture ureters without fetal calf serum, insulin and transferrin, and to assess whether smooth muscle differentiation was still able to proceed in *Tshz3*<sup>-/-</sup> ureters in the absence of these factors.

Despite the presence of  $\alpha$ SMA in *Tshz3*<sup>-/-</sup> ureters *in vitro*, the proximal ureter fails to contract in culture, so if smooth muscle differentiation was found to be rescued *in vitro* an alternative explanation for the aperistaltic phenotype would need to be sought. The expression of cellular components required for the propagation of peristalsis may be missing in the proximal ureter. The propagation of peristaltic movements through the ureter is thought to be dependent on gap junctions between pacemaker cells and smooth muscle cells, which allows networks of cells to be joined together to form functional syncytia (Schwentner et al., 2005). Therefore if expression of an important gap junction component, for example connexin43 (Nemeth et al., 2000; Sui et al., 2002), was downregulated in the proximal ureter, then the signal that triggers contraction could not be propagated from the initiation site into the proximal ureter, and the proximal ureter would fail to contract.

Therefore an absence of functional smooth muscle is not the only possible explanation for the failure of the proximal ureters of *Tshz3*<sup>-/-</sup> mice to peristalse.

### ***Ureter Elongation is impaired in Tshz3<sup>-/-</sup> ureters***

In addition to the defects in peristalsis observed in *Tshz3*<sup>-/-</sup> ureters, there is a defect in the elongation of these ureters. The underlying causes of the elongation defect remain to be elucidated. One possible reason for the smaller percentage increase in length in the *Tshz3*<sup>-/-</sup> ureters is that they have a smaller increase in cell number than *Tshz3*<sup>+/+</sup> ureters, this could be the result of differences in higher rates of apoptosis or lower rates of proliferation compared with the *Tshz3*<sup>+/+</sup>. *In vivo* analysis of apoptosis and proliferation failed to uncover differences in “cell turnover” between *Tshz3*<sup>+/+</sup> and *Tshz3*<sup>-/-</sup>, suggesting that differences in rates of apoptosis and proliferation are unlikely to be the cause of the defect in ureter elongation *in vitro*; however such a possibility cannot be formally excluded. Cell rearrangement can lead to striking elongation, even in the absence of cell turnover: for example the Malpighian tubules of *Drosophila* elongate by cell re-arrangement (rather than by an increase of cell numbers) (Jung et al., 2005). Therefore, an alternative explanation would be that cell number is not affected in *Tshz3*<sup>-/-</sup> ureters, but cell rearrangement is impaired leading to the ureters elongating less than *Tshz3*<sup>+/+</sup> ureters. Indeed, a defect in the organisation of the condensing mesenchymal cell layer was observed *in vivo*, suggesting that control of cell shape and cell re-arrangement may be impaired in *Tshz3*<sup>-/-</sup> ureters.

*In vivo*, ureter elongation is important to allow the correct positioning and rotation of the kidneys; when ureters are short it results in kidneys being closer to bladders, and

kidneys being rotated through 90° so that the ureter joins the kidney at its posterior apex, rather than medially, as is observed in *Tbx18*<sup>-/-</sup> mice (Airik et al., 2006). It is notable that no such defect was observed *in vivo*, however *in vivo* ureter length was not measured accurately, so a subtle defect of ureter elongation *in vivo* may exist.

## Summary of results in Chapter Seven

1. The proximal section of ureters from *Tshz3*<sup>-/-</sup> mice fail to contract *in vitro*. Thus, *in vivo*, *Tshz3*<sup>-/-</sup> ureters are most likely functionally-obstructed, providing an explanation for the *in vivo* phenotype described in Chapter Six.
2.  $\alpha$ SMA expression was not found to be overtly perturbed in *Tshz3*<sup>-/-</sup> ureters in culture. This is in contrast to *in vivo* results described in Chapter Six.
3. *Tshz3*<sup>-/-</sup> ureter peristalsis more frequently than *Tshz3*<sup>+/+</sup> ureters, indicating that the control of peristaltic timing may be affected in *Tshz3*<sup>-/-</sup> ureters.
4. Percentage length increase of *Tshz3*<sup>-/-</sup> ureters in culture is significantly less than that of *Tshz3*<sup>+/+</sup> ureters, revealing a possible subtle defect in ureter elongation.

## Chapter Eight - Final Discussion

### Summary of main findings

The overall aim of the research presented in this thesis was to explore whether *Teashirt* family genes are involved in the regulation of mouse urinary tract development.

I found that *Tshz1-3*, and a putative transcriptional target, *Larp*, transcripts are present in developing mouse kidneys. Furthermore, I found that they continue to be expressed in the kidney in adulthood (though for *Tshz2* and *3* at a lower level than at embryonic stages). Whilst attempting to investigate by Western blotting whether mTshz protein was present in the developing urinary tract, I discovered that Tshz3 protein is approximately twice its predicted size (and this is likely to be the case also for Tshz1 and 2), indicating that mouse Tshz proteins may undergo extensive post-translational modification.

I also found that *Tshz3*<sup>-/-</sup> embryonic mice display bilateral hydronephrosis and hydroureter, resulting from a defect in the development of their ureter. Specifically, the phenotype is a result of a failure of ureteric smooth muscle differentiation and the inability of the proximal ureter to peristalt. I characterised expression of *Tshz3* in the developing mouse urinary tract and found it to be expressed in the mesenchymal cells of the ureter and bladder, as well as in a subset of kidney stromal cells. In adult mouse kidneys *Tshz3* was expressed in a subset of interstitial cells, in the mesangial cells of the glomerulus and in the smooth muscle of the renal pelvis. Despite

expression of *Tshz3* in the developing kidney and bladder I found no defects in the development of these organs.

In conclusion I have found that *Tshz3* has a crucial role in mouse urinary tract development. The functions of *Tshz1* and *Tshz2* remain to be investigated, but their expression in developing kidneys is consistent with the possibility that they are also involved in the regulation of mouse urinary tract development.

### ***Teashirt3 and mesenchymal cell lineages in urinary tract development***

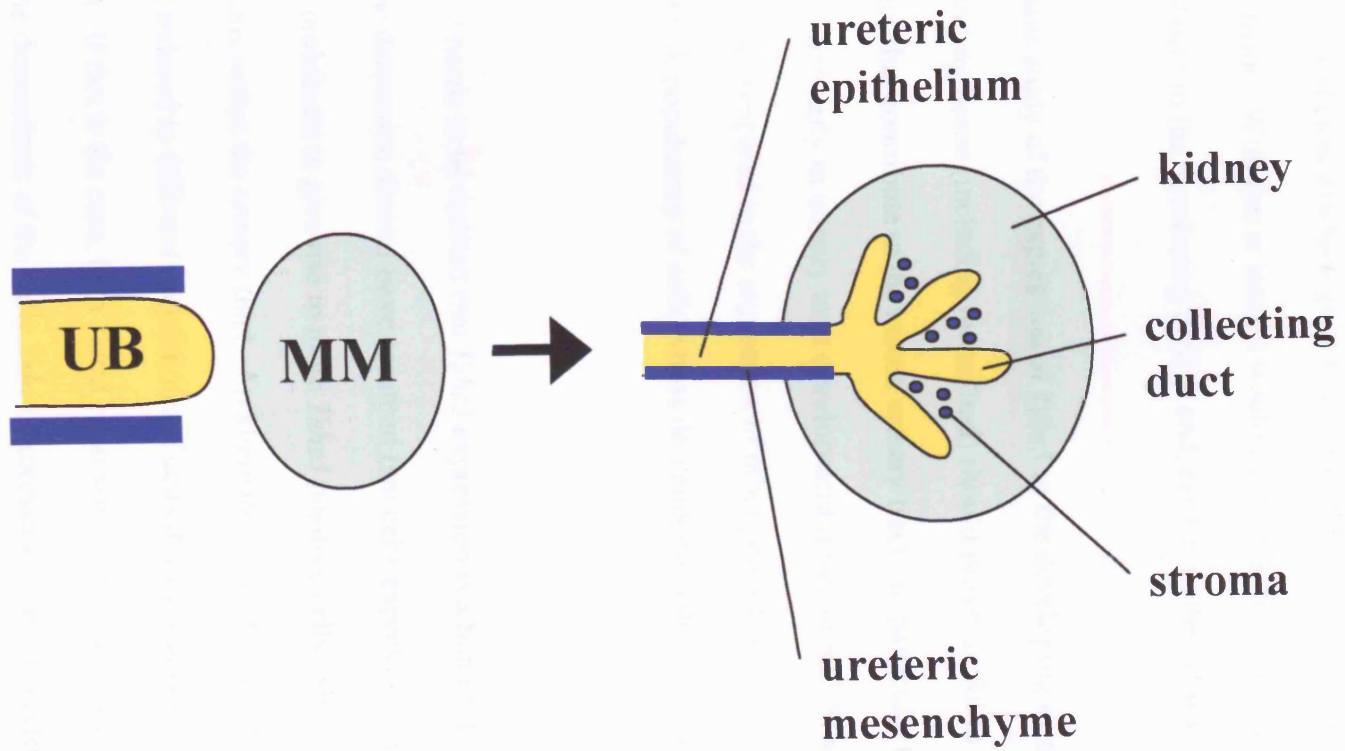
The expression pattern of *Tshz3* during the development of the urinary tract is intriguing. At E12.5 it is expressed in mesenchymal cells that surround the stalk of the ureteric bud, but is not expressed in the ureteric bud itself, or the metanephric mesenchyme (Figure 8.1) (Caubit et al., submitted). Later (E15-18; as described in Chapter Five and Caubit et al., submitted) *Tshz3* positive cells are found in the mesenchyme of the ureter (in both the Raldh2 positive and  $\alpha$ SMA positive layers), the stroma of the kidney (Figure 8.1) and the mesenchyme (both the lamina propria and the smooth muscle) of the bladder. This expression pattern is reminiscent of the expression of c-kit in the urinary tract: c-kit-positive cells are found outside the metanephric mesenchyme and the ureteric bud early in development (c-kit is expressed in a domain surrounding the metanephric mesenchyme, with particularly high numbers of c-kit-positive cells around the entry point of the ureteric bud into the metanephric mesenchyme) and later they populate both the mesenchymal layer of the ureter and the stroma of the kidney (Schmidt-Ott et al., 2006). Therefore the expression pattern of *Tshz3* is consistent with the current hypothesis that renal stromal cells derive from cells that originate outside of the metanephric mesenchyme. It remains to be investigated whether *Tshz3* and c-kit are co-expressed, or whether the expression of these markers represents two separate populations of cells.

**Figure 8.1 The expression of *Tshz3* during the development of the kidney and ureter**

In the conventional view of kidney development, the ureteric bud (UB, yellow) gives rise to the collecting system (ureter and collecting ducts, yellow) of the kidney; whereas the metanephric mesenchyme (MM, green) gives rise to the rest of the kidney (green), including the nephrons and stroma. *Tshz3* expression (blue) is detected in the mesenchymal cells surrounding the UB early in development (E12.5) and later (E15-E18) in the mesenchymal cells of the ureter and the medullary stromal cells. As discussed in the text, this expression pattern of *Tshz3* suggests that the medullary stromal cells may share a common origin with the ureteric mesenchymal cells.



**Figure 8.1**



The expression of *Tshz3* in the mesenchymal cells of the ureter and bladder raises the possibility that these *Tshz3*-positive cells may represent mesenchymal cells that derive from the tailbud, because Brenner-Anantharan et al. (2007) recently showed that the origin of the mesenchymal cells surrounding (and contributing to) the developing ureter and cloaca (which gives rise to the bladder and urethra) was the tailbud mesenchyme. With this in mind it would be interesting to investigate the expression of *Tshz3* in the developing urethra and, earlier, in the cloaca.

A more extensive study of the expression of *Tshz3* in the developing urinary tract and the surrounding tissue (including the tailbud) should prove useful to help define the cell lineages that contribute to the mouse urinary tract. In particular the expression of *Tshz3* early in urinary tract development (prior to E12.5) needs to be characterised, and compared to the expression of other genes that have been postulated to mark populations of cells whose descendants will contribute to the urinary tract.

Additionally, it needs to be verified that *Tshz3* expression is a bona fide lineage marker. In the discussion above I have assumed that cells expressing *Tshz3* early in development proliferate to give rise to more *Tshz3* positive cells, which then take up certain positions within the urinary tract. An alternative possibility is that *Tshz3* expression is induced in different populations of cells throughout development due to their location. If this is the case, then *Tshz3* expression cannot be used to follow the location of the descendants of the early *Tshz3* expressing cells. Therefore, early in development *Tshz3* positive cells, and their descendants, should be irreversibly 'marked' and their fates followed. This marking could be achieved by crossing mice

transgenic for tamoxifen-inducible Cre-recombinase expressed under the control of the *Tshz3* promoter with 'reporter mice', which have a floxed transcriptional STOP cassette inserted into the Rosa26 locus which prevents lacZ expression (as has been used to mark embryonic hematopoietic stem cells (Gothert et al., 2005)). Upon exposure to tamoxifen, *Tshz3*-expressing cells would express Cre recombinase, the STOP cassette would be removed by homologous recombination, and *lacZ* expression would be permanently induced. The expression of *lacZ* could then be followed to discover the fate of the descendants of these early *Tshz3*-expressing cells. The expression of *Tshz3* could be compared to that of *lacZ* in order to ascertain whether *Tshz3* expression itself is in fact a true lineage marker.

### ***Teashirt 3* is required for ureter development, a site of mesenchymal-epithelial interactions**

As shown in Chapter Six and in Caubit et al. (submitted), *Teashirt 3* is required for the correct development of the ureter; specifically it is required for the development of ureteric smooth muscle and stromal (Raldh2 positive) cell layer (in *Tshz3*<sup>-/-</sup> embryos the smooth muscle layer of the proximal ureter does not differentiate and the number of Raldh2 positive cells in the ureter is reduced) (Figure 8.2).

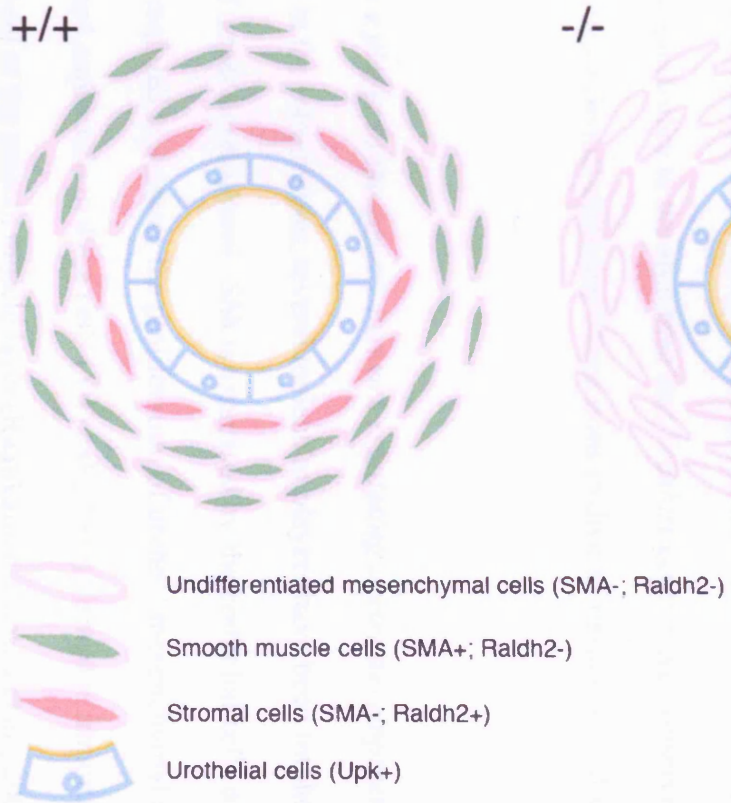
## Figure 8.2 Failed ureteric development in *Tshz3*<sup>-/-</sup> mouse

Diagram to summarise the failed differentiation of the ureter in *Tshz3*<sup>-/-</sup> null mutants: cross-sections through a *Tshz3*<sup>-/-</sup> (-/-) and wildtype (+/+) ureter are shown. Note the lack of  $\alpha$ SMA expressing smooth muscle cells and the reduction of *Raldh2* expressing stromal cells (which lie between urothelium and muscle) in the mutant ureter.

This figure was kindly provided by L. Fasano and appears in Caubit et al.

(submitted).

## Figure 8.2



Mesenchymal-epithelial interactions are important for the correct differentiation of the ureter, and *Teashirt* genes are known to be expressed in vertebrates during development at a number of sites at which mesenchymal-epithelial interactions occur such as the limb-buds, branchial arches, lung, middle ear and feather anlagen (Long et al., 2001a; Manfroid et al., 2006; Core et al., 2007), and indeed have been shown to be functionally important at some of these sites; for example, the limb-bud and middle ear ( Long et al., 2001a; Core et al., 2007) . Additionally, both members of the *teashirt* family in *Drosophila* are expressed in the Malpighian tubules during their development, and the development of the Malpighian tubules also requires mesenchymal-epithelial interactions (Denholm et al., 2003; Laugier et al., 2005). Therefore the observation that *Teashirt 3* is required for the correct differentiation of the ureter adds credibility to the argument that *Teashirt* genes have conserved roles in regulating mesenchymal-epithelial interactions in diverse tissues from diverse species.

### ***Teashirt 3 as a player in the genetic network regulating ureter development***

As discussed in the Introduction, several molecular players have been implicated in the control of ureter development. Shh is expressed by the epithelial cells of the ureter and is required to promote the proliferation of ureteral mesenchymal cells and to induce Bmp4 expression in these cells (Yu et al., 2002). Bmp4 is important for the development of the smooth muscle layer (Raatikainen-Ahokas et al., 2000; Miyazaki et al., 2003; Brenner-Anantharam et al., 2007), and also appears to act as a mesenchymal-to-epithelial signal to bring about the differentiation of the urothelium (Brenner-Anantharam et al., 2007). Additionally, Shh itself inhibits smooth muscle differentiation, and this is thought to be important to allow the formation of the

subepithelial ureteral mesenchymal or 'stromal' cell layer, which is missing in Shh conditional null mutant mice (Yu et al., 2002). Because Bmp4 play a role in ureteric smooth muscle development downstream of Shh signalling, and *Drosophila* Teashirt has been shown to physically interact with Ci (the transcription factor downstream of Hedgehog signalling (Angelats et al., 2002)), and *Tshz3*<sup>-/-</sup> ureters have defects in smooth muscle development (indeed it is virtually absent in the proximal part) (Chapter Six), I decided to investigate the expression of Bmp4 in *Tshz3*<sup>-/-</sup> ureters. I found no defect in Bmp4 expression by immunohistochemistry (Chapter Six), and this has subsequently been confirmed by *in-situ* hybridisation (Caubit et al., submitted). The fact that no defects in urothelial differentiation were observed in *Tshz3*<sup>-/-</sup> is consistent with this finding. Additionally *in-situ* hybridisation shows that *Shh* and *Patched1* expression are unaffected in *Tshz3*<sup>-/-</sup> ureters (Caubit et al., submitted). Together, these results show that in the absence of *Tshz3* the ureteral mesenchymal cells receive and respond to Shh signals, produce Bmp4, but fail to differentiate into smooth muscle, suggesting that *Tshz3* acts either downstream of these factors, or in a parallel pathway. A diagram to illustrate how *Tshz3* may act downstream of Shh and Bmp4 to promote ureteric smooth muscle differentiation can be seen in Figure 8.3.

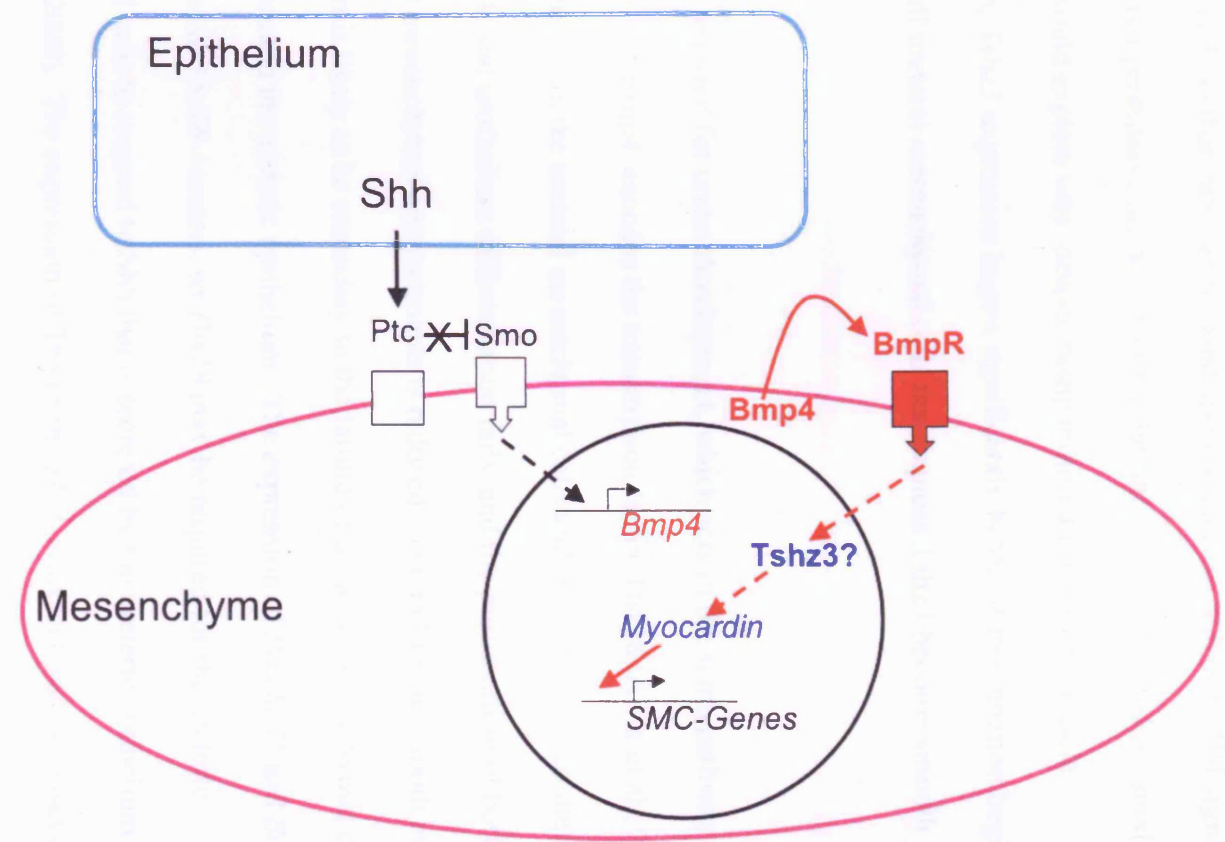
**Figure 8.3 *Tshz3* may act downstream of BMP4, and upstream of myocardin, to control smooth muscle differentiation in the ureter**

Observations made in this thesis, and in Caubit et al (submitted), are consistent with *Tshz3* acting (as a permissive factor) downstream of Bmp4 signalling (which is itself under the control of Shh signalling via Ptc) to promote the expression of myocardin, which acts to bring about smooth muscle differentiation through its control of transcription of smooth muscle cell (SMC) specific genes.

This figure was kindly provided by L. Fasano and appears in Caubit et al. (submitted).



**Figure 8.3**



There are two possible ways in which *Tshz3* may act downstream of the Shh/Patched1/Bmp4 pathway. Firstly, *Tshz3* expression may be induced by Shh or Bmp4. Secondly, *Tshz3* may act as a permissive factor, being required in ureteric mesenchymal cells so that they can respond appropriately to Shh or BMP4 signals. If *Tshz3* acts as a permissive factor (either for the Shh/Patched1/Bmp4, or another, pathway), it would explain why, despite being required for smooth muscle differentiation, *Tshz3* expression begins significantly before differentiation begins, and why not all ureteral mesenchymal cells that express *Tshz3* become smooth muscle.

Another gene required for ureter development, which acts in the same pathway as Shh, Patched1 and Bmp4, encodes the transcription factor *Tbx18* (Airik et al., 2006). *Tbx18* is expressed in the ureteral mesenchymal cells and in *Tbx18*<sup>-/-</sup> mice ureteric smooth muscle and urothelium differentiation fails, and the proliferation of both the epithelial and mesenchymal compartments is reduced. The failure of smooth muscle differentiation is likely to be secondary to the failure of ureteric mesenchymal cells to condense around the ureteric epithelium. The expression of *Patched1* and *Bmp4* is downregulated in *Tbx18*<sup>-/-</sup> ureters, so *Tbx18* may be required for the ureteric mesenchymal cells to respond to Shh that is secreted by the ureteric epithelium (Airik et al., 2006). The expression of *Tbx18* in *Tshz3*<sup>-/-</sup> ureters was not assessed, but as *Tbx18* acts upstream of Patched1 and Bmp4 to promote proliferation and condensation of mesenchymal cells (and the expression of Patched1 and Bmp4 are unaffected in *Tshz3*<sup>-/-</sup> ureters), I would hypothesise that its expression would be unaffected in *Tshz3*<sup>-/-</sup> ureters.

A strong argument exists for the possibility that *Tshz3* acts in a parallel pathway to Shh and Bmp4 (rather than downstream of them), because while Shh appears to be required for the proliferation of ureteric mesenchymal cells (Yu et al., 2002) and Bmp4 appears to promote smooth muscle development through its promotion of condensation of ureteric mesenchymal cells (Miyazaki et al., 2003), my data (Chapter Six) suggests that *Tshz3* is required for the process of differentiation itself (and the processes of proliferation, condensation and differentiation of smooth muscle precursor cells are likely to be regulated by independent regulatory pathways).

Indeed, although it is clear that Bmp4 is required for the correct development of the smooth muscle layer of the ureter, several observations point towards the fact that other regulators of ureteric smooth muscle development must exist. Firstly, in the Shh conditional knockout mouse, the development of smooth muscle is merely delayed, not blocked, despite the fact that Bmp4 expression is missing in the ureters of these mutants (Yu et al., 2002). Secondly Bmp4-soaked beads implanted into ureteric culture promote accumulation of ureteric mesenchymal cells around the beads, but do not induce expression of  $\alpha$ SMA (Miyazaki et al., 2003). Thirdly, although smooth muscle differentiation does not begin until around E15 (Yu et al., 2002), if Bmp4 function is genetically-deleted in mice after E12.5, no abnormalities in ureter development occur (Brenner-Anantharam et al., 2007). Finally I have shown in Chapter Six and Caubit et al. (submitted) that smooth muscle development can fail even in the presence of Bmp4.

Various other factors have been implicated in the control of ureteric development, and some of these may be regulators of smooth muscle development. In *Tbx18*<sup>-/-</sup> mice, sFRP2 (a modulator of Wnt signalling, expressed in the ureteral mesenchyme) is downregulated in the developing ureter, whereas the expression of Wnt7b (in the ureteric epithelium) is unaffected (Airik et al., 2006). The expression of Wnt7b and sFRP2 in wildtype ureters suggests that Wnt signalling may play a role in the control of ureter development. Additionally there is much evidence that *Teashirts* interact with the Wnt signalling pathway (for full details see Tables 1.1.1, 1.1.2 and 1.1.3 in Introduction), having been found to be both genetically upstream and downstream of Wnts in a variety of organisms, and having been shown to interact physically with  $\beta$  catenin (Armaddillo in *Drosophila*) and Tcf3, which are both downstream effectors of the Wnt signalling pathway. Thus, the regulation of ureteric smooth muscle development by Wnts and *Tshz3*, in collaboration with each other, is an intriguing possibility.

Raldh2 is also known to be expressed in the ureter, specifically in the 'stromal' cells that are located between the urothelium and the smooth muscle layer (Mahoney et al., 2006). As Raldh2 is required for the synthesis of retinoic acid from vitamin A, retinoic acid signalling may be involved in the control of ureteric development. In *Tshz3*<sup>-/-</sup> ureters Raldh2 expression is downregulated in the proximal part of the ureter (Caubit et al., submitted), so retinoic acid signalling would be deficient in this section of the ureter. Interestingly, *zTshz1* is induced by retinoic acid in the developing nervous system of zebrafish, (Wang et al., 2007), so *Teashirts* have been implicated as acting in pathways with retinoic acid previously. Also in Shh conditional knockout mice the stromal cells are reported to be missing (though

Raldh2 expression is not investigated (Yu et al., 2002)), therefore retinoic acid signalling may also be affected in the ureters of these mice and this may contribute to the phenotype. PI3 kinase signalling has also been shown to be required for ureteric smooth muscle development (Bush et al., 2006), highlighting another potential pathway that *Tshz3* may interact with.

Mice lacking either calcineurin (a  $\text{Ca}^{2+}$  dependent serine-threonine phosphatase) function or angiotensin signalling also have defects in ureteric smooth muscle, specifically a reduced proliferation rate of the smooth muscle cells (assessed postnatally) (Miyazaki et al., 1998; Chang et al., 2004). The mice lacking angiotensin signalling also have a thinner layer of smooth muscle in the proximal ureter at the neonatal stage, suggesting that the reduced proliferation of smooth muscle cells also occurs during prenatal development (Miyazaki et al., 1998). Although both of these phenotypes affect smooth muscle, the phenotypes are relatively mild suggesting that these pathways only play a minor role in the control of ureteric smooth muscle development. As the phenotype of *Tshz3*<sup>-/-</sup> mouse ureters is so much more severe it seems unlikely that *Tshz3* acts in the same pathway as either calcineurin or angiotensin.

ADAMTS-1 (an ADAM protease associated with the extracellular matrix) is also involved in ureter development. The phenotype of *ADAMTS-1* homozygous null mice is very specific; they have excess collagen fibres between the urothelial and smooth muscle layers of the ureter, but urothelial and smooth muscle differentiation do not appear to be affected (Shindo et al., 2000). Thus *ADAMTS-1* probably acts in an independent pathway to *Tshz3*.

*Dlgh1* (which encodes a PDZ domain protein) has a role in ureter development, being required for the differentiation of Raldh2 positive stromal cells and for the correct orientation of circular smooth muscle cells (Mahoney et al., 2006). The possibility that *Dlgh1* and *Tshz3* may act in the same pathways remains to be investigated.

Clearly it would be worthwhile to investigate the expression of these various genes that have been implicated in ureteric development in *Tshz3*<sup>-/-</sup> ureters, in particular those thought to be involved in smooth muscle development (such as PI3kinase), in order to further define the role of *Tshz3* in ureteric development, and to better understand the regulatory network (or networks) that act to bring about the correct development of the ureter. Micro-arrays could also be used to compare the expression of hundreds of genes in *Tshz3*<sup>-/-</sup> and wildtype ureter. This approach would have the advantage that it would most likely identify novel genes required for ureter development.

### ***Transcriptional pathways that may link Teashirt3 to smooth muscle differentiation***

Little is known about the transcriptional control of smooth muscle development in the ureter of the mouse. However, vascular smooth muscle differentiation requires serum response factor (SRF), which acts in concert with co-factors to activate the transcription of smooth muscle specific genes (such as  $\alpha$ SMA, SM22 $\alpha$  and SM-MHC) (Pipes et al., 2006). Bladder mesenchymal cells express SRF, so the differentiation of bladder smooth muscle might involve a similar gene expression programme as the differentiation of vascular smooth muscle (Li et al., 2006), and this

may also be the case for ureteric smooth muscle. Myocardin is an important co-factor for SRF, and it is involved in activating smooth muscle specific genes. Myocardin is upregulated during ureteral development, and the timing of this upregulation co-incides with smooth muscle differentiation (Mitchell et al., 2006). Myocardin expression is missing from *Tshz3*<sup>-/-</sup> ureters (at E16.5, when myocardin is expressed in wildtype ureteric cells that also expressed  $\alpha$ SMA), suggesting that *Tshz3* may regulate smooth muscle differentiation through the expression of myocardin (see Figure 8.2) (Caubit et al., submitted). Thus, *Tshz3* appears to play an important role in the transcriptional programme regulating ureteric smooth muscle differentiation.

***Teashirt3 may promote smooth muscle differentiation by regulating cell shape***

The ureteric mesenchymal cells in *Tshz3*<sup>-/-</sup> embryos appear to fail to adopt the characteristic shape and organisation that they do in wildtype (Chapter Six). Whilst this observation requires confirmation (for example by transmission electron microscopy), it raises the intriguing possibility that the failure of smooth muscle development in *Tshz3*<sup>-/-</sup> ureters arises from a failure of the precursor cells to adopt the correct conformation (as cell shape change has been shown to be vital for smooth muscle differentiation (Yang et al., 1999)). *Tshz3* may be required for ureteric mesenchymal cells to adopt a certain shape, in order that they differentiate to become smooth muscle. Such control over cell shape might be achieved by controlling how cells interact with other cells because re-arrangement of cell-cell contacts can modulate changes in cell shape (Jamora and Fuchs, 2002), and *Tsh* expression contributes to differences in cell adhesive properties in the developing leg of *Drosophila* (Erkner et al., 1999). Therefore *Tshz3* may control the shape of ureteric

mesenchymal cells by regulating their physical interactions with other cells, and this may be required for their subsequent differentiation into smooth muscle.

***Teashirt3 is required for normal ureteric peristalsis, in vitro***

The most striking phenotype observed in cultured *Tshz3*<sup>-/-</sup> ureters was the failure of their proximal sections to contract (Chapter Seven). This phenotype is presumably caused by a failure of smooth muscle function, although this requires further investigation as  $\alpha$ SMA expression was normal in the proximal section of cultured *Tshz3*<sup>-/-</sup> ureters. Other possible causes of the peristaltic failure of the proximal ureter are discussed in Chapter Seven. I noted that *Tshz3*<sup>-/-</sup> ureters peristalt more frequently than wildtype ureters and this phenotype also requires further characterisation. Movies could be analysed to determine whether this higher frequency is due to faster propagation of the peristaltic wave, or shorter periods of inactivity between peristaltic waves. The results of such analysis may provide clues as to what the defect at the cellular level is that causes the increased peristaltic frequency, and this could then be investigated.

***Teashirt3 is required for the elongation of the ureter, in vitro***

In Chapter Seven I showed that *Tshz3*<sup>-/-</sup> ureters do not elongate as much as wildtype ureters in culture. The cause of this defect is unknown, and the number of proliferative and apoptotic cells in cultured *Tshz3*<sup>-/-</sup> ureters should be quantified and compared to wildtype. If no differences in cell turnover can be found, then this would indicate that the defect in elongation was probably due to a failure of cells to adopt the appropriate positions in *Tshz3*<sup>-/-</sup> ureters. Such a possibility could be investigated by assessing cell shape and position through histological examination



and /or electron microscopy of cultured ureters. Additionally, whether similar defects occurs *in vivo* should be investigated; by measuring the lengths of *Tshz3*<sup>-/-</sup> ureters and comparing them to ureters from wildtype littermates.

### ***Teashirt3*<sup>-/-</sup> mice as a model of human pelviureteric junction obstruction**

Pelviureteric junction obstruction (PUJO) is a common cause of pathological hydronephrosis in neonatal humans, occurring in approximately 1 in 2000 children, and is diagnosed when there is hydronephrosis in the absence of any visible ureteral or bladder abnormality (Woodward and Frank, 2002). PUJO is often associated with renal parenchymal changes (Huang et al., 2006), and congenital PUJO may lead to decreased kidney function, eventually requiring surgical intervention (Decramer et al., 2006), and as such is a clinically important condition. As *Tshz3*<sup>-/-</sup> mice develop hydronephrosis *in-utero*, and only the proximal part of the ureter (at least part of which will form the pelviureteric junction postnatally) develops hydroureter, the phenotype of *Tshz3*<sup>-/-</sup> strongly resembles the human condition of congenital PUJO and therefore could provide a useful model in which to study the etiology of this condition. I have shown that in the case of *Tshz3*<sup>-/-</sup> mice the cause of the apparent ‘obstruction’ at the level of the pelviureteric junction (or proximal ureter) is a failure of peristaltic function. This, so called, ‘functional obstruction’ results in a failure of urine to move along the ureter to the bladder, thus it accumulates in the kidneys causing hydronephrosis (Mendelsohn, 2004). Other evidence also points to functional obstruction as a cause for PUJO. In mice lacking calcineurin function in the mesenchyme of the developing urinary tract a phenotype resembling PUJO develops due to defective pyeloureteral peristalsis resulting from abnormal postnatal development of the renal pelvis and ureter (Chang et al., 2004). Mice lacking

angiotensin type I receptor genes have a strikingly similar phenotype, with hypoplasia of the smooth muscle at the level of the pelviureteric junction, which lacks peristaltic movements (Miyazaki et al., 1998). *ADAMTS-1*<sup>-/-</sup> mice also have a phenotype resembling PUJO, which is likely to be caused by a thickened collagen layer at the pelviureteric junction restricting peristaltic movements (Shindo et al., 2000).

Additionally, studies on samples from human PUJO patients indicate abnormalities in the smooth muscle and innervation of the pelviureteric junctions, suggesting that functional obstruction may be the cause of (or at least contribute to) their hydronephrosis (Kajbafzadeh et al., 2006). In conclusion, the analysis of the phenotype of *Tshz3*<sup>-/-</sup> mice, and other mouse models of hydronephrosis, point to functional obstruction as a major cause of PUJO, even if some cases of PUJO are associated with physical stenosis (Pates and Dashe, 2006). Further studies on these mouse models of PUJO may define molecular pathways that lead to PUJO when they go awry, which might lead to the development of new treatments for this condition in the future. Additionally, screening human PUJO patients for mutations in their *Tshz3* gene would be worthwhile.

### **Regionalisation of the ureter**

The restriction of the severe ureter phenotype to the proximal portion (lack of  $\alpha$ SMA *in vivo*, and lack of peristaltic contractions *in vitro*) in *Tshz3*<sup>-/-</sup> embryos is striking. From this we can conclude that the ureter is regionalised (despite there being no obvious specialisation along its length). *Teashirt* genes themselves have been implicated in specifying regional identity, for example in the trunk and the leg of

*Drosophila* (Fasano et al., 1991; Roder et al., 1992; de Zulueta et al., 1994; Erkner et al., 1999; Wu and Cohen, 2000). However *Tshz3* is expressed along the entire length of the developing mouse ureter (Chapter Five) and *Tshz1* and *Tshz2* also show no regionalisation of expression within the ureter (*Tshz1* expression not being observable in the ureter, and *Tshz2* being expressed in the ureter in the same pattern as *Tshz3*) (Caubit et al., submitted), and therefore the regional expression of *Tshz* genes cannot account for the regionalisation of the ureter. *Tshz3* must function differently at different locations along the ureter, its function being far more important in the proximal section. This finding is not entirely surprising, as the activity of *Teashirt* genes is known to be context dependent; for example, in the developing eye of *Drosophila* *tsh* expression promotes eye development dorsally and suppresses it ventrally (Singh et al., 2002). The regionalisation of *Teashirt* function must depend on differences of expression of other genes between different regions. The *Hox* genes would be strong candidates for genes whose expression may be localised to particular regions within the ureter to specify regional identity, as they are well known for their ability to confer positional identity on the cells in which they are expressed (Lewis, 1978). Furthermore, *Teashirt* genes interact with *Hox* genes, both genetically and physically (Andrew et al., 1994; Mathies et al., 1994; Rauskolb and Wieschaus, 1994; McCormick et al., 1995; Rusch and Kaufman, 2000; Waltzer et al., 2001; Saller et al., 2002; Singh et al., 2002; Taghli-Lamalle et al., 2007) and thus the expression of different *Hox* genes in different parts of the ureter could account for regional differences in *Tshz3* function. Recently the expression of all the *Hox* genes was mapped in the developing mouse kidney (Patterson and Potter, 2004), and the authors noted no segment-specific expression within the ureteric bud. However, it is unclear whether their analysis included the whole length of the distal,

non-branching section of the ureteric bud (i.e. the ureter), so it remains a possibility that differences in *Hox* gene expression along the ureter could account for its regionalisation. Microarray experiments to compare gene expression profiles between proximal and distal segments of developing mouse ureters might be useful in identifying the genes responsible for the regionalisation of the ureter.

### **Possible role for *Teashirt 3* in the development of the renal stroma**

I found (Chapter Five) that *Tshz3* is expressed in the medullary stromal cells of the kidney during development, and kidney stromal cells are known to be important for kidney development (Cullen-McEwen et al., 2005). However, I discovered no defect in kidney development when functional *Tshz3* protein was missing from the renal stroma; the only phenotype seen in *Tshz3*<sup>-/-</sup> embryos in the kidney was an apparently “missing” papilla, but this was found to be due to the pressure of accumulating urine in the renal pelvis compressing the papilla. The possibility remains that there is a subtle defect in kidney development (that would not be apparent from examination of whole and sectioned kidneys); for example the branching of the ureteric bud, or the number of nephrons that form may be affected (and indeed the renal stroma has been shown to modulate ureteric bud branching (Mendelsohn et al., 1999)).

These possibilities could be investigated by analysing branching patterns of the ureteric bud of *Tshz3*<sup>-/-</sup> kidneys in culture (in comparison to wildtype) and by counting glomerular numbers by stereological methods (see Bertram (2001) for a review of this technique). Additionally, testing whether the expression of other genes in the kidneys of *Tshz3*<sup>-/-</sup> mice was normal may help to uncover a role for

*Tshz3* in kidney development. Although I tested the expression of several different genes (either known to be important in kidney development, or acting as markers of differentiation of specific cell populations within the kidney) in *Tshz3*<sup>-/-</sup> embryonic kidneys and found them unchanged (compared with wildtype), this investigation was by no means exhaustive. The expression of many other genes could be investigated, and such an analysis might uncover subtle defects in the *Tshz3*<sup>-/-</sup> kidney. For example if the expression of genes known to be expressed in stromal cells, such as RAR $\alpha$ , RAR $\beta$ 2, Raldh2, sFRP1, Wnt4 and Bmp4 (Mendelsohn et al., 1999; Yoshino et al., 2001; Itaranta et al., 2006), was found to be affected, this would point to a cell autonomous role for *Tshz3* in the development of renal stromal cells. As so many genes have been implicated in the development of the kidney, microarray analysis to compare the expression of genes in *Tshz3*<sup>-/-</sup> kidneys with wildtype is an attractive way of identifying target genes in the kidney (in contrast to the more laborious, and less inclusive, candidate approach).

If, after exhaustive investigation, no abnormalities could be found in *Tshz3*<sup>-/-</sup> kidneys, this would suggest either that *Tshz3* has no role in kidney development, or that *Tshz3* acts redundantly with other genes expressed in the renal stroma to regulate kidney development. A strong candidate for such a gene would be *Tshz2*, as it also is expressed in the renal stroma (Caubit et al., submitted). Such a possibility could be investigated by the generation of double mutant mice.

Additionally, in the future (because *Tshz3* is not expressed by cortical stromal cells) a comparison of the function of *Tshz3* in the kidney, with the function (in the kidney) of other genes expressed in renal stromal cells, may help to elucidate whether

cortical and medullary stromal cells have distinct roles in kidney development (as I suggested in the introduction of this thesis).

### **Possible role for *Teashirt 3* in the development of the bladder**

*Tshz3* is also expressed in the mesenchymal cells of the developing bladder; at E15 the expression is most prominent in the cells of the lamina propria, whereas at later stages the expression levels appear higher in the smooth muscle cells (see Chapter Five). Therefore *Tshz3* expression may be required for the development of the lamina propria and/or the smooth muscle of the bladder. Mesenchymal-epithelial interactions are known to be important for the development of the bladder (Baskin et al., 1997; Tash et al., 2001; Haraguchi et al., 2007; Shiroyanagi et al., 2007), and therefore the development of the urothelium may also depend on *Tshz3*. However, I observed no gross structural abnormalities in the bladders of *Tshz3*<sup>-/-</sup> embryos (as assessed by gross morphology and histology) and  $\alpha$ SMA expression was normal in the smooth muscle layers of *Tshz3*<sup>-/-</sup> bladders. Nevertheless, a function for *Tshz3* in bladder development cannot be excluded until further experiments have been undertaken. To confirm that *Tshz3* is not required for smooth muscle development, the expression of other markers of smooth muscle differentiation (such as SM-MHC) should be investigated. Additionally the expression of differentiation markers of the lamina propria and urothelial layers should be assessed in order to identify whether defects in development of these cell types occur. Finally the physiological development of the embryonic bladders could be assessed by utilising methods developed on sheep fetal bladders (Thiruchelvam et al., 2003). Relatively little is known about the molecular players involved in the development of the bladder, and therefore a microarray experiment to compare gene expression in embryonic *Tshz3*<sup>-/-</sup>

bladders with wildtype embryonic bladders could prove highly informative, as the changes in expression of genes previously not known to be important in bladder development may be found, and this would open new avenues of exploration in the study of bladder development. Additionally, results from such an experiment would allow the investigator to ask whether any genes previously implicated in bladder development, such as *Shh* (Haraguchi et al., 2007; Shiroyanagi et al., 2007) and *Fgf7* (Tash et al., 2001), are downstream of *Tshz3*. As with the kidney, *Tshz3* may act redundantly with other genes in the bladder, in which case it may be necessary to generate and analyse doubly mutant mice.

#### **Possible role for *Teashirt3* in the adult kidney**

*Tshz3* is expressed in the adult kidney (Chapters Three and Five); in a subset of interstitial cells (located mainly in the medulla) and in cells within the glomerulus (Chapter Five) and also expressed in the adult ureter (Chapter Five). Possible roles for *Tshz3* in adult renal systems were discussed in Chapter Five, including the maintenance of smooth muscle phenotype in adult ureteric smooth muscle, the function of mesangial cells in the glomeruli of adult kidneys and the function of adult interstitial cells. These proposed functions have not been investigated because *Tshz3*<sup>-/-</sup> mice die as neonates, precluding phenotypic analysis of the adult kidney. This difficulty could be overcome through the use of the Cre-lox system to engineer conditional knockout mice (i.e. mice that lack *Tshz3* in specific cell types/lineages) or even an inducible conditional knockout mice (where the *Tshz3* gene could be lost from certain cell types at a time controlled by the investigator). For example, *Tshz3* could be deleted from smooth muscle after they had completed differentiation by inducing Cre-recombinase in adult smooth muscle cells (Bockamp et al., 2002).

In Chapter Five, I proposed that *Tshz3* might be a marker of adult renal stem cells, because *Tshz3* positive cells are found in the medullary interstitium of the adult kidney, a proposed niche for renal stem cells (Al-Awqati and Oliver, 2002). This could be investigated by seeing whether BrdU-retaining cells in the kidney express *Tshz3* and/or by inflicting injury (for example by folic acid treatment (Long et al., 2001b)) to a *Tshz3*<sup>+/-</sup> mouse and observing whether  $\beta$ -galactosidase positive (i.e. *Tshz3* expressing) cells contribute to regenerating structures (indicating that they are multipotent precursors). Additionally whether *Tshz3* function was required for the renal stem cells to contribute to regeneration after injury could be investigated by comparing the amount of regeneration that occurred after injury between *Tshz3*<sup>+/-</sup> and wildtype mice. If wildtype mice had a better ability to regenerate their kidneys than *Tshz3*<sup>+/-</sup> mice this would suggest that *Tshz3* was important for renal stem cell function.

### **A role for *Teashirt 1*, *Teashirt 2* and *Larp* (a putative transcriptional target of *Teashirts*) in urinary tract development?**

The overall aim of this thesis was to explore whether *Teashirt* genes are involved in the regulation of the development of the mouse urinary tract, in an attempt to gain insight into conserved roles for these in the development of the renal systems of highly divergent animals, and in epithelial-mesenchymal cell interactions during the development of organs. In the first part of my thesis my specific aim was to establish whether *Teashirt* genes were expressed in the developing urinary tract, and if they were, to characterise their expression patterns.



I showed (Chapter Three) that transcripts of *Tshz 1, 2* and *3*, and one of their putative transcriptional targets, *Larp*, were present in developing (from E11) and adult mouse kidneys. Indeed the expression of *Tshz2* and *3* is higher in embryonic than adult kidneys, suggesting a developmental role for these genes in the kidney. The expression of *Tshz3* has been discussed extensively elsewhere (because it was also investigated using a *lacZ/Tshz3* transgenic mouse). The lower expression of *Tshz3* in adult compared with embryonic kidneys (as determined by real time-PCR), is in agreement with the expression patterns of *Tshz3* observed by analysis of the *lacZ/Tshz3* transgenic mouse, since *Tshz3* was found to be expressed in the renal stroma of the embryonic kidney, and in the interstitial cells and mesangial cells of the adult kidney. The embryonic renal stroma makes a higher contribution to the total volume of the embryonic kidney than the interstitial plus mesangial cells make to the adult kidney: therefore the overall expression of *Tshz3* in the adult kidney is lower than that of the embryonic kidney.

In Chapter Four I attempted to investigate the expression of Tshz1, 2 and 3 proteins in the developing urinary tract by developing specific antibodies against them, to be used in western blotting and immunohistochemistry experiments. My attempts to identify Tshz1, 2 or 3 proteins in tissue from developing mouse urinary tracts were unsuccessful. However, I did show that both my anti-Tshz1 and anti-Tshz3 antibodies were specific against Myc-tagged Tshz1 and Tshz3 proteins respectively. Failure to detect endogenous Tshz1 and Tshz3 proteins in tissue from developing mouse urinary tracts is probably due to the antibodies not being sensitive enough to detect the proteins using the protocols followed. Hopefully this will be resolved in future through further optimisation of the western blotting and

immunohistochemistry protocols. My anti-Tshz2 antibody failed to show any specific reactivity, and so another will need to be generated in the future.

With the exception of *Tshz3* (discussed above), further work is required to establish any role for *Teashirt* genes in the development of the mouse urinary tract. Although I have demonstrated that *Tshz1* and *2*, and *Larp*, are expressed in the kidney during development, and have begun to characterise their temporal expression pattern, I have not characterised their spatial expression within the developing kidney. The development of the kidneys is a highly complex process, and therefore without data about which cells of the developing kidney express the *Tshz1* and *2*, and *Larp* genes it is difficult to speculate about their possible roles in this process. In the future the spatial expression patterns of *Tshz1* and *2*, and *Larp* could be investigated by immunohistochemistry (using antibodies generated by myself and characterised in Chapter Four of this thesis, as well as antibodies from other sources) and/or by *in-situ* hybridisation. Additionally, further expression analysis is required to investigate whether *Tshz1* and *2*, and *Larp* are expressed in other parts of the urinary tract such as the bladder and the ureters. This could be achieved by RT-PCR and Real Time PCR experiments, as well as by immunohistochemistry and *in-situ* hybridisation.

Detailed spatial expression patterns would allow hypothetical roles for these genes in urinary tract development to be formulated, which could be tested using knockout mice. I have performed such an analysis for the *Tshz3* knockout mouse (Chapters Five, Six and Seven). A *Tshz1* knockout mouse has been generated and no renal defects have been reported (Core et al., 2007), however specific analysis of the urinary tract of these mice may lead to the identification of previously unidentified

renal abnormalities. RNAi could also be used to investigate *Teashirt* function, by knocking down function of these genes in organ culture (this has been done before for *Wt1* (Davies et al., 2004)). As all three *Teashirts* are expressed in a renal cell line derived from uninduced metanephric mesenchymal cells, they may have a function in early kidney development (as shown in Chapter Three), for example in controlling the outgrowth of the ureteric bud, but without *in vivo* expression and functional studies such a role is merely speculative.

When studying the function of the *Teashirt* genes it will be important to keep in mind that they may act redundantly in some contexts. Mouse *Teashirt* genes are very similar to each other, and contain the same functional domains and they have been shown to act in essentially the same way as each other when mis-expressed in *Drosophila* embryos (Manfroid et al., 2004). This strongly suggests that they have the capacity to perform common functions. Indeed, the *Drosophila teashirt* genes, *tiptop* and *teashirt*, have partially redundant functions in the development of the *Drosophila* trunk (Laugier et al., 2005). Further, *teashirt* and *tiptop* can repress each other's expression (Laugier et al., 2005). This might also be the case for mouse *Teashirt* genes, which would mean that even if two *Teashirt* genes are not normally expressed in the same cells, they can still compensate for the loss of the other in the mutant (as their expression may be de-repressed in the mutant). Therefore in order to gain a complete understanding of *Teashirt* gene function in mice, double and triple mutant phenotypes will need to be analysed in addition to single mutants.

Once the roles of the *Teashirt* genes in urinary tract development have been established it will be interesting to determine the regulatory pathways in which they

act. As discussed in the introduction *Teashirt* genes have been shown to interact, either genetically or physically, with a number of different genes/proteins. Many of these have themselves been shown to be important in the development of the urinary tract in mice, raising the possibility that *Teashirt* genes act collaboratively with these genes to regulate the development of the urinary tract. For example in *Xenopus* *XTshz1* induces the expression of *Wnt4* (Koebernick et al., 2006) and *Wnt4* is known to be required for metanephric mesenchymal cells to undergo mesenchymal-to-epithelial transition (Stark et al., 1994). Indeed *Teashirt* genes have been shown to act both upstream and downstream of *Wnt* signalling (Gallet et al., 2000; Zirin and Mann, 2004), and have even been shown to interact physically with the downstream effector of *Wnt* signalling,  $\beta$  catenin (known as Armadillo in *Drosophila*) (Gallet et al., 1998; Gallet et al., 1999; Onai et al., 2007). *Drosophila* Tsh has also been shown to bind Ci, the transcription factor downstream of Hedgehog signalling (Angelats et al., 2002). This is interesting in view of the role of Shh signalling in ureter (Yu et al., 2002) and bladder (Haraguchi et al., 2007; Shiroyanagi et al., 2007) development. *tsh* has also been shown to interact with *eyes Absent (eya)* in *Drosophila* (Pan and Rubin, 1998; Bessa et al., 2002; Bessa and Casares, 2005) and *Eya1* is expressed in the metanephric mesenchyme in mouse, where it is involved in the control of *Gdnf* expression (Xu et al., 1999; Brodbeck and Englert, 2004; Sajithlal et al., 2005).

### **Role for Teashirts in the development of urinary tracts in general?**

In this thesis I have shown that all members of the *Teashirt* gene family are expressed in the developing urinary tract of mice, and that at least one of these *Teashirt* genes (*Teashirt3*) is critically required for the correct development of the

mouse urinary tract (specifically for the differentiation of ureteric smooth muscle). *teashirt* genes are also expressed in the renal tract of *Drosophila* during its development, and may play important developmental roles in that context (Denholm et al., 2003; Laugier et al., 2005). Thus *Teashirt* genes may have conserved roles in renal tract development in highly divergent species. In order to explore this possibility, the expression and function of *Teashirt* genes in the renal tracts of other model organisms (such as *Xenopus* and zebrafish) should be investigated.

## Chapter Nine – References

- AIRIK, R., BUSSEN, M., SINGH, M. K., PETRY, M. & KISPERS, A. (2006) Tbx18 regulates the development of the ureteral mesenchyme. *J. Clin. Invest.*, 116, 663-674.
- AIRIK, R. & KISPERS, A. (2007) Down the tube of obstructive nephropathies: The importance of tissue interactions during ureter development. *Kidney Int.*, 72, 1459-1467.
- AL-AWQATI, Q. & OLIVER, J. A. (2002) Stem cells in the kidney. *Kidney Int.*, 61, 387- 395.
- ALEXANDRE, E., GRABA, Y., FASANO, L., GALLET, A., PERRIN, L., DE ZULUETA, P., PRADEL, J., KERRIDGE, S. & JACQ, B. (1996) The *Drosophila* teashirt homeotic protein is a DNA-binding protein and modulator, a HOM-C regulated modifier of variegation, is a likely candidate for being a direct target gene. *Mech. Dev.*, 59, 191-204.
- ANDREW, D. J., HORNER, M. A., PETITT, M. G., SMOLIK, S. M. & SCOTT, M. P. (1994) Setting limits on homeotic gene function: restraint of Sex combs reduced activity by teashirt and other homeotic genes. *EMBO J.*, 13, 1132-1144.
- ANGELATS, C., GALLET, A., THEROND, P., FASANO, L. & KERRIDGE, S. (2002) Cubitus interruptus acts to specify naked cuticle in the trunk of *Drosophila* embryos. *Dev. Biol.*, 241, 132-44.
- AOKI, Y., MORI, S., KITAJIMA, K., YOKOYAMA, O., KANAMARU, H., OKADA, K. & YOKOTA, Y. (2004) Id2 haploinsufficiency in mice leads to congenital hydronephrosis resembling that in humans. *Genes Cells*, 9, 1287-1296.
- AZPIAZU, N. & MORATA, G. (2000) Function and regulation of homothorax in the wing imaginal disc of *Drosophila*. *Development*, 127, 2685-2693.
- BACHMANN, S., METZGER, R. & BUNNEMANN, B. (1990) Tamm-Horsfall protein-mRNA synthesis is localized to the thick ascending limb of Henle's loop in rat kidney. *Histochemistry*, 94, 517-523.
- BASCANDS, J. L., KLEIN, J. & SCHANSTRA, J. P. (2007) A nest in renal fibrosis? *Kidney Int.*, 72, 242-244.
- BASKIN, L. S., HAYWARD, S. W., SUTHERLAND, R. A., DISANDRO, M. S., THOMSON, A. A. & CUNHA, G. R. (1997) Cellular Signaling in the Bladder. *Front. Biosci.*, 2, 592-595.

- BASSON, M. A., AKBULUT, S., WATSON-JOHNSON, J., SIMON, R., CARROLL, T. J., SHAKYA, R., GROSS, I., MARTIN, G. R., LUFKIN, T., MCMAHON, A. P., WILSON, P. D., COSTANTINI, F., MASON, I. J. & LICHT, J. D. (2005) Sprouty1 is a critical regulator of GDNF/RET-mediated kidney induction. *Dev. Cell*, 8, 229-239.
- BATOURINA, E., TSAI, S., LAMBERT, S., SPRENKLE, P., VIANA, R., DUTTA, S., HENSLE, T., WANG, F., NIEDERREITHER, K., MCMAHON, A. P., CARROLL, T. J. & MENDELSON, C. L. (2005) Apoptosis induced by vitamin A signaling is crucial for connecting the ureters to the bladder. *Nat. Genet.*, 37, 1082-1089.
- BERTRAM, J. F. (2001) Counting in the kidney. *Kidney Int.*, 59, 792-796.
- BESSA, J. & CASARES, F. (2005) Restricted teashirt expression confers eye-specific responsiveness to Dpp and Wg signals during eye specification in *Drosophila*. *Development*, 132, 5011-5020.
- BESSA, J., GEBELEIN, B., PICHAUD, F., CASARES, F. & MANN, R. S. (2002) Combinatorial control of *Drosophila* eye development by Eyeless, Homothorax, and Teashirt. *Genes Dev.*, 16, 2415-2427.
- BLANK, R. S., SWARTZ, E. A., THOMPSON, M. M., OLSON, E. N. & OWENS, G. K. (1995) A retinoic acid-induced clonal cell line derived from multipotential P19 embryonal carcinoma cells expresses smooth muscle characteristics. *Circ. Res.*, 76, 742-749.
- BOCKAMP, E., MARINGER, M., SPANGENBERG, C., FEES, S., FRASER, S., ESHKIND, L., OESCH, F. & ZABEL, B. (2002) Of mice and models: improved animal models for biomedical research. *Physiol. Genomics*, 11, 115-132.
- BRENNER-ANANTHARAM, A., CEBRIAN, C., GUILLAUME, R., HURTADO, R., SUN, T.-T. & HERZLINGER, D. (2007) Tailbud-derived mesenchyme promotes urinary tract segmentation via Bmp4 signaling. *Development*, 134, 1967-1975.
- BRODBECK, S. & ENGLERT, C. (2004) Genetic determination of nephrogenesis: the Pax/Eya/Six gene network. *Pediatr. Nephrol.*, 19, 249-255.
- BROPHY, P. D., OSTROM, L., LANG, K. M. & DRESSLER, G. R. (2001) Regulation of ureteric bud outgrowth by Pax2-dependent activation of the glial derived neurotrophic factor gene. *Development*, 128, 4747-4756.
- BUSH, K. T., VAUGHN, D. A., LI, X., ROSENFELD, M. G., ROSE, D. W., MENDOZA, S. A. & NIGAM, S. K. (2006) Development and differentiation of the ureteric bud into the ureter in the absence of a kidney collecting system. *Dev. Biol.*, 298, 571-584.

- CASARES, F. & MANN, R.S. (2000) A dual role for homothorax in inhibiting wing blade development and specifying proximal wing identity in *Drosophila*. *Development*, 127, 1499-1508.
- CAUBIT, X., CORE, N., BONED, A., KERRIDGE, S., DJABALI, M. & FASANO, L. (2000) Vertebrate orthologues of the *Drosophila* region-specific patterning gene *teashirt*. *Mech. Dev.*, 91, 445-8.
- CAUBIT, X., GANNON, C.M., MARTIN, E., JENKINS, D., CORE, N., VOLA, C., LONG, D.A., SKAER, H.S., WOOLF, A.S. & FASANO, L. *Tshz3* deficiency causes functional renal tract obstruction by impeding ureteric smooth muscle differentiation. *Submitted and bound in appendix of this thesis*.
- CAUBIT, X., TIVERON, M. C., CREMER, H. & FASANO, L. (2005) Expression patterns of the three *Teashirt*-related genes define specific boundaries in the developing and postnatal mouse forebrain. *J. Comp. Neurol.*, 486, 76-88.
- CHANG, C.-P., MCDILL, B. W., NEILSON, J. R., JOIST, H. E., EPSTEIN, J. A., CRABTREE, G. R. & CHEN, F. (2004) Calcineurin is required in urinary tract mesenchyme for the development of the pyeloureteral peristaltic machinery. *J. Clin. Invest.*, 113, 1051-1058.
- CHAUVET, S., MAUREL-ZAFFRAN, C., MIASSOD, R., JULLIEN, N., PRADEL, J. & ARAGNOL, D. (2000) *dlarp*, a new candidate *Hox* target in *Drosophila* whose orthologue in mouse is expressed at sites of epithelium/mesenchymal interactions. *Dev. Dyn.*, 218, 401-413.
- COHEN, G. M. (1997) Caspases: the executioners of apoptosis. *Biochem. J.*, 326, 1-16.
- CORE, N., CAUBIT, X., METCHAT, A., BONED, A., DJABALI, M. & FASANO, L. (2007) *Tshz1* is required for axial skeleton, soft palate and middle ear development in mice. *Developmental Biology*, 308, 407-420.
- CORE, N., CHARROUX, B., MCCORMICK, A., VOLA, C., FASANO, L., SCOTT, M.P., KERRIDGE, S. (1997) Transcriptional regulation of the *Drosophila* homeotic gene *teashirt* by the homeodomain protein *Fushi tarazu*. *Mech. Dev.*, 68, 157-172.
- CULI, J., PILAR, A., MODOLELL, J., MANN, R.S. (2006) *jing* is required for wing development and to establish the proximo-distal axis of the leg in *Drosophila melanogaster*. *Genetics*, 173, 255-266.
- CULLEN-MCEWEN, L. A., CARUANA, G. & BERTRAM, J. F. (2005) The Where, What and Why of the Developing Renal Stroma. *Nephron Exp. Nephrol.*, 99, E1-E8.



- DAVID, S. G., CEBRIAN, C., VAUGHAN, J. E. D. & HERZLINGER, D. (2005) C-KIT AND URETERAL PERISTALSIS. *J. Urol.*, 173, 292-295.
- DAVIES, J. A., LADOMERY, M., HOHENSTEIN, P., MICHAEL, L., SHAFE, A., SPRAGGON, L. & HASTIE, N. (2004) Development of an siRNA-based method for repressing specific genes in renal organ culture and its use to show that the Wt1 tumour suppressor is required for nephron differentiation. *Hum. Mol. Genet.*, 13, 235-246.
- DE ZULUETA, P., ALEXANDRE, E., JACQ, B. & KERRIDGE, S. (1994) Homeotic complex and teashirt genes co-operate to establish trunk segmental identities in *Drosophila*. *Development*, 120, 2287-2296.
- DECRAMER, S., WITTKKE, S., MISCHAK, H., ZURBIG, P., WALDEN, M., BOUISSOU, F., BASCANDS, J.-L. & SCHANSTRA, J. P. (2006) Predicting the clinical outcome of congenital unilateral ureteropelvic junction obstruction in newborn by urinary proteome analysis. *Nat. Med.*, 12, 398-400.
- DENHOLM, B., SUDARSAN, V., PASALODOS-SANCHEZ, S., ARTERO, R., LAWRENCE, P., MADDRELL, S., BAYLIES, M. & SKAER, H. (2003) Dual origin of the renal tubules in *Drosophila*: mesodermal cells integrate and polarize to establish secretory function. *Curr. Biol.*, 13, 1052-1057.
- DESMOULIERE, A., GEINOZ, A., GABBIANI, F. & GABBIANI, G. (1993) Transforming growth factor- $\beta$ 1 induces  $\alpha$ -smooth muscle actin expression in granulation tissue myofibroblasts and in quiescent and growing cultured fibroblasts. *J. Cell Biol.*, 122, 103-111.
- EKBLOM, P., THESLEFF, I., SAXEN, L., MIETTINEN, A. & TIMPL, R. (1983) Transferrin as a fetal growth factor: acquisition of responsiveness related to embryonic induction. *Proc. Nat. Acad. Sci. U. S. A.*, 80, 2651-2655.
- ERKNER, A., GALLET, A., ANGELATS, C., FASANO, L. & KERRIDGE, S. (1999) The role of Teashirt in proximal leg development in *Drosophila*: ectopic Teashirt expression reveals different cell behaviours in ventral and dorsal domains. *Dev. Biol.*, 215, 221-32.
- ERKNER, A., ROURE, A., CHARROUX, B., DELAAGE, M., HOLWAY, N., CORE, N., VOLA, C., ANGELATS, C., PAGES, F., FASANO, L., KERRIDGE, S. (2002) Grunge, related to human Atrophin-like proteins, has multiple functions in *Drosophila* development. *Development*, 129, 1119-1129.
- FASANO, L., RODER, L., CORE, N., ALEXANDRE, E., VOLA, C., JACQ, B. & KERRIDGE, S. (1991) The gene teashirt is required for the development of *Drosophila* embryonic trunk segments and encodes a protein with widely spaced zinc finger motifs. *Cell*, 64, 63-79.

- GALLET, A., ANGELATS, C., ERKNER, A., CHARROUX, B., FASANO, L. & KERRIDGE, S. (1999) The C-terminal domain of armadillo binds to hypophosphorylated teashirt to modulate wingless signalling in *Drosophila*. *EMBO J.*, 18, 2208-17.
- GALLET, A., ANGELATS, C., KERRIDGE, S. & THEROND, P. P. (2000) Cubitus interruptus-independent transduction of the Hedgehog signal in *Drosophila*. *Development*, 127, 5509-5522.
- GALLET, A., ERKNER, A., CHARROUX, B., FASANO, L. & KERRIDGE, S. (1998) Trunk-specific modulation of wingless signalling in *Drosophila* by teashirt binding to armadillo. *Curr. Biol.*, 8, 893-902.
- GOTHERT, J. R., GUSTIN, S. E., HALL, M. A., GREEN, A. R., GOTTGENS, B., IZON, D. J. & BEGLEY, C. G. (2005) In vivo fate-tracing studies using the Scl stem cell enhancer: embryonic hematopoietic stem cells significantly contribute to adult hematopoiesis. *Blood*, 105, 2724-2732.
- GRAHAM, F. L., SMILEY, J., RUSSELL, W. C. & NAIRN, R. (1977) Characteristics of a human cell line transformed by DNA from human adenovirus type 5. *J. Gen. Virol.*, 36, 59-72.
- GRIESHAMMER, U., LE, M., PLUMP, A. S., WANG, F., TESSIER-LAVIGNE, M. & MARTIN, G. R. (2004) SLIT2-mediated ROBO2 signaling restricts kidney induction to a single site. *Dev. Cell*, 6, 709-717.
- GRUPP, C. & MÜLLER, G. A. (1999) Renal Fibroblast Culture. *Nephron Exp. Nephrol.*, 7, 377-385.
- HAN, S.W., RHA, K.H., LEE, H-Y. (2006) Ureteropelvic Junction Obstruction. In: Cilento, B.G., Windle, M.L., Koo, H.P., Rauch, D., Cromie, W.J. (eds) *Pediatrics Urology*, e-medicine website ([www.emedicine.com](http://www.emedicine.com)), WebMD.
- HARAGUCHI, R., MOTOYAMA, J., SASAKI, H., SATOH, Y., MIYAGAWA, S., NAKAGATA, N., MOON, A. & YAMADA, G. (2007) Molecular analysis of coordinated bladder and urogenital organ formation by Hedgehog signaling. *Development*, 134, 525-533.
- HAYASHI, K. I., SAGA, H., CHIMORI, Y., KIMURA, K., YAMANAKA, Y. & SOBUE, K. (1998) Differentiated phenotype of smooth muscle cells depends on signaling pathways through insulin-like growth factors and phosphatidylinositol 3-kinase. *J. Biol. Chem.*, 273, 28860-28867.
- HENDERSON, K. D., ISAAC, D. D. & ANDREW, D. J. (1999) Cell fate specification in the *Drosophila* salivary gland: the integration of homeotic gene function with the DPP signaling cascade. *Dev. Biol.*, 205, 10-21.
- HIRSCHI, K. K., ROHOVSKY, S. A. & D'AMORE, P. A. (1998) PDGF, TGF- $\beta$ , and heterotypic cell-cell interactions mediate endothelial cell-induced

- recruitment of 10T1/2 cells and their differentiation to a smooth muscle fate. *J. Cell Biol.*, 141, 805-814.
- HOFFER, F. A. & LEBOWITZ, R. L. (1985) Intermittent hydronephrosis: a unique feature of ureteropelvic junction obstruction caused by a crossing renal vessel. *Radiology*, 156, 655-658.
- HOLYCROSS, B. J., BLANK, R. S., THOMPSON, M. M., PEACH, M. J. & OWENS, G. K. (1992) Platelet-derived growth factor-BB-induced suppression of smooth muscle cell differentiation. *Circ. Res.*, 71, 1525-1532.
- HU, P., DENG, F.-M., LIANG, F.-X., HU, C.-M., AUERBACH, A. B., SHAPIRO, E., WU, X.-R., KACHAR, B. & SUN, T.-T. (2000) Ablation of uroplakin III gene results in small urothelial plaques, urothelial leakage, and vesicoureteral reflux. *J. Cell Biol.*, 151, 961-972.
- HUANG, W. Y., PETERS, C. A., ZURAKOWSKI, D., BORER, J. G., DIAMOND, D. A., BAUER, S. B., MCLELLAN, D. L. & ROSEN, S. (2006) Renal biopsy in congenital ureteropelvic junction obstruction: Evidence for parenchymal maldevelopment. *Kidney Int.*, 69, 137-143.
- ICHIKAWA, I., KUWAYAMA, F., POPE, J. C. I. V., STEPHENS, F. D. & MIYAZAKI, Y. (2002) Paradigm shift from classic anatomic theories to contemporary cell biological views of CAKUT. *Kidney Int.*, 61, 889-898.
- ICHIMURA, K., KURIHARA, H. & SAKAI, T. (2006) Involvement of mesangial cells expressing  $\alpha$ -smooth muscle actin during restorative glomerular remodeling in Thy-1.1 nephritis. *J. Histochem. Cytochem.*, 54, 1291-1301.
- IIZUKA-KOGO, A., ISHIDAO, T., AKIYAMA, T. & SENDA, T. (2007) Abnormal development of urogenital organs in Dlg1-deficient mice. *Development*, 134, 1799-1807.
- ITARANTA, P., CHI, L., SEPPANEN, T., NIKU, M., TUUKKANEN, J., PELTOKETO, H. & VAINIO, S. (2006) Wnt-4 signaling is involved in the control of smooth muscle cell fate via Bmp-4 in the medullary stroma of the developing kidney. *Dev. Biol.*, 293, 473-483.
- IWANO, M. & NEILSON, E. G. (2004) Mechanisms of tubulointerstitial fibrosis. *Curr. Opin. Nephrol. Hypertens.*, 13, 279-284.
- JAMORA, C. & FUCHS, E. (2002) Intercellular adhesion, signalling and the cytoskeleton. *Nat. Cell Biol.*, 4, E101-E108.
- JUNG, A.C., DENHOLM, B., SKAER, H. & AFFOLTER, M. (2005) Renal tubule development in *Drosophila*: a closer look at the cellular level. *J. Am. Soc. Nephrol.*, 16, 322-328.

- KAJBAFZADEH, A.-M., PAYABVASH, S., SALMASI, A. H.,  
MONAJEMZADEH, M. & TAVANGAR, S. M. (2006) Smooth muscle cell  
apoptosis and defective neural development in congenital ureteropelvic  
junction obstruction. *J. Urol.*, 176, 718-723.
- KOEBERNICK, K., KASHEF, J., PIELER, T. & WEDLICH, D. (2006) *Xenopus*  
Teashirt1 regulates posterior identity in brain and cranial neural crest. *Dev.*  
*Biol.*, 298, 312-326.
- KONG, X.-T., DENG, F.-M., HU, P., LIANG, F.-X., ZHOU, G., AUERBACH, A.  
B., GENIESER, N., NELSON, P. K., ROBBINS, E. S., SHAPIRO, E.,  
KACHAR, B. & SUN, T.-T. (2004) Roles of uroplakins in plaque formation,  
umbrella cell enlargement, and urinary tract diseases. *J. Cell Biol.*, 167, 1195-  
1204.
- KUME, T., DENG, K. & HOGAN, B. L. (2000) Murine forkhead/winged helix  
genes *Foxc1* (*Mf1*) and *Foxc2* (*Mfh1*) are required for the early  
organogenesis of the kidney and urinary tract. *Development*, 127, 1387-1395.
- LANDSCHULZ, W., THESLEFF, I. & EKBLUM, P. (1984) A lipophilic iron  
chelator can replace transferrin as a stimulator of cell proliferation and  
differentiation. *J. Cell Biol.*, 98, 596-601.
- LAUGIER, E., YANG, Z., FASANO, L., KERRIDGE, S. & VOLA, C. (2005) A  
critical role of teashirt for patterning the ventral epidermis is masked by  
ectopic expression of tiptop, a paralog of teashirt in *Drosophila*. *Dev. Biol.*,  
283, 446-58.
- LEMLEY, K. V. & KRIZ, W. (1991) Anatomy of the renal interstitium. *Kidney Int.*,  
39, 370-381.
- LEVINSON, R. S., BATOURINA, E., CHOI, C., VORONTCHIKHINA, M.,  
KITAJEWSKI, J. & MENDELSON, C. L. (2005) *Foxd1*-dependent signals  
control cellularity in the renal capsule, a structure required for normal renal  
development. *Development*, 132, 529-539.
- LEWIS, E. B. (1978) A gene complex controlling segmentation in *Drosophila*.  
*Nature*, 276, 565-570.
- LI, J., SHIROYANAGI, Y., LIN, G., HAQQ, C., LIN, C.-S., LUE, T. F.,  
WILLINGHAM, E. & BASKIN, L. S. (2006) Serum response factor, its  
cofactors, and epithelial-mesenchymal signaling in urinary bladder smooth  
muscle formation. *Differentiation*, 74, 30-39.
- LIANG, F. X., RIEDEL, I., DENG, F. M., ZHOU, G., XU, C., WU, X. R., KONG,  
X. P., MOLL, R. & SUN, T. T. (2001) Organization of uroplakin subunits:  
transmembrane topology, pair formation and plaque composition. *Biochem.*  
*J.*, 355, 13-18.

- LONG, Q., PARK, P. K. & EKKER, M. (2001a) Expression and regulation of mouse *Mtsh1* during limb and branchial arch development. *Dev. Dyn.*, 222, 308-312.
- LONG, D. A., WOOLF, A. S., SUDA, T. & YUAN, H. T. (2001b) Increased renal angiotensin-1 expression in folic acid-induced nephrotoxicity in mice. *J. Am. Soc. Nephrol.*, 12, 2721-31.
- LOUGHNA, S., HARDMAN, P., LANDELS, E., JUSSILA, L., ALITALO, K. & WOOLF, A. S. (1997) A molecular and genetic analysis of renal glomerular capillary development. *Angiogenesis*, 1, 84-101.
- LOUGHNA, S., YUAN, H. T. & WOOLF, A. S. (1998) Effects of oxygen on vascular patterning in Tie1/LacZ metanephric kidneys in vitro. *Biochem Biophys. Res. Commun.*, 247, 361-6.
- MACKIE, G. G. & STEPHENS, F. D. (1975) Duplex kidneys: a correlation of renal dysplasia with position of the ureteral orifice. *J. Urol.*, 114, 274-280.
- MAHONEY, Z. X., SAMMUT, B., XAVIER, R. J., CUNNINGHAM, J., GO, G., BRIM, K. L., STAPPENBECK, T. S., MINER, J. H. & SWAT, W. (2006) Discs-large homolog 1 regulates smooth muscle orientation in the mouse ureter. *Proc. Natl. Acad. Sci. U. S. A.*, 103, 19872-19877.
- MANFROID, I., CAUBIT, X., KERRIDGE, S. & FASANO, L. (2004) Three putative murine Teashirt orthologues specify trunk structures in *Drosophila* in the same way as the *Drosophila* teashirt gene. *Development*, 131, 1065-73.
- MANFROID, I., CAUBIT, X., MARCELLE, C. & FASANO, L. (2006) Teashirt 3 expression in the chick embryo reveals a remarkable association with tendon development. *Gene Expr. Patterns*, 6, 908-12.
- MARIC, C., RYAN, G. B. & ALCORN, D. (1997) Embryonic and postnatal development of the rat renal interstitium. *Anat. Embryol. (Berl)*. 195, 503-514.
- MARXER-MEIER, A., HEGYI, I., LOFFING, J. & KAISLING, B. (1998) Postnatal maturation of renal cortical peritubular fibroblast in the rat. *Anat. Embryol. (Berl)*. 197, 143-153.
- MATA, J., MARGUERAT, S. & BAHLER, J. (2005) Post-transcriptional control of gene expression: a genome-wide perspective. *Trends Biochem. Sci.*, 30, 506-514.
- MATHEWS, M. B., BERNSTEIN, R. M., FRANZA, B. R. J. & GARRELS, J. I. (1984) Identity of the proliferating cell nuclear antigen and cyclin. *Nature*, 309, 374-376.

- MATHIES, L. D., KERRIDGE, S. & SCOTT, M. P. (1994) Role of the teashirt gene in *Drosophila* midgut morphogenesis: secreted proteins mediate the action of homeotic genes. *Development*, 120, 2799-2809.
- MATSUI, K., BREITENEDER-GELEFF, S. & KERJASCHKI, D. (1998) Epitope-specific antibodies to the 43-kD glomerular membrane protein podoplanin cause proteinuria and rapid flattening of podocytes. *J. Am. Soc. Nephrol.*, 9, 2013-2026.
- MAXWELL, P.H., OSMOND, M.K., PUGH, C.W., HERYET, A., NICHOLLS, L.G., TAN, C.C., DOE, B.G., FERGUSON, D.J., JOHNSON, M.H. & RATCLIFFE, P.J. (1993) Identification of the renal erythropoietin-producing cells using transgenic mice. *Kidney Int.*, 44, 1149-1162.
- MCCORMICK, A., CORE, N., KERRIDGE, S. & SCOTT, M. P. (1995) Homeotic response elements are tightly linked to tissue-specific elements in a transcriptional enhancer of the teashirt gene. *Development*, 121, 2799-2812.
- MCHUGH, K., M. (1995) Molecular analysis of smooth muscle development in the mouse. *Dev. Dyn.*, 204, 278-290.
- MENDELSON, C. (2004) Functional obstruction: the renal pelvis rules. *J. Clin. Invest.*, 113, 957-959.
- MENDELSON, C. (2006) Going in circles: conserved mechanisms control radial patterning in the urinary and digestive tracts. *J. Clin. Invest.*, 116, 635-637.
- MENDELSON, C., BATOURINA, E., FUNG, S., GILBERT, T. & DODD, J. (1999) Stromal cells mediate retinoid-dependent functions essential for renal development. *Development*, 126, 1139-1148.
- MITCHELL, E. K. L., TAYLOR, D. F., WOODS, K., DAVIS, M. J., NELSON, A. L., TEASDALE, R. D., GRIMMOND, S. M., LITTLE, M. H., BERTRAM, J. F. & CARUANA, G. (2006) Differential gene expression in the developing mouse ureter. *Gene Expr. Patterns*, 6, 519-538.
- MIYAGAWA, Y., OKA, T., TAKANO, Y., TAKAHA, M., CHOI, S. & ISOBE, F. (2001) Renal artery aneurysm causing hydronephrosis. *Int. J. Urol.*, 8, 463-466.
- MIYAZAKI, Y., TSUCHIDA, S., NISHIMURA, H., POPE, J. C., IV, HARRIS, R. C., MCKANNA, J. M., INAGAMI, T., HOGAN, B. L. M., FOGO, A. & ICHIKAWA, I. (1998) Angiotensin induces the urinary peristaltic machinery during the perinatal period. *J. Clin. Invest.*, 102, 1489-1497.
- MIYAZAKI, Y., OSHIMA, K., FOGO, A., HOGAN, B. L. M. & ICHIKAWA, I. (2000) Bone morphogenetic protein 4 regulates the budding site and elongation of the mouse ureter. *J. Clin. Invest.*, 105, 863-873.

- MIYAZAKI, Y., OSHIMA, K., FOGO, A. & ICHIKAWA, I. (2003) Evidence that bone morphogenetic protein 4 has multiple biological functions during kidney and urinary tract development. *Kidney Int.*, 63, 835-844.
- MOORE, M. W., KLEIN, R. D., FARINAS, I., SAUER, H., ARMANINI, M., PHILLIPS, H., REICHARDT, L. F., RYAN, A. M., CARVER-MOORE, K. & ROSENTHAL, A. (1996) Renal and neuronal abnormalities in mice lacking GDNF. *Nature*, 382, 76-79.
- MORSTYN, G., HSU, S. M., KINSELLA, T., GRATZNER, H., RUSSO, A. & MITCHELL, J. B. (1983) Bromodeoxyuridine in tumors and chromosomes detected with a monoclonal antibody. *J. Clin. Invest.*, 72, 1844-1850.
- MUNDLOS, S., PELLETIER, J., DARVEAU, A., BACHMANN, M., WINTERPACHT, A. & ZABEL, B. (1993) Nuclear localization of the protein encoded by the Wilms' tumor gene WT1 in embryonic and adult tissues. *Development*, 119, 1329-1341.
- MURAWSKI, I. J. & GUPTA, I. R. (2006) Vesicoureteric reflux and renal malformations: a developmental problem. *Clin. Genet.*, 69, 105-117.
- MYAT, M. M., ISAAC, D. D. & ANDREW, D. J. (2000) Early genes required for salivary gland fate determination and morphogenesis in *Drosophila melanogaster*. *Adv. Dent. Res.*, 14, 89-98.
- NEMETH, L., MADDUR, S. & PURI, P. (2000) Immunolocalization of the gap junction protein connexin43 in the interstitial cells of Cajal in the normal and Hirschsprung's disease bowel. *J. Pediatr. Surg.*, 35, 823-828.
- NEUFELD, G., COHEN, T., GENGRINOVITCH, S. & POLTORAK, Z. (1999) Vascular endothelial growth factor (VEGF) and its receptors. *FASEB J.*, 13, 9-22.
- OLIVER, J. A., MAAROUF, O., CHEEMA, F. H., MARTENS, T. P. & AL-AWQATI, Q. (2004) The renal papilla is a niche for adult kidney stem cells. *J. Clin. Invest.*, 114, 795-804.
- ONAI, T., MATSUO-TAKASAKI, M., INOMATA, H., ARAMAKI, T., MATSUMARA, M., YAKURA, R., SASAI, N. & SASAI, Y. (2007) XTsh3 is an essential enhancing factor of canonical Wnt signaling in *Xenopus* axial determination. *EMBO J.*, 26, 2350-2360.
- ORLANDI, A., ROPRAZ, P. & GABBIANI, G. (1994) Proliferative activity and  $\alpha$ -smooth muscle actin expression in cultured rat aortic smooth muscle cells are differently modulated by transforming growth factor- $\beta$ 1 and heparin. *Exp. Cell Res.*, 214, 528-536.
- PAN, D. & RUBIN, G. M. (1998) Targeted expression of teashirt induces ectopic eyes in *Drosophila*. *Proc. Natl. Acad. Sci. U. S. A.*, 95, 15508-15512.

- PAPPIN, D. J. C., HOJRUP, P. & BLEASBY, A. J. (1993) Rapid identification of proteins by peptide-mass fingerprinting. *Curr. Biol.*, 3, 327-332.
- PATES, J. A. & DASHE, J. S. (2006) Prenatal diagnosis and management of hydronephrosis. *Early Hum. Dev.*, 82, 3-8.
- PATTERSON, L. T. & POTTER, S. S. (2004) Atlas of Hox gene expression in the developing kidney. *Dev. Dyn.*, 229, 771-779.
- PICHEL, J. G., SHEN, L., SHENG, H. Z., GRANHOLM, A.-C., DRAGO, J., GRINBERG, A., LEE, E. J., HUANG, S. P., SAARMA, M., HOFFER, B. J., SARIOLA, H. & WESTPHAL, H. (1996) Defects in enteric innervation and kidney development in mice lacking GDNF. *Nature*, 382, 73-76.
- PIPES, G. C. T., CREEMERS, E. E. & OLSON, E. N. (2006) The myocardin family of transcriptional coactivators: versatile regulators of cell growth, migration, and myogenesis. *Genes Dev.*, 20, 1545-1556.
- RAATIKAINEN-AHOKAS, A., HYTÖNEN, M., TENHUNEN, A., SAINIO, K. & SARIOLA, H. (2000) Bmp-4 affects the differentiation of metanephric mesenchyme and reveals an early anterior-posterior axis of the embryonic kidney. *Dev. Dyn.*, 217, 146-158.
- RAUCHMAN, M. I., NIGAM, S. K., DELPIRE, E. & GULLANS, S. R. (1993) An osmotically tolerant inner medullary collecting duct cell line from an SV40 transgenic mouse. *Am. J. Physiol. Renal Physiol.*, 265, F416-424.
- RAUSKOLB, C. & WIESCHAUS, E. (1994) Coordinate regulation of downstream genes by extradenticle and the homeotic selector proteins. *EMBO J.*, 13, 3561-3569.
- RELAN, N. K., YANG, Y., BEQAJ, S., MINER, J. H. & SCHUGER, L. (1999) Cell elongation induces laminin  $\alpha 2$  chain expression in mouse embryonic mesenchymal cells: role in visceral myogenesis. *J. Cell Biol.*, 147, 1341-1350.
- ROBERTSON, L. K., BOWLING, D. B., MAHAFFEY, J. P., IMIOLCZYK, B. & MAHAFFEY, J. W. (2004) An interactive network of zinc-finger proteins contributes to regionalization of the Drosophila embryo and establishes the domains of HOM-C protein function. *Development*, 131, 2781-2789.
- RODER, L., VOLA, C. & KERRIDGE, S. (1992) The role of the teashirt gene in trunk segmental identity in Drosophila. *Development*, 115, 1017-1033.
- ROGERS, S. A., RYAN, G. & HAMMERMAN, M. R. (1991) Insulin-like growth factors I and II are produced in the metanephros and are required for growth and development in vitro. *J. Cell Biol.*, 113, 1447-1453.



- ROJEK, A., FUCHTBAUER, E.-M., KWON, T.-H., FROKIAER, J. & NIELSEN, S. (2006) Severe urinary concentrating defect in renal collecting duct-selective AQP2 conditional-knockout mice. *Proc. Natl. Acad. Sci. U. S. A.*, 103, 6037-6042.
- ROMAN, J. & MCDONALD, J. A. (1992) Expression of fibronectin, the integrin alpha 5, and alpha-smooth muscle actin in heart and lung development. *Am. J. Respir. Cell Mol. Biol.*, 6, 472-480.
- ROMIH, R., KOROŠEC, P., DE MELLO, W. & JEZERNIK, K. (2005) Differentiation of epithelial cells in the urinary tract. *Cell Tissue Res.*, 320, 259-268.
- ROMIO, L., WRIGHT, V., PRICE, K., WINYARD, P. J., DONNAI, D., PORTEOUS, M. E., FRANCO, B., GIORGIO, G., MALCOLM, S., WOOLF, A. S. & FEATHER, S. A. (2003) OFD1, the gene mutated in oral-facial-digital syndrome type 1, is expressed in the metanephros and in human embryonic renal mesenchymal cells. *J. Am. Soc. Nephrol.*, 14, 680-9.
- ROOKS, V. J. & LEBOWITZ, R. L. (2001) Extrinsic ureteropelvic junction obstruction from a crossing renal vessel: demography and imaging. *Pediatr. Radiol.*, 31, 120-124.
- RUSCH, D. B. & KAUFMAN, T. C. (2000) Regulation of proboscipedia in *Drosophila* by homeotic selector genes. *Genetics*, 156, 183-194.
- SAINIO, K., SUVANTO, P., DAVIES, J., WARTIOVAARA, J., WARTIOVAARA, K., SAARMA, M., ARUMAE, U., MENG, X., LINDAHL, M., PACHNIS, V. & SARIOLA, H. (1997) Glial-cell-line-derived neurotrophic factor is required for bud initiation from ureteric epithelium. *Development*, 124, 4077-87.
- SAJITHLAL, G., ZOU, D., SILVIUS, D. & XU, P. X. (2005) *Eya1* acts as a critical regulator for specifying the metanephric mesenchyme. *Dev. Biol.*, 284, 323-336.
- SALLER, E., KELLEY, A. & BIENZ, M. (2002) The transcriptional repressor Brinker antagonizes Wingless signaling. *Genes Dev.*, 16, 1828-1838.
- SANCHEZ, M. P., SILOS-SANTIAGO, I., FRISEN, J., HE, B., LIRA, S. A. & BARBACID, M. (1996) Renal agenesis and the absence of enteric neurons in mice lacking GDNF. *Nature*, 382, 70-73.
- SCHMIDT-OTT, K. M., CHEN, X., PARAGAS, N., LEVINSON, R. S., MENDELSON, C. L. & BARASCH, J. (2006) *c-kit* delineates a distinct domain of progenitors in the developing kidney. *Dev. Biol.*, 299, 238-249.

- SCHUCHARDT, A., D'AGATI, V., PACHNIS, V. & COSTANTINI, F. (1996) Renal agenesis and hypodysplasia in ret-k- mutant mice result from defects in ureteric bud development. *Development*, 122, 1919-1929.
- SCHUGER, L., SKUBITZ, A. P. N., ZHANG, J., SOROKIN, L. & HE, L. (1997) Laminin alpha 1 chain synthesis in the mouse developing lung: requirement for epithelial-mesenchymal contact and possible role in bronchial smooth muscle development. *J. Cell Biol.*, 139, 553-562.
- SCHWARTZ, R. D., STEPHENS, F. D. & CUSSEN, L. J. (1981) The pathogenesis of renal dysplasia. II. The significance of lateral and medial ectopy of the ureteric orifice. *Invest. Urol.*, 19, 97-100.
- SCHWENTNER, C., OSWALD, J., LUNACEK, A., FRITSCH, H., DEIBL, M., BARTSCH, G. & RADMAYR, C. (2005) Loss of interstitial cells of cajal and gap junction protein connexin 43 at the vesicourethral junction in children with vesicourethral reflux. *J. Urol.*, 174, 1981-1986.
- SHARPE, J., AHLGREN, U., PERRY, P., HILL, B., ROSS, A., HECKSHER-SORENSEN, J., BALDOCK, R. & DAVIDSON, D. (2002) Optical projection tomography as a tool for 3D microscopy and gene expression studies. *Science*, 296, 541-545.
- SHINDO, T., KURIHARA, H., KUNO, K., YOKOYAMA, H., WADA, T., KURIHARA, Y., IMAI, T., WANG, Y., OGATA, M., NISHIMATSU, H., MORIYAMA, N., OH-HASHI, Y., MORITA, H., ISHIKAWA, T., NAGAI, R., YAZAKI, Y. & MATSUSHIMA, K. (2000) ADAMTS-1: a metalloproteinase-disintegrin essential for normal growth, fertility, and organ morphology and function. *J. Clin. Invest.*, 105, 1345-1352.
- SHIROYANAGI, Y., LIU, B., CAO, M., AGRAS, K., LI, J., HSIEH, M. H., WILLINGHAM, E. J. & BASKIN, L. S. (2007) Urothelial sonic hedgehog signaling plays an important role in bladder smooth muscle formation. *Differentiation*, (Epub ahead of print May 9).
- SIMFOROOSH, N., TABIBI, A., NOURALIZADEH, A., NOURI-MAHDAVI, K. & SHAYANINISAH, H. (2005) Laparoscopic management of ureteropelvic junction obstruction by division of anterior crossing vein and cephalad relocation of anterior crossing artery. *J. Endourol.*, 19, 827-830.
- SINGH, A., KANGO-SINGH, M. & SUN, Y. H. (2002) Eye suppression, a novel function of teashirt, requires Wingless signaling. *Development*, 129, 4271-4280.
- SOANES, K. H. & BELL, J. B. (2001) The drosophila aeroplane mutant is caused by an I-element insertion into a tissue-specific teashirt enhancer motif. *Genome*, 44, 919-928.

- SOANES, K. H., MACKAY, J. O., CORE, N., HESLIP, T., KERRIDGE, S. & BELL, J. B. (2001) Identification of a regulatory allele of teashirt (tsh) in *Drosophila melanogaster* that affects wing hinge development. An adult-specific tsh enhancer in *Drosophila*. *Mech. Dev.*, 105, 145-151.
- STAEHLING-HAMPTON, K. & HOFFMANN, F. M. (1994) Ectopic decapentaplegic in the *Drosophila* midgut alters the expression of five homeotic genes, dpp, and wingless, causing specific morphological defects. *Dev. Biol.*, 164, 502-512.
- STARK, K., VAINIO, S., VASSILEVA, G. & MCMAHON, A. P. (1994) Epithelial transformation of metanephric mesenchyme in the developing kidney regulated by Wnt-4. *Nature*, 372, 679-683.
- STRYER, L. (1995) Exploring Proteins. In: Stryer, L. *Biochemistry, Fourth Edition*, Chapter Three. W.H. Freeman and Company, New York, USA.
- SUI, G. P., ROTHERY, S., DUPONT, E., FRY, C. H. & SEVERS, N. J. (2002) Gap junctions and connexin expression in human suburothelial interstitial cells. *BJU Int.*, 90, 118-129.
- TAGHLI-LAMALLEM, O., GALLET, A., LEROY, F., MALAPERT, P., VOLA, C., KERRIDGE, S. & FASANO, L. (2007) Direct interaction between Teashirt and Sex combs reduced proteins, via Tsh's acidic domain, is essential for specifying the identity of the prothorax in *Drosophila*. *Dev. Biol.*, 307, 142-51.
- TASH, J. A., DAVID, S. G., VAUGHAN, J. E. D. & HERZLINGER, D. A. (2001) Fibroblast growth factor-7 regulates stratification of the bladder urothelium. *J. Urol.*, 166, 2536-2541.
- THELIER, K. (Ed.) (1989) *The House Mouse*, New York, Springer-Verlag.
- THESLEFF, I., PARTANEN, A. M., LANDSCHULZ, W., TROWBRIDGE, I. S. & EKBLUM, P. (1985) The role of transferrin receptors and iron delivery in mouse embryonic morphogenesis. *Differentiation*, 30, 152-158.
- THIRUCHELVAM, N., WU, C., DAVID, A., WOOLF, A.S., CUCHOW, P.M. & FRY, C.H. (2003) Neurotransmission and viscoelasticity in the ovine fetal bladder after in utero bladder outflow obstruction. *Am. J. Physiol. Regul. Integr. Comp. Physiol.*, 284, R1296-1305.
- TOOTLE, T. L. & REBAY, I. (2005) Post-translational modifications influence transcription factor activity: A view from the ETS superfamily. *Bioessays*, 27, 285-298.
- TORBAN, E., DZIARMAGA, A., IGLESIAS, D., CHU, L. L., VASSILIEVA, T., LITTLE, M., ECCLES, M., DISCENZA, M., PELLETIER, J. &

- GOODYER, P. (2006) PAX2 activates WNT4 expression during mammalian kidney development. *J. Biol. Chem.*, 281, 12705-12712.
- TREANOR, J. J. S., GOODMAN, L., DE SAUVAGE, F., STONE, D. M., POULSEN, K. T., BECK, C. D., GRAY, C., ARMANINI, M. P., POLLOCK, R. A., HEFTI, F., PHILLIPS, H. S., GODDARD, A., MOORE, M. W., BUJ-BELLO, A., DAVIES, A. M., ASAI, N., TAKAHASHI, M., VANDLEN, R., HENDERSON, C. E. & ROSENTHAL, A. (1996) Characterization of a multicomponent receptor for GDNF. *Nature*, 382, 80-83.
- VERANIC, P., ROMIH, R. & JEZERNIK, K. (2004) What determines differentiation of urothelial umbrella cells? *Eur. J. Cell Biol.*, 83, 27-34.
- VELARDO, J.T. (1981) Histology of the Ureter. In: Bergman, H. (ed) *The Ureter*, Second Edition, Chapter Two. Sringer-Verlag, New York, USA.
- WALTZER, L., VANDEL, L. & BIENZ, M. (2001) Teashirt is required for transcriptional repression mediated by high Wingless levels. *EMBO J.*, 20, 137-145.
- WANG, H., LEE, E. M.-J., SPERBER, S. M., LIN, S., EKKER, M. & LONG, Q. (2007) Isolation and expression of zebrafish zinc-finger transcription factor gene tsh1. *Gene Expr. Patterns*, 7, 318-322.
- WEISS, D. J., LIGGITT, D. & CLARK, J. G. (1997) In situ histochemical detection of beta-galactosidase activity in lung: assessment of X-gal reagent in distinguishing lacZ gene expression  $\beta$ -galactosidase activity. *Hum. Gene Ther.*, 8, 1545-1554.
- WOODWARD, M. & FRANK, D. (2002) Postnatal management of antenatal hydronephrosis. *BJU Int.*, 89, 149-156.
- WOOLF, A. S., KOLATSI-JOANNOU, M., HARDMAN, P., ANDERMARCHER, E., MOORBY, C., FINE, L. G., JAT, P. S., NOBLE, M. D. & GHERARDI, E. (1995) Roles of hepatocyte growth factor/scatter factor and the met receptor in the early development of the metanephros. *J. Cell Biol.*, 128, 171-184.
- WU, J. & COHEN, S. M. (2000) Proximal distal axis formation in the Drosophila leg: distinct functions of teashirt and homothorax in the proximal leg. *Mech. Dev.*, 94, 47-56.
- XU, P.-X., ADAMS, J., PETERS, H., BROWN, M. C., HEANEY, S. & MAAS, R. (1999) Eya1-deficient mice lack ears and kidneys and show abnormal apoptosis of organ primordia. *Nat. Genet.*, 23, 113-117.
- YANG, Y., RELAN, N. K., PRZYWARA, D. A. & SCHUGER, L. (1999) Embryonic mesenchymal cells share the potential for smooth muscle

differentiation: myogenesis is controlled by the cell's shape. *Development*, 126, 3027-3033.

YOSHINO, K., RUBIN, J. S., HIGINBOTHAM, K. G., UREN, A., ANEST, V., PLISOV, S. Y. & PERANTONI, A. O. (2001) Secreted Frizzled-related proteins can regulate metanephric development. *Mech. Dev.*, 102, 45-55.

YU, J., CARROLL, T. J. & MCMAHON, A. P. (2002) Sonic hedgehog regulates proliferation and differentiation of mesenchymal cells in the mouse metanephric kidney. *Development*, 129, 5301-5312.

ZIRIN, J. D. & MANN, R. S. (2004) Differing strategies for the establishment and maintenance of teashirt and homothorax repression in the *Drosophila* wing. *Development*, 131, 5683-5693.

## Appendix

Caubit, X., **Gannon, C.M.**, Martin, E., Jenkins, D, Core, N, Vola, C., Long, D.A.,  
Skaer, H.S., Woolf, A.S. and Fasano, L. *Submitted.*

"Tshz3 deficiency causes functional renal tract obstruction by impeding ureteric  
smooth muscle differentiation."

**Tshz3 deficiency causes functional renal tract obstruction by impeding ureteric smooth muscle differentiation.**

Xavier Caubit<sup>1\*</sup>, Claire M. Gannon<sup>2\*</sup>, Elise Martin<sup>1</sup>, Dagan Jenkins<sup>3</sup>, Nathalie Coré<sup>1</sup>, Christine Vola<sup>1</sup>, David A. Long<sup>2</sup>, Helen Skaer<sup>4</sup>, Adrian S. Woolf<sup>2+</sup> & Laurent Fasano<sup>1+</sup>.

(\*These two individuals contributed equally to the study; <sup>+</sup>Joint communicating authors)

<sup>1</sup>Institut de Biologie du Développement de Marseille-Luminy (IBDML), UMR6216, CNRS, Université de la Méditerranée, F-13288 Marseille cedex 09, France ; <sup>2</sup>Nephro-Urology Unit, UCL Institute of Child Health, 30 Guilford Street, London WC1N 1EH, United Kingdom ; <sup>3</sup>Weatherall Institute of Molecular Medicine, University of Oxford, John Radcliffe Hospital, Oxford OX3 9DS, United Kingdom ; <sup>4</sup>Department of Zoology, University of Cambridge, Downing Street, Cambridge CB2 3EJ, United Kingdom.

<sup>+</sup>Joint communicating authors: Laurent Fasano, Institut de Biologie du Développement de Marseille-Luminy (IBDML), UMR6216, CNRS, Université de la Méditerranée, F-13288 Marseille cedex 09, France Email [fasano@ibdml.univ-mrs.fr](mailto:fasano@ibdml.univ-mrs.fr) Tel 00 33 (0) 491 269 603 Fax 00 33 (0) 491 820 682 and Adrian S Woolf, Nephro-Urology Unit, UCL Institute of Child Health, 30 Guilford Street, London WC1N 1EH, United Kingdom. Email [a.woolf@ich.ucl.ac.uk](mailto:a.woolf@ich.ucl.ac.uk) Tel 00 44 (0)20 7905 2615 Fax 00 44 (0)20 7905 2133

**ABSTRACT**

*Teashirt (Tshz)* genes encode transcription factors conserved between flies and mammals. We show that mouse ureteric smooth muscle cell (SMC) precursors express *Tshz3*, and that *Tshz3* null mutant mice have congenital hydronephrosis without anatomically-impaired urine flow. *In vivo*, failed ureteric muscle differentiation antedated urinary tract dilatation while *ex vivo*, wild-type but not mutant fetal proximal ureter segments contracted spontaneously. Moreover, the expression of myocardin, an essential component of the regulatory pathway for SMC differentiation, and of myocardin-dependent SMC genes was markedly downregulated in *Tshz3*-null mouse ureters prior to the onset of hydronephrosis. The data are consistent with a model in which *Tshz3* expression is required for SMC differentiation by pathways involving myocardin-dependent SMC transcription. These findings provide new insights into molecular pathways linking visceral SMC differentiation with muscle function, and they also emphasise the central role of the proximal ureter in the physiological transit of fetal urine from the kidney to the urinary bladder, with defects leading to congenital hydronephrosis.



## INTRODUCTION

The metanephric precursor of the adult mammalian kidney develops through reciprocal inductive interactions between ureteric bud (UB) epithelium and metanephric mesenchyme (MM) (1). Between mouse embryonic day (E) 10 and 11, MM signals trigger UB outgrowth from the mesonephric duct and enhance UB elongation and entry into the MM. Thereafter, UB branching morphogenesis generates kidney collecting ducts and UB branched UB tip signals induce MM cells to aggregate and undergo mesenchymal-to-epithelial transition, forming nephrons.

The unbranched UB 'stalk' outside the MM elongates to form the ureter tube epithelium, the 'urothelium', and signaling between these and surrounding mesenchymal cells is required for further maturation (2, 3). UB stalk epithelia secrete Sonic hedgehog (Shh) which signals *via* Patched1 (Ptch1) to induce Bone morphogenetic protein 4 (Bmp4) in peri-urothelial mesenchymal cells (4). Bmp4 recruits these cells and enhances their differentiation into SMC (5-7). Inactivation of *Shh* in the urinary tract causes delays in ureteric SMC maturation (4). A hallmark of smooth muscle cells (SMC) differentiation is elevated expression of SMC-selective differentiation marker genes, including *smooth muscle  $\alpha$ -actin* (*SM $\alpha$ -A*), *SM myosin heavy chain* (*SMMHC*), and *SM22* (8). Stromal cells between urothelial and SMC layers express retinaldehyde dehydrogenase 2 (*Raldh2*) (9) and this layer may be the precursor of the lamina propria which confers elastic properties. UB stalk epithelia mature into urothelia, and express uroplakin (UP)-rich plaques on their apical surfaces (10) maintaining the 'water-tight' properties of this epithelium.

*Drosophila teashirt* (*tsh*) was discovered as a region-specific zinc finger-containing homeotic gene specifying embryonic trunk identity and was subsequently shown to have multiple roles in

fly development (11-14). Based on sequence homology, three *tsh*-like mouse genes (*Tshz1-3*) are known and their expression patterns in the nervous system, trunk, limbs and gut (15, 16) raise the possibility that they play developmental roles in mammals. Indeed, each substitutes for fly *tsh* in genetic rescue experiments (17) and *Tshz1* is functionally-implicated in mouse skeletal, ear and palate development (18).

In the current study, we demonstrate that *Tshz3* has a critical role in mammalian ureteric development. Specifically, our data show that ureteric mesenchymal cells express *Tshz3* transcripts and protein and our loss of function approach in mice shows that *Tshz3* expression is required for ureteric SMC differentiation. Furthermore, our data demonstrate that loss of function of *Tshz3* induces dilatation of the fetal renal pelvis and proximal ureter and that this phenotype correlates with, and is preceded by, the absence of expression of genes encoding contractile SMC markers. In vascular SMCs, expression of some of these same genes is regulated by a myocardin-dependent transcriptional program (19) and we here demonstrate that although myocardin is expressed in developing wild-type ureteric SMCs, it is downregulated in *Tshz3*-null mutant mouse ureters. These findings provide new insights into molecular pathways linking visceral SMC differentiation with muscle function, and they also emphasise the central role of the proximal ureter in the physiological transit of fetal urine from the kidney to the urinary bladder, with defects leading to congenital hydronephrosis.

## RESULTS

### ***Tshz3* targeted inactivation.**

The mouse *Tshz3* locus comprises two exons separated by a 70 kb-long intron, the first exon encoding only 13 amino acids. To inactivate *Tshz3*, we deleted most of exon 2 that encodes 1068 amino acids, including zinc-finger motifs predicted to be required for transcription factor function (**Figure 1, A-D**). The targeted allele contains only a short stretch of *Tshz3* coding sequence, fused to *LacZ*, and is devoid of *Tshz3* putative functional domains, apart from a nuclear localisation signal. Male chimeras were initially mated to C57BL/6J females. Surprisingly, no heterozygotes were recovered, although the recombined allele was confirmed in progeny by genotyping embryos, revealing the embryonic lethality of *Tshz3* haplo-insufficiency in this mixed background. Chimeras were mated to CD1 females and several chimeras achieved germline transmission. Crossing *Tshz3*<sup>+/-</sup> parents failed to produce viable null mutant offspring but genotyping E18.5 litters showed a normal Mendelian ratio of genotypes. *Tshz3*<sup>-/-</sup> pups were born but were unable to gasp, becoming cyanotic and dying within an hour. There were no external anatomical differences between wild-type and *Tshz3*<sup>-/-</sup> littermates. Analyses of X-Gal staining allowed us to conclude that patterns of  $\beta$ -galactosidase activity in *Tshz3*<sup>+/-</sup> embryos reliably reported endogenous *Tshz3* expression as assessed by *in situ* hybridisation (ISH; **Figure 1, E** and data not shown). Immunohistochemistry (IHC) failed to detect *Tshz3* protein in *Tshz3*<sup>-/-</sup> embryos (data not shown), indicating the allele to be null.

### **Urinary tract malformations in *Tshz3*<sup>-/-</sup> embryos.**

*Tshz3*<sup>-/-</sup> urinary tracts were markedly hydronephrotic (**Figure 2, A-C**), a fully penetrant, bilateral phenotype evident from E16.5, affecting both sexes. Proximal ureters of *Tshz3*<sup>-/-</sup> embryos displayed distortions and severe dilatation (**Figure 2, C**). In heterozygous embryos, rare cases (4/63) of unilateral hydroureter occurred. On histology, gross hydronephroses were

confirmed in null mutants (**Figure 2, D and E**) and their dilated proximal ureters were thin-walled (**Figure 2, F-I**). No 'crossing blood vessels' were found at termini of dilated segments and *Tshz3*<sup>-/-</sup> vesico-ureteric junctions and bladders were anatomically normal (data not shown). We injected India ink into the E18.5 null mutant renal pelvis and, upon exerting gentle pressure, ink flowed down the ureter into the bladder, excluding the possibility of complete anatomical obstruction (**Figure 2, J, K, K'**). Each null mutant kidney had a 'flat' papilla which, upon draining pelvic urine at autopsy, recovered its normal pointed shape, suggesting that urine had been under increased hydrostatic pressure (**Supplementary Figure 1, F**). E18.5 null mutant kidneys were otherwise similar to wild-types, with several layers of glomeruli, uromodulin-expressing thick ascending limbs of loops of Henle, and aquaporin 2-expressing collecting ducts; condensing MM was observed in the nephrogenic cortex of wild-type and null mutant kidneys (**Supplementary Figure 1**). Wild-type, +/- and -/- metanephroi were similar in appearance at E12.5, with the UB initiated branching within the MM: mesonephric ducts were intact and ectopic ureteric buds were not observed in *Tshz3*<sup>-/-</sup> embryos (**Supplementary Figure 2, A-D**). As described (4), we found that wild-type ureteric SMC differentiation proceeded in a proximal to distal direction, starting at E15.5. At E15.5 no difference was observed in diameters of nascent renal pelvises or ureters between wild-type and *Tshz3*<sup>-/-</sup> embryos (**Figure 3, A-D**). On close inspection, however, a compact layer of mesenchymal cells was apparent around urothelia of the wild-type proximal ureter but these cells appeared less orderly in mutants (**Figure 3, B and D; Supplementary Figure 2, E and F**). At E16.5, wild-type proximal ureters had matured such that urothelia were surrounded by SM (**Figure 3, E and F**), whereas *Tshz3*<sup>-/-</sup> embryos showed marked pelvic and proximal ureteric dilatation and their muscular layers were not apparent (**Figure 3, G and H**). At E16.5, peri-urothelial cells just distal to dilated ureteric segments in *Tshz3*<sup>-/-</sup> embryos appeared less aggregated than in wild-types (**Supplementary Figure 2, G and H**). In null mutants, urinary tract dilatation became more marked at E17.5 and E18.5 and, although some irregularly-arranged cells were found around E18.5 proximal ureteric

urothelia, they did not form orderly muscle bundles (**Figure 3, I-P**). The first layer of mouse metanephric glomeruli acquires capillary loops, and would therefore start to filter blood, between E14.5-15.5. Hence, in normal development, initiation of urine production harmonises with proximal ureteric SMC formation whereas, in mutants, there appears to be a problem with SMC development and urine production would start just before the onset of hydronephrosis.

### **Tshz3 is expressed in ureteric mesenchymal cells.**

In wild-type embryos, we compared expression of *Tshz3* and *Pax2*, the latter of which is expressed in UB branches and MM (1): *Tshz3* was detected in undifferentiated mesenchymal cells around the UB stalk and there was no coexpression of *Tshz3* and *Pax2* (**Figure 4, A**). X-Gal staining of heterozygous E12.5 urinary tracts showed signal along and around the UB stalk (**Figure 4, B and C**) and, additionally, a few scattered *LacZ*-expressing cells were found in the metanephric stroma (**Figure 4, C**). At E15.5, *Tshz3* expression was maintained in peri-urothelial cells around the elongating ureter and adjacent to renal pelvic epithelia (**Figure 4, D**). *Tshz3* protein was detected in E15.5 mesenchymal cells starting to aggregate around urothelia and in loosely-organised cells with cell bodies arranged tangentially (**Figure 4, E**) and expression persisted in both layers at E16.5 (data not shown). We suggest that the inner layer comprises predominantly SMC precursors, whereas the outer ring represents adventitial fibroblast precursors. *Tshz3* IHC patterns in wild-type embryos were similar to *LacZ* expression patterns in +/- mice (Compare **Figure 4, D** and **Figure 4, F**). *Tshz3* was also expressed in bladder mesenchyme and around mesonephric ducts (data not shown). We compared *LacZ* expression in heterozygous mice with  $\alpha$  smooth muscle actin ( $\alpha$ SMA) protein, a marker of SMC differentiation (4, 20). Between E15.5 and E18.5, *LacZ* expression was detected not only in differentiating ureteric SMCs but also in cells directly peripheral to nascent muscle (**Figure 4, G and H**). At E18.5, we observed *Raldh2*/ $\beta$ -galactosidase double positive cells immediately adjacent to urothelia (**Figure 4, I**). Using ISH (**Supplementary Figure 3**), we confirmed the

overall patterns of *Tshz3* expression described above: we also found that *Tshz2* was expressed in ureteric mesenchyme but no significant ureteric ISH signal was obtained for *Tshz1*.

### **Tshz3 deficiency causes perturbed development of ureteric SMC.**

Given the null mutant hydronephrosis phenotype and the apparent problems in ureteric smooth muscle formation (as observed by histology), which were suggestive of “functional” obstruction, we examined SMC development in *Tshz3* null mutant kidneys using  $\alpha$ SMA IHC. In wild-type embryos,  $\alpha$ SMA was first detected at E14.5 in a subset of cells within aggregated mesenchyme of the proximal ureter and the nascent renal pelvis (not shown). In E15.5 wild-type ureters, most aggregated mesenchymal cells in these locations expressed both  $\alpha$ SMA and two other muscle differentiation proteins, smooth muscle myosin heavy chain (SM-MHC) and smooth muscle 22 $\alpha$  (SM22 $\alpha$ ). In *Tshz3*<sup>-/-</sup> mice, however, all three SMC markers were downregulated (**Figure 5, A-F**). ISH confirmed deficient  $\alpha$ SMA (**Figure 5, G and H**) and SM22 $\alpha$  (data not shown) expression in E15.5 mutant proximal ureters. Critically, at this time, urinary tract dilatation was not yet present, so observed downregulation of SMC marker expression in the mutant could not be the result of damage. The fact that early activation of SMC-specific genes failed in *Tshz3* null ureters was consistent with the hypothesis that Tshz3 is needed for early differentiation of the ureteral mesenchyme into SMC. In wild-types from E16.5 to E18.5,  $\alpha$ SMA immunostaining revealed that proximal ureteric SMC layers became more organised and thicker: in contrast, during the period when gross upper urinary tract dilatation was developing in *Tshz3*<sup>-/-</sup> mutants,  $\alpha$ SMA expression was restricted to a few disorganised peri-urothelial cells in the proximal-most ureter (**Figure 5, I-T**). At the distal terminus of the dilated segment, ureteric calibre became almost normal, coinciding with some  $\alpha$ SMA expression (**Figure 5, P**). Similar aberrant expression patterns were noted with SM-MHC and SM22 $\alpha$  IHC (data not shown). Notably, normal  $\alpha$ SMA expression was maintained in null mutant aorta, renal arteries and kidney stroma (**Figure 5, K,O,S** and data not shown). In addition, we examined *Tshz3*<sup>-/-</sup> distal ureters, which

were of normal (or minimally-dilated) diameter.  $\alpha$ SMA upregulated in wild-type distal ureters between E15.5 and E17.5, whereas  $\alpha$ SMA was undetectable in mutant ureters at E15.5 and barely detectable at E17.5. At this latter stage, peri-urothelial cells appeared less compact than those in wild-types (**Supplementary Figure 4**). Hence, *Tshz3* null ureters have aberrant SMC development, with the most profound deficiency where the ureter joins the renal pelvis.

#### **Cellular and molecular characterisation of *Tshz3*<sup>-/-</sup> ureters.**

Next, we determined whether the failure of SMC development might be caused by reduced proliferation and/or increased apoptosis of periureteric cells (**Supplementary Figure 5** and **Supplementary Table 1**). As assessed by IHC for proliferating cell nuclear antigen (PCNA), we noted a tendency for decreased proliferation in E15.5 *Tshz3* null mutant urothelia and aggregated ureteric mesenchyme. However, after statistical analyses, the percentage point prevalences of positive nuclei in urothelia, aggregated mesenchyme and looser mesenchyme outside this zone were not significantly different between wild-type and *Tshz3*<sup>-/-</sup> proximal ureters at either E15.5 (before hydronephrosis) or E16.5 (when hydronephrosis was present). Apoptosis, as assessed by terminal deoxynucleotidyl transferase-mediated dUTP nick end labeling was never detected in aggregated cells around the urothelium in either genotype, whereas there was a similar, low prevalence in urothelia and also mesenchymal cells outside the aggregated mesenchymal layer. Furthermore, plentiful periureteric cells expressed *LacZ* in null mutant urinary tracts (**Supplementary Figure 5, D**). Thus, *Tshz3* is not essential for SMC precursor proliferation or survival, and therefore must be required for differentiation of SMCs. Because of Shh's known role in ureteric SMC differentiation (4), we sought evidence for Shh signaling by ISH for *Shh*, *Ptch1* and *Bmp4*. *Shh* was expressed by E15.5 urothelia of both wild-type and *Tshz3* null mutants, and transcripts for *Ptch1* and *Bmp4* were expressed in peri-urothelial cells in both genotypes (**Figure 6, A-F**). Taken together these results suggest that in absence of *Tshz3*, the

ureteral mesenchymal cells are Shh responsive but nevertheless fail to differentiate into SMCs in the developing ureter.

Although little is known about the transcriptional mechanisms that link Shh signalling pathway to the program of visceral SMC gene expression, significant progress has, however, been made with respect to characterizing the promoter and regulatory regions of SMC-restricted genes. Several studies have shown that vascular SMC differentiation is controlled by a serum response factor (SRF) and myocardin-dependent transcriptional regulatory program (21). Interestingly, comparison of the expression profiles of ureters at E12.5 and E15.5 identifies *myocardin* as one of the upregulated genes in the developing ureter (22). To establish whether a myocardin-dependent transcriptional program might exist in ureteric SMC, we sought *myocardin* expression in developing ureters. We found that wild-type ureteric SMC precursors start to express *myocardin* at E15.5 (data not shown). We next sought to determine whether *myocardin* expression was altered in *Tshz3* mutant ureters. In E16.5 wild-type ureters, mesenchymal cells co-expressed myocardin and  $\alpha$ SMA. In *Tshz3*<sup>-/-</sup> mice, however, myocardin and  $\alpha$ SMA were downregulated (**Figure 6, G and H**). At E15.5 and E16.5, ISH confirmed deficient *myocardin* expression in mutant proximal ureters (data not shown). Between embryonic urothelial and SM layers there normally exists a mesenchymal population expressing Raldh2 (9) and we investigated whether *Tshz3* is involved in differentiation of these cells. At E18.5, the numbers of Raldh2 expressing cells adjacent to urothelia appeared either reduced (data not shown) or nearly absent in some *Tshz3* null mutants *versus* wild-types (**Figure 6, I and J**), suggesting that loss of *Tshz3* in the ureteral mesenchyme perturbs the differentiation of another mesenchymal cell lineage in the developing ureter. The ureter differentiates by the interaction of an epithelium and a mesenchyme and recent studies suggested a requirement for a signalling from the SMC layer to the ureteric epithelium (23). We thus investigated whether loss of *Tshz3* in the ureteral mesenchyme would compromise differentiation of the ureteric epithelium. Apical expression of



UPIb was detected in mutant and wild-type epithelia (**Figure 6, K and L**), indicating that, despite failed mesenchymal differentiation, urothelia matured normally.

**Lack of *Tshz3* perturbs peristalsis in forming ureters.**

The failure of ureteric SMC differentiation, and the lack of physical obstruction, suggested that urinary tract dilatation in mutants was due to functional obstruction caused by impaired peristalsis (2). When maintained in organ culture for up to six days, wild-type E15.5 ureters elongated and underwent spontaneous contractions several times/minute (**Figure 7 and Supplementary videos 1 and 2**). Contractions initiated approximately a fifth of the way down the ureter and were followed by distal propagation: the most proximal parts of the explants also contracted and, *in vivo*, this would probably ‘squeeze’ the renal papilla which protrudes into the pelvis and proximal ureter. Null mutant ureters explanted at E15.5 (when urinary tract dilatation is not yet present) also grew, initiated contractions at a similar proximal/distal level and propagated a pulse-wave distally. Significantly, however, null mutant proximal ureters completely failed to contract.

## DISCUSSION

### ***Tshz3* is expressed in ureteric mesenchymal precursors.**

*Tshz3* is expressed early in mouse metanephrogenesis in mesenchymal cells surrounding the UB stalk. Furthermore, *Tshz3* is expressed in these mesenchymal cells as they mature into SMCs, the peristaltic machinery of the ureter. Other *Tshz3* expressing cells, immediately adjacent to urothelium, co-express *Raldh2* rather than  $\alpha$ SMA, consistent with the idea that *Tshz3* is also expressed in stromal precursors which will form the ureteric elasticated lamina propria. Recent studies indicate that tailbud mesenchyme is required for formation of several structures in the murine urogenital system (5, 24). Fate-mapping experiments in developing birds indicate that the UB is surrounded by two distinct mesenchymal populations: the MM derived from the intermediate mesoderm and also tail bud-derived mesoderm which, in part, will differentiate into ureteric SMC (5). Our results suggest that this model may also hold true for mammals, with *Tshz3* positive cells marking precursors which give rise to ureteric SMC and also to ureteric stromal cells (Figure 8, A).

### ***Tshz3* is required for the differentiation of ureteric SM and its harmonised peristalsis.**

Our data has shown that *Tshz3* has critical roles in urinary tract development. Indeed, we showed that a lack of *Tshz3* was associated with bilateral hydronephroses, with an onset before birth. Urinary tract dilatation started at E16, soon after the first filtering glomeruli form (mouse E16 anatomically-equates to a late first trimester human fetus) but hydronephroses were not caused by anatomical obstruction of the urinary tract. Critically, we also demonstrated that, *in vivo*, failed ureteric muscle differentiation antedated urinary tract dilatation and, furthermore, our embryonic ureteric organ culture data support the contention that hydronephroses results from 'functional' urinary flow impairment caused by defective ureteric contractility.

**The role of *Tshz3* in SMC differentiation.**

Several genes are known to have roles in differentiation of ureteric SMC (e.g. *Shh* pathway) and urothelia (e.g. UPs). The current model (2, 3) is based on the analysis of *Shh*, *Bmp4* and *Tbx18* mutant mice and proposes that embryonic ureteric urothelia secrete *Shh* signals to surrounding mesenchymal precursors which respond by proliferating and upregulating secreted molecules like *Bmp4* (4) and transcription factors like *Tbx18* (23) which themselves may enhance SMC differentiation. Nevertheless, because ureteric SM formation is delayed (rather than absent) in mice with urinary tract deletion of *Shh* (4), SMC progenitor cells may also receive and/or produce other SM differentiation factors (e.g. Angiotensin/Calcineurin signaling) (25).

As reciprocal epithelial-mesenchymal interactions between prospective urothelia and SMCs are considered important for ureteric development, we also ascertained the phenotype of urothelia in *Tshz3* mutant ureters. As in wild-types, *Tshz3* mutant urothelia expressed *Shh* transcripts, and we also noted that adjacent mesenchymal cells upregulated *Bmp4* and *Ptch1*, ‘functional read outs’ of *Shh* bioactivity (4), in both wild-types and mutants. It was striking that SMCs were deficient in the *Tshz3*<sup>-/-</sup> proximal ureters despite expression of *Bmp4* in ureteric mesenchyme. Our observations indicated that a deficiency of *Tshz3* was not associated with lack of peri-urothelial mesenchymal cells themselves and suggested that *Tshz3*, as *Bmp4* (4), did not mediate the proliferative function of *Shh*. Collectively, the data suggests that, in the absence of functional *Tshz3*, SMC precursors have lost competence to respond to *Bmp4* (**Figure 8, A**).

Studies of (non-ureteric) mesenchymal cells suggest that signals modulate SMC gene expression by regulating the association of serum response factor (SRF) with cofactors (26). SRF activates a subset of SMC genes, including  $\alpha$ SMA, *SM22 $\alpha$*  and *SM-MHC*, by recruiting the transcriptional coactivator myocardin which itself acts in concert with other factors to activate the full repertoire of SMC-specific genes (26). Mitchell *et. al.* (22) reported *myocardin* upregulation during murine ureteric maturation and our data shows that, whereas myocardin is normally

detected in mouse ureteric SMC between E15.5-E16.5, it is barely detectable in littermate *Tshz3*<sup>-/-</sup> ureters. In normal ureters,  $\alpha$ SMA, SM22 $\alpha$  and SM-MHC are upregulated between E15-16 but this fails to take place in proximal ureters of *Tshz3* null mutants. Taken together our data suggest that Bmp4 might induce SMC differentiation through Tshz3, an essential factor for *myocardin* expression (**Figure 8, B**). Several potential possibilities might, however, explain Bmp4-mediated inducibility of SMC gene expression during ureter differentiation. Future experiments will help us to determine whether Shh/Bmp4 and Tshz3 work in parallel or converging pathways rather than be in a direct single pathway. During mouse embryogenesis, *myocardin* is expressed in SMC of the stomach, bladder, and intestine, where *Tshz3* expression also occurs ((27) and our unpublished data)). Hence, our conclusions about *Tshz3* in ureteric development may have relevance to understanding molecular pathways controlling differentiation of visceral smooth muscle in other organs.

Finally, our data may help in a better understanding of the relationship between the epithelium and the mesenchyme during ureter differentiation. To a large extent, the water-tight properties of the urothelium results from apical expression of UPs by specialised umbrella cells (10). We noted that flat, ‘umbrella-like’ cells adjacent to the urinary lumen were evident in E18.5 mutant ureters (**Supplementary Figure 2, H**) and urothelia in *Tshz3* mutant mice expressed UP1b. Furthermore, the lack of edema in mutant ureters, and the fact that injected India ink was retained in the urinary tract lumen were consistent with the contention that no major disruption of the urothelial barrier had occurred. Thus, our data suggest that the signal from the ureteral mesenchyme (23) require to fully differentiate the epithelium into an urothelium does not depend on differentiation of ureteral mesenchymal cells into either  $\alpha$ SMA-expressing SMCs or Raldh2-expressing stromal cells.

### **Conservation of *Teashirt* genes in fly and mammalian urinary tracts.**

Several genes are significantly enriched in *Drosophila* renal (Malpighian) tubules and some, which code for plasma and lysosomal membrane proteins, have human homologues which, when mutated, cause defective tubular physiological functions (28). These observations suggest a close conservation of renal function across several million years of divergent evolution. One such enriched gene is *tsh* (28), and within the Malpighian tubule, *tsh* is expressed in mesodermally-derived stellate cells (29), and *tiptop*, a *tsh* paralogue, is also expressed in the tubule (30). Our results provide a striking example of a gene which is conserved between flies and mammals, which is expressed in the developing renal systems of these highly-diverged species and which, when mutated, causes a major urinary tract malformation in mammals. Our previous work in *Drosophila* (12, 17, 31-34) showed that *tsh*, the fly homologue of *Tshz3*, is a key component of several gene networks (*Hox*, *wg/Wnt*, *hh/Shh* and *ey/Pax6/Pax2*) conserved in vertebrates and involved in urinary tract formation (1). In *Drosophila* and *Xenopus*, Teashirt proteins have been implicated in canonical Wnt signaling; like fly Tsh and Armadillo, *Xenopus* Tshz3 and  $\beta$ -catenin interact physically (34, 35). Interestingly, mouse ureter expression of *Wnt7b* and *Sfrp2*, respectively in epithelia and mesenchyme, suggests that the canonical Wnt pathway regulates ureteric mesenchymal proliferation and SM development (23), as shown for the lung (36). *Wnt* signaling is deregulated in a rat strain with congenital obstructive uropathy (37) and future *in vivo* and *in vitro* studies may allow us to determine whether *Tshz3* enhances Wnt signaling activity in a  $\beta$ -catenin-dependent manner in ureteric mesenchyme.

### **TSHZ3 and human renal tract malformations**

A dilated upper urinary tract, or hydronephrosis, occurs in 7% of human gestations (38). Some hydronephroses are transient normal variants explained by high flow rates of hypotonic fetal urine. When dilatation persists, a common diagnosis is 'pelviureteric junction obstruction' (PUJO), present in up to 0.5% of all gestations (38, 39). PUJO ureters are not anatomically

blocked but have aberrant SM arrangement where the proximal (top of the) ureter joins the renal pelvis (40, 41). Congenital PUJO requires careful clinical follow-up and surgical intervention may be indicated if kidney function is decreased (42). Despite the clinical impact of this common malformation, its pathogenesis is unknown. Ureteric peristalsis propels urine from the renal pelvis towards the urinary bladder, and a failure of this activity is envisaged to cause 'functional' flow impairment leading to urinary tract dilatation and kidney damage (2). Mouse models have guided candidate-gene screens for identification of mutations causing human congenital urinary tract malformations (10, 43). In *Tshz3* null mutant mice, SMC differentiation was particularly impaired in the renal pelvis and the proximal ureter, a common site for congenital defects in humans (1). To date, malformations of the human urinary system have not yet been associated with specific mutations of *TSHZ* genes but we suggest that they (especially *TSHZ2* and *TSHZ3*, because they are both expressed in fetal ureteric SMC) should be examined as candidates for congenital PUJO and related disorders, such as multicystic dysplastic kidney, an entity characterised by severely disorganised ureteric and renal pelvic morphogenesis (44). In this regard, we note that translocations and a chromosomal deletion disrupting the 19q12 region in which *TSHZ3* resides have also been reported in patients with multi-organ malformations, including congenital hydronephrosis and multicystic dysplastic kidney (45, 46), implicating the disruption of long-range elements regulating the expression of *TSHZ3* in generating this phenotype. In future, it may also be informative to seek mutations in duplicated conserved non-coding elements of *TSHZ3* because mutations in cis-regulatory elements have been shown to cause human disease (47) and the *Tshz* family is known to have a large number of such duplicated elements (48).

## METHODS

### Gene targeting of the *Tshz3* locus.

DNA fragments from the *Tshz3* locus were isolated from a 129/Ola mouse genomic library. To generate the targeting construct, we used a vector (pKO) containing a *neo*-resistance gene derived from the pMC1NeoPolyA vector (49) flanked in 5' with a multiple cloning site and separated in 3' from the HSV-*tk* cassette by *Sall* and *BamHI* site. A 0.53-kb short arm, comprising the start of exon 2, was generated by PCR and fused in frame with a *lacZ* coding sequence. The *lacZ* sequence followed by the SV40 polyadenylation signal was excised from pETL as a 4.25 kb *BamHI* fragment (50). The 0.53-kb-*lacZ* fragment was inserted 5' to the *neo* gene and a 5.8 kb fragment 3' of the *Tshz3* gene was inserted between the *neo* and HSV-*tk* genes of pKO. This targeting vector was designed to allow the deletion of most of exon 2 that contains the putative DNA binding zinc fingers. E14 (129/Ola) ES cells were electroporated by 20 µg of the recombinant plasmid. Transfected ES cells were incubated in presence of 300 µg/ml G418 for positive selection. Two days later, negative selection was applied using 2µM gancyclovir. Homologous recombinants were tested by hybridisation of *XbaI*-digested genomic DNA using a fragment generated by PCR as a 3' external probe. The neomycin sequence was used as a probe to check unique integration event. To control correct recombination 5' to the locus, PCR amplifications were performed with a forward primer upstream to the 5' homology region, (5'TTACAAATAAATGCGCCCGT 3') and a reverse primer in the *lacZ* coding sequence (5'CCTCTTCGCTATTACGCCAG 3').

### Generation of *Tshz3*-null mice.

All animals were treated according to protocols approved by the French Ethical Committee. Male chimeras were generated after injection of *Tshz3*<sup>+/-</sup> ES cells into C57BL/6J blastocysts and mated to C57BL/6J females, and the resulting offspring were assayed for germ line transmission

of the *Tshz3*<sup>LacZ</sup> allele by PCR. As no transmission of the *Tshz3*<sup>LacZ</sup> allele was detected after the analysis of 249 newborns, male chimeras were mated to CD1 females; seven chimeras gave rise to germ line transmission. F1 heterozygous offspring were intercrossed to obtain homozygous mice for *Tshz3* mutation. Alternatively, F1 heterozygous males were crossed to CD-1 females to generate *Tshz3* mutants on CD-1 genetic background. Mice were analysed after six generations on the CD-1 background. Genotyping was performed by PCR on genomic DNA. Two primers from the *neo* sequence allowed a 478-bp amplification from the recombinant allele (5'-GGA AGG GAC TGG CTG CTA TTG-3' and 5'-CGA TAC CGT AAA GCA CGA GG-3'), two primers from exon 2 allowed a 630-bp amplification from the wild type allele (5'-CGGAGCATCTGGACCGCTATT-3' and 5'-CTGATATACGTGGAAGGAGTC-3'). PCR conditions were as follows: 1 cycle at 94°C for 5mn, 30 cycles at 94°C for 45s, 60°C for 30s, 72°C for 45s. To visualise urinary tract lumens, India ink solution was injected into renal pelves of whole urogenital systems using a pulled-out Pasteur pipette. Gentle hydrostatic pressure was then applied to push the ink through the ureter to the bladder.

#### **General histology, X-Gal reaction and IHC.**

Mouse tissues were fixed in 4% paraformaldehyde, paraffin-embedded, and sectioned to 5 or 10  $\mu\text{m}$ . Sections were stained with heamatoxylin and eosin, toluidine blue or Masson's trichrome. The X-gal reaction was performed to detect  $\beta$ -galactosidase activity: tissues were fixed for 30 min at 4°C in PBS containing 1% formaldehyde, 2mM MgCl<sub>2</sub>, 5mM EGTA, and 0.02% NP-40, washed in PBS and incubated at 37°C in PBS containing 5mM K<sub>3</sub>Fe(CN)<sub>6</sub>, 5 mM K<sub>4</sub>Fe(CN)<sub>6</sub>, 2 mM MgCl<sub>2</sub>, 0.01% Na deoxycholate , 0.02% NP-40, and 1 mg/ml X-gal. Specimens were postfixed in 4% paraformaldehyde, and tissues were cryoprotected in sucrose, embedded and sectioned to 10  $\mu\text{m}$ . We used a guineapig anti-Tshz3 antibody generated against mouse amino acids 557-664 (a gift from A. Garratt, Max-Delbrück-Center for Molecular Medicine, Berlin). Other antibodies were: mouse anti- $\alpha$ SMA, conjugated to FITC or to horseradish peroxidase



(Sigma, clone 1A4; Dako); rabbit anti-aquaporin 2 (Chemicon); rabbit anti- $\beta$ -galactosidase (Cappel); rabbit anti-Pax2 (Zymed); mouse anti-PCNA (BD Pharmingen); rabbit anti-Raldh2 (a gift from P. McCaffery, University of Aberdeen, UK); goat anti-myocardin (sc-21559 from Santa-Cruz); rabbit anti-SM-MHC (anti-MHC204/200, described in Kelley *et al.* (51); a gift from M. Conti and R. Adelstein, Laboratory of Molecular Cardiology, Bethesda, USA); rabbit anti-SM22 $\alpha$  (a gift from M. Gimona, Austrian Academy of Sciences, Salzburg, Austria); sheep anti-uromodulin (Bioscience Resource Project, AMS Biotechnology Distribution); rabbit anti-UIPb (a gift from T. T. Sun, New York School of Medicine, USA). Immunostaining was performed either on 14  $\mu$ m cryosections of tissues fixed with 4% paraformaldehyde or on 5  $\mu$ m sections of paraffin-embedded tissues after quenching endogenous peroxidase and antigen retrieval followed by reaction with secondary antibodies followed by peroxidase-based or fluorescent-based detection methods, as appropriate for the individual primary antibodies (details available on request). Apoptotic cells were detected using the In Situ Death Detection kit, Fluorescein (Roche). For each sample, the number of apoptotic cells, and the total number of cells were counted for each of the following cell populations in the proximal ureter: urothelium, compacted mesenchyme and loose mesenchyme.

## ISH.

Mouse embryos were fixed overnight in 4% PFA, cryoprotected in 30% sucrose and embedded in OCT (Tissue-teck). ISH on 16  $\mu$ m-thick sections using digoxigenin-labeled probes were performed as described (52). Radioactive ISH were performed in paraffin wax-embedded tissue sections as described (53), with minor modifications by Caubit *et al.* (16). *Tshz1-3* riboprobes have been described (16). Other probes used were: *Bmp4* (a gift from B. Hogan, Duke University, Durham, USA); *Ptch1* (a gift from M Scott, Howard Hughes Medical Institute, Stanford University School of Medicine, Stanford, CA) ; *Shh* (a gift from D. Epstein, University of Pennsylvania School of Medicine, USA);  *$\alpha$ SMA* and *myocardin* (kindly provided

by E. Osion, University of Texas Southwestern Medical Center, Dallas, USA); and *SM22 $\alpha$*  (a gift from A. Kispert, Hannover Medical School, Hannover, Germany).

#### **Embryonic ureter culture and video microscopy.**

E15.5 ureters explanted onto platforms (Millipore; pore size 0.4  $\mu\text{m}$ ) and cultured in defined, serum-free media, as described for embryonic mouse urinary bladders (54). The timelapse imaging of ureters was done on the 5th day of culture on an inverted Axiovert 200M (Zeiss) equipped with a spinning-disc confocal head (Perkin Elmer) using a 5x, 0.16 NA (Carl Zeiss). Images were acquired every 0.5 second for 2 minutes by using a cooled, 14-bit CCD camera (CoolSnap HQ; Roper Scientific, Trenton, NJ) operated by Metamorph Image Software (Universal Imaging Corporation, West Chester, PA). Images were analyzed using Metamorph software.

**ACKNOWLEDGEMENTS**

The work was supported by the Biotechnology and Biological Sciences Research Council, the British Council, the Company of Biologists, Egidie Alliance Program and the Association Française contre les Myopathies (AFM) and Kids Kidney Research. We thank D. Rampling for performing Masson's trichrome staining, and B. Hogan, D. Epstein, M. Scott, A. Kispert, E. Olson, for ISH probes. We thank P. McCaffery, M. Gimona, M. Conti, B. Adelstein and T.T. Sun for antibodies and we are especially grateful to A. Garratt for providing us with the anti-mouse Tshz3 antibody before its publication. We thank J. Davies, V. Tasic, A. Dimovski and Z. Gucev for helpful discussions.

**AUTHOR CONTRIBUTIONS**

XC generated the mutant mouse and performed morphology and gene expression analyses; CMG performed morphology, histology, gene expression studies and the ureteric cultures; EM performed gene expression studies; NC generated mutant mice and performed histology and gene expression analyses; CV and DAL performed histology and gene expression analyses; DJ advised on human genetic perspectives; HS initiated the project, comparing fly and mammalian renal genes; ASW and LF directed the experiments, helped to interpret them and drafted the paper; and all individuals made input into, and approved, the submitted article.

**COMPETING INTERESTS STATEMENT**

The authors declare no competing financial interests.



## REFERENCES

1. Schedl, A. 2007. Renal abnormalities and their developmental origin. *Nat Rev Genet* 8:791-802.
2. Mendelsohn, C. 2004. Functional obstruction: the renal pelvis rules. *J Clin Invest* 113:957-959.
3. Mendelsohn, C. 2006. Going in circles: conserved mechanisms control radial patterning in the urinary and digestive tracts. *J Clin Invest* 116:635-637.
4. Yu, J., Carroll, T.J., and McMahon, A.P. 2002. Sonic hedgehog regulates proliferation and differentiation of mesenchymal cells in the mouse metanephric kidney. *Development* 129:5301-5312.
5. Brenner-Anantharam, A., Cebrian, C., Guillaume, R., Hurtado, R., Sun, T.T., and Herzlinger, D. 2007. Tailbud-derived mesenchyme promotes urinary tract segmentation via BMP4 signaling. *Development* 134:1967-1975.
6. Miyazaki, Y., Oshima, K., Fogo, A., and Ichikawa, I. 2003. Evidence that bone morphogenetic protein 4 has multiple biological functions during kidney and urinary tract development. *Kidney Int* 63:835-844.
7. Raatikainen-Ahokas, A., Hytonen, M., Tenhunen, A., Sainio, K., and Sariola, H. 2000. BMP-4 affects the differentiation of metanephric mesenchyme and reveals an early anterior-posterior axis of the embryonic kidney. *Dev Dyn* 217:146-158.
8. Owens, G.K. 1995. Regulation of differentiation of vascular smooth muscle cells. *Physiol Rev* 75:487-517.
9. Mahoney, Z.X., Sammut, B., Xavier, R.J., Cunningham, J., Go, G., Brim, K.L., Stappenbeck, T.S., Miner, J.H., and Swat, W. 2006. Discs-large homolog 1 regulates smooth muscle orientation in the mouse ureter. *Proc Natl Acad Sci U S A* 103:19872-19877.
10. Jenkins, D., and Woolf, A.S. 2007. Uroplakins: new molecular players in the biology of urinary tract malformations. *Kidney Int* 71:195-200.
11. Andrew, D.J., Horner, M.A., Petitt, M.G., Smolik, S.M., and Scott, M.P. 1994. Setting limits on homeotic gene function: restraint of Sex combs reduced activity by teashirt and other homeotic genes. *Embo J* 13:1132-1144.
12. Fasano, L., Roder, L., Core, N., Alexandre, E., Vola, C., Jacq, B., and Kerridge, S. 1991. The gene teashirt is required for the development of Drosophila embryonic trunk segments and encodes a protein with widely spaced zinc finger motifs. *Cell* 64:63-79.
13. Roder, L., Vola, C., and Kerridge, S. 1992. The role of the teashirt gene in trunk segmental identity in Drosophila. *Development* 115:1017-1033.

14. Taghli-Lamalle, O., Gallet, A., Leroy, F., Malapert, P., Vola, C., Kerridge, S., and Fasano, L. 2007. Direct interaction between Teashirt and Sex combs reduced proteins, via Tsh's acidic domain, is essential for specifying the identity of the prothorax in *Drosophila*. *Dev Biol* 307:142-151.
15. Caubit, X., Core, N., Boned, A., Kerridge, S., Djabali, M., and Fasano, L. 2000. Vertebrate orthologues of the *Drosophila* region-specific patterning gene teashirt. *Mech Dev* 91:445-448.
16. Caubit, X., Tiveron, M.C., Cremer, H., and Fasano, L. 2005. Expression patterns of the three Teashirt-related genes define specific boundaries in the developing and postnatal mouse forebrain. *J Comp Neurol* 486:76-88.
17. Manfroid, I., Caubit, X., Kerridge, S., and Fasano, L. 2004. Three putative murine Teashirt orthologues specify trunk structures in *Drosophila* in the same way as the *Drosophila* teashirt gene. *Development* 131:1065-1073.
18. Core, N., Caubit, X., Metchat, A., Boned, A., Djabali, M., and Fasano, L. 2007. Tshz1 is required for axial skeleton, soft palate and middle ear development in mice. *Dev Biol* 308:407-420.
19. Wang, D.Z., and Olson, E.N. 2004. Control of smooth muscle development by the myocardin family of transcriptional coactivators. *Curr Opin Genet Dev* 14:558-566.
20. McHugh, K.M. 1995. Molecular analysis of smooth muscle development in the mouse. *Dev Dyn* 204:278-290.
21. Miano, J.M. 2003. Serum response factor: toggling between disparate programs of gene expression. *J Mol Cell Cardiol* 35:577-593.
22. Mitchell, E.K., Taylor, D.F., Woods, K., Davis, M.J., Nelson, A.L., Teasdale, R.D., Grimmond, S.M., Little, M.H., Bertram, J.F., and Caruana, G. 2006. Differential gene expression in the developing mouse ureter. *Gene Expr Patterns* 6:519-538.
23. Airik, R., Bussen, M., Singh, M.K., Petry, M., and Kispert, A. 2006. Tbx18 regulates the development of the ureteral mesenchyme. *J Clin Invest* 116:663-674.
24. Haraguchi, R., Motoyama, J., Sasaki, H., Satoh, Y., Miyagawa, S., Nakagata, N., Moon, A., and Yamada, G. 2007. Molecular analysis of coordinated bladder and urogenital organ formation by Hedgehog signaling. *Development* 134:525-533.
25. Chang, C.P., McDill, B.W., Neilson, J.R., Joist, H.E., Epstein, J.A., Crabtree, G.R., and Chen, F. 2004. Calcineurin is required in urinary tract mesenchyme for the development of the pyeloureteral peristaltic machinery. *J Clin Invest* 113:1051-1058.
26. Pipes, G.C., Creemers, E.E., and Olson, E.N. 2006. The myocardin family of transcriptional coactivators: versatile regulators of cell growth, migration, and myogenesis. *Genes Dev* 20:1545-1556.

27. Wang, D., Chang, P.S., Wang, Z., Sutherland, L., Richardson, J.A., Small, E., Krieg, P.A., and Olson, E.N. 2001. Activation of cardiac gene expression by myocardin, a transcriptional cofactor for serum response factor. *Cell* 105:851-862.
28. Wang, J., Kean, L., Yang, J., Allan, A.K., Davies, S.A., Herzyk, P., and Dow, J.A. 2004. Function-informed transcriptome analysis of *Drosophila* renal tubule. *Genome Biol* 5:R69.
29. Denholm, B., Sudarsan, V., Pasalodos-Sanchez, S., Artero, R., Lawrence, P., Maddrell, S., Baylies, M., and Skaer, H. 2003. Dual origin of the renal tubules in *Drosophila*: mesodermal cells integrate and polarize to establish secretory function. *Curr Biol* 13:1052-1057.
30. Laugier, E., Yang, Z., Fasano, L., Kerridge, S., and Vola, C. 2005. A critical role of teashirt for patterning the ventral epidermis is masked by ectopic expression of tiptop, a paralog of teashirt in *Drosophila*. *Dev Biol* 283:446-458.
31. Angelats, C., Gallet, A., Therond, P., Fasano, L., and Kerridge, S. 2002. Cubitus interruptus acts to specify naked cuticle in the trunk of *Drosophila* embryos. *Dev Biol* 241:132-144.
32. Gallet, A., Angelats, C., Erkner, A., Charroux, B., Fasano, L., and Kerridge, S. 1999. The C-terminal domain of armadillo binds to hypophosphorylated teashirt to modulate wingless signalling in *Drosophila*. *Embo J* 18:2208-2217.
33. Gallet, A., Angelats, C., Kerridge, S., and Therond, P.P. 2000. Cubitus interruptus-independent transduction of the Hedgehog signal in *Drosophila*. *Development* 127:5509-5522.
34. Gallet, A., Erkner, A., Charroux, B., Fasano, L., and Kerridge, S. 1998. Trunk-specific modulation of wingless signalling in *Drosophila* by teashirt binding to armadillo. *Curr Biol* 8:893-902.
35. Onai, T., Matsuo-Takasaki, M., Inomata, H., Aramaki, T., Matsumura, M., Yakura, R., Sasai, N., and Sasai, Y. 2007. XTsh3 is an essential enhancing factor of canonical Wnt signaling in *Xenopus* axial determination. *Embo J* 26:2350-2360.
36. Shu, W., Jiang, Y.Q., Lu, M.M., and Morrisey, E.E. 2002. Wnt7b regulates mesenchymal proliferation and vascular development in the lung. *Development* 129:4831-4842.
37. Hermens, J., Thelen, P., Ringert, R., and Seseke, F. 2007. Alterations of selected genes of the Wnt signal chain in rat kidneys with spontaneous congenital obstructive uropathy. *J Pediatr Urol* 3:86-95.
38. Gunn, T.R., Mora, J.D., and Pease, P. 1995. Antenatal diagnosis of urinary tract abnormalities by ultrasonography after 28 weeks' gestation: incidence and outcome. *Am J Obstet Gynecol* 172:479-486.
39. Ismaili, K., Hall, M., Piepsz, A., Wissing, K.M., Collier, F., Schulman, C., and Avni, F.E. 2006. Primary vesicoureteral reflux

- detected in neonates with a history of fetal renal pelvis dilatation: a prospective clinical and imaging study. *J Pediatr* 148:222-227.
40. dell'Agnola, C.A., Carmassi, L.M., Merlo, D., and Tadini, B. 1990. Duration and severity of congenital hydronephrosis as a cause of smooth muscle deterioration in pyelo-ureteral junction obstruction. *Z Kinderchir* 45:286-290.
  41. Zhang, P.L., Peters, C.A., and Rosen, S. 2000. Ureteropelvic junction obstruction: morphological and clinical studies. *Pediatr Nephrol* 14:820-826.
  42. Decramer, S., Wittke, S., Mischak, H., Zurbig, P., Walden, M., Bouissou, F., Bascands, J.L., and Schanstra, J.P. 2006. Predicting the clinical outcome of congenital unilateral ureteropelvic junction obstruction in newborn by urinary proteome analysis. *Nat Med* 12:398-400.
  43. Lu, W., van Erde, A.M., Fan, X., Quintero-Rivera, F., Kulkarni, S., Ferguson, H., Kim, H.G., Fan, Y., Xi, Q., Li, Q.G., et al. 2007. Disruption of ROBO2 is associated with urinary tract anomalies and confers risk of vesicoureteral reflux. *Am J Hum Genet* 80:616-632.
  44. Woolf, A.S., Price, K.L., Scambler, P.J., and Winyard, P.J. 2004. Evolving concepts in human renal dysplasia. *J Am Soc Nephrol* 15:998-1007.
  45. Groenen, P.M., Garcia, E., Debeer, P., Devriendt, K., Fryns, J.P., and Van de Ven, W.J. 1996. Structure, sequence, and chromosome 19 localization of human USF2 and its rearrangement in a patient with multicystic renal dysplasia. *Genomics* 38:141-148.
  46. Kulharya, A.S., Michaelis, R.C., Norris, K.S., Taylor, H.A., and Garcia-Heras, J. 1998. Constitutional del(19)(q12q13.1) in a three-year-old girl with severe phenotypic abnormalities affecting multiple organ systems. *Am J Med Genet* 77:391-394.
  47. Kleinjan, D.A., and van Heyningen, V. 2005. Long-range control of gene expression: emerging mechanisms and disruption in disease. *Am J Hum Genet* 76:8-32.
  48. McEwen, G.K., Woolfe, A., Goode, D., Vavouri, T., Callaway, H., and Elgar, G. 2006. Ancient duplicated conserved noncoding elements in vertebrates: a genomic and functional analysis. *Genome Res* 16:451-465.
  49. Mansour, S.L., Thomas, K.R., and Capecchi, M.R. 1988. Disruption of the proto-oncogene int-2 in mouse embryo-derived stem cells: a general strategy for targeting mutations to non-selectable genes. *Nature* 336:348-352.
  50. Mombaerts, P., Wang, F., Dulac, C., Chao, S.K., Nemes, A., Mendelsohn, M., Edmondson, J., and Axel, R. 1996. Visualizing an olfactory sensory map. *Cell* 87:675-686.



51. Kelley, C.A., Kawamoto, S., Conti, M.A., and Adelstein, R.S. 1991. Phosphorylation of vertebrate smooth muscle and nonmuscle myosin heavy chains in vitro and in intact cells. *J Cell Sci Suppl* 14:49-54.
52. Tiveron, M.C., Hirsch, M.R., and Brunet, J.F. 1996. The expression pattern of the transcription factor Phox2 delineates synaptic pathways of the autonomic nervous system. *J Neurosci* 16:7649-7660.
53. Sassoon, D., and Rosenthal, N. 1993. Detection of messenger RNA by in situ hybridization. *Methods Enzymol* 225:384-404.
54. Burgu, B., McCarthy, L.S., Shah, V., Long, D.A., Wilcox, D.T., and Wolf, A.S. 2006. Vascular endothelial growth factor stimulates embryonic urinary bladder development in organ culture. *BJU Int* 98:217-225.

## FIGURE LEGENDS

### Figure 1. Targeted disruption of *Tshz3*.

(A) Gene targeting strategy to knock-in the *LacZ* gene into exon 2 (ex2; light dotted box) of mouse *Tshz3*. The *LacZ* coding sequence (hatched box) and the *neomycin* expression cassette (*pTK-neo*; black box) were inserted into exon 2, resulting in removal of most of exon 2 and creating an *XbaI* digest size difference between wild-type and targeted loci. Dark dotted box represents the *herpes simplex virus thymidine kinase* cassette (*HSV-tk*). The white box indicates the 3' external probe (3'probe) used for Southern blotting. Short arrows denote locations of primers used for PCR screening. Restriction sites are abbreviated as follows: B, *BamHI*; E, *EcoRI*; S, *Sall*; N, *NotI*; X, *XbaI*. (B) Southern analysis of DNA from representative wild-type (+/+) and targeted (+/-) ES cell clones. The wild-type allele yields a 9.3 kb band and the targeted allele a 6.1 kb band when genomic DNA is digested with *XbaI* and hybridized with the 3' probe. (C) Appropriate recombination 5' to the locus was confirmed by PCR amplification using a forward primer located upstream to the 5' homology region and a reverse primer located in the *LacZ* gene (short arrows in A). (D) PCR-based genotyping of wild-type (+/+), heterozygous (+/-) and homozygous null (-/-) embryos. (E) X-Gal staining of *Tshz3*<sup>+/-</sup> whole mount embryo at E12.5 (*LacZ*; right panel) compared to endogenous *Tshz3* transcripts assessed by ISH in a wild-type embryo (*Tshz3*; left panel). X-Gal staining reproduced the expression pattern of *Tshz3*, as illustrated in the telencephalon, external ear (arrowhead), vibrissae (double arrow) and hand plates (arrows).

### Figure 2. *Tshz3*<sup>-/-</sup> mice develop congenital hydronephrosis.

Note that for this and subsequent Figures, representative images are shown from at least five mice of each genotype analysed at each developmental stage. (A and B) Whole E18.5 urinary tracts showing paired kidneys and ureters, and urinary bladder. Versus wild-type littermates (A),

*Tshz3*<sup>-/-</sup> kidneys had bilateral hydronephroses (**B**). (**C**) Higher magnification view of hydronephrosis and proximal hydroureter shown in **B**. (**D-I**) Heamatoxylin and eosin-stained transverse sections through E17.5 embryos (**D** and **E**) and ureters (**F-I**). Urothelia and surrounding mesenchyme were multilayered in the wild-type embryo in proximal (**F**) and distal (**H**) ureter. In the *Tshz3*<sup>-/-</sup> ureter, both layers appeared abnormally thin in the proximal ureter (**G**) but they were grossly normal distally (**I**). (**J** and **K**) E16.5 autopsies in which India ink was injected into the right renal pelvis of a normal (**J**) and a null mutant (**K, K'**) mouse: in both, ink flowed into the bladder (arrowhead). (**K'**) Inset shows dilated proximal ureter filled with ink. bl, bladder; k, kidney; p, pelvis; u, ureter; ue, ureteric epithelium; um, ureteral mesenchyme; ut, uterus.

### Figure 3. Ontogeny of urinary tract dilatation.

Sections are stained with Masson's trichrome and haematoxylin which results in a red colour for muscles, blue for nuclei and a blue/green for collagens (epithelia also appear red). **A, B, E, F, I, J, M** and **N** are wild-type (+/+) urinary tracts and **C, D, G, H, K, L, O** and **P** are null mutant (-/-) littermates. (**A-D**) E15.5, with mesenchymal cells surrounding proximal ureter epithelia indicated by arrows in **B** and arrowheads **D**. (**E-H**) E16.5. (**I-L**) E17.5. (**M-P**) E18.5.

### Figure 4. Expression of *Tshz3* in the developing ureter and metanephros.

(**A-C**) E12.5 urinary tracts. (**A**) Wild-type with double IHC for the UB and MM marker Pax2 transcription factor (red nuclei) and for *Tshz3* (green nuclei): *Tshz3* was specifically-expressed by mesenchymal cells around the UB stalk. (**B** and **C**) Heterozygous *Tshz3* embryos stained with X-Gal. Note cells around the ureter expressed *LacZ* (blue in **B**) as did scattered cells in the metanephric medullary interstitium (arrow in **C**). (**D-G**) Sections of E15.5 urinary tracts with all nuclei stained with DAPI (blue). *Tshz3* IHC in wild-type embryos (green in **D** and **E**) and  $\beta$ -galactosidase IHC in heterozygous embryos (green in **F**) show positive periureteric and kidney

stromal cells. **(G)** Transverse section of a E15.5 *Tshz3* heterozygote ureter immunostained for  $\beta$ -galactosidase (red) and  $\alpha$ SMA (green). **(H and I)** E18.5 *Tshz3* heterozygote ureters. **(H)** IHC for  $\beta$ -galactosidase (red) and  $\alpha$ SMA (green) with DAPI nuclear stain (blue). Arrowheads indicate the outer layer of cells, which expressed  $\beta$ -galactosidase but not  $\alpha$ SMA. Inset shows  $\beta$ -galactosidase positive,  $\alpha$ SMA negative cells (arrow) **(I)** IHC for Raldh2 (brown) and with *LacZ* expression detected by the X-Gal reaction (blue): inset shows Raldh2/*LacZ* double positive cells. u, ureter; ub, ureteric bud branch.

**Figure 5. Ureteric SMC differentiation in wild-type and *Tshz3* null mutants.**

Wild-types (+/+; **A, C, E, G, I, J, M, N, Q and R**) and *Tshz3* null mutants (-/-; **B, D, F, H, K, L, O, P, S and T**). **(A-H)** Transverse sections of E15.5 proximal ureters; asterix indicates the lumen of the ureter. In **A-F**, all nuclei were stained blue with DAPI and immunohistochemistry (green positive signals) is shown for SM-MHC (**A and B**), SM22 $\alpha$  (**C and D**) and  $\alpha$ SMA (**E and F**). **(G and H)** ISH for  $\alpha$ SMA (positive purple signal): arrowheads point to the  $\alpha$ SMA positive signal in arteries near ureters. **(I-T)**. Brightfield images, with all nuclei counterstained with haematoxylin (blue) and positive signal for  $\alpha$ SMA IHC in brown. **(I-L)** E16.5 renal tracts. **(M-P)** E17.5 renal tracts. **(Q-T)** E18.5 renal tracts.

**Figure 6. Molecular characterisation of *Tshz3*<sup>-/-</sup> ureters.**

**(A-F)** ISH on transverse sections of E15.5 proximal ureters of wild-types (**A, C, E**) and *Tshz3* null mutants (**B, D, F**). Patterns of expression (black dots) were similar in both genotypes, with *Shh* expressed in urothelia (**A, B**) and *Ptch1* (**C, D**) and *Bmp4* (**E, F**) expressed in peri-urothelial cells. **(G and H)** E16.5 proximal ureter sections from wild-type (**G**) or null mutant (**H**) stained with anti- $\alpha$ SMA antibody (green positive signal), DAPI (all nuclei are blue) and anti-myocardin antibody (red positive signal). Inset in **(G)** shows positive cells which co-express myocardin and  $\alpha$ SMA. Inset in **(H)** shows that in the mutant ureter, rare  $\alpha$ SMA

positive cells are positive for myocardin. (**I** and **J**) E18.5 proximal ureter sections from wild-type (**I**) or null mutant (**J**) stained with anti- $\alpha$ SMA antibody (green positive signal), DAPI (all nuclei are blue) and anti-Raldh2 antibody (red positive signal). Inset in (**I**) shows Raldh2 positive cells which do not express  $\alpha$ SMA: these are ureteric stromal cells. Note that few peri-urothelial express either  $\alpha$ SMA or Raldh2 in null mutant proximal ureters. (**K** and **L**) UP1b ICH (brown positive signal) on E18.5 wildtype (**K**) and null mutant (**L**) ureters.

**Figure 7. *Tshz3* is required for harmonised ureteric peristalsis.**

(**A** and **B**) An explanted wild-type (**A**) and *Tshz3*<sup>-/-</sup> (**B**) E15.5 ureter after six days culture: the ends on the left of each frame represent the proximal ureteric segments. (**C** and **D**) Graphs illustrating peristaltic contractions of cultured ureters of wild-type (**C**) and *Tshz3*<sup>-/-</sup> (**D**) ureters. Measurements of luminal diameters were made at four different positions from their proximal to distal ends from a 20 second digital recording of contracting ureters (**Supplementary movie 1 and 2**). Data are presented as the percentage of the relaxed diameter. In the trace from the wild-type ureter (**C**) the contraction (downward motion from baseline) initiates about one fifth of the way down (red line) the ureter; this is rapidly followed by both contraction of the more proximal segment (blue line) and also by distal propagation (pink and yellow lines). Null mutant trace (**D**) shows absent proximal proximal segment contraction together with a variable delay of distal relaxation (pink line). Representative traces are shown for at least five samples from each genotype.

**Figure 8. Ureteric differentiation.** A) Summary of failed differentiation in *Tshz3* null mutants. Note lack of  $\alpha$ SMA expressing SMCs in the mutant ureter, which also has a reduction of *Raldh2* expressing stromal cells between urothelium and muscle. B) Proposed molecular signalling required for full SMC differentiation. *Shh* is expressed by the nascent urothelium, and the secreted factor binds Ptch1 in mesenchyme, activating Smoothened (Smo) which leads

to *Bmp4* expression. Subsequently, this growth factor is available to bind its receptor (BmpR) and facilitate SMC differentiation. For the latter process to proceed efficiently and completely in the proximal ureter, however, *Tshz3* expressed in ureteric mesenchyme must act with (or perhaps drive) myocardin expression (blue), resulting in transcription of SMC-genes (black) such as *aSMA* and *SMMHC*.

Figure 1

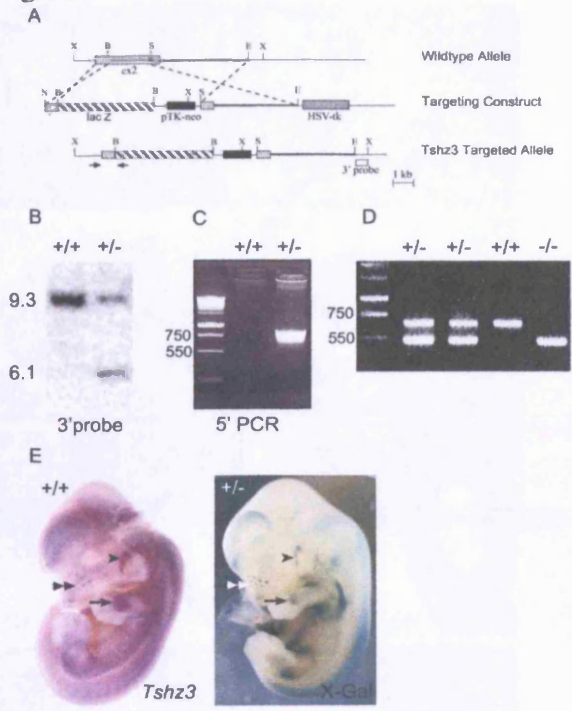


Figure 2

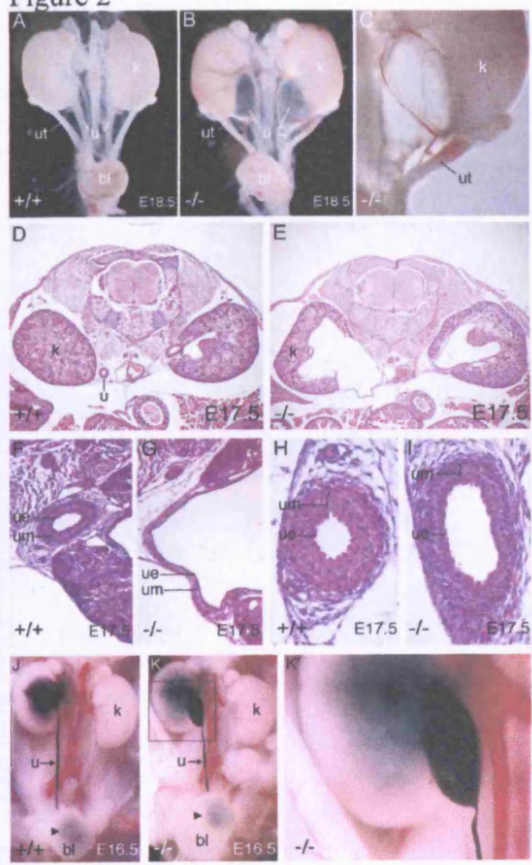




Figure 3

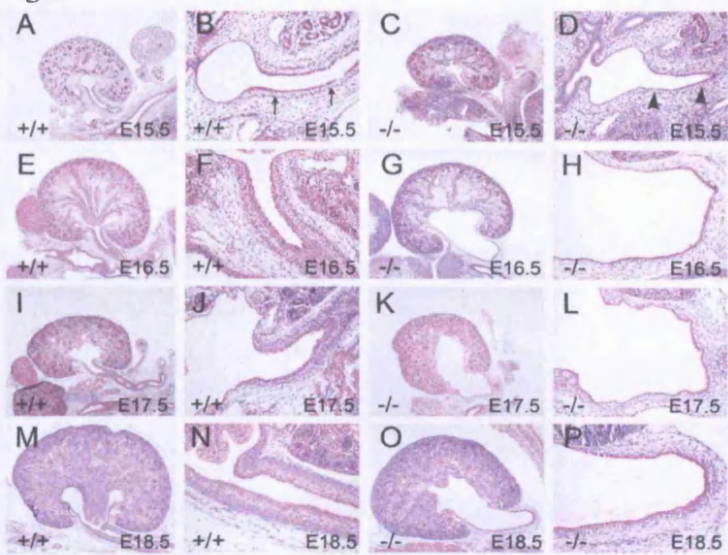


Figure 4

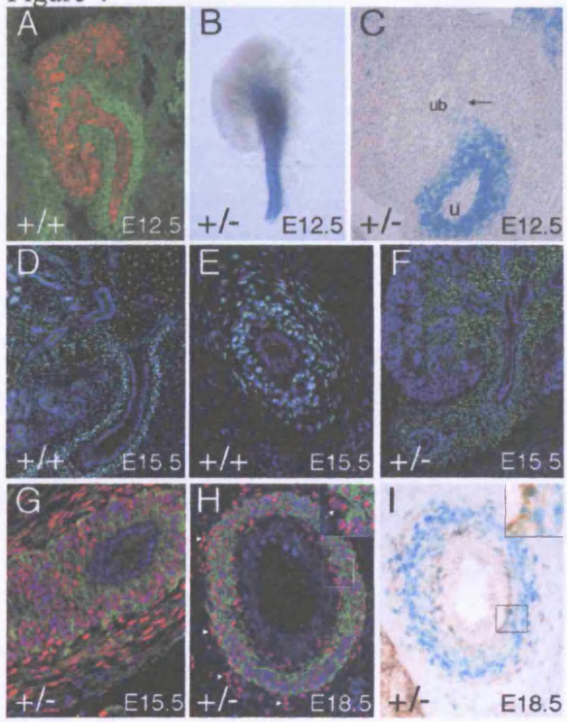


Figure 5

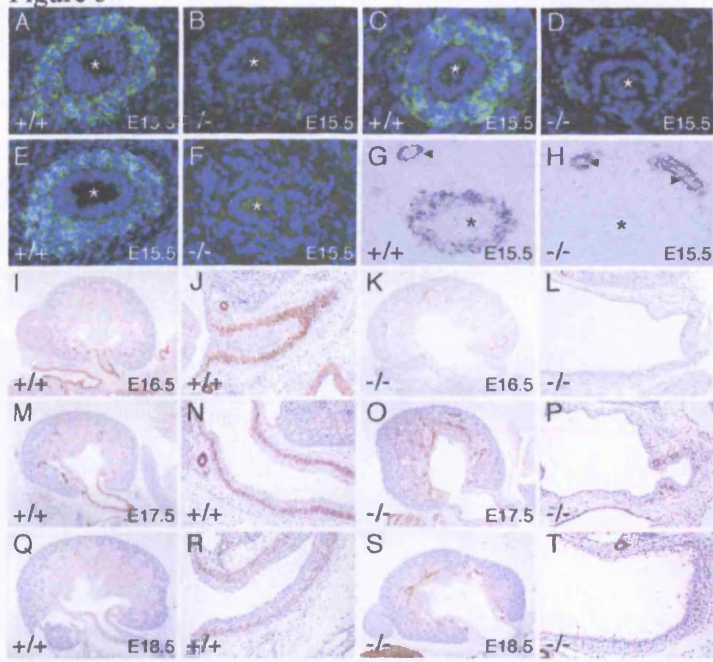


Figure 6

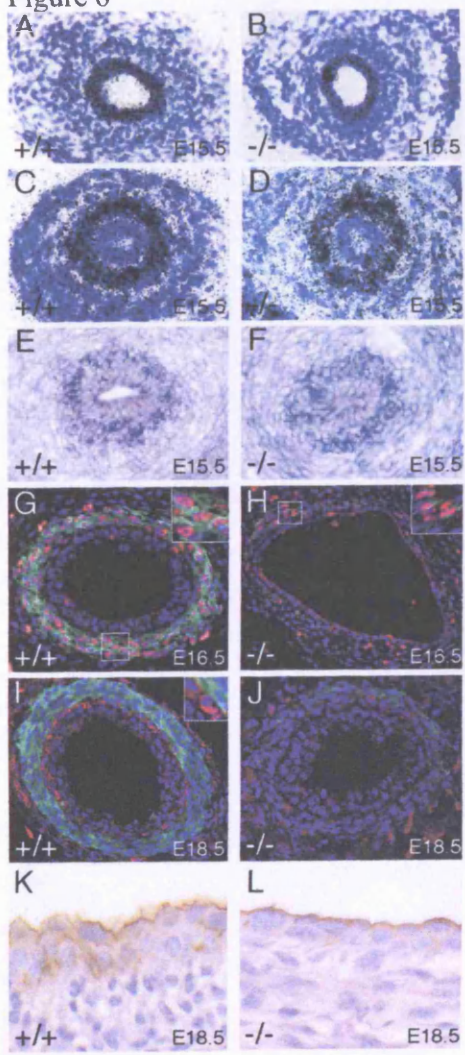


Figure 7

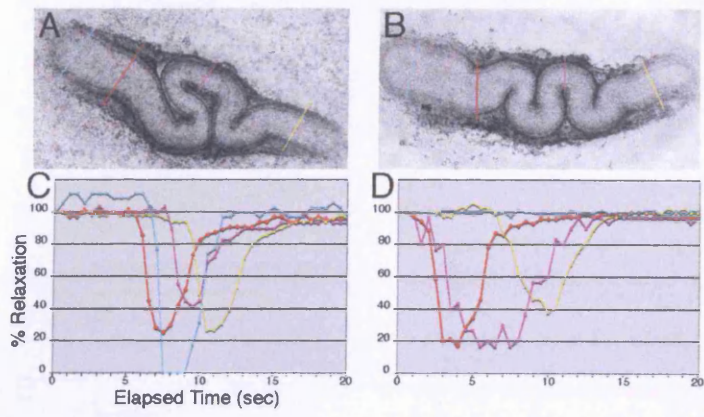
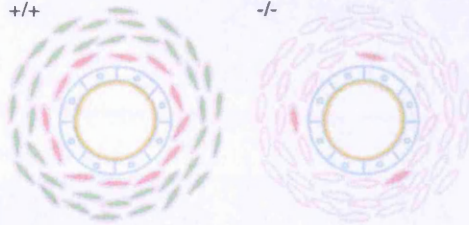






Figure 8

A

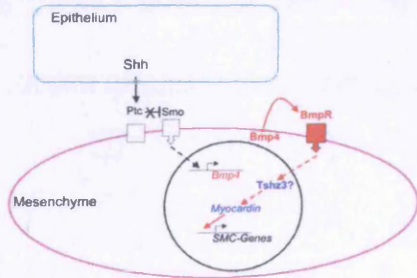
+/+

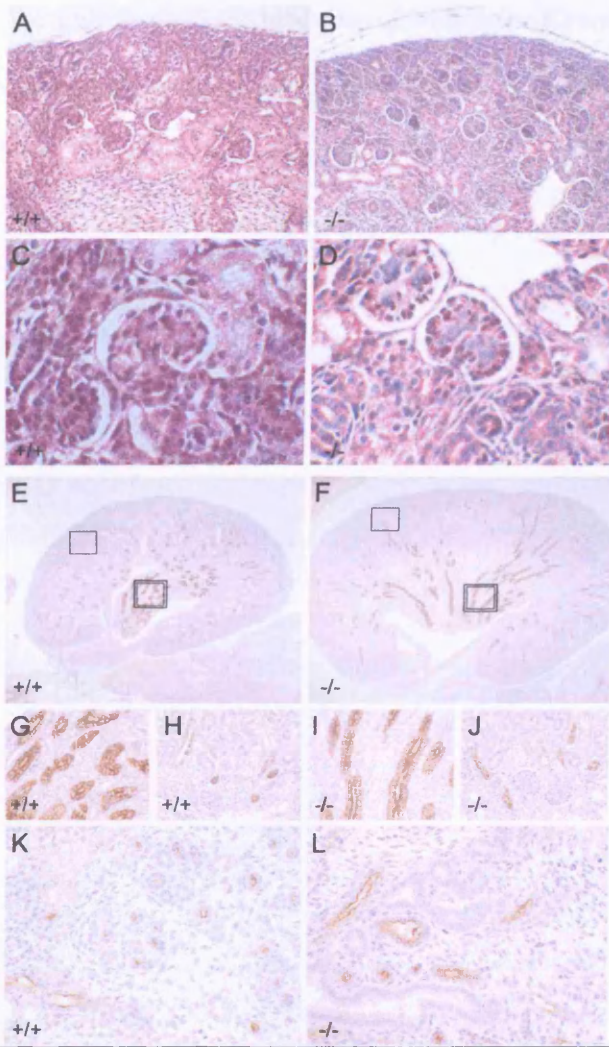
-/-



-  Undifferentiated mesenchymal cells (SMA<sup>-</sup>; Ralgh2<sup>-</sup>)
-  Smooth muscle cells (SMA<sup>+</sup>; Ralgh2<sup>-</sup>)
-  Stromal cells (SMA<sup>-</sup>; Ralgh2<sup>+</sup>)
-  Urothelial cells (UP<sup>+</sup>)

B



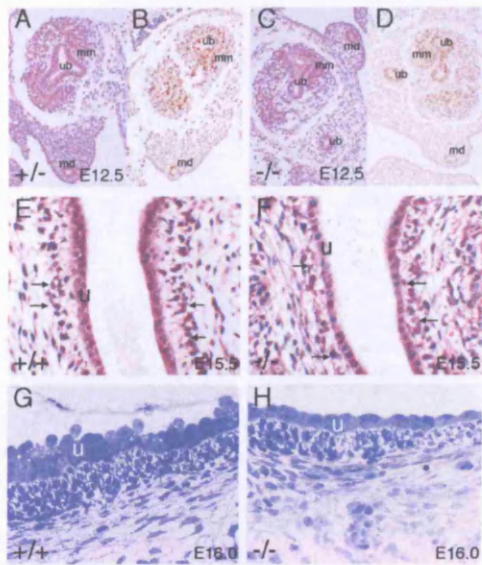


**Supplementary Figure 1. E18.5 kidneys.**

A, C, E, G, H, and K are section of a wild-type E18.5 kidney, whereas B, D, F, I, J, and L are from a *Tshz3* null-mutant kidney. Note that, in F, the null mutant papilla is pointed, as this kidney had pelvic urine drained on autopsy. The kidney cortex is grossly similar in the wild-type (A) and null mutant (B). In both genotypes, glomeruli had capillary loops (C and D). Low power views of wild-type (E) and null (F) kidneys with brown signal generated by IHC for aquaporin 2 (brown), a collecting duct marker: boxes define regions shown in high magnification in G-J. High power view of medullary (G and I) and cortical (H and J) collecting ducts. (K and

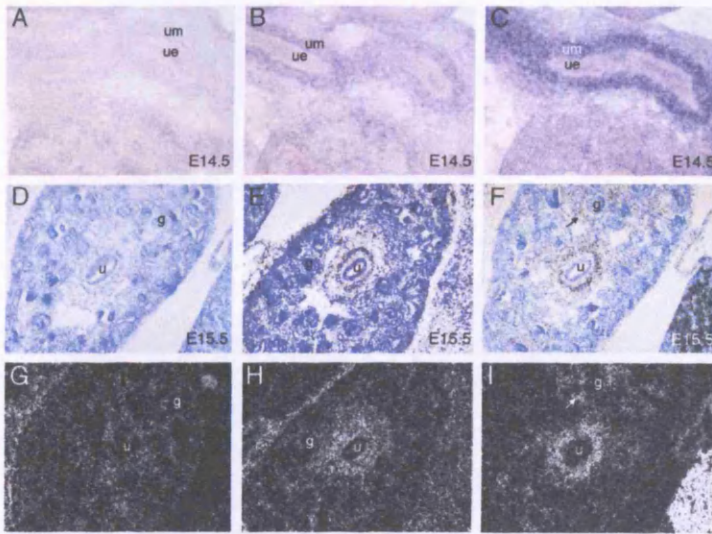
**L)** Sections through the medullas of wild-type (**K**) and *Tshz3*<sup>-/-</sup> (**L**) kidneys immunostained for uromodulin (brown): thick ascending limbs of loops of Henle are present in both genotypes.





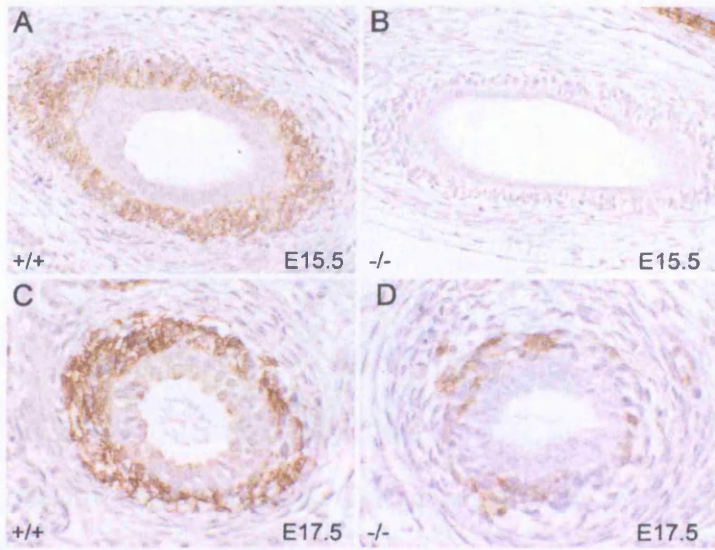
**Supplementary Figure 2. Early metanephric development and ureteric mesenchymal cell morphology.**

(A-D) Sections of E12.5 metanephroi from *Tshz3*<sup>+/-</sup> (A and C) and *Tshz3*<sup>-/-</sup> (B and D) embryos stained either with Masson's trichrome (A and C) or immunostained to detect the Pax2 transcription factor (brown in B and D) showing intact ureteric bud branches (ub), induced metanephric mesenchyme (mm) and mesonephric ducts (md): note that there is an artefactual shear through the metanephros in B. (E and F) High power images of longitudinal sections from wild-type (E) and *Tshz3*<sup>-/-</sup> (F) E15.5 proximal ureters stained with Masson's trichrome demonstrate aggregating mesenchyme in wild-type and early disorganisation of mesenchymal cells in mutants: mesenchymal cells indicated by arrows. (G and H) Toluidine blue staining of E16.0 ureter longitudinal sections at a level immediately distal to the proximal ureter. In the wild-type (G), radially-organised mesenchymal cells were observed: the cells form a thinner and less compact layer in the null mutant (H). u, urothelium.



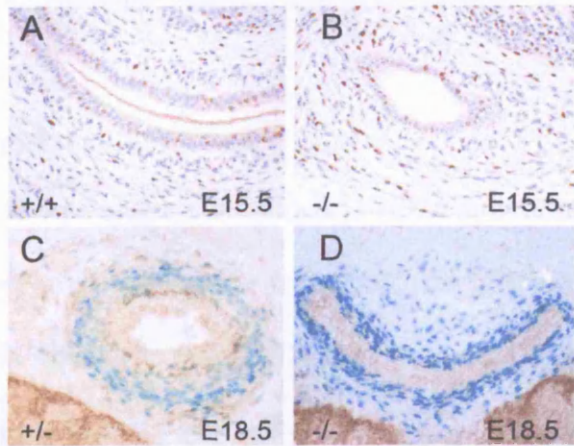
**Supplementary Figure 3. *Tshz1-3* expression, as assessed by ISH.**

(A-C) Longitudinal sections of E14.5 wild-type ureters with ISH for *Tshz1* (A), *Tshz2* (B) and *Tshz3* (C). *Tshz2* and *Tshz3* but not *Tshz1* were expressed (purple colour) in ureteral mesenchyme. (D-I) Transverse sections of E15.5 wild-type kidneys for *Tshz1* (D and G), *Tshz2* (E and H) and *Tshz3* (F and I). (D-F) and (G-I) are respectively brightfield and darkfield views of the same sections, with a positive signal detected as black dots in the former and white dots in the latter fields. *Tshz2* and *Tshz3* were expressed in mesenchymal cells surrounding proximal ureteric urothelia. *Tshz3* was also expressed in the medullary and inner cortical interstitium (arrowed in F and I). *Tshz2* signals were also detected in the medullary interstitium. With regard to *Tshz1*, signals above background were not obtained. g, glomerulus; u, ureter; ue, ureteral epithelium; um, ureteral mesenchyme.



**Supplementary Figure 4. Maturation of the distal ureter.**

All fields are transverse sections of distal ureters, immunostained for  $\alpha$ SMA (brown positive signal) with nuclei counterstained with haematoxylin (blue). In wildtypes (+/+), note upregulation of  $\alpha$ SMA in aggregating peri-urothelial cells between E15.5 (A) and E17.5 (C). In contrast, IHC signal for  $\alpha$ SMA was deficient in *Tshz3* null mutants at E15.5 (B) and was reduced versus wildtypes at E17.5 (D).



**Supplementary Figure 5. Cell turnover in the proximal ureter.**

(**A and B**) PCNA IHC (brown nuclear signal) of a wild-type (+/+; **A**) and a *Tshz3* null mutant (-/-; **B**) proximal ureter. Note there is no lack of PCNA expressing cells in either the mutant urothelium or surrounding mesenchymal layers. (**C and D**) X-Gal staining.  $\beta$ -galactosidase expressing cells (blue) around ureteric urothelium in a heterozygous (**C**) and a null mutant (**D**) embryo. There is no lack of periurothelial cells in the null mutant ureter which express *LacZ* inserted into the *Tshz3* locus. Note that the *Tshz3*<sup>-/-</sup> proximal ureter shown in **D** has collapsed during processing, hence the transverse section appears as a ‘smile’ shape.

## **SUPPLEMENTARY VIDEO LEGENDS**

### **Supplementary movie 1**

Wild type ureter; contraction initiated approximately a fifth of the way down the ureter, then the most proximal part contracted and was followed by distal propagation. Proximal ureter is on the right side of the movie. The Quicktime movie is played at approximately 4x actual speed.

### **Supplementary movie 2**

*Tshz3*<sup>-/-</sup> ureter; contraction initiated approximately a fifth of the way down the ureter and, as in wild type was followed by distal propagation. Significantly, however, the proximal ureter completely failed to contract. Proximal ureter is on the right side of the movie. The Quicktime movie is played at approximately 4x actual speed.

